

# DISSERTATION

## Rotary kiln biomass pyrolysis – Comprehensive investigations of a 3 MW operating pilot plant over a period of two years

ausgeführt zum Zwecke der Erlangung des akademischen Grades eines  
Doktors der technischen Wissenschaften

unter der Leitung von  
Univ. Prof. Dipl.-Ing. Dr. techn. Hermann HOFBAUER

am Institut für Verfahrenstechnik,  
Umwelttechnik und Technische Biowissenschaften (E 166)

eingereicht an der Technischen Universität Wien  
Fakultät für Maschinenwesen und Betriebswissenschaften

von

Michael Halwachs  
Hochart 99  
7423 Pinkafeld  
Matrikelnummer: 0527411

Hochart, 26.09.2011

.....  
Michael Halwachs

***I never saw a wild thing sorry for itself.  
A small bird will drop frozen dead from a bough  
without ever having felt sorry for itself.***

("Self pity" by D.H. Lawrence)

## Preface

The concentrations of greenhouse gases (GHG) in the atmosphere have reached unprecedentedly high levels and climate change is no longer a threat, but a reality. Atmospheric carbon dioxide (CO<sub>2</sub>) concentration has risen from 280 ppm prior to the industrial revolution to 379 ppm in 2005 [Forster et al., 2007]. The rate of increase between 2000 and 2005 was 3.3 per cent per annum, attributed to expansion of economic activity, increased GHG intensity of economic activity, and declining strength of the oceanic and terrestrial C sinks [Canadell et al., 2007].

The Intergovernmental Panel on Climate Change's Fourth Assessment Report (IPCC, 2007) clearly outlines the projected impacts of climate change, which are anticipated to be catastrophic unless atmospheric CO<sub>2</sub> level is stabilized at or below 550 ppm. The Kyoto protocol committed industrialized countries (those listed under the Kyoto Protocol's Annex I) to legally binding targets for the period 2008 to 2012, aimed to deliver a 5 per cent reduction in emissions compared with 1990. However, it is estimated that stabilization at 550 ppm will require developed countries to reduce their emissions by 60 per cent below 2000 levels by 2050 [Defra, 2003].

Given the potentially catastrophic impacts of climate change, particularly the evidence of non-linear and non-reversible changes or "tipping points", some argue that a reduction in emissions is not sufficient to address the risk of impacts due to elevated CO<sub>2</sub> levels, and propose strategies to withdraw CO<sub>2</sub> from the atmosphere to stabilize atmospheric CO<sub>2</sub> levels more rapidly [Lehmann and Joseph, 2009].

The scope of the challenge that faces us is significant. The Vattenfall report [Vattenfall, 2007], for example, estimates that stabilizing CO<sub>2</sub> at 450 ppm requires approximately 27 Gt CO<sub>2</sub>e (all greenhouse gases on the basis of CO<sub>2</sub> equivalents) to be withdrawn from the atmosphere by 2030.

The need for Annex I countries to encourage emissions mitigation so that they may reach their targets under the Kyoto Protocol has spawned the emergence of mandatory emissions trading schemes, while voluntary schemes have emerged to satisfy the growing demand from individuals and business seeking to offset their GHG emissions. Pyrolysis of biomass to produce renewable energy and biochar, and the use of biochar as a soil amendment, can contribute to mitigating GHG emissions through several routes and thus could constitute and offset activity within emissions trading schemes [Lehmann and Joseph, 2009].

A pyrolysis process can be used to split up the biomass in a volatile fraction poor in undesired substances (Cl, N, S, Na and K) and a char fraction where these substances are concentrated. In this way cheap biomass can be used for co-firing in existing fossil fuel power stations without the danger of corrosion, deposition, and emission problems. The aim of the project is the development and demonstration of a biomass pretreatment process based on pyrolysis in the temperature range between 450 to 630 °C to split the energy in the biomass into volatiles with a low content of the above mentioned undesired components and char, where most of these elements are concentrated. Based on the results of the pilot plant a scale up to a capacity of 30 MW<sub>th</sub> fuel input and the connection with the coal fired power plant is also discussed.

Thanks to the support of several people - which I greatly appreciate - this thesis was elaborated, which may contribute to a better understanding of the pyrolysis technology and its chances and possibilities to contribute to the mitigation of GHG emissions.

My sincere thanks go to Prof. Dr. Hermann Hofbauer, my supervisor, who not only supported my scientific career in many aspects, but also provided me the chance to collect international experience on several conferences all around the world.

I owe special thanks to Dr. Tobias Pröll for his support in doing first steps in IPSEpro modelling and his technical and scientific steering during the first part of the project.

Furthermore I would like to thank DI Gerhard Kampichler, Ringseis Reinhard and the whole crew of the pilot plant - I really enjoyed the time in Dürnröhr.

Thanks are also due to DI Markus Kleinhappl, DI Johannes Zeisler and DI Norbert Kienzl for their excellent analytical work.

Equally I would like to thank my master students Stefan Kern and Ute Wolfesberger, who contributed with their theses on various aspects of pyrolysis. Especially I would say thank you to DI Stefan Kern who has done really great work.

Finally, I am grateful to my family, who have always supported my education, be it financially or emotionally.

My dearest thanks go to my girlfriend Bettina, for her love and understanding throughout many years.



## Abstract

Co-firing of biomass is in many cases feasible for coal fired power plants. However, there are some limiting factors for using biomass in these plants. One of these factors is the composition of the biomass. Corrosive components like chloride, potassium or sodium can be harmful for the boiler of the coal fired power plant, because these power plants with a dust firing are optimized for a high efficiency. Therefore, the steam parameters temperature and pressure have to be as high as possible. At these high temperatures the mentioned components (Cl, K, Na, etc.) cause high temperature corrosion in the boiler especially at the super heater surface. So there has to be an intermediate step for the co-firing of e.g. straw, which is a local and cheap feedstock, in the coal fired power plant.

A pyrolysis process can be used to split up the biomass in a volatile fraction poor in undesired substances (Cl, N, S, Na and K) and a char fraction where these substances are concentrated. In this way cheap biomass can be used for co-firing in existing fossil fuel power stations without the danger of corrosion, deposition, and emission problems. The aim of the project is the development and demonstration of a biomass pretreatment process based on pyrolysis in the temperature range between 450 to 630 °C to split the energy in the biomass into volatiles with a low content of the above mentioned undesired compounds and char where most of these elements are concentrated.

This specific application of pyrolysis of biomass is still a new technology that has not been published in literature very often before. Due to this fact a pilot plant with an externally heated rotary kiln pyrolysis reactor that is designed for a fuel power of 3 MW has been built and operated at the EVN AG coal fired power plant in Dürnröhr.

Based on the results of comprehensive investigations carried out at the pilot plant a scale up to a capacity of 30 MW<sub>th</sub> fuel input and integration into the coal fired power plant is also discussed in this work.

## Kurzfassung

Mitverbrennung (Co-firing) von Biomasse stellt in vielen Fällen eine mögliche Option für bestehende Kohlekraftwerke dar. Es gibt jedoch einige limitierende Faktoren für den Einsatz von Biomasse in diesen Kraftwerken, einer dieser Faktoren ist die Zusammensetzung der Biomasse. Korrosive Bestandteile wie Chlorid, Kalium oder Natrium können schädliche Auswirkungen für den Kessel des Kohlekraftwerkes haben. Kohlekraftwerke mit einer Staubfeuerung werden für einen hohen Wirkungsgrad optimiert, deshalb müssen die Dampfparameter, Druck und Temperatur, so hoch wie möglich sein. Bei diesen hohen Temperaturen führen die genannten Komponenten (Cl, K, Na, etc.) zu Hochtemperaturkorrosion im Kessel und da speziell an der Oberfläche des Überhitzers. Daher muss es einen Zwischenschritt für die Mitverbrennung von landwirtschaftlichen Rückständen (z.B. Stroh), die ein lokaler und billiger Rohstoff sind, für die Nutzung in einem bestehenden Kohlekraftwerk geben.

Ein Pyrolyseverfahren kann zur Auftrennung der Biomasse in eine flüchtige Fraktion, welche geringe Mengen an unerwünschten Substanzen (Cl, N, S, Na und K) enthält, und eine Koksfraktion, wo diese Stoffe aufkonzentriert sind, genutzt werden. Auf diese Weise kann bisher ungenutzte, billige Biomasse für die Mitverbrennung in bestehenden fossilen Kraftwerken ohne die Gefahr von Korrosion, Ablagerung und Emissionsproblemen verwendet werden. Ziel des Projektes ist die Entwicklung und Demonstration eines Biomasse-Vorbehandlungsprozesses basierend auf der Pyrolysetechnologie in einem Temperaturbereich von 450-630°C. Die Biomasse und damit auch die Energie in der Biomasse wird dabei in einen flüchtigen Bestandteil (Pyrolysegas und Pyrolyseöl) mit einem geringen Gehalt an den oben genannten unerwünschten Verbindungen und dem Pyrolysekoks (Biochar), wo die meisten dieser Elemente aufkonzentriert sind, aufgetrennt.

Dieser Verwendungszweck für eine Pyrolyseanlage stellt eine neue, innovative Prozesstechnologie dar, die bisher nur selten betrachtet wurde. Aufgrund dieser Ausgangslage wurde eine Pilotanlage, dessen Kernstück ein indirekt beheizter Drehrohrpyrolysereaktor mit einer Brennstoffwärmeleistung von 3 MW bildet, am Gelände der EVN AG in Dürnröhr errichtet.

Basierend auf den Ergebnissen der Pilotanlage wird ein Scale-up der Anlage mit einer Brennstoffwärmeleistung von 30 MW<sub>th</sub> und die Anbindung an das bestehende Kohlekraftwerk diskutiert.

---

## Table of contents

<b>1</b>	<b>Introduction .....</b>	<b>13</b>
1.1	Biomass as a renewable energy resource.....	13
1.1.1	Classification of biomass .....	14
1.2	Straw as renewable energy resource.....	15
<b>2</b>	<b>Theoretical background .....</b>	<b>17</b>
2.1	Biomass composition .....	17
2.2	Energetic use of biomass.....	20
2.2.1	Thermo-chemical conversion .....	22
2.2.2	Bio-chemical conversion .....	24
2.2.3	Physical-chemical conversion.....	24
2.3	Pyrolysis of biomass .....	25
2.3.1	Pyrolysis mechanisms and pyrolysis reaction kinetics .....	27
2.4	Flash Pyrolysis .....	39
2.4.1	Reactor types for flash pyrolysis.....	40
2.5	Slow Pyrolysis.....	46
2.5.1	Carbonisation .....	46
2.5.2	Torrefaction .....	46
2.6	Combustion of agricultural residues in a thermal power plant .....	48
2.6.1	Technologies for Co-firing .....	48
2.6.2	Co-firing of biomass in a pulverised coal fired power plant .....	56
2.6.3	High temperature corrosion.....	58
2.7	The coal fired power plant Dürnrrohr.....	59
<b>3</b>	<b>Pyrolysis pilot plant Dürnrrohr.....</b>	<b>63</b>
3.1.1	Process description .....	66
3.1.2	Pyrolysis operation.....	67
3.1.3	Fluidised bed operation.....	68
3.1.4	Spray type cooler.....	69
3.1.5	Gas cleaning of the pilot plant .....	70
3.1.6	Data logging .....	72
<b>4</b>	<b>Experimental work and chemical analyses .....</b>	<b>73</b>
4.1	Feedstock and pyrolysis charcoal characterisation .....	73
4.2	Detection of pyrolysis oil .....	75
4.2.1	Gravimetric analysis for pyrolysis oil.....	76
4.2.2	GC-MS/FID analysis for pyrolysis oil .....	77
4.3	Pyrolysis gas characterisation .....	79
4.3.1	Measurement of NH <sub>3</sub> .....	81
4.3.2	Measurement of H <sub>2</sub> S .....	82

---

4.3.3	Measurement of HCl .....	84
4.4	Determination of the ash melting behaviour .....	85
<b>5</b>	<b>Overall plant mass and energy balances .....</b>	<b>87</b>
5.1	Process simulation .....	87
5.1.1	About IPSEpro .....	88
5.2	System modelling .....	90
5.2.1	General approach .....	90
5.2.2	Modelling of the pyrolysis pilot plant .....	91
5.3	Calculating balances with the IPSEpro model .....	95
5.3.1	Calculating the pyrolysis oil elemental composition .....	98
<b>6</b>	<b>Experimental and simulation results .....</b>	<b>99</b>
6.1	Fuel and pyrolysis char analysis .....	100
6.1.1	Carbon content and LHV .....	103
6.1.2	Volatiles .....	106
6.1.3	Ash content .....	107
6.1.4	Elemental analysis .....	109
6.2	Results of the gravimetric detection of pyrolysis oils from pyrolysis pilot plant .....	121
6.3	Water content of pyrolysis gas and fuel samples .....	128
6.4	Dust and entrained char .....	130
6.5	Ash melting behaviour of fuel and pyrolysis char samples .....	131
6.6	Operation with indoor stored wheat straw .....	134
6.6.1	Characterization of feedstock .....	135
6.6.2	Pyrolysis char from wheat straw .....	136
6.6.3	Elemental analysis of pyrolysis char from wheat straw .....	138
6.6.4	Pyrolysis gas composition .....	148
6.6.5	Pyrolysis oil composition .....	163
6.6.6	Detection of gravimetric pyrolysis oil .....	165
6.6.7	Dust and entrained char .....	166
6.6.8	Variation of the pyrolysis temperature .....	168
6.6.9	Variation of the residence time .....	172
6.7	Distribution of chemical elements in the pyrolysis products .....	175
6.8	Efficiency .....	179
6.8.1	Chemical efficiency .....	179
6.8.2	Plant efficiency .....	181
<b>7</b>	<b>Conclusion and outlook .....</b>	<b>185</b>
7.1	Conclusion .....	185
7.2	Outlook – Scale up of pilot plant .....	188
7.3	Outlook – Biochar production .....	190
<b>8</b>	<b>Bibliography .....</b>	<b>193</b>

---

---

<b>9 Appendix .....</b>	<b>211</b>
9.1 Measured values and name of their measuring points in the process control system.....	211
9.2 Design data of the pyrolysis pilot plant Dürrohr .....	211
9.3 Analyses of black coal .....	213
9.4 Process simulation flow sheet.....	216
9.5 Energy flow in the pilot plant .....	217
9.6 Balanced results.....	217
9.7 Chromatograms from the GC-MS/FID detection .....	272

## Figures

FIGURE 1-1: PHOTOSYNTHESIS AND EXHALATION IN A GREEN PLANT [KERN, 2010].....	13
FIGURE 1-2: CLASSIFICATION OF BIOMASS [KALTSCHMITT ET AL., 2009].....	14
FIGURE 1-3: AVAILABLE AMOUNTS OF STRAW 1980 – 2007 [HASLINGER ET WOPIENKA, 2009].....	15
FIGURE 1-4: ACREAGE, STRAW- AND CORN YIELDS 1980 – 2007 [HASLINGER ET WOPIENKA, 2009], DT/HA = 0,1 T/HA.....	16
FIGURE 2-1: FORMATION AND COMPOSITION OF BIOMASS, ADAPTED [HOFBAUER, 2008] .....	17
FIGURE 2-2: CELLULOSE STRUCTURE (N= DEGREE OF POLYMERIZATION) [KLEMM, 2005] .....	18
FIGURE 2-3: HEMICELLULOSE STRUCTURE [UNGER ET ISING, 2002].....	18
FIGURE 2-4: STRUCTURE OF P-COUMARYL ALCOHOL, CONIFERYL ALCOHOL AND SINAPYL ALCOHOL [STEEN, 2011].....	19
FIGURE 2-5: POSSIBLE STRUCTURE OF LIGNIN [STEEN, 2011] .....	19
FIGURE 2-6: A TENTATIVE CHEMICAL STRUCTURE OF WHEAT STRAW LIGNIN [SUN ET AL., 1997].....	19
FIGURE 2-7: MAIN CONVERSION OPTIONS FOR BIOMASS TO SECONDARY ENERGY CARRIERS (HTU= HYDRO THERMAL UPGRADING) [FAAJ, 2006].....	21
FIGURE 2-8: PRINCIPLE OF A COMPLETE THERMO-CHEMICAL CONVERSION OF BIOMASS, ADAPTED [KALTSCHMITT ET AL., 2009] .....	22
FIGURE 2-9: SUB-PROCESSES OF COMBUSTION, ADAPTED [KALTSCHMITT ET AL., 2009] .....	25
FIGURE 2-10: THERMAL BEHAVIOUR OF WOOD DURING HEATING WITHOUT OXYGEN [KALTSCHMITT ET AL., 2009].....	26
FIGURE 2-11: SIMPLIFIED REPRESENTATION OF BIOMASS PYROLYSIS [BROWNSORT, 2009].....	28
FIGURE 2-12: THERMAL DECOMPOSITION OF WOOD, ADAPTED [KALTSCHMITT ET AL., 2009] .....	29
FIGURE 2-13: THERMAL DECOMPOSITION OF WOOD INTO CELLULOSE, HEMICELLULOSE AND LIGNIN, ADAPTED [KALTSCHMITT ET AL., 2009] .....	30
FIGURE 2-14: DISSOCIATION MECHANISMS OF CELLULOSE [FAIX ET AL., 1988].....	32
FIGURE 2-15: REACTION PATHWAYS FOR CELLULOSE DECOMPOSITION [MOK ET ANTAL, 1983] .....	32
FIGURE 2-16: THE MECHANISM OF CELLULOSE PYROLYSIS PROPOSED BY BANYASZ ET AL. [BANYASZ ET AL., 2001], [BANYASZ ET AL., 2001].....	34
FIGURE 2-17: TIC CHROMATOGRAM FROM PY-GC/MS OF HEMICELLULOSE AT DIFFERENT TEMPERATURES [WU ET AL., 2009].....	35
FIGURE 2-18: TYPICAL PRODUCTS OF THERMAL DECOMPOSITION OF LIGNIN [KALTSCHMITT ET AL., 2009].....	36
FIGURE 2-19: TYPICAL REACTIONS OF A PYROLYTIC DECOMPOSITION OF LIGNIN, ADAPTED [KALTSCHMITT ET AL., 2009].....	37
FIGURE 2-20: BUBBLING FLUID BED REACTOR [BRIDGWATER, 2003] .....	41
FIGURE 2-21: CIRCULATING FLUID BED REACTOR [BRIDGWATER, 2003] .....	42
FIGURE 2-22: PRINCIPLE OF ROTATING CONE PYROLYSIS REACTOR [BRIDGWATER ET GRASSI, 1991] .....	43
FIGURE 2-23: UNIVERSITY OF TWENTE ROTATING CONE FLASH PYROLYSIS REACTOR [BRIDGWATER ET PEACOCKE, 2000].....	44
FIGURE 2-24: PRINCIPLE OF A REACTOR WITH A ROTATING PLATE, ADAPTED [KALTSCHMITT ET AL., 2009]....	44
FIGURE 2-25: VORTEX ABLATIVE REACTOR [BRIDGWATER, 2003] .....	45
FIGURE 2-26: FIXED BED TORREFACTION REACTOR WITH DIRECT HEAT SUPPLY, ADAPTED [KALTSCHMITT ET AL., 2009].....	47
FIGURE 2-27: JACKED ROTARY KILN REACTOR, ADAPTED [KALTSCHMITT ET AL., 2009] .....	47
FIGURE 2-28: PROCESS LAYOUT OF UNIT PERFORMING DIRECT CO-FIRING .....	49
FIGURE 2-29: CO-FIRING CONCEPT FOR DIRECT CO-FIRING OF BIOMASS AND COAL. [ORJALA ET HEISKANEN, 2004].....	51
FIGURE 2-30: FLOW SHEET OF THE LAHTI ENERGIA OY GASIFIER [ORAVAINEN, 2008] .....	52
FIGURE 2-31: FLOW SHEET OF THE ZELTWEG BioCoComb POWER PLANT [SIMADER ET MORITZ, 2002].....	53
FIGURE 2-32: UPFRONT PYROLYSIS UNIT OF HAMM POWER STATION [CREMERS, 2009], (1) RESIDUAL BUNKER, (2) SHREDDER, (3) BUNKER, (4) CRANE, (5) MATERIAL LOCK, (6) PYROLYSIS ROTARY KILN, (7) BURNER SYSTEM, (8) DISCHARGE PYROLYSIS SOLIDS, (9) FAN, (10) DUST PRECIPITATOR .....	54
FIGURE 2-33: CO-FIRING OF BIO-OIL IN A POWER STATION [WAGENAAR ET AL., 2004].....	55
FIGURE 2-34: INFLUENCED PARTS OF A PLANT BY CO-FIRING OF BIOMASS, ADAPTED [KALTSCHMITT ET AL., 2009].....	56
FIGURE 2-35: THE COAL FIRED POWER PLANT DÜRNROHR [VERBUND, 2004].....	59
FIGURE 2-36: CROSS-SECTIONAL VIEW THROUGH THE DÜRNROHR POWER PLANT, ADAPTED [NEWAG NIOGAS, 1987].....	60

FIGURE 2-37: TANGENTIAL COAL DUST FIRING IN THE DÜRNROHR POWER PLANT, ADAPTED [NEWAG NIOGAS, 1987] .....	61
FIGURE 3-1: PYROLYSIS PILOT PLANT AT DÜRNROHR/AUSTRIA.....	63
FIGURE 3-2: FLOW SHEET OF THE PYROLYSIS PILOT PLANT .....	65
FIGURE 3-3: SCREENSHOT OF THE PLANT SCHEME FROM THE PROCESS CONTROL SYSTEM .....	66
FIGURE 3-4: ROTARY KILN REACTOR IN THE PROCESS CONTROL SYSTEM.....	67
FIGURE 3-5: FLUIDISED BED REACTOR/AFTERBURNER .....	69
FIGURE 3-6: GAS CLEANING OF THE PILOT PLANT: SPRAY COOLER, SPRAY ABSORBER AND FABRIC FILTER.....	70
FIGURE 4-1: COMPARISON OF THE DETECTION OF PYROLYSIS OIL BY GC-MS AND GRAVIMETRY [HOFBAUER ET AL., 2003].....	76
FIGURE 4-2: SCHEME OF THE TAR MEASURING SYSTEM, ADAPTED [HOFBAUER ET AL., 2003] .....	77
FIGURE 4-3: TEST RIG FOR H <sub>2</sub> S SAMPLING [KLEINHAPPL ET ZEISLER, 2010] .....	82
FIGURE 4-4: ASH MELTING – BEGINNING OF SINTERING (SIT).....	85
FIGURE 4-5: ASH MELTING – BEGINNING OF SOFTENING (SOT) .....	85
FIGURE 4-6: ASH MELTING – HEMISPHERIC POINT (HT) .....	86
FIGURE 4-7: ASH MELTING - FLOWING POINT (FT) .....	86
FIGURE 5-1: STRUCTURE OF IPSEPRO, ADAPTED [SIMTECH, 2009] .....	88
FIGURE 5-2: PROCESS SIMULATION FLOW SHEET OF THE PILOT PLANT IN IPSEPRO.....	91
FIGURE 5-3: IPSEPRO MODEL OF THE ROTARY KILN PYROLYSIS REACTOR.....	92
FIGURE 5-4: ILLUSTRATION OF THE COMMUNICATION BETWEEN IPSEPRO PSE AND MICROSOFT EXCEL [KERN, 2010].....	97
FIGURE 6-1: DIFFERENT FUEL SAMPLES:(1) PALM NUT SHELLS, (2) REED STRAW, (3) SORGHUM STRAW, (4) STRAW PELLETS, (5) MISCANTHUS, (6) WALDVIERTLER ENERGY GRASS, (7) PAPER RESIDUAL MATERIAL .....	100
FIGURE 6-2: DIFFERENT PYROLYSIS CHAR SAMPLES FROM THE PILOT PLANT:(1) PALM NUT SHELLS, (2) REED STRAW, (3) SORGHUM STRAW, (4) STRAW PELLETS, (5) MISCANTHUS, (6) WALDVIERTLER ENERGY GRASS, (7) PAPER RESIDUAL MATERIAL .....	101
FIGURE 6-3: CARBON CONTENT AND LHV OF DIFFERENT FUEL SAMPLES (DM).....	103
FIGURE 6-4: CARBON CONTENT AND LHV OF DIFFERENT PYROLYSIS CHAR SAMPLES (DM).....	104
FIGURE 6-5: CORRELATION OF CARBON CONTENT AND LHV OF PYROLYSIS CHAR SAMPLES .....	105
FIGURE 6-6: CONTENT OF VOLATILES OF DIFFERENT FUELS (DM).....	106
FIGURE 6-7: CONTENT OF VOLATILES OF DIFFERENT PYROLYSIS CHAR SAMPLES (DM) .....	106
FIGURE 6-8: ASH CONTENT OF DIFFERENT FUELS (DM).....	107
FIGURE 6-9: ASH CONTENT OF DIFFERENT PYROLYSIS CHAR SAMPLES (DM) .....	107
FIGURE 6-10: HYDROGEN CONTENT OF DIFFERENT FUEL SAMPLES (DM).....	109
FIGURE 6-11: HYDROGEN CONTENT OF DIFFERENT PYROLYSIS CHAR SAMPLES (DM).....	110
FIGURE 6-12: NITROGEN CONTENT OF DIFFERENT FUEL SAMPLES (DM) .....	111
FIGURE 6-13: NITROGEN CONTENT OF DIFFERENT PYROLYSIS CHAR SAMPLES (DM) .....	111
FIGURE 6-14: SULPHUR CONTENT OF DIFFERENT FUEL SAMPLES (DM) .....	113
FIGURE 6-15: SULPHUR CONTENT OF DIFFERENT PYROLYSIS CHAR SAMPLES (DM) .....	114
FIGURE 6-16: CHLORINE CONTENT OF DIFFERENT FUEL SAMPLES (DM).....	115
FIGURE 6-17: CHLORINE CONTENT OF DIFFERENT PYROLYSIS CHAR SAMPLES (DM).....	115
FIGURE 6-18: COMPARISON OF CHLORINE RELEASE DURING THE PYROLYSIS OF DIFFERENT TYPES OF BIOMASS [HRBEK, 2005].....	116
FIGURE 6-19: POTASSIUM CONTENT OF DIFFERENT FUEL SAMPLES (DM).....	117
FIGURE 6-20: POTASSIUM CONTENT OF DIFFERENT PYROLYSIS CHAR SAMPLES (DM).....	118
FIGURE 6-21: CHANGES IN K CONTENTS OF RICE STRAW BIOCHAR AS A FUNCTION OF TEMPERATURE DURING PYROLYSIS [YU ET AL., 2005].....	119
FIGURE 6-22: SODIUM CONTENT OF DIFFERENT FUEL SAMPLES (DM) .....	120
FIGURE 6-23: SODIUM CONTENT OF DIFFERENT PYROLYSIS CHAR SAMPLES (DM) .....	120
FIGURE 6-24: GRAVIMETRIC PYROLYSIS OIL CONTENT OF PALM NUT SHELLS .....	121
FIGURE 6-25: GRAVIMETRIC PYROLYSIS OIL CONTENT OF REED STRAW.....	122
FIGURE 6-26: GRAVIMETRIC PYROLYSIS OIL CONTENT OF SORGHUM STRAW .....	122
FIGURE 6-27: GRAVIMETRIC PYROLYSIS OIL CONTENT OF STRAW PELLETS.....	123
FIGURE 6-28: GRAVIMETRIC PYROLYSIS OIL CONTENT OF MISCANTHUS STRAW .....	123
FIGURE 6-29: GRAVIMETRIC PYROLYSIS OIL CONTENT OF WALDVIERTLER ENERGY GRASS.....	124
FIGURE 6-30: GRAVIMETRIC PYROLYSIS OIL CONTENT OF PAPER RESIDUAL MATERIAL .....	124
FIGURE 6-31: INTERMEDIATE PYROLYSIS OF POWDERED STRAW: HALOCLEAN PROCESS YIELDS [HORNUNG, 2008].....	126

FIGURE 6-32: INTERMEDIATE PYROLYSIS OF STRAW PELLETS: HALOCLEAN PROCESS YIELDS [HORNUNG, 2008]	126
FIGURE 6-33: FAST PYROLYSIS OF PINE/SPRUCE: BIOTHERM PROCESS YIELDS [BROWNSORT, 2009]	127
FIGURE 6-34: WATER CONTENT OF PYROLYSIS GAS AND FUEL SAMPLES	128
FIGURE 6-35: CORRELATION OF WATER CONTENT GAS AND WATER CONTENT FUEL	129
FIGURE 6-36: DUST AND ENTRAINED CHAR OF DIFFERENT FUEL SAMPLES	130
FIGURE 6-37: ASH MELTING BEHAVIOUR OF DIFFERENT BIOMASS SAMPLES	131
FIGURE 6-38: ASH MELTING BEHAVIOUR OF TWO STRAW SAMPLES COMPARED WITH THE DATA FROM THE DATABASE BIOBIB	132
FIGURE 6-39: ASH MELTING BEHAVIOUR OF THE DIFFERENT PYROLYSIS CHAR SAMPLES	132
FIGURE 6-40: ASH MELTING BEHAVIOUR OF FOUR PYROLYSIS CHAR SAMPLES FROM WHEAT STRAW	133
FIGURE 6-41: A TYPICAL STRAW SAMPLE (LASSEE) WHICH WAS USED FOR PLANT BALANCING	135
FIGURE 6-42: A TYPICAL PYROLYSIS CHAR FROM THE FEEDSTOCK STRAW	136
FIGURE 6-43: PYROLYSIS CHAR YIELD DURING THE ON-SITE BALANCING 2010 AND THE YIELD WHICH WAS CALCULATED FROM THE MODEL	137
FIGURE 6-44: CARBON CONTENT OF PYROLYSIS CHAR AT DIFFERENT PYROLYSIS TEMPERATURES	138
FIGURE 6-45: CHANGES IN ELEMENTS WITH INCREASING TEMPERATURE DURING THE CHARRING PROCESS OF WOOD [BALDOCK ET SMERNIK, 2002], PYROLYSIS PRODUCTS ... FAST PYROLYSIS PRODUCTS [ TSAI ET AL., 2006], BC ... BIOCHAR [CHENG ET AL., 2006]	139
FIGURE 6-46: HYDROGEN CONTENT OF PYROLYSIS CHAR AT DIFFERENT PYROLYSIS TEMPERATURES	140
FIGURE 6-47: NITROGEN CONTENT OF PYROLYSIS CHAR AT DIFFERENT PYROLYSIS TEMPERATURES	140
FIGURE 6-48: SULPHUR CONTENT OF PYROLYSIS CHAR AT DIFFERENT PYROLYSIS TEMPERATURES	141
FIGURE 6-49: CHLORINE CONTENT OF PYROLYSIS CHAR AT DIFFERENT PYROLYSIS TEMPERATURES	142
FIGURE 6-50: RELEASE OF CHLORINE AND POTASSIUM DURING PYROLYSIS OF STRAW [DAM-JOHANSEN ET AL., 1997]	143
FIGURE 6-51: POTASSIUM CONTENT OF PYROLYSIS CHAR AT DIFFERENT PYROLYSIS TEMPERATURES	144
FIGURE 6-52: COMPARISON OF K RELEASE TO THE GAS PHASE; STRAW AND WOOD PYROLYSIS [JENSEN ET AL., 2000]	145
FIGURE 6-53: SODIUM CONTENT OF PYROLYSIS CHAR AT DIFFERENT PYROLYSIS TEMPERATURES	145
FIGURE 6-54: LOWER HEATING VALUE OF AND ORIGINAL STRAW AND PYROLYSIS CHAR (DM) AT DIFFERENT PYROLYSIS TEMPERATURES	146
FIGURE 6-55: FRACTION OF VOLATILES OF PYROLYSIS CHAR AT DIFFERENT PYROLYSIS TEMPERATURES	147
FIGURE 6-56: PYROLYSIS GAS COMPOSITION OF STRAW	149
FIGURE 6-57: CORRELATION OF WATER CONTENT OF PYROLYSIS GAS AND PYROLYSIS TEMPERATURE	151
FIGURE 6-58: MECHANISM OF NH <sub>3</sub> AND HCN DISPOSAL DURING DEVOLATILISATION [BASSILAKIS ET AL., 1993]	153
FIGURE 6-59: CONCENTRATION OF NH <sub>3</sub> IN THE PYROLYSIS GAS (PYROLYSIS GAS TEMPERATURE 550 °C)	153
FIGURE 6-60: CONCENTRATION OF NH <sub>3</sub> IN THE PYROLYSIS GAS (PYROLYSIS GAS TEMPERATURE 500 °C)	154
FIGURE 6-61: CONCENTRATION OF NH <sub>3</sub> IN THE PYROLYSIS GAS (PYROLYSIS GAS TEMPERATURE 450 °C)	154
FIGURE 6-62: CONCENTRATION OF HCL IN THE PYROLYSIS GAS (PYROLYSIS GAS TEMPERATURE 550°C)	155
FIGURE 6-63: COMPARISON OF CL RELEASE TO THE GAS PHASE; STRAW AND WOOD PYROLYSIS [JENSEN ET AL., 2000]	156
FIGURE 6-64: PERCENTAGE OF RELEASED CHLORINE AS A FUNCTION OF THE PYROLYSIS TEMPERATURE FOR DIFFERENT BIOMASS [BJÖRKMANN ET STRÖMBERG, 1997]	156
FIGURE 6-65: CHROMATOGRAM OF SULPHUR SAMPLING (PERMANENT GASES) AT A PYROLYSIS TEMPERATURE OF 650°C AND WHEAT STRAW AS FUEL [LETTNER ET AL., 2008]	158
FIGURE 6-66: H <sub>2</sub> S SAMPLING AT A PYROLYSIS TEMPERATURE OF 550 °C	159
FIGURE 6-67: H <sub>2</sub> S SAMPLING AT A PYROLYSIS TEMPERATURE OF 500 °C	160
FIGURE 6-68: H <sub>2</sub> S SAMPLING AT A PYROLYSIS TEMPERATURE OF 600 °C	161
FIGURE 6-69: ALL MEASURED H <sub>2</sub> S CONCENTRATIONS DURING THE SAMPLING PERIOD	162
FIGURE 6-70: TYPICAL DISTRIBUTION OF MAIN FRACTIONS OF PYROLYSIS OIL [KALTSCHMITT ET AL., 2009]	163
FIGURE 6-71: RELATIVE PROPORTIONS OF GROUP COMPOUNDS OF GC/MS TAR [WOLFESBERGER, 2008]	164
FIGURE 6-72: MEASURED AMOUNTS OF PYROLYSIS OIL BY THE GRAVIMETRIC METHOD	165
FIGURE 6-73: TEMPERATURE DEPENDENCY OF PYROLYSIS OIL	165
FIGURE 6-74: TEMPERATURE DEPENDENCY OF DUST	166
FIGURE 6-75: TEMPERATURE DEPENDENCY OF ENTRAINED CHAR	167
FIGURE 6-76: MASS FRACTIONS OF THE PYROLYSIS PRODUCTS FOR TEMPERATURE VARIATION DURING PYROLYSIS OF STRAW	168
FIGURE 6-77: TRENDS OF THE MASS FRACTIONS OF THE PYROLYSIS PRODUCTS FOR TEMPERATURE VARIATION DURING PYROLYSIS OF STRAW	169



FIGURE 6-78: STRAW PYROLYSIS: EFFECT OF TEMPERATURE ON THE DECOMPOSITION PRODUCT [FAGBEMI ET AL., 2001] .....	170
FIGURE 6-79: FRACTIONS OF THE PYROLYSIS PRODUCTS FOR TEMPERATURE VARIATION DURING PYROLYSIS OF STRAW .....	171
FIGURE 6-80: TRENDS OF THE ENERGY FRACTIONS OF THE PYROLYSIS PRODUCTS FOR TEMPERATURE VARIATION DURING PYROLYSIS OF STRAW.....	171
FIGURE 6-81: MASS FRACTIONS OF THE PYROLYSIS PRODUCTS FOR RESIDENCE TIME VARIATION DURING PYROLYSIS OF STRAW AT 560 °C .....	172
FIGURE 6-82: TRENDS OF THE MASS FRACTIONS OF THE PYROLYSIS PRODUCTS FOR RESIDENCE TIME VARIATION DURING PYROLYSIS OF STRAW AT 560 °C .....	173
FIGURE 6-83: ENERGY FRACTIONS OF THE PYROLYSIS PRODUCTS FOR RESIDENCE TIME VARIATION DURING PYROLYSIS OF STRAW AT 560 °C .....	173
FIGURE 6-84: TRENDS OF THE ENERGY FRACTIONS OF THE PYROLYSIS PRODUCTS FOR RESIDENCE TIME VARIATION DURING PYROLYSIS OF STRAW AT 560 °C.....	174
FIGURE 6-85: DISTRIBUTION OF THE CHEMICAL ELEMENTS IN THE PYROLYSIS PRODUCTS FOR INDOOR STORED STRAW AT A PYROLYSIS TEMPERATURE OF 450 °C .....	176
FIGURE 6-86: DISTRIBUTION OF THE CHEMICAL ELEMENTS IN THE PYROLYSIS PRODUCTS FOR INDOOR STORED STRAW AT A PYROLYSIS TEMPERATURE OF 500 °C .....	177
FIGURE 6-87: DISTRIBUTION OF THE CHEMICAL ELEMENTS IN THE PYROLYSIS PRODUCTS FOR INDOOR STORED STRAW AT A PYROLYSIS TEMPERATURE OF 550 °C .....	178
FIGURE 6-88: SANKEY-DIAGRAM OF DIVIDING THE FEEDSTOCK’S CHEMICAL ENERGY BY THE PYROLYSIS REACTOR FOR PYROLYSIS OF STRAW AT A PYROLYSIS TEMPERATURE OF 560 °C, VALUES IN [kW].....	180
FIGURE 6-89: CHEMICAL EFFICIENCIES FOR INDOOR STORED WHEAT STRAW AT DIFFERENT PYROLYSIS TEMPERATURES .....	181
FIGURE 6-90: TYPICAL ENERGY BALANCE OF THE PYROLYSIS REACTOR FOR PYROLYSIS OF STRAW AT A TEMPERATURE OF 550 °C .....	182
FIGURE 6-91: IPSEPRO MODEL FOR THE CASE OF ENERGY SUPPLY BY PYROLYSIS GAS, VALUES ARE FOR THE SIZE OF THE PILOT PLANT (ABOUT 3 MW) [KERN, 2010] .....	183
FIGURE 6-92: SANKEY-DIAGRAM FOR THE PILOT PLANT SIZE AND STRAW PYROLYSIS FOR THE CASE OF ENERGY SUPPLY BY PYROLYSIS GAS, ENERGY FLOWS, VALUES IN [kW].....	184
FIGURE 7-1: SCENARIO ONE: ONE 30 MW PYROLYSIS REACTOR, SUPPLY OF PYROLYSIS ENERGY BY COMBUSTION OF PYROLYSIS GAS .....	188
FIGURE 7-2: SCENARIO TWO: THREE PARALLEL OPERATING PYROLYSIS REACTORS, SUPPLY OF PYROLYSIS ENERGY BY COMBUSTION OF CHAR AND BIOMASS .....	189
FIGURE 7-3: CONCEPTUAL MODEL OF C REMAINING FROM BIOMASS USING A DOUBLE-EXPONENTIAL DECAY MODEL WITH A MEAN RESIDENCE TIME OF 10 YEARS FOR THE LABILE C POOL AND 1000 YEARS FOR THE STABLE C POOL BUT DIFFERENT PROPORTIONS OF LABILE C [LEHMANN AND JOSEPH, 2009] .....	191
FIGURE 7-4: CARBON SEQUESTRATION BY PHOTOSYNTHESIS AND BIOCHAR SEQUESTRATION [IBI, 2011].....	192
FIGURE 9-1: PROCESS SIMULATION FLOW SHEET OF THE PILOT PLANT .....	216
FIGURE 9-2: ENERGY FLOW IN THE PILOT PLANT, PYROLYSIS OPERATION OF STRAW .....	217
FIGURE 9-3: SAMPLE 7948 – LIQUID PHASE.....	272
FIGURE 9-4: SAMPLE 7948 – LIQUID PHASE.....	273
FIGURE 9-5: SAMPLE 7948 – LIQUID PHASE.....	274
FIGURE 9-6: SAMPLE 7948 – TARRY PHASE .....	275
FIGURE 9-7: SAMPLE 7948 – TARRY PHASE .....	276
FIGURE 9-8: SAMPLE 7948 – TARRY PHASE .....	277
FIGURE 9-9: SAMPLE 7948 – TARRY PHASE .....	278
FIGURE 9-10: SAMPLE 7949 .....	279
FIGURE 9-11: SAMPLE 7949 .....	280
FIGURE 9-12: SAMPLE 7949 .....	281
FIGURE 9-13: SAMPLE 7950 .....	282
FIGURE 9-14: SAMPLE 7950 .....	283

## Tables

TABLE 2-1 COMPOSITION OF VARIOUS BIOMASSES IN WT. % [HOFBAUER, 2008].....	18
TABLE 2-2: CHROMATOGRAPHIC PEAK IDENTIFICATION OF MAIN PYROLYSIS PRODUCTS FROM HEMICELLULOSE [WU ET AL., 2009] .....	35
TABLE 2-3: TYPICAL YIELDS OF DIFFERENT PYROLYSIS TECHNOLOGIES [BROWNSORT, 2009].....	38
TABLE 2-4: COMPOSITION OF SOLID FUELS AND BIOMASS TYPES [KALTSCHMITT ET AL., 2009] .....	57
TABLE 2-5: MAIN FIGURES FOR THE COAL FIRED POWER PLANT DÜRNROHR .....	61
TABLE 2-6: CHLORINE (CL), SODIUM (NA), POTASSIUM (K) AND SULPHUR (S) CONTENT OF THE FOUR BLACK COAL SAMPLES.....	62
TABLE 3-1: DESIGN DATA OF THE PILOT PLANT FOR PYROLYSIS OPERATION.....	64
TABLE 3-2: DESIGN DATA OF THE PILOT PLANT FOR FLUIDISED BED OPERATION.....	64
TABLE 4-1: APPLICABLE DIN AND ÖNORM STANDARDS FOR THE DIFFERENT ANALYSES .....	74
TABLE 5-1: CONNECTIONS OF THE UNIT U_PYROL_HTD_ .....	93
TABLE 5-2: VARIABLES OF THE ROTARY KILN PYROLYSIS REACTOR .....	94
TABLE 5-3: MEASUREMENTS USED FOR THE IPSEPRO BALANCE AND THEIR ASSOCIATED KKS NUMBER .....	96
TABLE 5-4: EXTRACT OF THE RESULT FROM THE GC-MS ANALYSIS [KERN, 2010] .....	98
TABLE 5-5: RESULT OF A CONVERSION TO ELEMENTAL PYROLYSIS OIL COMPOSITION .....	98
TABLE 6-1: PLANT SETTINGS DURING THE SAMPLING PERIOD OF THE DIFFERENT PYROLYSIS CHAR SAMPLES .....	102
TABLE 6-2: CONDITIONS FOR INVESTIGATIONS WITH WHEAT STRAW .....	134
TABLE 6-3: ELEMENTAL ANALYSIS OF STRAW .....	135
TABLE 6-4: ELEMENTAL ANALYSIS OF PYROLYSIS CHAR FROM STRAW AT DIFFERENT PYROLYSIS TEMPERATURES .....	136
TABLE 6-5: TYPICAL PRODUCT YIELDS (DRY BASIS) FOR DIFFERENT MODES OF PYROLYSIS [BRIDGWATER, 2007].....	137
TABLE 6-6: PYROLYSIS GAS COMPOSITION CONCERNING PERMANENT GASES AT A PYROLYSIS TEMPERATURE OF 550°C .....	148
TABLE 6-7: YIELDS OF THE MAJOR GASES (IN % VOLUME; A, WOOD; B, COCONUT SHELL; C, STRAW) [FAGBEMI ET AL., 2001] .....	150
TABLE 6-8: DETECTED SUBSTANCE GROUPS IN THE PYROLYSIS OIL BY GC-MS/FID .....	164
TABLE 6-9: REMAINING FRACTIONS OF ELEMENTS IN THE PYROLYSIS CHAR OF STRAW AT DIFFERENT PYROLYSIS TEMPERATURES [SOUKUP, 2005] .....	175
TABLE 9-1: MEASURED VALUES AND THE NAME OF THEIR MEASURING POINTS IN THE PROCESS CONTROL SYSTEM.....	211
TABLE 9-2: DESIGN DATA OF THE PILOT PLANT FOR PYROLYSIS OPERATION.....	211
TABLE 9-3: DESIGN DATA OF THE PILOT PLANT FOR FLUIDISED BED OPERATION.....	212
TABLE 9-4: BLACK COAL MURCKI .....	213
TABLE 9-5: BLACK COAL CENTRUM .....	213
TABLE 9-6: BLACK COAL RYDULTOWY.....	214
TABLE 9-7: BLACK COAL KRU TRADE .....	214
TABLE 9-8: ELEMENTAL ANALYSIS OF DIFFERENT FUEL SAMPLES .....	215
TABLE 9-9: ELEMENTAL ANALYSIS OF DIFFERENT PYROLYSIS CHAR SAMPLES.....	215
TABLE 9-10: DETECTED SINGLE COMPONENTS IN THE PYROLYSIS OIL SAMPLES BY USING GC-MS/FID.....	284

# 1 Introduction

## 1.1 Biomass as a renewable energy resource

Biomass can be called the backbone of the renewable energies and amounts for nearly 60 per cent of all renewable energies in Austria and the European Union [Kopetz, 2010]. To build up biomass, green plants convert  $\text{CO}_2$  into organic matter with the use of sunlight. Biomass represents stored solar energy that can be used at the time the energy is required. A part of the generated biomass by photosynthesis is used again for the maintenance of the metabolism operation, as  $\text{CO}_2$  has lower energy content than the organic molecules. This procedure is called  $\text{CO}_2$  exhalation. During vegetation, only a small part of the primary irradiated energy is chemically bound. The plant is able to use the radiation range from 400 to 700 nm. For the formation of glucose there is a theoretical efficiency of 33.2 per cent achieved. Considering the  $\text{CO}_2$  exhalation and energy losses, the efficiency of the biomass formation is much lower than the theoretical efficiency. The average utilization of the radiation ranges between 0.04 % in the desert and almost 2 per cent in the rain forest. In the larger part of Europe the net efficiency is between 0.8 and 1.2 per cent. For example in a central European hornbeam forest, there is an annual growth of 5.7 t/ha above ground and 2.4 t/ha in the form of roots, if an efficiency of 1 % is assumed [Hofbauer, 2008].

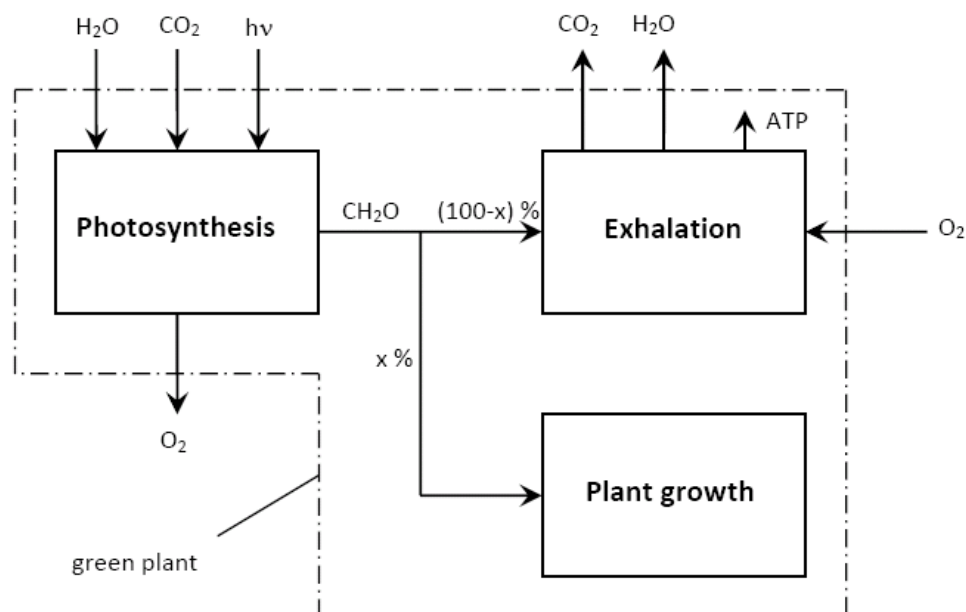


Figure 1-1: Photosynthesis and exhalation in a green plant [Kern, 2010]

### 1.1.1 Classification of biomass

The term “biomass” contains all organic matter. It contains all plants and animals, their residua, dead animals and plants (e.g. straw) and all organics which have been a result of a technical conversion (e.g. black liquor, paper and cellulose, organic customer waste fraction, vegetable oil, alcohol). The borderline between biomass and fossil fuels is peat, the secondary fossil product of rotting [Hofbauer, 2008].

Biomass can be divided into primary and secondary products [Hofbauer, 2008]:

- Primary products are the whole biomass which is the result of direct photosynthesis by sunlight.
- Secondary products are built per conversion or decomposition by higher plants or animals. They source their energy indirectly from the sunlight. To the secondary products belong all animals, their residua and sewage sludge.

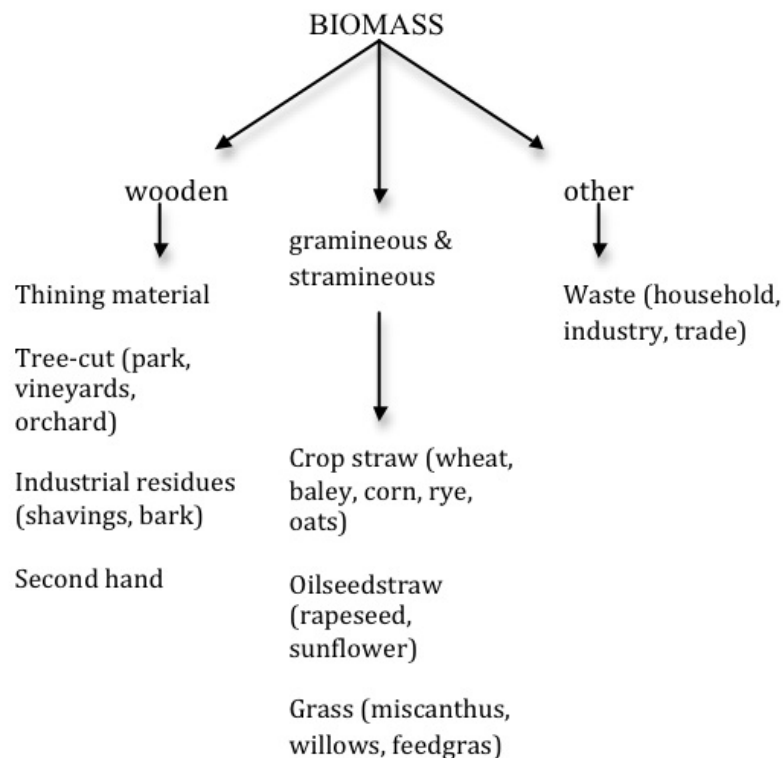


Figure 1-2: Classification of biomass [Kaltschmitt et al., 2009]

## 1.2 Straw as renewable energy resource

Beside the main product (cereal, fruit, vegetable), a certain amount of biomass is produced as by-products during agricultural production. Among the by-products that can be used for energetic purposes, a distinction is made between straw as the main by-product suitable as a source of energy and other organic residues of minor importance. [Kaltschmitt et Bridgwater, 1997]

The use of straw in different conversions processes is becoming of more and more interest. Several treatments for a broad range of applications are in the focus of science [Weinwurm, 2010]. Due to this growing interest it is a necessity to keep in mind how much straw is available for these processes. First estimations of the availability of straw for a thermal conversion process in Austria, more precisely for the coal fired power plant at Dürnrohr was carried out in the past [Stoifl, 2000]. Figure 1-3 shows the available amount of straw over the last decades in Austria.

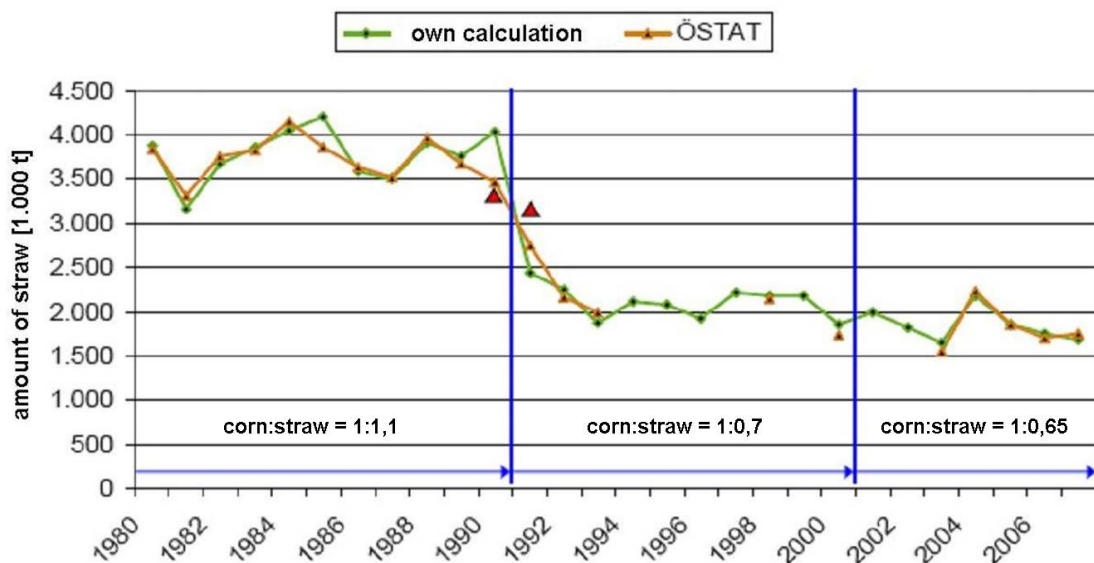


Figure 1-3: Available amounts of straw 1980 – 2007 [Haslinger et Wopienka, 2009]

Figure 1-4 shows the development of the straw and corn yields and the covered acreage over the years.

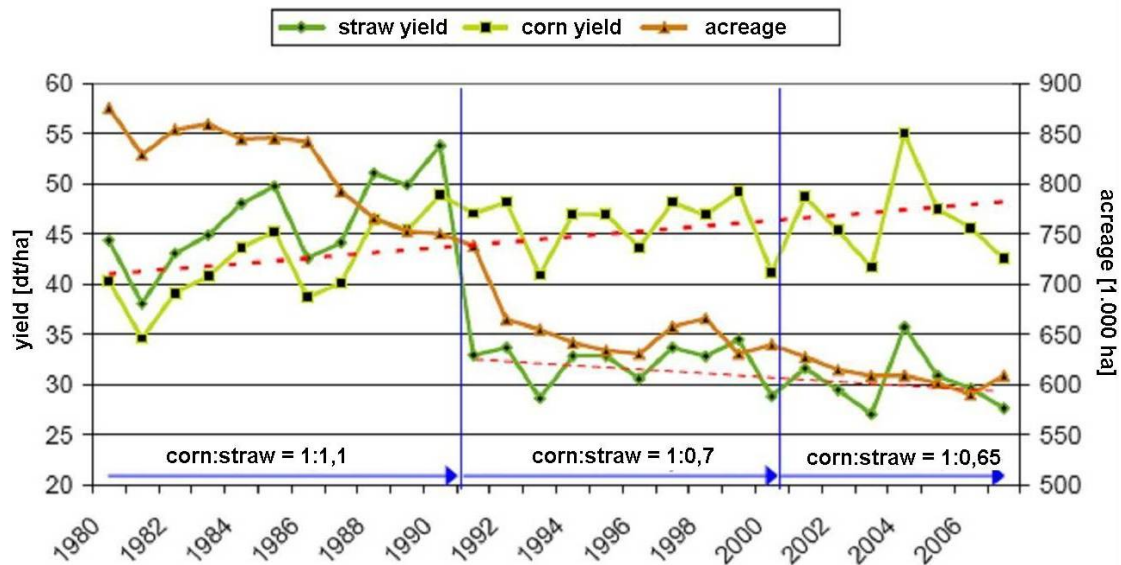


Figure 1-4: Acreage, straw- and corn yields 1980 – 2007 [Haslinger et Wopienka, 2009], dt/ha = 0,1 t/ha

Beside the already discussed straw, a huge variety of other agricultural wastes are available within the agricultural crop and animal production like olive stones, residues from the vegetable production, peels, shells, and husks [Kaltschmitt et Bridgwater, 1997].

## 2 Theoretical background

### 2.1 Biomass composition

The dry matter of green plants consists about 90 % of carbon and oxygen and about 6 per cent of hydrogen. These elements are absorbed by the vegetable in the atmosphere in form of carbon dioxide ( $\text{CO}_2$ ), oxygen ( $\text{O}_2$ ), water ( $\text{H}_2\text{O}$ ) or  $\text{HCO}_3^-$ . The plants contain some more elements than carbon, oxygen and hydrogen. They are called plant nutrients and depending on the demanded amount of them, they are subdivided into macro nutrients and micro nutrients. The main macro nutrients, which can be found in plants in an amount of up to 5 per cent of its dry matter, are nitrogen (N), potassium (K), and calcium (Ca). Furthermore, phosphorus (P), magnesium (Mg) and sulphur (S) are macro nutrients. The micro nutrients are boron (B), manganese (Mn), copper (Cu), zinc (Zn) and molybdenum (Mo). They can be found in a concentration from 0.001 to 0.03 per cent in the dry matter of plants. Iron (Fe) can be dedicated to the macro or to the micro nutrients [Hofbauer, 2008].

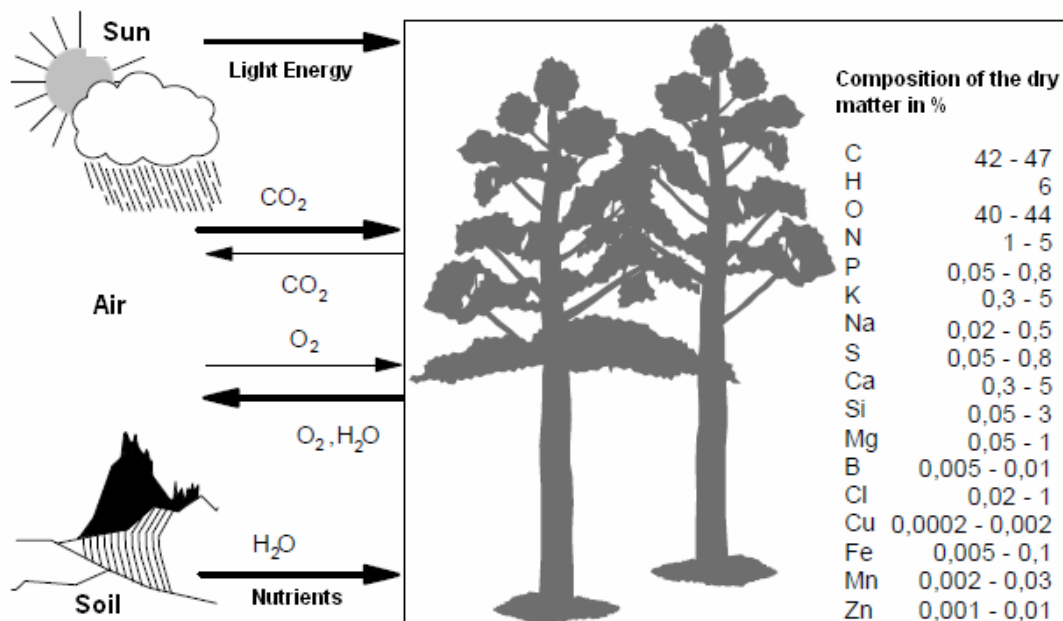


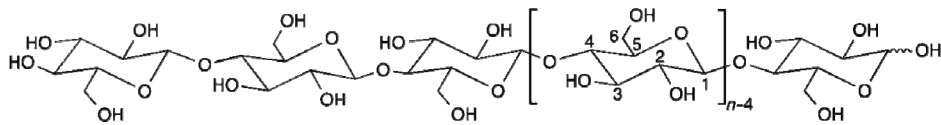
Figure 2-1: Formation and composition of biomass, adapted [Hofbauer, 2008]

The main carbon containing components of biomass are cellulose, lignin and hemicellulose. Furthermore biomass contains extractives and ash. A composition of various biomasses is displayed in Table 2-1.

Table 2-1 Composition of various biomasses in wt. % [Hofbauer, 2008]

	Cellulose	Hemicellulose	Lignin	Extractives/ashes
Hardwood	40-42	30-35	20-22	2-3
Softwood	40-43	21-23	27-28	3-5
Annual crops	38-42	25-30	15-21	5-10

Cellulose consists of a long polymer of glucose ( $\beta$ -D-Glucose,  $\beta$ -1,4 linked) without branches (Figure 2-2). The macromolecules contain between 2000 and 15000 repeating glucopyranose units. Cellulose is a structural substance in plant cells and the most common macromolecule in nature.

Figure 2-2: Cellulose structure ( $n$ = degree of polymerization) [Klemm, 2005]

Hemicellulose contains many different sugar monomers, including xylose, mannose, galactose, rhamnose and arabinose. The, in contrary to cellulose, branched hemicellulose consists of 300-5000 sugar units. Hemicellulose supports the cell membrane in addition it also seals the cell walls.

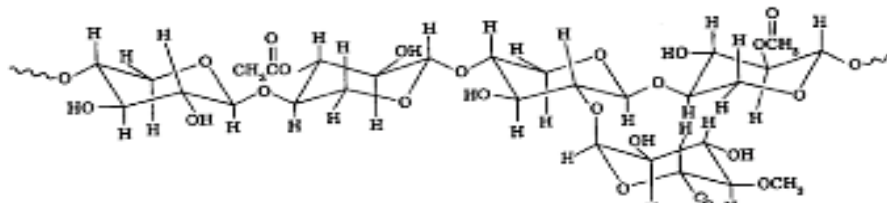


Figure 2-3: Hemicellulose structure [Unger et Ising, 2002]

Lignin is a large, cross-linked racemic macromolecule. The molecule consists of various substructures, like *p*-coumaryl alcohol, coniferyl alcohol and sinapyl alcohol (Figure 2-4), which appear to repeat in a haphazard manner. As a major cell wall component, lignin provides rigidity, internal transport of water and nutrients and protection against attack of micro organism. Caused by the chemical nature of the lignin, it is practically impossible to extract lignin in pure form (Figure 2-5) [Buranov et Mazza, 2008].

Figure 2-6 shows a tentative chemical structure of wheat straw lignin [Sun et al., 1997].



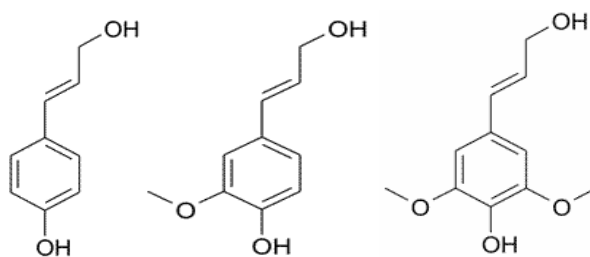


Figure 2-4: Structure of p-coumaryl alcohol, coniferyl alcohol and sinapyl alcohol [Steen, 2011]

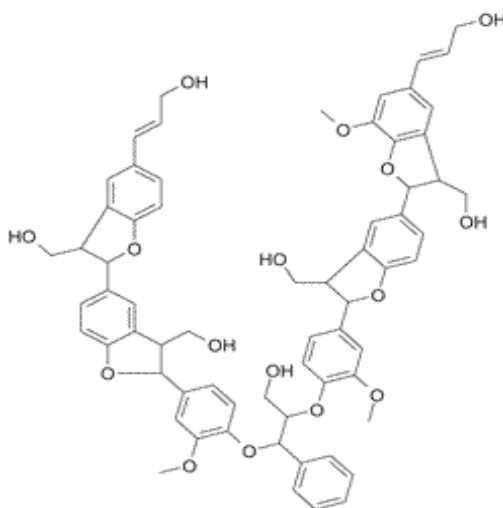


Figure 2-5: Possible structure of lignin [Steen, 2011]

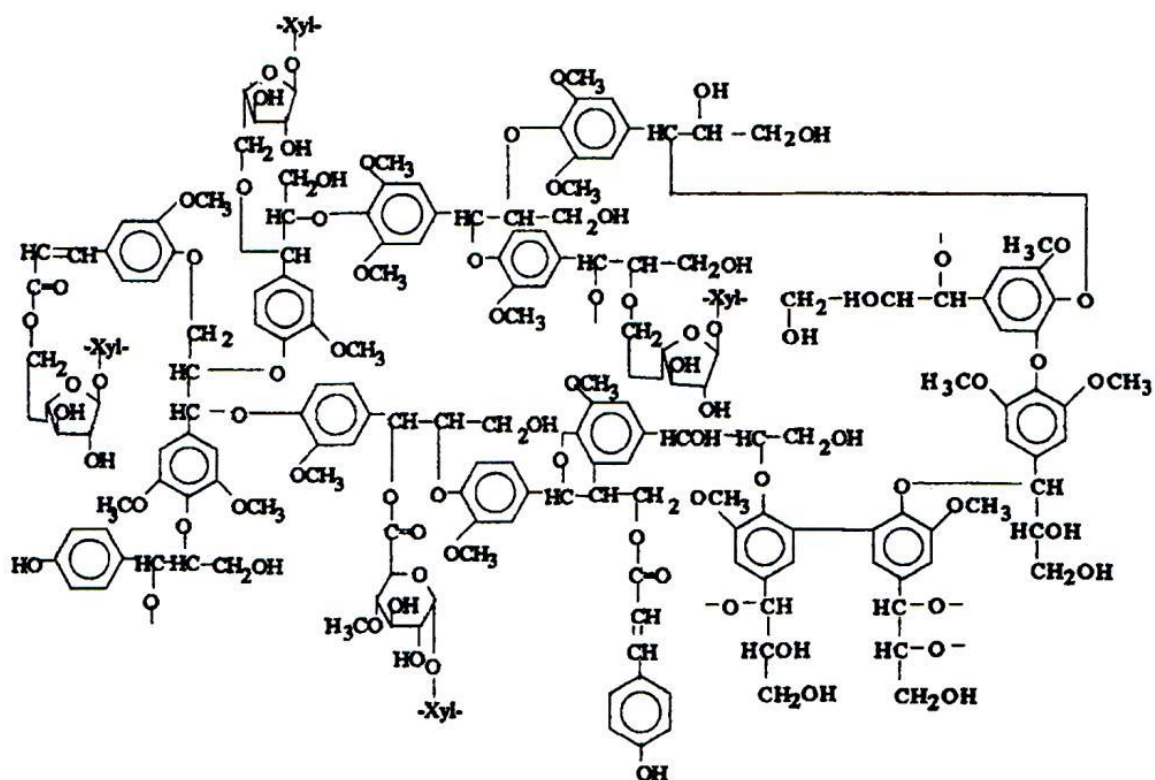


Figure 2-6: A tentative chemical structure of wheat straw lignin [Sun et al., 1997]

## 2.2 Energetic use of biomass

Depending on the type of biomass and the desired form of energy, there are many different technologies available. In addition with the traditional combustion of solid biomass for heat production, there is the possibility of transforming the solid biomass into solid, liquid or gaseous secondary energy sources, in which a reevaluation takes place on one or more of the following characteristics:

- Energy density
- Handling
- Storage- and transport characteristics
- Compatibility of environment
- Potential of fossil fuel substitution
- Usability of residua

The desire of the energy conversion of biomass is to obtain useful products. The choice of the conversion process depends on the type and quantity of biomass feedstock, the desired form of energy, end use requirements, environmental standards and economic conditions.

The three main processes to convert biomass into energy are thermo-chemical processes and bio-chemical processes [Goyal et al., 2008]. The different thermo-chemical processes include combustion, gasification, liquefaction, hydrogenation and pyrolysis. Bio-chemical processes are aerobic and anaerobic decomposition, which include the alcoholic and methane fermentation. Finally, physico-chemical processes summarize processes such as extraction of oilseeds to produce biodiesel.

In Figure 2-7 these main biomass conversion options are displayed and further more the most frequently used conversion steps into secondary energy is shown.

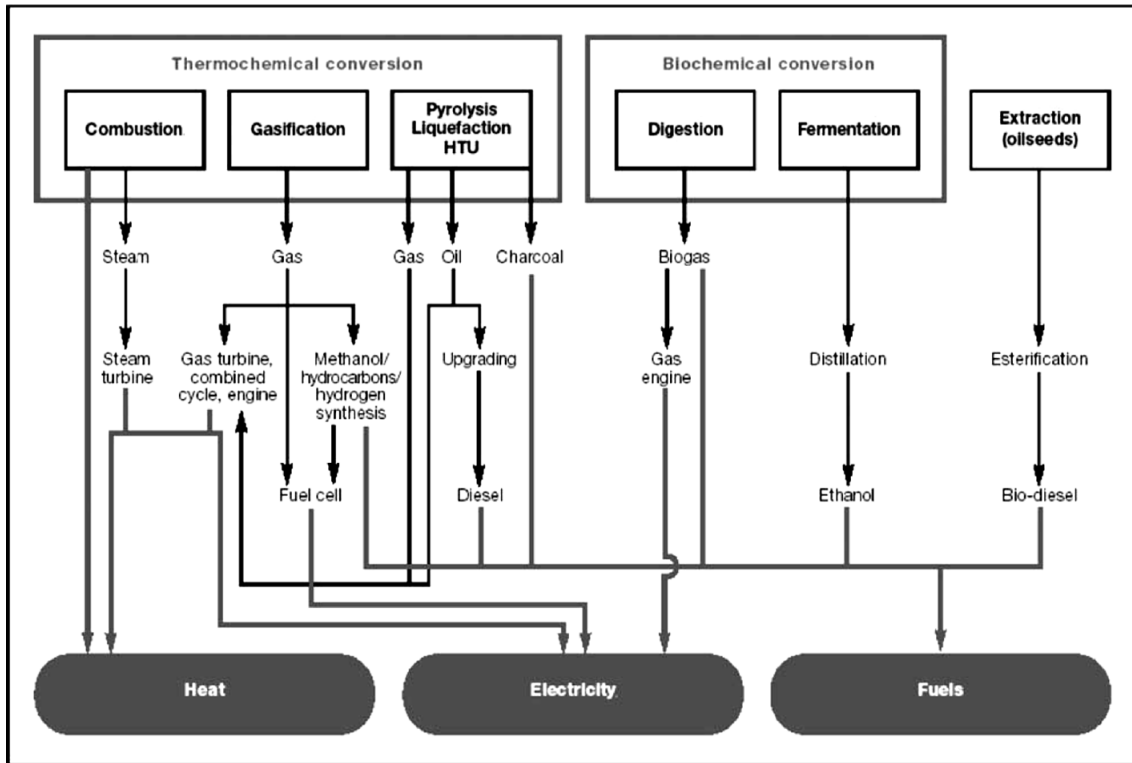


Figure 2-7: Main conversion options for biomass to secondary energy carriers (HTU= hydro thermal upgrading) [Faaij, 2006]

### 2.2.1 Thermo-chemical conversion

In thermo-chemical conversion processes, solid biomass is transformed due to the influence of heat into solid, liquid or gaseous secondary energy sources. The aim of the conversion processes is the supply of secondary energy sources whose properties can be well defined.

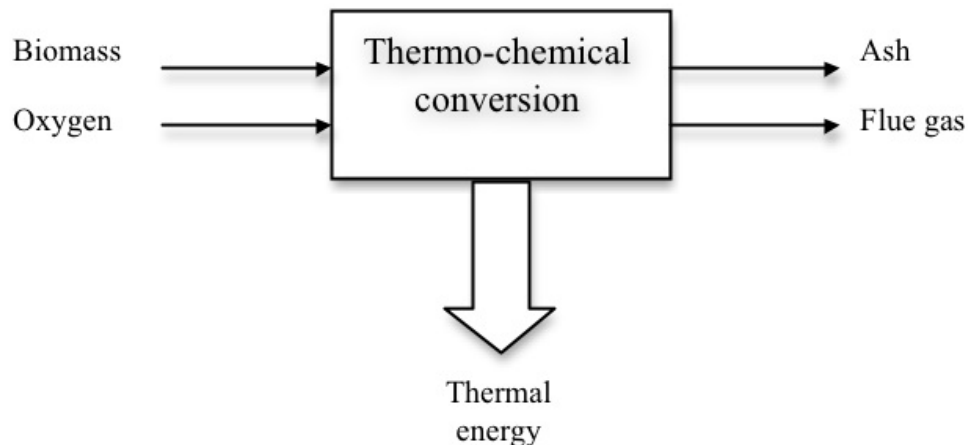


Figure 2-8: Principle of a complete thermo-chemical conversion of biomass, adapted [Kaltschmitt et al., 2009]

#### **Combustion**

The combustion of biomass, e.g. wood, is the oldest principle of thermal biomass conversion. The biomass is directly burned in presence of air ( $\lambda > 1$ ) to convert chemical energy stored in biomass into heat, mechanical power, or electricity. Combustion can be divided into different physical and chemical steps, like heating, drying (100-150 °C), pyrolysis (250-500 °C), gasification of solid carbon to carbon monoxide (above 700 °C) followed by an oxidation of flammable gases to carbon dioxides (from 900-1500 °C) and finally the heat output which has to be used immediately for heat and/or power generation [Kaltschmitt et al., 2009].

#### **Gasification**

The gasification of biomass is a process at high temperatures where the biomass is converted into flammable gases, which are called producer gas or synthesis gases. The gasification process is operated under oxygen deficiency conditions ( $\lambda < 1$ ) with a gasification agent that contains oxygen, like water or air. Under these conditions the carbon stored in the biomass is oxidised mainly to carbon monoxide and carbon dioxide and the required heat to keep the process going must be provided by reaction with free oxygen ( $O_2$ ). This

gasification process is called autothermal gasification. In case of allothermal gasification heat is indirectly delivered through a heat exchanger or heat carrier (e.g. circulating bed material). As gasification agent steam can be used which leads to a hydrogen rich and nitrogen free producer gas. The composition of the product gas in general depends on the biomass feedstock, temperature, residence time, pressure and the gasification medium. The out coming low calorific gas from e.g. air gasification can be used in gas engines or gas turbines for power generation. The producer gas from autothermal gasification with pure oxygen or from allothermal gasification can be transformed to gaseous or liquid secondary energy sources like methanol, methane, bio dimethyl ether, Fischer Tropsch diesel or bio hydrogen [Kaltschmitt et al., 2009].

### **Pyrolysis**

Pyrolysis is the decomposition of organic compounds by thermal energy in the absence of oxygen ( $\lambda = 0$ ). It happens at temperatures above 200 to 300 °C in an inert atmosphere. During normal operation, pyrolysis gases and pyrolysis oil are produced and a solid residue with rich carbon content is left back. The shares of the products and their properties are determined by the process conditions. Pyrolysis oil can be used as a fuel for boilers, diesel engines or gas turbines. Furthermore, the products of the pyrolysis process could be used for several conversion processes [Kaltschmitt et al., 2009].

### **Liquefaction**

The processes that are able to convert solid biomass into liquid secondary energy sources are called liquefaction processes. Generally, this happens as a result of thermo-chemical conversion processes with a focus on production of liquid secondary energy sources. In most cases liquid is obtained by thermo-chemical conversion at low temperatures (250-320 °C) and high pressures (5-20 MPa) using a catalyst in the presence of hydrogen. [Demirbas, 2000] Liquefaction can happen in one single step (e.g. flash pyrolysis) or during more steps (e.g. Fischer-Tropsch synthesis) [Kaltschmitt et al., 2009].

### **Carbonisation**

Carbonisation is also a thermo-chemical conversion process. During the carbonisation, the process parameters are controlled in the way to maximise the production of solid products (e.g. wood charcoal) [Kaltschmitt et al., 2009].

### 2.2.2 Bio-chemical conversion

The technology to convert biomass into secondary energy sources by micro organisms is called bio-chemical conversion.

Biomass that contains e.g. sugar or starch can be converted into ethanol by alcoholic fermentation and the ethanol is then separated from the mash by distillation. The ethanol can be used as a fuel for Otto engines or it can be burned for heat and/or power production.

Biogas, which contains up to two thirds of methane, can be produced from biomass by anaerobic decomposition through certain single cell micro bacteria. The biogas can be used as a fuel in gas engines or gas burners. After suitable preparation to natural gas quality, the biogas can be fed into the gas grid as synthetic natural gas. The other way of biomass decomposition is the aerobic decomposition, whereas single cell micro bacteria oxidise the biomass with oxygen from air. This process is called composting [Kaltschmitt et al., 2009].

### 2.2.3 Physical-chemical conversion

A physical chemical conversion process of biomass is for example the production of vegetable oil. The source is a plant that contains oil, whose liquid oil phase has to be separated from the solid part of the plant. This can be done by mechanical squeezing or by extraction. The oil of the oily seed or the oily press cake is extracted with a solvent and after the extraction oil and solvent are separated again via distillation. The solid residue can be used as feeding stuff and the oil can be used natural or treated (e.g. RME) as a fuel for several diesel engines or in a combined heat and power station (CHP) [Kaltschmitt et al., 2009].

## 2.3 Pyrolysis of biomass

Pyrolysis is the decomposition of organic compounds by thermal energy. It happens at temperatures above 300 °C for wood in an inert atmosphere. During normal operation, pyrolysis gases and pyrolysis oil are produced, and a solid residue with high carbon content is left [Kaltschmitt et al., 2009]. The shares of the products and their properties are determined by the process conditions. Pyrolysis oil can be used as a fuel for boilers, diesel engines, gas turbines and Stirling engines. Furthermore, the products of pyrolysis can be converted into other products like chemicals from pyrolysis oil [Czernik et Bridgwater, 2004]. The progress of thermo-chemical conversion of biomass can be split into separate sub-areas that are restricted by temperature and air ratios. Depending on the process parameters, they may happen in parallel or independently of each other. As is shown in Figure 2-9 and in Equation 2-1, the sub-processes are characterized by the excess air ratio  $\lambda$  that is defined as the amount of air used in the process in relation to the amount of air needed for a complete stoichiometric reaction [Kaltschmitt et al., 2009].

$$\lambda = \frac{\dot{m}_{air}}{\dot{m}_{air,stoichiom.}} \quad (2-1)$$

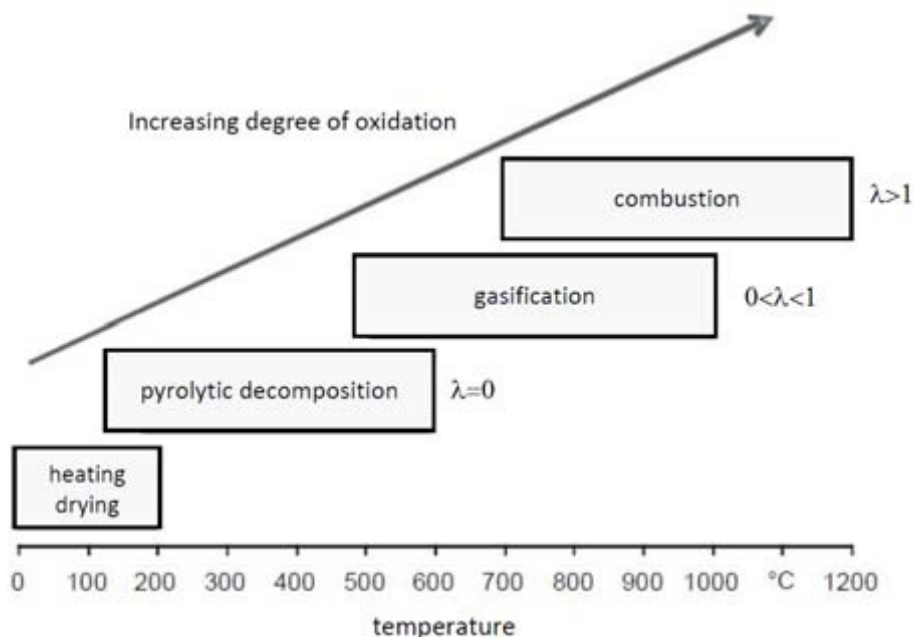


Figure 2-9: Sub-processes of combustion, adapted [Kaltschmitt et al., 2009]

Up to 220 °C the water, which is in the porous structure of the solid biomass free and latent, evaporates. This is an endothermic process. Until most of the water in the solid biomass has been evaporated, the temperature does not rise significantly as a consequence of the high enthalpy of evaporation. The process of heating, drying and pyrolytic decomposition is shown in Figure 2-10 [Kaltschmitt et al., 2009].

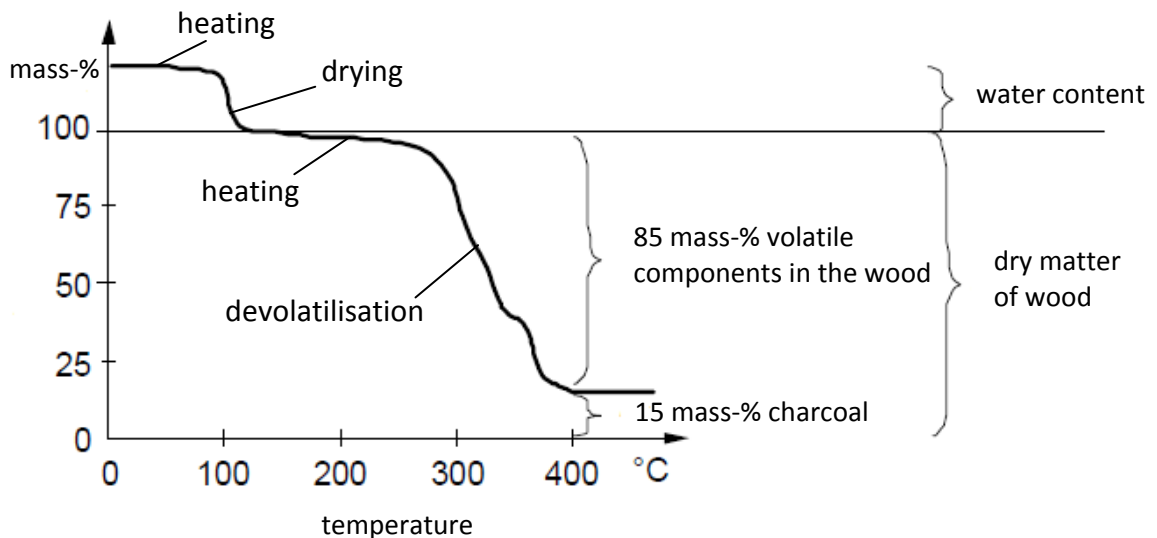


Figure 2-10: Thermal behaviour of wood during heating without oxygen [Kaltschmitt et al., 2009]

Figure 2-10 shows if the pyrolytic decomposition is largely completed at temperatures of around 500 °C, a solid residue, which consists predominantly of carbon and ash remains. In general, about 80 to 85 % of the organic material is converted into gaseous products by pyrolytic decomposition [Rüdiger, 1997].



### 2.3.1 Pyrolysis mechanisms and pyrolysis reaction kinetics

Up to now there are no standard results for the decomposition processes of lignin, cellulose and hemicellulose available. Most of the knowledge exists of the thermal decomposition of cellulose because it is the major part of the wood and cellulose is not that complex than hemicellulose or lignin [Bridgwater et al., 1999].

Biomass is generally composed of three main groups of natural polymeric materials: cellulose, hemicellulose and lignin. Other typical components are grouped as "extractives" (generally smaller organic molecules or polymers) and minerals (inorganic compounds). These are present in differing proportions in different biomass types and these proportions influence the product distributions on pyrolysis [Antal and Grønli, 2003], [Brown, 2009], [Mohan et al, 2006].

The variance in the yields of the various classes is attributable to several factors, the most important of which are [Bridgwater et al., 2003]:

- Feedstock (e.g. cellulose, hemicellulose and lignin content)
- Pyrolysis conditions (e.g. particle size, temperature, residence time)

On heating to pyrolysis temperatures the main components contribute to product yields broadly as follows [Antal and Grønli, 2003]. Primary products of hemicellulose and cellulose decomposition are condensable vapours (hence liquid products) and gas. Lignin decomposes to liquid, gas and solid char products. Extractives contribute to liquid and gas products either through simple volatilisation or decomposition. Minerals in general remain in the char where they are termed ash. This distribution of components into products is shown schematically in Figure 2-11.

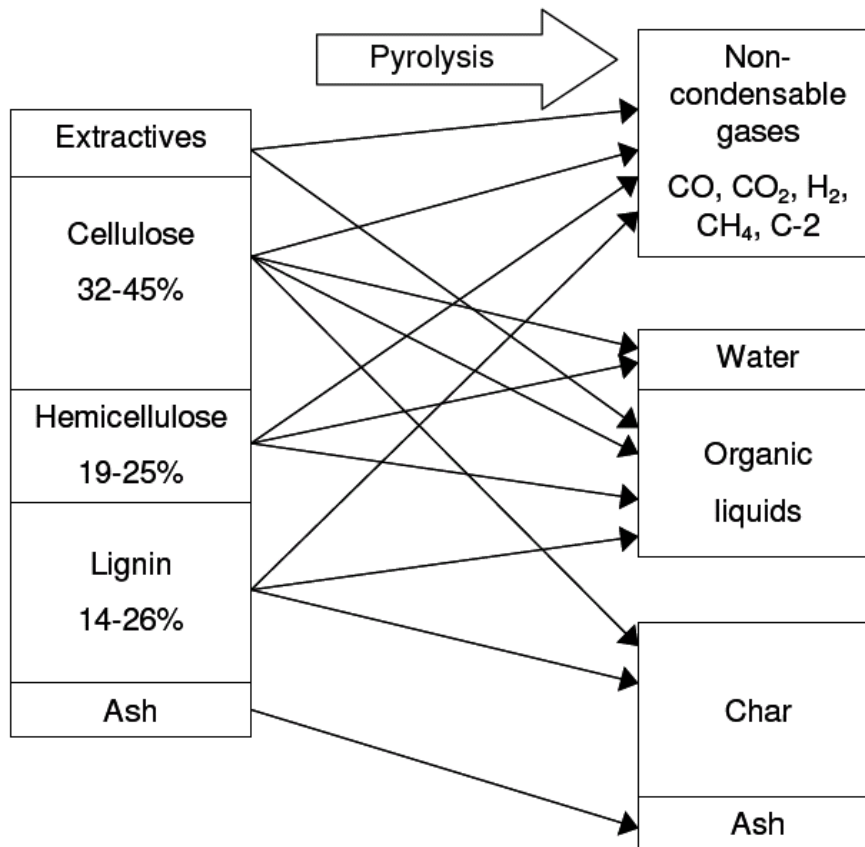


Figure 2-11: Simplified representation of biomass pyrolysis [Brownsort, 2009]

Figure 2-12 shows an example of the pyrolytic degradation of dry beech wood. The pyrolytic decomposition of organic matter in this example starts at about 200 °C with the formation of water (H<sub>2</sub>O), carbon dioxide (CO<sub>2</sub>), carbon monoxide (CO) and methanol (CH<sub>3</sub>OH). In the range of 320 to 340 °C for approximately 30 per cent of the wood substance has been degraded. More hydrocarbon compounds are formed, which condense at room temperature and ambient pressure and are then obtained as pyrolysis oil. As already mentioned all lignocellulosic biomass consist mainly of cellulose, hemicellulose and lignin.

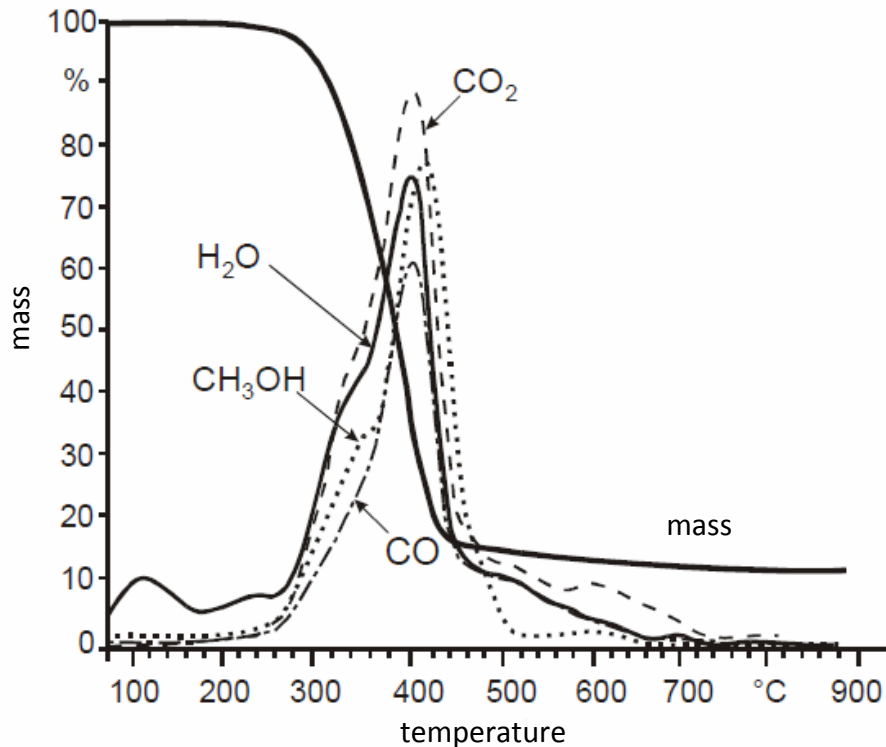


Figure 2-12: Thermal decomposition of wood, adapted [Kaltschmitt et al., 2009]

These different components decompose at different temperatures. For example, all the curves in Figure 2-12 show a shoulder at temperatures ranging from 320 to 350 °C the maximum of the decomposition of hemicellulose. From this temperature the contribution from the pyrolytic decomposition products of hemicellulose decreases. The maxima in the gases and vapors at about 400 °C, equivalent to about 70 per cent weight loss, mark the maximum of the cellulose degradation, which is completed at about 450 °C.

The small amounts of measurable substances above 450 °C derived from the decomposition of lignin which occurs over a wide temperature range. In Figure 2-12 this decomposition of lignin is finished at a temperature of 700 °C.

The mass fractions of gaseous decomposition products are thus determined by the biomass components, cellulose, hemicellulose and lignin. Therefore, Figure 2-13 shows the pyrolytic decomposition of these three components, and additionally those of wood. The course of the pyrolytic decomposition of wood could be summed up by the gradient of the individual single components. Consequently no significant interactions between the individual wood components during the pyrolytic decomposition occur.

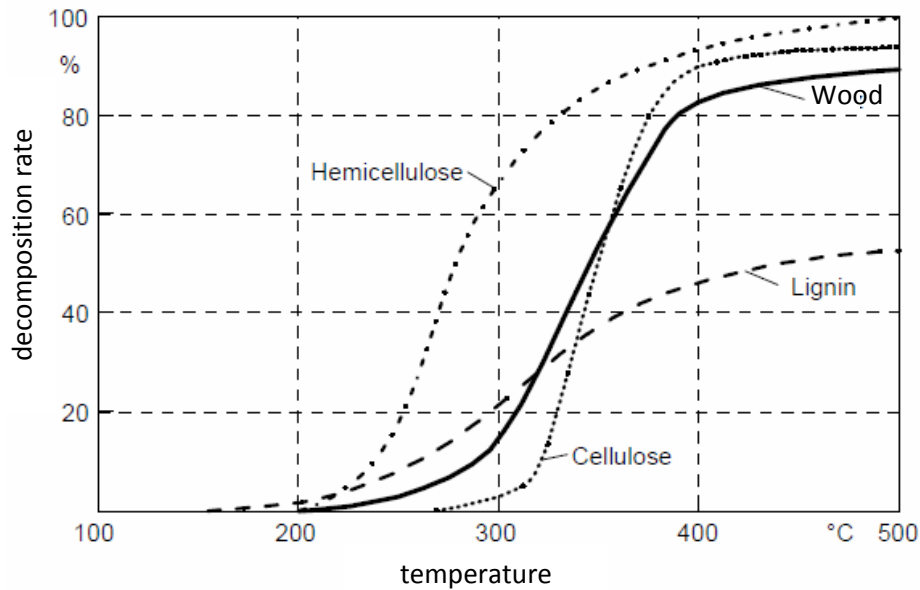


Figure 2-13: Thermal decomposition of wood into cellulose, hemicellulose and lignin, adapted [Kaltschmitt et al., 2009]

Figure 2-13 shows that charcoal is initially formed from lignin, since it is degraded during the pyrolytic decomposition to only about 60 %. The behaviour of the pyrolytic decomposition of grass and straw differs only very slightly from that of wood [Kaltschmitt et al., 2009].

Depending on the conditions under which the pyrolytic decomposition is realized, the cleavage reactions can occur differently. In the production of charcoal - a "classical" pyrolytic conversion of wood - the following phases could be distinguished:

The production of charcoal is a classical pyrolytic process that can be divided into four sections [Yang et al., 2007]:

In the first section, the solid biomass is heated up and dried at temperatures of up to 220 °C. Larger quantities of steam and small amounts of carbon dioxide (CO<sub>2</sub>), acetic acid and formic acid discharge along the way.

During step two the pyrolytic decomposition starts and releases the major parts of carbon dioxide (CO<sub>2</sub>), acetic acid and formic acid at temperatures up to 280 °C. This process is like step one an endothermic process and most of the produced gases are not flammable.

Step three occurs in the temperature range from 280 °C to 500 °C. In this process step flammable gases like carbon monoxide (CO), methane (CH<sub>4</sub>), formaldehyde (CH<sub>2</sub>O), acetic acid (C<sub>2</sub>H<sub>4</sub>O<sub>2</sub>), formic acid (CH<sub>2</sub>O<sub>2</sub>), methanol (CH<sub>3</sub>OH) and hydrogen (H<sub>2</sub>) are built during a strong exothermic reaction. If the feedstock is wood, the reaction releases a heat quantity of 880 kJ per kg wood.

The produced, invisible gases escape the wood matrix very fast, so the gas stream carries small droplets of condensable organic compounds. The residue of this process is charcoal that changes its structural composition to a crystalline configuration at 400 °C [Kaltschmitt et al., 2009].

The following reactions after the exothermic reactions of step three are only endothermic processes. During step four the gases are cracked by passing through the charcoal at temperatures above 500 °C. Mainly combustible gases like carbon monoxide (CO) and hydrogen (H<sub>2</sub>) are formed.

### **Pyrolysis of cellulose**

Pyrolysis of cellulose is a complex process with several reactions. Up to now, many kinetic models for the pyrolysis process of cellulose have been investigated [Bradbury et al., 1979], [Piskorz et al., 1988], [Banyasz et al., 2001], [Luo et al., 2004]. The pyrolysis of cellulose is characterized by a decreasing polymerization grade by splitting glycolic compounds between the glucose units by heat. The thermal degradation of cellulose happens by two types of reactions that proceed in parallel and are influenced by parameters like the temperature, heating rate or ash content of the biomass [Shafizadeh, 1982]. The starting material for these two parallel reactions is made by an intermediate pre-reaction that produces an unstable, reactive form of cellulose called "active cellulose" [Bradbury et al., 1979]. One of the two processes is a gradual degradation, dehydration, decarboxylation and charring upon heating at temperatures less than 300 °C. During this step, char, non-condensable gases like carbon dioxide and carbon monoxide and water vapour are produced. The second process includes depolymerization and cleavage. It is a rapid volatilization accompanied by the formation of levoglucosan, which further leads to condensable gases and tar, upon pyrolysis at higher temperatures. If the condensable vapours produced by this reaction are not removed immediately out of the hot reactor, they can be cracked by a secondary reaction into char and gas. This reaction is undesired in the production of liquid products by fast pyrolysis [Bradbury et al., 1979], [Shafizadeh, 1982], [Shafizadeh et Fu, 1973], [Demirbas, 2000], [Antal et Varhegyi, 1995]. The activation energy for the depolymerization reaction at higher temperatures is the highest, followed by the dehydration reaction that occurs at lower temperatures and the secondary cracking of the condensable gases which has the lowest activation energy [Basu, 2010]

Figure 2-14 shows the dissociation mechanisms of cellulose. The transglycosylation leads by intramolecular substitution of the glycosidic bond

through the free hydroxyl groups to the elimination of water and thus to the formation of monomeric and oligomeric anhydrosugars (e.g. levoglucosan, cellobiosan). These anhydrosugars may additionally split water, which then leads ultimately to the formation of tar and char [Richards, 1988], [Shafizadeh, 1982]. The cyclo- and aldol-reversion causes a ring cleavage and leads to the formation of low molecular fragments such as acetaldehyde, acetol, hydroxyacetaldehyde, ethanedial, furfural and furanone.

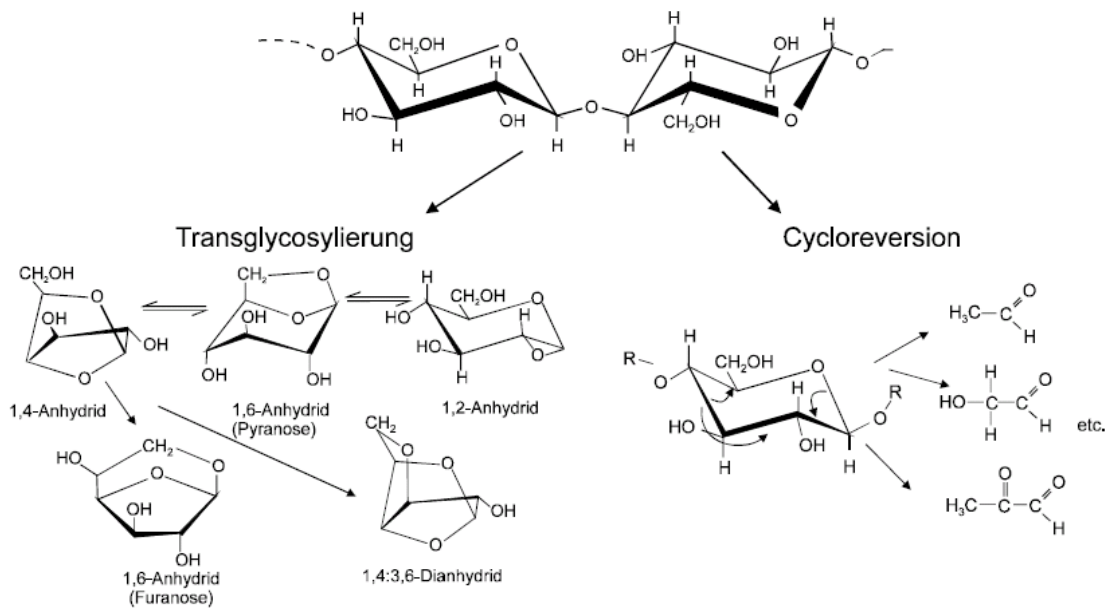


Figure 2-14: Dissociation mechanisms of cellulose [Faix et al., 1988]

The products of cellulose decomposition can vary noticeably depending upon reaction conditions. Figure 2-15 illustrates the detailed reaction mechanism proposed by Mok and Antal [Mok et Antal, 1983].

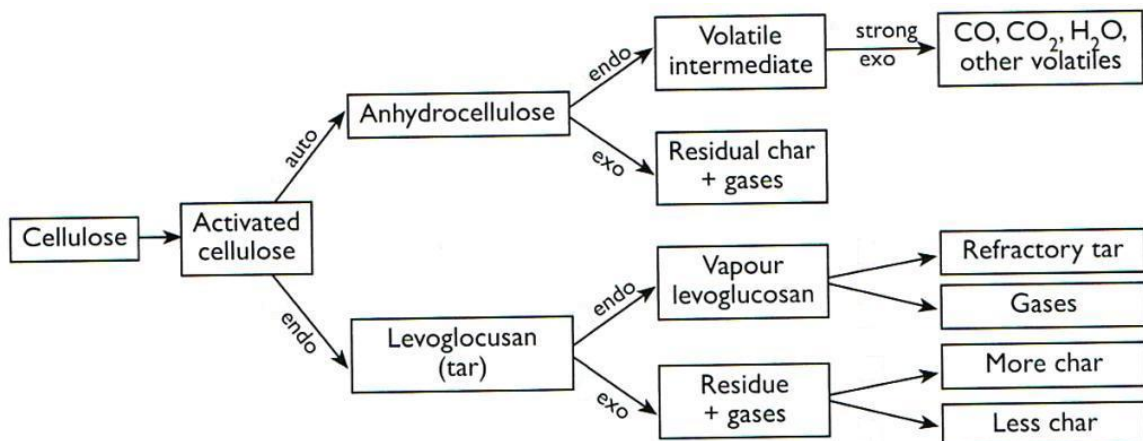


Figure 2-15: Reaction pathways for cellulose decomposition [Mok et Antal, 1983]

Cellulose decomposition includes both an exothermic pathway via anhydrocellulose and an endothermic pathway via levoglucosan. The anhydrocellulose pathway yields char and non-condensable gases in a process that is overall exothermic, but it occurs at extremely slow heating rates making this pathway of little practical importance. The levoglucosan (anhydroglucose) pathway is an endothermic devolatilisation process that can lead to either predominately tarry vapours or char at the final product. A combination of temperature, residence time and naturally occurring catalysts in biomass determine the extent of secondary reactions, which yield a wide variety of organic compounds, including aldehydes, ketones, carboxylic acids, alcohols, and anhydrosugars from cellulose pyrolysis [Mohan et al, 2006].

Another mechanism for pyrolysis of cellulose is proposed by Piskorz et al. [Piskorz et al., 1988] who proposed a modified version of the mechanism by Bradbury et al. [Bradbury et al., 1979]. The initial stage takes into account the competitive formation of char (with carbon dioxide and steam), which is again favored by low temperatures, and a rapid reduction in the degree of polymerization associated with the formation of active cellulose. Successively, a further competition is established between two pathways. The first is ring fragmentation (decarbonylation, dehydration) with the formation of hydroxyacetaldehyde (and other products including formic acid, acetic acid, glyoxal, methylglyoxal, etc.), which is favoured by high temperatures and catalyzed by metallic compounds. The low-temperature process, favoured by the absence of impurities in the substrate, is depolymerization by transglycosylation with the formation of levoglucosan, cellobiosan (and other sugars, such as glucose, fructose) in high yields. Possible decomposition of cellobiosan is indicated as the major route for formaldehyde production.

Figure 2-16 shows the mechanism of cellulose pyrolysis proposed by Banyasz et al. [Banyasz et al., 2001], [Banyasz et al., 2001] which differs from the mechanism proposed by Piskorz et al. [Piskorz et al., 1988] only in the way that the formation of hydroxyacetaldehyde occurs through the formation of reaction intermediates.

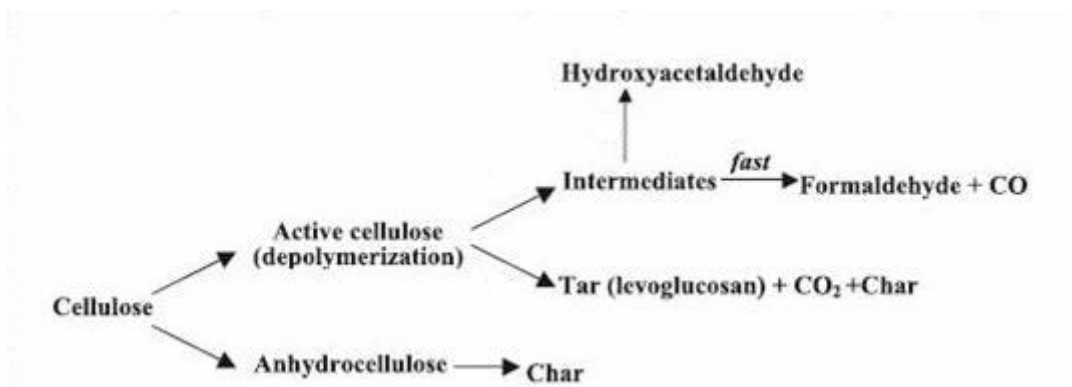


Figure 2-16: The mechanism of cellulose pyrolysis proposed by Banyasz et al. [Banyasz et al., 2001], [Banyasz et al., 2001]

### Pyrolysis of hemicelluloses

In contrast to cellulose, which is a homopolysaccharide, hemicelluloses are heteropolysaccharides. The monomeric components of hemicellulose are primarily D-glucose, D-mannose, D-galactose, D-xylose, L-arabinose but to some extent it can be L-rhamnose in addition to D-glucuronic acid, D-galacturonic acid and 4-O-methyl-D-glucuronic acid.

Hemicellulose is an inhomogenous glycan composed of two or more kinds of monosaccharide and has short side chains, which are cracked first during pyrolysis. Then, polymer chain depolymerization and intramolecular dehydration condensation occurred subsequently. Therefore, hemicellulose is thermal unstable [Wu et al., 2009]. Hemicellulose is the first to decompose beginning at 220 °C and substantially completed at 315 °C [Yang et al., 2007].

Pyrolysis products of hemicellulose include non-condensable gases (primarily CO, CO<sub>2</sub>, H<sub>2</sub> and CH<sub>4</sub>), low molecular weight organic compounds (carboxylic acids, aldehydes, alkanes and ethers), and some water [Rutherford et al., 2004]. Some of these compounds can be recovered in commercially significant quantities. For example, both acetic acid and furfural have been manufactured by thermal processing of hemicellulose-rich biomass. On the other hand, heavy molecular weight (tarry) compounds are produced in relatively small amounts compared to pyrolysis of cellulose and lignin [Rutherford et al., 2004].

In Figure 2-17, the Py-GC/MS total ion chromatograms of hemicellulose at 260, 320, and 550 °C are shown. The pyrolysis products are listed in Table 2-2.



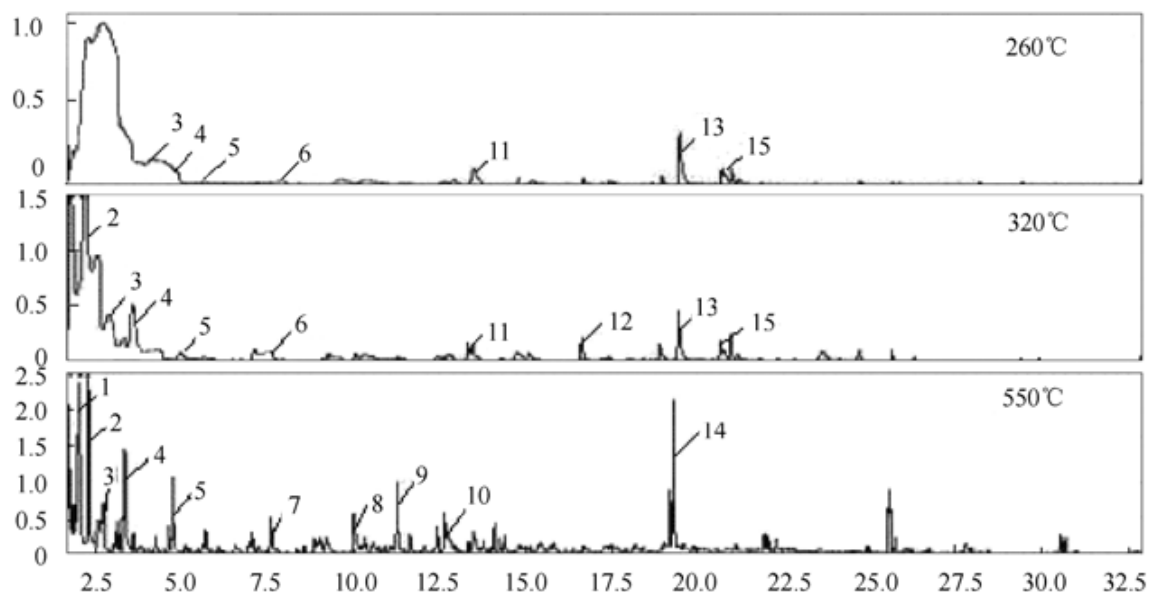


Figure 2-17: TIC chromatogram from Py-GC/MS of hemicellulose at different temperatures [Wu et al., 2009]

Table 2-2: Chromatographic peak identification of main pyrolysis products from hemicellulose [Wu et al., 2009]

Peak number	Compound	Formula	Area /%		
			260°C	320°C	550°C
1	2-butanone	C <sub>4</sub> H <sub>8</sub> O	-	-	4.41
2	acetic acid	C <sub>2</sub> H <sub>4</sub> O <sub>2</sub>	-	27.86	12.81
3	1-hydroxy-propanone	C <sub>3</sub> H <sub>6</sub> O <sub>2</sub>	10.54	8.66	13.98
4	1-hydroxy-2-butanone	C <sub>4</sub> H <sub>8</sub> O <sub>2</sub>	21.55	12.73	6.67
5	furfural	C <sub>5</sub> H <sub>4</sub> O <sub>2</sub>	2.30	2.00	5.52
6	4-hydroxy-3-hexanone	C <sub>6</sub> H <sub>12</sub> O <sub>2</sub>	3.21	7.60	-
7	cyclopentanedione	C <sub>5</sub> H <sub>6</sub> O <sub>2</sub>	-	-	2.49
8	2,4-dimethyl-pentanal	C <sub>7</sub> H <sub>14</sub> O	-	-	3.98
9	3-methyl-2-cyclopentanedione	C <sub>6</sub> H <sub>8</sub> O <sub>2</sub>	-	-	4.83
10	pentanal	C <sub>5</sub> H <sub>10</sub> O	-	-	3.20
11	4,5-dimethyl-4-hexenal	C <sub>8</sub> H <sub>14</sub> O	10.37	4.86	-
12	2,4,6-trimethyl-phenol	C <sub>9</sub> H <sub>12</sub> O	-	2.50	-
13	1-tert-butoxy-2-methylpropane	C <sub>8</sub> H <sub>18</sub> O	16.04	7.08	-
14	1,4-cyclohexadiene-1-carboxylic acid, methyl ester	C <sub>8</sub> H <sub>10</sub> O <sub>2</sub>	-	-	8.19
15	2,2-dimethyl- 3-pentanol	C <sub>7</sub> H <sub>16</sub> O	4.96	2.72	-

At 260 °C, the pyrolysis products include 1-hydroxy-propanone, 1-hydroxy-2-butanone, 4,5-dimethyl-4-hexenal, and 1-tert-butoxy-2-methylpropane. In comparison with the pyrolysis products at 260 °C, more pyrolysis products were found at 320 °C, such as acetic acid and 2,4,6-trimethyl-phenol. Moreover, 27 % of the pyrolysis products are in the form of acetic acid, which

is believed to be derived from the acetyl groups of hemicellulose [Gullu et Demirbas, 2001]. At 550 °C, the pyrolysis products are mainly composed of acetic acid, 1-hydroxy-propanone, 1,4-cyclohexadiene -1-carboxylic acid, and methyl ester, which accounts for 12.81 %, 13.98 %, and 8.19 % of the products, respectively.

### Pyrolysis of lignin

Lignin is one of the major constituents of biomass. Due to its three dimensional structure and its multitude of boundary types it is very complex to characterise its behaviour during pyrolysis.

For example, the pyrolysis of one lignin-trimer results in 42 different components [Vorher, 1976]. Figure 2-18 shows a typical example of thermal decomposition products from a lignin-dimer. Therefore, predominantly phenolic cleavage products are produced with different side chain conformations. The process starts at a temperature of 175 °C and ends at about 700 °C [Kaltschmitt et al., 2009]. This is the reason why the decomposition mechanisms of lignin can only be estimated. An overview about the kinetics of lignin pyrolysis is given in Radlein et al. [Radlein et al., 1991].

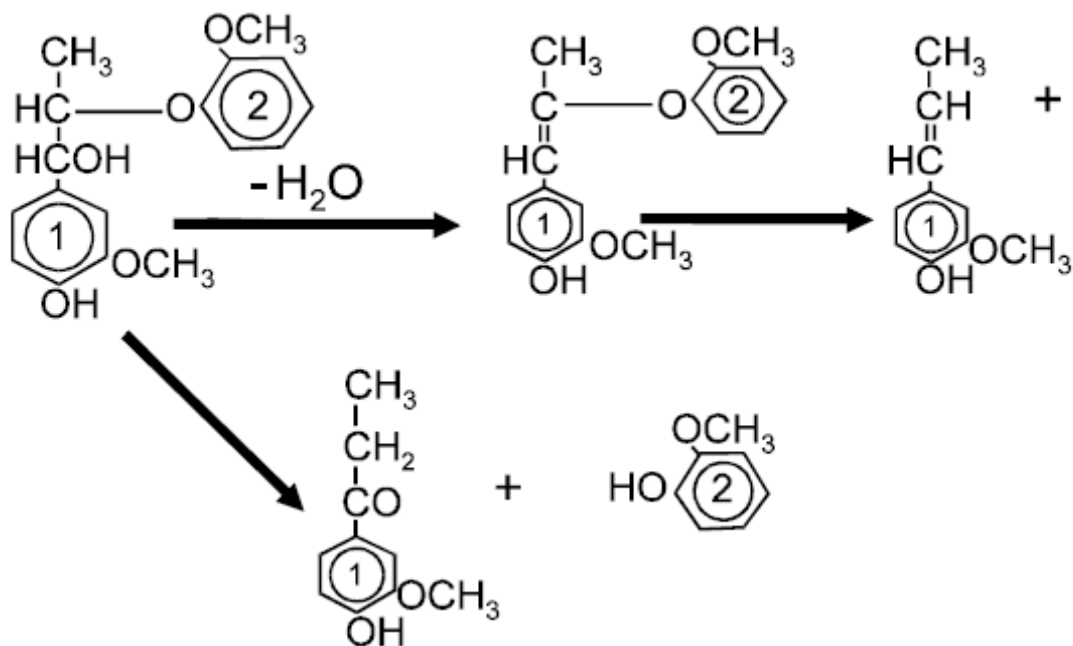


Figure 2-18: Typical products of thermal decomposition of lignin [Kaltschmitt et al., 2009]

Figure 2-19 shows a simplified kinetic scheme of the decomposition of lignin, with the main reaction paths. There are three parallel reactions possible during the process, each with a different rate constant  $k_1$ ,  $k_2$  and  $k_3$ . The activation energies rise from  $E_1$  to  $E_3$  ( $E_1 < E_2 < E_3$ ).

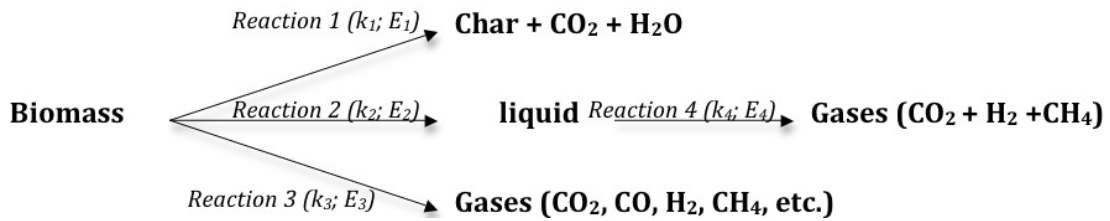


Figure 2-19: Typical reactions of a pyrolytic decomposition of lignin, adapted [Kaltschmitt et al., 2009]

Charcoal, carbon dioxide ( $\text{CO}_2$ ) and water are the products of reaction 1 ( $k_1$ ). This process works at low temperatures. Liquid products are a result of reaction 2 ( $k_2$ ) that happens at higher temperatures. In this temperature range flash-pyrolysis takes place and forms liquid energy sources and chemical raw materials. A further secondary crack-reaction ( $k_4$ ) is able to convert the liquid products to carbon monoxide, hydrogen and methane. If the temperature is still higher than at reaction 2 the biomass is converted into gaseous products which happens during reaction 3 ( $k_3$ ) [Kaltschmitt et al., 2009].

The products of pyrolysis of biomass that contain lignocelluloses are solid (charcoal), liquid (pyrolysis oil) and gaseous (pyrolysis gases). Their distribution is depending on the temperature of the thermal decomposition.

Table 2-3 summarises the wider and typical ranges for key variables and product yields.

Table 2-3: Typical yields of different pyrolysis technologies [Brownsort, 2009]

		Slow Pyrolysis	Intermediate Pyrolysis	Fast Pyrolysis
Feed		Scores of feeds reported		
Temperature, °C	Range	250 - 750	320 - 500	400 - 750
	Typical	350 - 400	350 - 450	450 - 550
Time	Range	mins - days	1 - 15 mins	ms - s
	Typical	2 - 30 mins	4 mins	1 - 5 s
Yields, % wt on dry				
Char	Range	2 - 60	19 - 73	0 - 50
	Typical	25 - 35	30 - 40	10 - 25
Liquid	Range	0 - 60	18 - 60	10 - 80
	Typical	20 - 50	35 - 45	50 - 70
Gas	Range	0 - 60	9 - 32	5 - 60
	Typical	20 - 50	20 - 30	10 - 30

There are two fundamental technologies for pyrolysis that can be distinguished, flash-pyrolysis and slow-pyrolysis. The operation purpose of flash-pyrolysis is the production of liquid secondary energy sources like pyrolysis oil. Slow-pyrolysis is mainly used for the production of charcoal or the torrefaction process.

## 2.4 Flash Pyrolysis

Fast-pyrolysis or flash-pyrolysis is a process in which biomass is heated up very fast in the absence of oxygen. During this process the biomass decomposes to generate mostly vapours and aerosols and some charcoal. The residence time of the biomass in the hot area has to be very short to prevent the products from secondary reactions. Usually the residence time is shorter than one second. After the pyrolysis process, the vapours are cooled down and condensed, so dark pyrolysis oil is formed [Bridgwater et Grassi, 1991].

The aim of the flash-pyrolysis is to maximise the yield of liquid products. To reach the right conditions it is important that the essential features of the flash-pyrolysis are satisfied.

This means that

- The biomass particle has to be heated up very fast. Heating rates of more than 1000 °C per second are required.
- The pyrolysis temperature has to be controlled carefully. In the vapour phase there is a temperature of about 500 °C with a short residence time of less than two seconds.
- The pyrolysis vapours have to be cooled down very fast after the hot reactor.

There are several types of flash pyrolysis technologies proposed in literature [Goyal et al., 2008]:

- *Flash hydro-pyrolysis* is flash pyrolysis done in hydrogen atmosphere. It is carried out at a pressure up to 20 MPa [Gercel, 2002].
- *Rapid thermal process* is a particular heat transfer process with very short heat residence times (between 30 ms and 1.5 s). It is done at temperatures between 400 and 950 °C. Rapid de-polymerization and cracking of feedstock takes place. Rapid heating eliminates side reactions, whereby, obtaining products with comparable viscosity to diesel oil [Funino et al., 1999].
- *Vacuum flash pyrolysis*: In this process, pyrolysis is done under vacuum. It limits the secondary decomposition reactions, which gives high oil yields and low gas yields [Pakdel et al., 1999].

### 2.4.1 Reactor types for flash pyrolysis

As it can be seen from the requirements above, the construction of the reactors for flash-pyrolysis is a big challenge. A lot of research concerning the design of several reactor types has been done during the last years to optimise heat transfer and mass transport. In the following chapters several important techniques and processes for flash-pyrolysis are discussed in more detail. This area has been extensively reviewed by Bridgwater [Bridgwater et al., 1999], [Bridgwater et Peacocke, 1999].

In general the reactors can be divided into [Bridgwater et Peacocke, 2000]:

- Fluidised bed reactors
  - Bubbling fluidised beds
  - Circulating fluidised beds
- Ablative reactors
  - Ablative reactor with rotating cone
  - Ablative reactor with rotating plate
  - Vortex reactor ablative reactor
- Vacuum pyrolysis

## Bubbling fluidised bed reactors

One of the big advantages using a bubbling fluid bed reactor for flash-pyrolysis is that construction and operation of this system are very simple. The reactor is principally the same as for other well known bubbling fluid bed processes. The heat carrier inside the reactor is sand that provides a constant temperature distribution in the fluidised bed and performs a very efficient heat transfer to the biomass particles due to high solids density. The heating of the process can be provided in several ways, for example it is possible to heat the sand in an external combustion chamber or a fluidised bed reactor and return the sand to the pyrolysis reactor. This reactor type for pyrolysis has also a good and consistent performance with high liquid yields (typically 70-75 wt. % from wood on a dry feed basis). The residence time of solids and vapours is controlled by the fluidising gas flow rate and it is higher for char than for vapours. The char acts as an effective vapour cracking catalyst at flash-pyrolysis, so a fast and effective char separation is very important. The high heating rates require small and dry particles of biomass, so the biomass has to be grinded to a size of 2-3 mm and dried before fed into the pyrolysis reactor [Bridgwater, 2003]. Pyrolysis vapours exiting the cyclone are quenched and bio-oil is obtained. After the quenching step a electrostatic precipitator is installed to extract the droplets from the export gas.

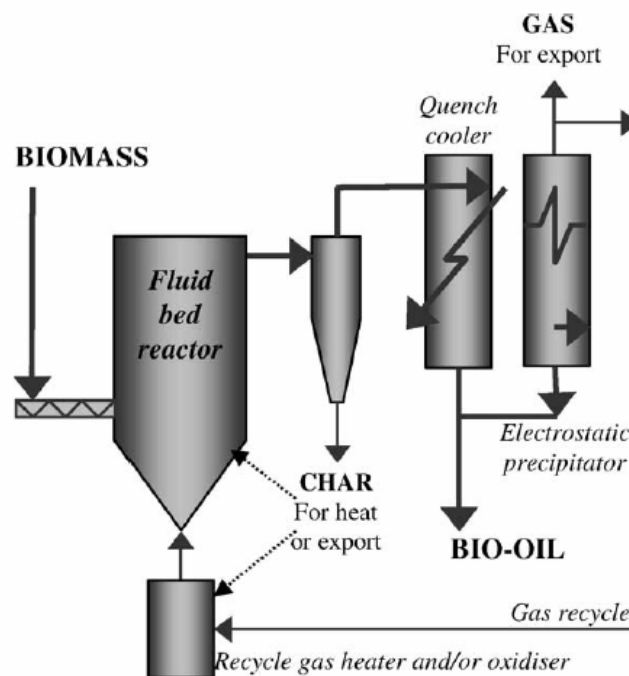


Figure 2-20: Bubbling fluid bed reactor [Bridgwater, 2003]

## Circulating fluidised bed reactors

Like inside the bubbling fluidised bed reactor sand is used as a bed material in the reactor. As a reason of that a good temperature control can be achieved in the reactor. The technology of fluidised bed reactors is also well explored, so operation and construction of such a plant is state of the art, but the hydrodynamics inside the reactor are more complex than in a bubbling fluidised bed reactor. Circulating fluidised bed reactors are suitable for very large throughputs and the residence time for char is almost the same as for vapours and gas. More fine char particles are produced due to the high gas velocity which are separated after the reactor by a cyclone and can be used in a second reactor to provide the required heat for the pyrolysis process [Bridgwater, 2003]. Bio-oil separation can be carried out in a similar way as described before.

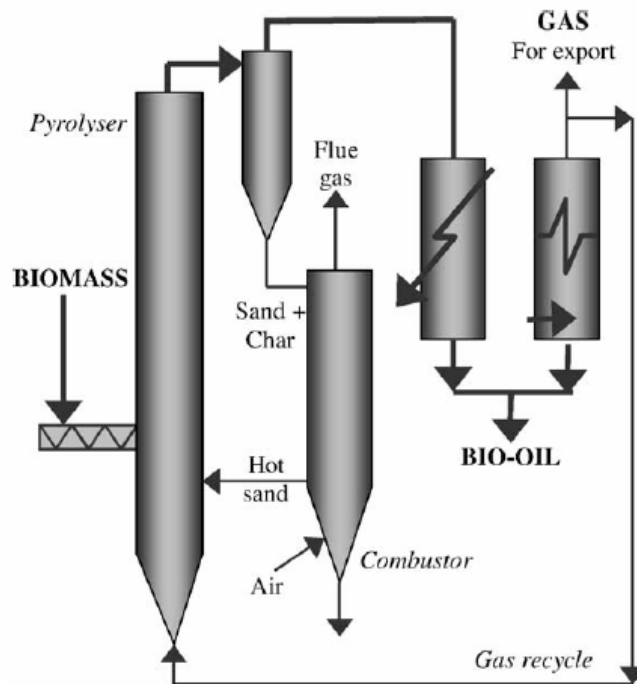


Figure 2-21: Circulating fluid bed reactor [Bridgwater, 2003]

## Ablative pyrolysis

During this process a biomass particle is pyrolysed by contacting a hot reactor surface. So the biomass is pressed against a heated, rapidly moving surface which melts the biomass and leaves an oil film behind that evaporates. Unlike the fluidised bed pyrolysis reactors, ablative pyrolysis processes are independent of a particular size of the feedstock. The performance of the process is limited by the heat transfer to the piece of biomass. It leads to



compact reactors that do not need a carrier gas, but they have the handicap of a surface area controlled system and moving parts at high temperature.

### **Ablative reactor with rotating cone**

The concept of this reactor is that biomass particles are fed into the top of a heated rotating turned around cone together with an inert material like sand or with catalytic active particles (Figure 2-22). As a reason of the rotating movement of the cone, the particles are pressed on to the heated surface and get pyrolysed while being transported spirally upwards along the hot cone wall.

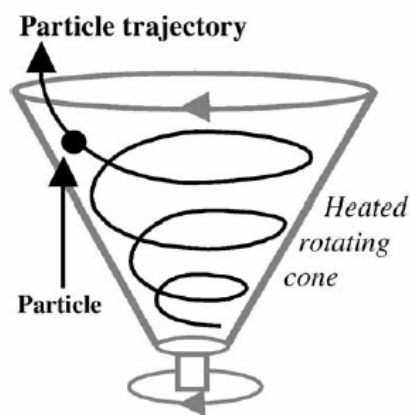


Figure 2-22: Principle of rotating cone pyrolysis reactor [Bridgwater et Grassi, 1991]

The residue of the process (ash, charcoal) is ejected from the top of the cone. An advantage of this process is that there is less carrier gas needed, so the reactor can be built very compact, but however, gas is needed for char burn off and for sand transport. The pyrolysis vapours leave the reactor via a separate tube (Figure 2-23). A disadvantage of this reactor type is that the system is very complex as the integrated operation of three subsystems is required. These systems are the rotating cone pyrolyser, the riser for sand recycling and the fluidised bed char combustor [Bridgwater et Grassi, 1991].

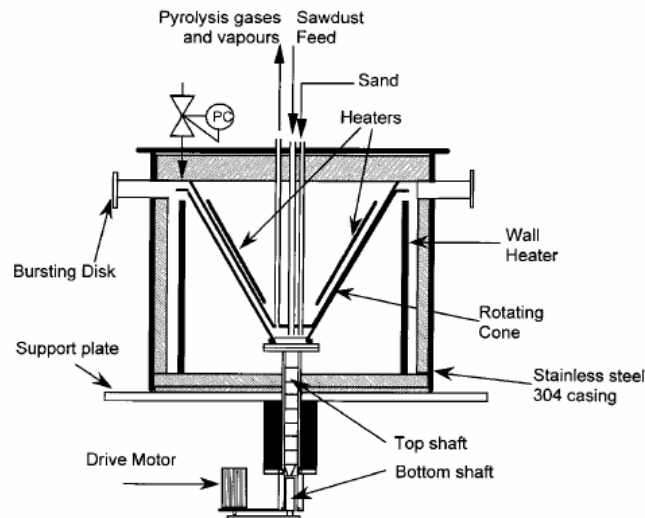


Figure 2-23: University of Twente rotating cone flash pyrolysis reactor [Bridgwater et Peacocke, 2000]

### Ablative reactor with rotating plate

In this reactor, the biomass particles fall through a shaft on a rotating, hot plate and are pressed on the plate by a hydraulic piston. A part of the biomass melts and leaves a thin liquid film on the plate that gets pyrolysed by the heat of the plate. There are also no carrier gases needed for the transportation of the pyrolysis products [Kaltschmitt et al., 2009].

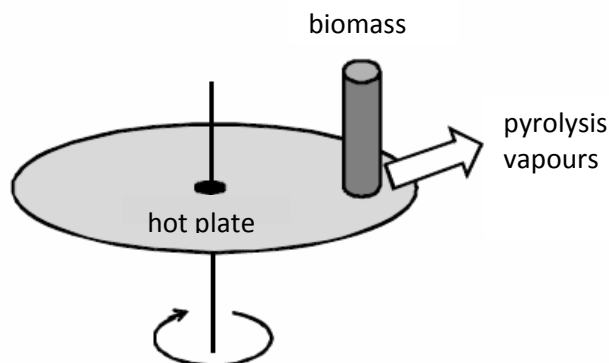


Figure 2-24: Principle of a reactor with a rotating plate, adapted [Kaltschmitt et al., 2009]

### Vortex ablative reactor

A reactor with a horizontal drum or a Vortex reactor works like a cyclone. The biomass particles with a size of approximately 5 mm are injected by a hot gas stream into the reactor and are accelerated to supersonic speed by additional injected steam or nitrogen. As a result of the high velocity and the tangential movement, the biomass particle gets pyrolysed on the hot drum surface (Figure 2-25) [Bridgwater, 2003].

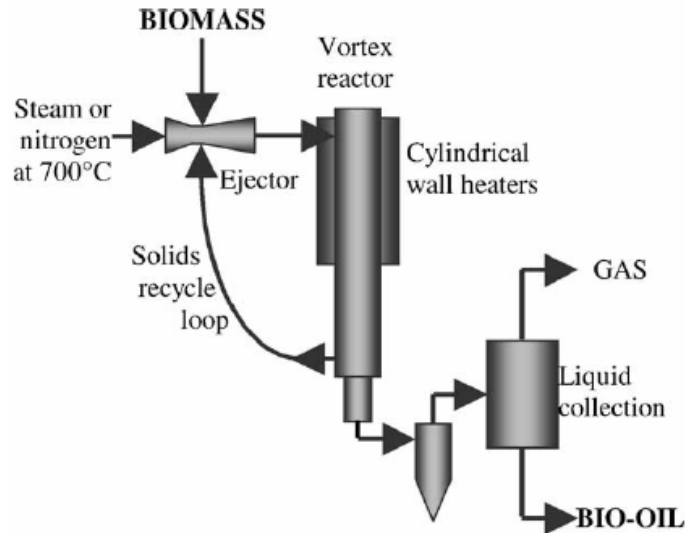


Figure 2-25: Vortex ablative reactor [Bridgwater, 2003]

### **Vacuum pyrolysis**

Vacuum pyrolysis is a special form of fast pyrolysis. It is not a real fast pyrolysis because the residence time of the solids is very long. The advantage of this process is that it can handle larger particles than all the other flash-pyrolysis processes. The residence time of the biomass in the reactor is here usually longer than half an hour, but that is not harmful for the fluid production because the produced pyrolysis gas is evacuated immediately. This process does not need a carrier gas and there is less char in the liquid product due to lower gas velocities. But vacuum pyrolysis is relatively complicated mechanically [Bridgwater et Grassi, 1991].

## 2.5 Slow Pyrolysis

The main product of slow pyrolysis is a solid product like charcoal or activated carbon. Therefore, lower process temperatures and longer residence times favour the production of charcoal. Slow pyrolysis is divided into two sections, carbonisation and torrefaction. Carbonisation is a complete pyrolysis process at about 500 °C with the aim of producing charcoal or activated carbon.

Drying and a partial pyrolysis at lower temperature happen during the torrefaction of biomass. Torrefaction is a preparation process that improves the properties of the feedstock for a further treatment [Kaltschmitt et al., 2009].

### 2.5.1 Carbonisation

There are many existing processes currently used for carbonisation. The well known way is to use a charcoal kiln. Thereby a part of the feedstock is combusted by a selective air supply. The resulting hot combustion gases flow through the biomass that is dried, heated up and devolatilized [Kaltschmitt et al., 2009].

### 2.5.2 Torrefaction

Torrefaction is a thermal treatment step in the relatively low temperature range of 225 to 300 °C, which aims to produce a fuel with increased energy density by decomposing the reactive hemicellulose fraction [Prins et al., 2006]. It is a partial pyrolysis process at temperatures between 225 and 300 °C slow heating rates and residence times of many minutes (up to 60 minutes). The aim is to make solid biomass suitable for further thermal conversion processes like combustion or gasification. Biomass that is treated by torrefaction has improved properties compared to natural finished biomass. Like the pyrolysis processes torrefaction acts at the absence of oxygen to prevent the conversion of carbon to carbon dioxide and to loose energy.

Up to now torrefaction has been state of the art for roasting coffee beans or cacao beans for many years. During the last years some draft proposals for wood torrefaction processes have been suggested. The heat for running the process can be provided directly to the biomass or indirectly.

For a direct heat supply hot gas passes through the biomass bed. The produced pyrolysis gas can be part of the hot gas. The reactor shown in Figure

2-26 is loaded from the top and the torrefaction product is taken from the bottom of the reactor.

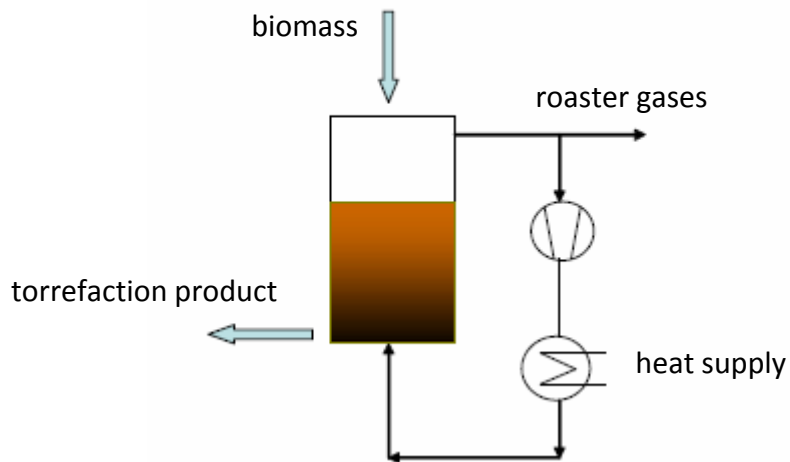


Figure 2-26: Fixed bed torrefaction reactor with direct heat supply, adapted [Kaltschmitt et al., 2009]

For an indirect heating of the biomass the walls of the reactor are heated or there are some internals (agitating arms, screw) to transfer the heat to the biomass. In Figure 2-27 a jacked rotary kiln reactor is used for torrefaction.

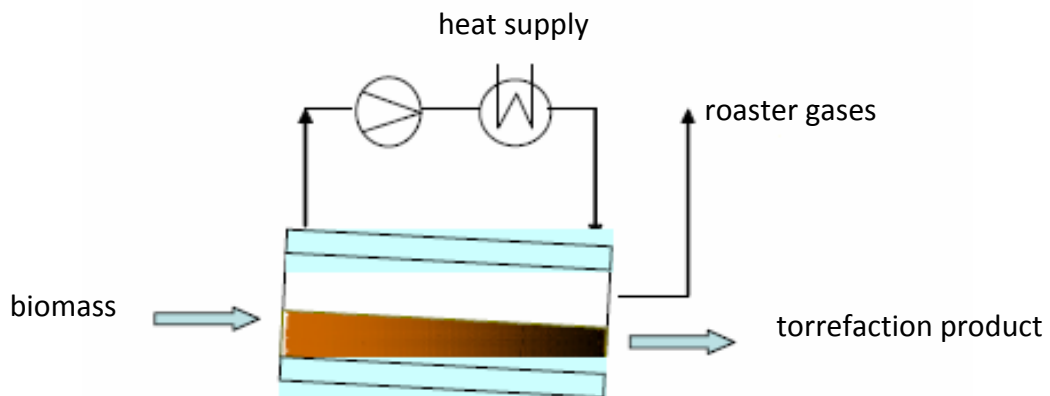


Figure 2-27: Jacked rotary kiln reactor, adapted [Kaltschmitt et al., 2009]

## 2.6 Combustion of agricultural residues in a thermal power plant

The background of the work carried out in this thesis is co-firing of low cost biomass fuels in existing coal fired power plants. Therefore, a short overview of previous proposed or realised methods for co-firing shall be given in this chapter. The most important technologies are:

- Direct co-firing
- Indirect co-firing
- Parallel co-firing

### 2.6.1 Technologies for Co-firing

Co-firing is defined as simultaneous combustion of different fuels in the same boiler. When biomass is used in co-firing, it represents one interesting alternative for reducing greenhouse gas emissions as well as most other emissions [Baxter et Koppejan, 2004]. An overview about the technical status of biomass co-firing is given by Cremers [Cremers, 2009] and van Loo et Koppejan [Loo et Koppejan, 2002].

In industrial coal-fired power plants, co-firing can be used to reduce CO<sub>2</sub> emissions without any loss in efficiency and with only minor changes to the plant's settings. Therefore, only low percentages of biomass are usually used. Co-combustion of biomass with coal is a matter of intensive research for different applications, and several comprehensive studies exist on this topic [Baxter, 2005], [Ghani et al., 2009], [Huang et al., 2006], [Nevalainen et al., 2007], [Sami et al., 2001], [Zulfiqar et al., 2006]. Co-firing can be accomplished via three different modifications, which are direct, indirect and parallel co-firing. For direct co-firing, a mixture of the standard fuel and the additional fuel is burned together in the boiler, while for parallel co-firing, a separate boiler where only the additional fuel is burned would be required. In this case, indirect co-firing would be the aim as only the gaseous products made by pyrolysis or gasification would be burned in the coal-fired boiler [Maciejewska et al., 2006].

The direct co-firing is the most popular option for biomass and coal co-firing currently in Europe [IEA, 2011], mostly due to relatively low investment cost of turning existing coal power plants into co-firing plants [Zuwala et Sciazko, 2005]. A recent inventory on the application of co-firing worldwide [Koppejan, 2004] shows that over 80 coal-powered plants have experience with co-firing

biomass or waste. Typical power stations where co-firing is applied are in the range from approximately 50 MW<sub>e</sub> to 700 MW<sub>e</sub>. The majority are equipped with pulverised coal boilers (tangentially fired, front-wall fired, back-wall fired, dual-wall fired and cyclone). Furthermore, bubbling and circulating fluidised bed boilers, cyclone boilers, and stoker boilers are used [Baxter et Koppejan, 2004].

Parallel co-firing units are also present, mostly in pulp and paper industrial power plants. The indirect co-firing options are currently considered to be too expensive for European markets, as proved by the co-firing experience in UK [Livingston, 2005]. However, when considering the future prospects for co-firing, the tendency is to increase the ratio of biomass/coal, and to be able to utilize a wide range of different biomass fuels including fuels blends. Therefore it may be in the future that the higher investment in more advanced co-firing configurations would pay back by better operability and flexibility of the system [Maciejewska et al., 2006].

### Co-firing of grinded biomass

In this option (Figure 2-28) biomass (a secondary fuel) enters the boiler together with coal (primary fuel).

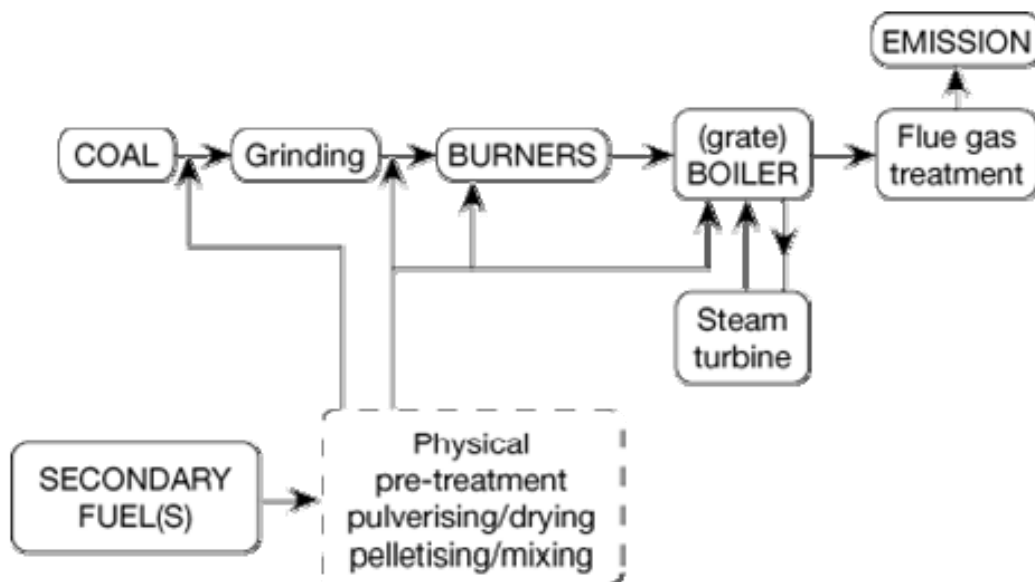


Figure 2-28: Process layout of unit performing direct co-firing

In case of direct co-firing of biomass with coal in large-scale PC (pulverised coal) boilers the following options are possible [Maciejewska et al., 2006]:

- Blending biomass with coal in the fuel yard and transportation of the mix through the coal system with the application of coal processing and

combustion equipment (coal mills, crushers, pulverizers, burners) [Livingston, 2005]. This is the cheapest and most straightforward option, however problems resulting from differences in the characteristics of the two mixed fuels can occur. Also, some types of biomass cannot be processed this way (for example herbaceous biomass is known to cause many problems during feeding and sizing). It can be applied to biomass like olive/palm kernels or cocoa shells as well as saw dust (in the last case, blending with coal takes place after the coal mills) [Kiel, 2005]. There are a number of projects in Europe based on this option, but its application is considered to be limited (i.e. to conventional wall or corner-fired furnaces) [Livingston, 2005].

- Separate milling of biomass, mechanical or pneumatic feeding to the boiler followed by firing of the biomass material through existing coal injection system and burners [Livingston, 2005]. In this case the fuel mixing takes place in the combustion chamber, thus without impacting the fossil fuel delivery system. This option involves higher investment.
- Installation of new, dedicated biomass milling and sometimes also burning equipment [Livingston, 2005]. This option increases the number of biomass materials, which can be fed to the boiler. There are projects in Europe based on this option, although it is relatively complex and expensive to install. In the direct co-firing configuration, a minimum investment is necessary, but may face various shortcomings resulting from differences between the properties of mixed feedstock. One of them is that the biomass ashes become mixed with coal ashes. Although coal ashes and, to a lesser extent, biomass ashes might be reused separately, the re-use of mixed ashes may be restricted substantially.



Figure 2-29 shows a co-firing concept for direct co-firing of biomass and coal.

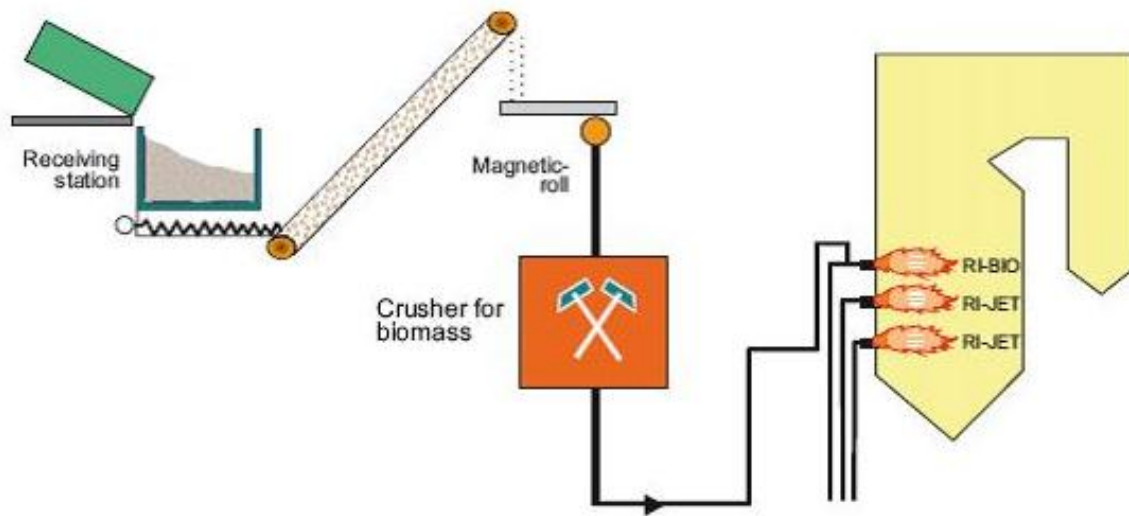


Figure 2-29: Co-firing concept for direct co-firing of biomass and coal. [Orjala et Heiskanen, 2004]

In this process (Figure 2-29) the biomass (e.g. forest residue chips, bark, clean demolition wood chips and agricultural wastes) is screened and ground in the crusher process and then fed to the boiler through separate bio-coal burners (RI-BIO). Mixing of biomass and coal can be carried out in two different ways. Biomass can be introduced to the coal flow just before the burner or biomass can be fed to the furnace through a center pipe and will be mixed with coal in the flame. This co-firing concept makes possible to substitute up to 20-30 % of coal on an energy basis with biomass resulting in equal reduction in greenhouse gas emissions [Kostamo, 1999], [Savolainen et Sormunen, 2001]. This co-firing concept was tested at Suomenoja Power Plant in Finland. Co-combustion did not have significant influence on boiler performance and ignition and stability of the flame [Savolainen et al., 2003].

### Co-firing of gasified biomass

In this option biomass is gasified (or combusted) separately and the produced gas is injected and burned in the coal boiler. This technique keeps the biomass ashes separated from the coal ashes, while allowing very high co-firing ratios. The drawback of indirect co-firing option is relatively high unit investment costs [Zuwala et Sciazko, 2005]. Indirect co-firing by pre-gasification has been operated in a number of demonstration plants in Austria (Zeltweg), Finland (Lahti) and the Netherlands (Geertruidenberg) [European Commission, 2000].

The most potential and feasible gasification technology to be applied for indirect co-firing is fluidised bed gasification. Both bubbling as well as circulating fluidised bed gasification can be applied. Both technologies are fuel flexible, which enables utilization of wide selection of different biofuels as well as waste derived fuels. Some fuel pretreatment is required, like crushing (roughly below 50 mm), but heating value, density and other characteristics of the fuel can vary in a wide range. One of the most successful commercial demonstration is gasification and co-firing of the product gas in PC (pulverized coal) boiler in Kymijärvi power plant in Lahti, Finland [Nieminen et Karki, 2007].

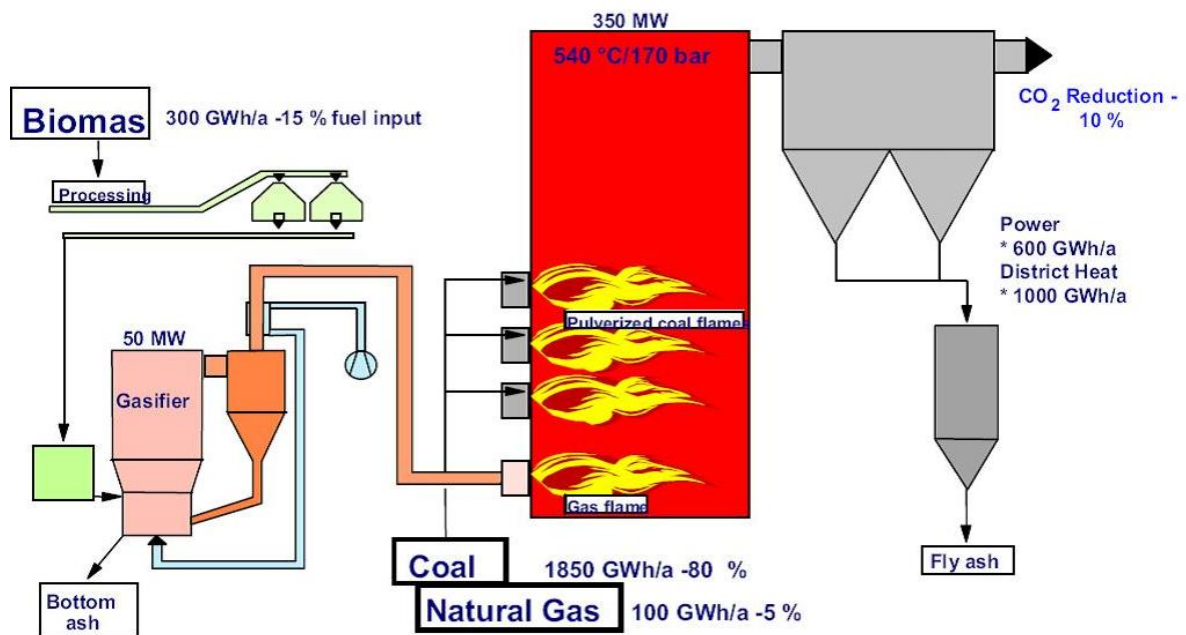


Figure 2-30: Flow sheet of the Lahti Energia Oy gasifier [Oravainen, 2008]

In the BioCoComb (Bio-fuel for Co-Combustion) demonstration project, a CFB gasifier for bark, wood chips, sawdust etc. was installed at the 137 MW<sub>e</sub> pulverised coal fired power plant of Verbund Austrian Hydropower AG in Zeltweg, Austria [Simader et Moritz, 2002].

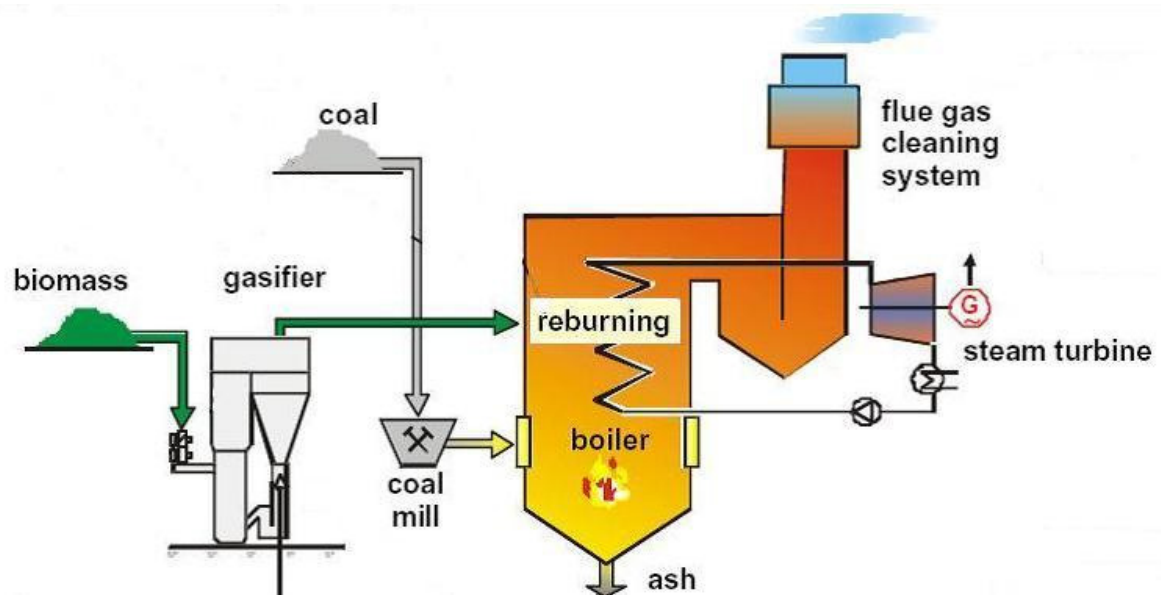


Figure 2-31: Flow sheet of the Zeltweg BioCoComb power plant [Simader et Moritz, 2002]

The process concept (Figure 2-31) is based on the gasification of biomass (bark, wood chips, sawdust with a water content of 40 to 50 %) in a fluidised bed. In this case, the air is fed to the system to exactly such an extent that part of the fuel burns and, while doing so, the heat is produced that is required for the gasification of the rest of the biomass, for the combustion of which not enough oxygen is available. Because it is neither a matter of total combustion nor a matter of total gasification it is called partial gasification. The gas is led uncooled from the gasifier to the boiler, where it serves as auxiliary fuel and replaces part of the coal. Apart from the CO<sub>2</sub>-reduction, the NO<sub>x</sub>-reduction through "reburning" is also of interest. For integration into the power plant the fluidised bed gasifier is installed near the coal-fired boiler. In the gasifier the biomass is converted to gas that is then directly conveyed to the boiler via a hot-gasline as a second fuel. The partial gasification taking place in the reactor is sufficient respectively desired. Due to this process, pre-drying of the biomass and cleaning of the emerging gas is not necessary. Furthermore, this process can be used to reduce NO<sub>x</sub>-emissions, due to the fact that, with the aid of the gas, a second combustion takes place in the coal [Simader et Moritz, 2002]. Due to the liberalisation of the European electricity market, the whole power plant Zeltweg was shutdown in 2001.

## Co-firing of pyrolysed biomass

For application of biomass pyrolysis as a pretreatment process, equipment is needed which can pyrolyse large amounts of straw or similar fuels in relatively low temperatures, however such equipment is not commercially available today [Jensen et al., 2001]. Nevertheless the use of biomass pyrolysis oil in co-firing with fossil fuel has been demonstrated in large-scale coal power station [Chiaramonti et al., 2005]. The application of pyrolysed biomass for co-firing can be sometimes challenging, as the liquid products obtained by means of pyrolysis are rich in water that is detrimental for ignition [Yaman et al., 2000].

Pyrolysis as a first stage in a two-stage gasification plant for straw and other agricultural materials does deserve consideration [Rösch et Wintzer, 1997]. Hamm Uentrop Power Station in Dortmund has installed a pyrolysis unit connected to a main coal-fired boiler, as illustrated in Figure 2-32. The products from the pyrolysis process are gas, char, metals and other inert material. The pyrolysis gas is injected directly into the boiler, whereas the char is milled in the existing coal mills and is injected in the boiler together with the coal.

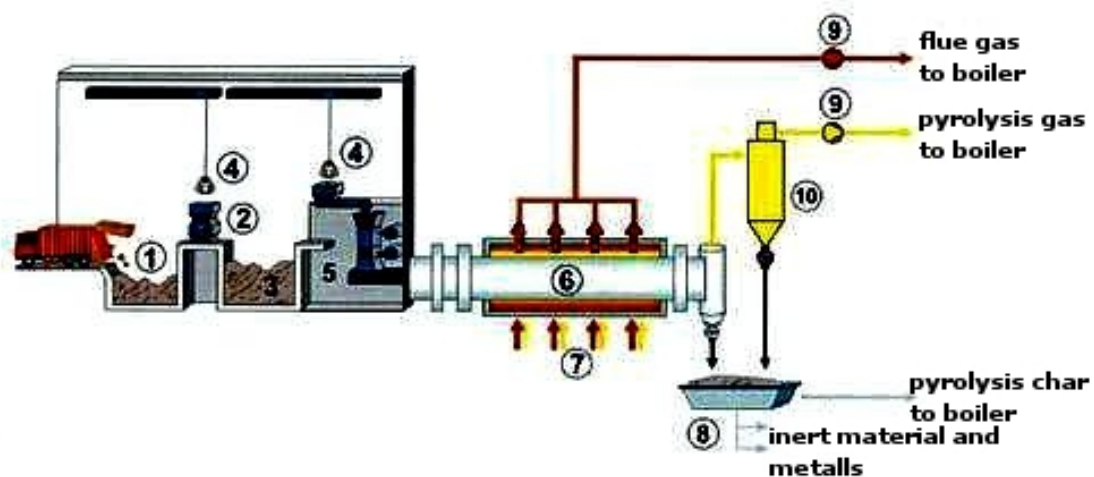


Figure 2-32: Upfront pyrolysis unit of Hamm Power Station [Cremers, 2009], (1) residual bunker, (2) shredder, (3) bunker, (4) crane, (5) material lock, (6) pyrolysis rotary kiln, (7) burner system, (8) discharge pyrolysis solids, (9) fan, (10) dust precipitator

The use of biomass pyrolysis oils in co-firing with fossil fuels has also been investigated and tested on commercial scale. In particular, the use of this biofuel in large coal and natural gas power station was demonstrated.

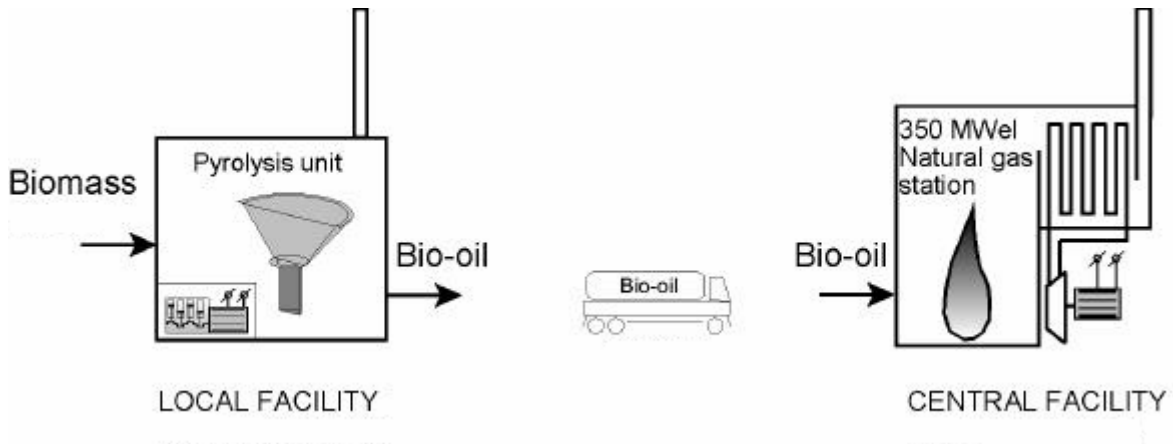


Figure 2-33: Co-firing of bio-oil in a power station [Wagenaar et al., 2004]

Pyrolysis oil, pyrolysis liquid, bio-oil, bio fuel oil, bio crude oil (PL) produced by Red Arrow Products Company by the RTP™ process (Ensyn Rapid Thermal Process) was co-fired in a coal station [Sturzl, 1997] at the Manitowoc public utilities power station, Wisconsin, a 20 MWe low-sulphur Kentucky coal-fired stocker boiler. A total of 370 h of operation have been accumulated, feeding 5 % of thermal input by PL, corresponding to 1 MW<sub>e</sub> power output generated by PL. The plant was operated without significant problems after cost-effective modification of the boiler to allow for co-firing. No adverse effects were observed on emission levels (sulphur emissions reduced by 5 %), maintenance programs or ash handling. Waagenar et al. [Wagenaar et al., 2002] have also reported of co-firing PL in a coal fired power plant.

Biomass PL from BTG (Biomass Technology Group) has also recently been fired in a combined cycle natural gas power station in Harculo in the Netherlands [Wagenaar et al., 2004]. This was the first time PL was co-fired at a power plant scale above 20 MW<sub>e</sub>. The 251 MW<sub>e</sub> power plant is equipped with a 90 MW<sub>e</sub> gas turbine (top cycle) and a 161 MW<sub>e</sub> steam turbine (bottom cycle). The exhaust gases from the gas turbine were directed to a boiler, which was fed with an additional natural gas input: this particular plant configuration offered the opportunity to replace part of its fossil fuel feed with biomass PL during a 2 day test campaign. PL was fed at a rate of 1.9 t/h (equivalent to 7.9–7.8 MW LHV thermal input) into one of the 12 burners of the boiler, and air-assisted atomized at pressure of approximately 4 bar. Tests lasted approximately 4 h per day, consuming a total of 15 t of PL. The power output setting of the plant remained unchanged. The oil gun operated well with PL, without the need for gun cooling, and after PL operation it was

visually similar to heavy oil operated guns. As far as emissions are concerned, a slight increase in  $\text{NO}_x$  emissions was observed, due to the replacement of a nitrogen free fuel (natural gas) with a nitrogen-containing one (PL) [Chiaramonti et al., 2005].

## 2.6.2 Co-firing of biomass in a pulverised coal fired power plant

Co-firing of solid biomass in conventional hard coal or lignite fired power plants is possible but its use is limited to some boundary conditions.

The fraction of biomass of the total thermal power of a conventional coal fired thermal power plant is limited by the mass flow rate of biomass that can be burned without expecting significant drawbacks. Drawbacks could be corrosion in the boiler, higher emissions or disadvantages concerning the flow of the gases in the power plant. Figure 2-34 shows possible effects on different parts of a plant by co-firing of biomass.

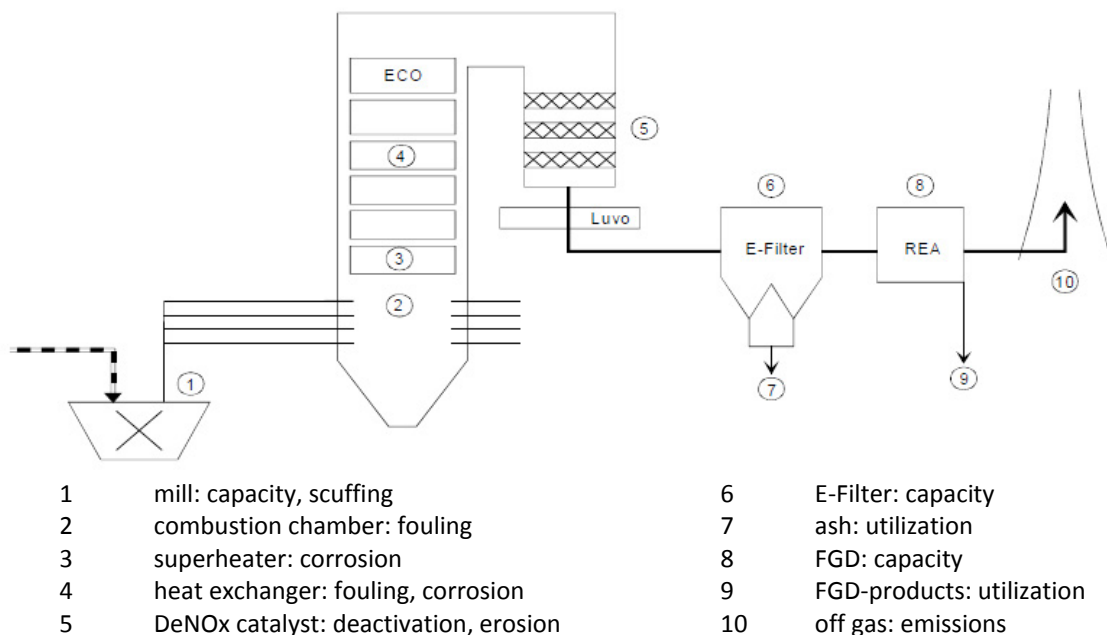


Figure 2-34: Influenced parts of a plant by co-firing of biomass, adapted [Kaltschmitt et al., 2009]

As a reason of the lower heating value of biomass than that of coal, the mass flow of fuel raises by co-firing of biomass, so the fuel supply units have to handle the higher flow of coal and biomass. For example, if 10 % of the fuel power in a coal fired power plant is substituted by straw, the fuel mass flow would be twice as much than using only coal as a fuel. This is the reason why grinding and drying of the biomass should happen separately. The mills for

coal are also in the majority of cases not suitable for the desired biomass types.

The gas flows during the combustion change their characteristics only in a very small range in the case of co-firing of biomass. Significant changes occur only due to the water content of the biomass that becomes noticeable in the water content and the volume flow of the off gas.

Fouling and slagging have also to be considered. Because of the lower melting points of most biomass ashes, like the ash of straw compared to the ash of coal, there is the risk of slag formation in the combustion chamber. For slag tap furnaces a low melting point of the ash is necessary but for a dust firing, like in the power plant Dürnröhr with a dry ash removal, it can be dangerous [Kaltschmitt et al., 2009].

Fact is that stramineous biomass has much higher chlorine content than hard coal or lignite. This is the reason why a straw firing has a very high potential of high temperature corrosion of the firing equipment [Baxter, 2005] [Jensen et al., 2001] [Kiel, 2005] [Davidsson et al., 2002] [European Commission, 2000]. Table 2-4 shows the chemical composition of straw, wood, and coal in mass-% of their dry matter.

Table 2-4: Composition of solid fuels and biomass types [Kaltschmitt et al., 2009]

biomass/fuel	C	H	O	N	K	Ca	Mg	P	S	Cl
mass-% of dry matter										
<b>hard coal</b>	72.5	5.6	11.1	1.3					0.94	<0.13
<b>Lignite</b>	65.9	4.9	23.0	0.7					0.39	<0.1
<b>spruce wood</b>	49.8	6.3	43.2	0.13	0.13	0.70	0.08	0.03	0.015	0.005
<b>rye straw</b>	46.6	6.0	42.1	0.55	1.68	0.36	0.06	0.15	0.085	0.40
<b>wheat straw</b>	45.6	5.8	42.1	0.48	1.01	0.31	0.10	0.10	0.082	0.19
<b>barley straw</b>	47.5	5.8	41.4	0.46	1.38	0.49	0.07	0.21	0.089	0.40
<b>rape straw</b>	47.1	5.9	40.0	0.84	0.79	1.70	0.22	0.13	0.27	0.47
<b>Maize straw</b>	45.7	5.3	41.7	0.65					0.12	0.35
<b>sunflower straw</b>	42.5	5.1	39.1	1.11	5.00	1.90	0.21	0.20	0.15	0.81

### 2.6.3 High temperature corrosion

On the inside of a fired steam boiler there can occur high temperature corrosion and low temperature corrosion. They can be caused by the combustion products of the firing of coal, oil, industrial waste, municipal waste or biomass. Low temperature corrosion can happen if the off gas, that contains  $\text{SO}_3$ , is cooled down below the dew point of  $\text{H}_2\text{SO}_4$  [Heitmann, 2000].

As a reason of slagging and fouling of biomass fired boilers, the steam temperature has been traditionally kept below 450 °C in order to limit the corrosion damage of the super heater tubes. Especially, straw fired boilers have been experiencing problems due to the inorganic metal constituents such as alkali metals and chlorine present in the straw. A demand to raise the temperature of the superheated steam to improve the electrical efficiency and to make the plants more economical has been an area of discussion especially with regards to corrosion of the boiler components. Some tests have shown that severe corrosion takes place at test probes with metal temperatures above 520 °C [Michelsen et al., 1998].

The power plant Dürnröhr is designed for a high electrical efficiency. The superheated steam has a temperature of 530 °C [Böhmer et al., 2003] at nominal value so co-firing of straw, that has a high amount of chlorine and potassium, would be dangerous for the durability of the parts of the power plant. A good overview about first calculations of the corrosion potential in the power station Dürnröhr taking into account co-firing of straw is given in the final report of the Technical University of Freiberg [Schreiner et al, 2009].



## 2.7 The coal fired power plant Dürnrohr

The power station in Dürnrohr is Austria's biggest coal fired power plant. It was built as a replacement for the Zwentendorf nuclear power station, a plant that never started up due to a 1978 referendum. The Dürnrohr power station (Figure 2-35) was built in order to use the already established power lines and other infrastructure of the nuclear power station. It consists of two blocks. One of the two blocks has an electrical output of 405 MW which is operated by Verbund Austrian Thermal Power AG and the other one has an electrical output of 352 MW operated by the Energie Versorgung Niederösterreich (EVN) AG. The plant was set into operation in 1987 [NEWAG NIOGAS, 1987].

In 2004 a heating plant (largest such in Austria, at the time) using waste heat from the power plant was opened.



Figure 2-35: The coal fired power plant Dürnrohr [Verbund, 2004]

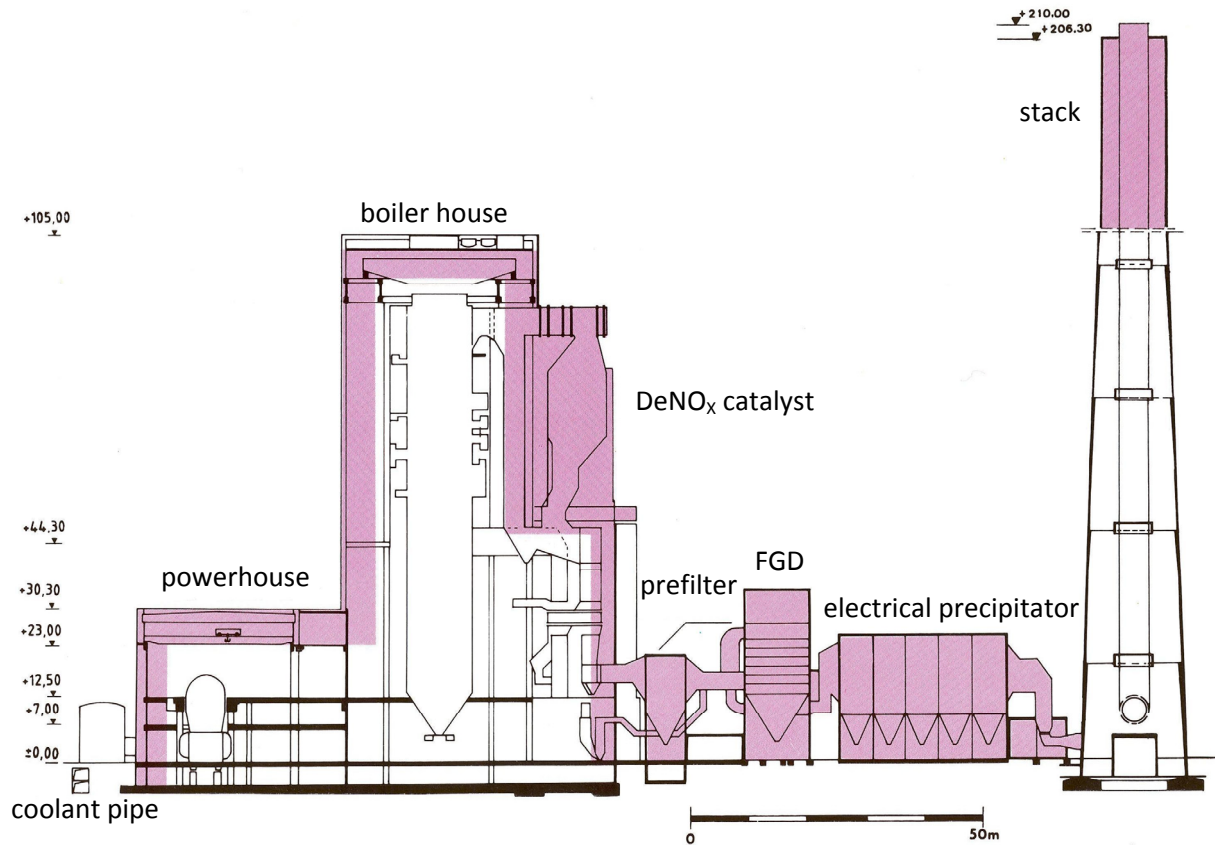


Figure 2-36: Cross-sectional view through the Dürnröhr power plant, adapted [NEWAG NIOGAS, 1987]

The plant (condensation power station with intermediate superheating and fresh water cooling as well as use of steam for district heating) is powered by black coal imported from the Czech Republic and Poland but it can also use natural gas as a fuel. The combustion chamber uses a tangential dust firing with four burner register, each located in an edge (Figure 2-37). Cooling water is provided by the Danube River that is just a few kilometres away. At the time the power station was built it set new standards concerning environmental sustainability. For an example Europe's first optimal working NO<sub>x</sub> reduction system (selective catalytic reduction) with ammonia as a reduction agent was realised in Dürnröhr. Further gas cleaning is carried out through a flue gas desulphurisation (FGD) system and an electrical dust precipitator (Figure 2-36) [16].

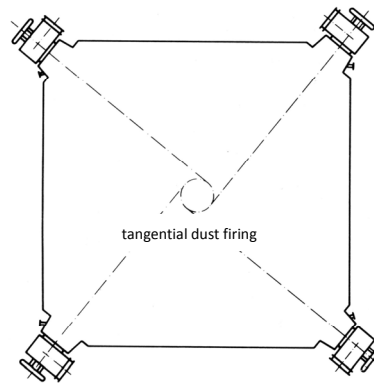


Figure 2-37: Tangential coal dust firing in the Dürnrrohr power plant, adapted [NEWAG NIOGAS, 1987]

Table 2-5 shows the main operating figures of the coal fired power plant. The co-firing of the pyrolysis gas is planned below the second coal burner level.

Table 2-5: Main figures for the coal fired power plant Dürnrrohr

Maximum capacity	352 MW
Net efficiency without district heating using coal	41.3 to 41.9 %
Net efficiency without district heating using natural gas	42.3 to 43.5 %
Main steam flow	1018 t/h
Main steam temperature	540 °C
Main steam pressure	206 bar (a)
Flue gas volume flow	~1 Mio. Nm <sup>3</sup> /h
Effective output generator	400 MVA
Use of steam for district heating	50 MW
Industrial steam extraction	50 MW
<b>Firing with coal</b>	
LHV	24.3 to 30 MJ/kg
Maximum coal consumption	~120t/h
<b>Firing with natural gas</b>	
LHV	36.6 MJ/Nm <sup>3</sup>
Maximum natural gas consumption	80000 Nm <sup>3</sup> /h

Four different sorts (Murcki, Centrum, Rydultowy, Kru Trade) of black coal imported from the Czech Republic and Poland are used for firing. Table 2-6 shows a part of the analyses of the four coal sorts. The full analyses can be found in the appendix (c.f. 9.3).

Table 2-6: Chlorine (Cl), sodium (Na), potassium (K) and sulphur (S) content of the four black coal samples

	<b>Murcki</b>	<b>Centrum</b>	<b>Rydultowy</b>	<b>Kru Trade</b>
	wt. %			
<b>Cl</b>	0.006	0.005	0.016	0.005
<b>Na</b>	0.260	0.371	0.964	0.101
<b>K</b>	1.930	1.962	1.571	1.953
<b>S</b>	2.130	2.510	2.700	0.070

### 3 Pyrolysis pilot plant Dürnrrohr

The pyrolysis pilot plant is located in Dürnrrohr/Austria just next to the coal fired power plant. The pilot plant is in operation since 2008 (Figure 3-1). Figure 3-2 shows the flow sheet with the most important parts of the plant. The two most important components are the rotary kiln pyrolysis reactor, where the thermal decomposition of the biomass takes place, and the fluidised bed combustion chamber for pyrolysis gas combustion as well as char combustion. Further important components are the fuel chopper, the char hopper and the biomass hopper, the spray type cooler, the spray absorber, the fabric filter and the stack.



Figure 3-1: Pyrolysis pilot plant at Dürnrrohr/Austria

The plant is fully automated by a process control system, so it can be controlled easily from a single control room. The process control system is also able to record the measured data from all of the sensors and actors of the plant. These datasets can be exported to an excel-file for an optional processing. In Figure 3-3 a screenshot can be seen showing a plant scheme including the process control system. Table 3-1 and Table 3-2 show the design data of the pilot plant for pyrolysis and fluidised bed operation.

Table 3-1: Design data of the pilot plant for pyrolysis operation

Fuel thermal output	3-5 MW
Biomass amount	600-1100 kg/h
Pyrolysis gas amount	500-850 kg/h
Pyrolysis charcoal amount	140-300 kg/h
Combustion air amount	2000-3000 Nm <sup>3</sup> /h
Flue gas amount combustion total	7300-12800 Nm <sup>3</sup> /h
Heating gas amount for rotary kiln reactor	2500-5900 Nm <sup>3</sup> /h
Flue gas amount over fabric filter	6600-10800 Nm <sup>3</sup> /h
Exhaust gas amount over stack	4300-6600 Nm <sup>3</sup> /h
Recirculation gas for combustion	1000-4200 Nm <sup>3</sup> /h
Water injection total	1.4-2.4 m <sup>3</sup> /h
Absorber addition	2-4 kg/h
Amount fabric filter ash	5-8.5 kg/h
Heating temperature	800-1000° C
Pyrolysis gas temperature	350-650° C
Flue gas temperature stack	150-200° C
O <sub>2</sub> -content combustion	2.5-3.5 %

Table 3-2: Design data of the pilot plant for fluidised bed operation

Fuel thermal output	3-5 MW
Pyrolysis charcoal amount	0-300 kg/h
Combustion air amount	1200-2600 Nm <sup>3</sup> /h
Flue gas amount combustion total	4000-8500 Nm <sup>3</sup> /h
Flue gas amount over fabric filter	5600-11200 Nm <sup>3</sup> /h
Exhaust gas amount over stack	2800-5700 Nm <sup>3</sup> /h
Recirculation gas for combustion	2800-5600 Nm <sup>3</sup> /h
Water injection total	1.4-2.4 m <sup>3</sup> /h
Absorber addition	2-4 kg/h
Amount fabric filter ash	28-67 kg/h
Combustion chamber temperature	800-850° C
Flue gas temperature stack	150-200° C
O <sub>2</sub> -content combustion	3-4 %



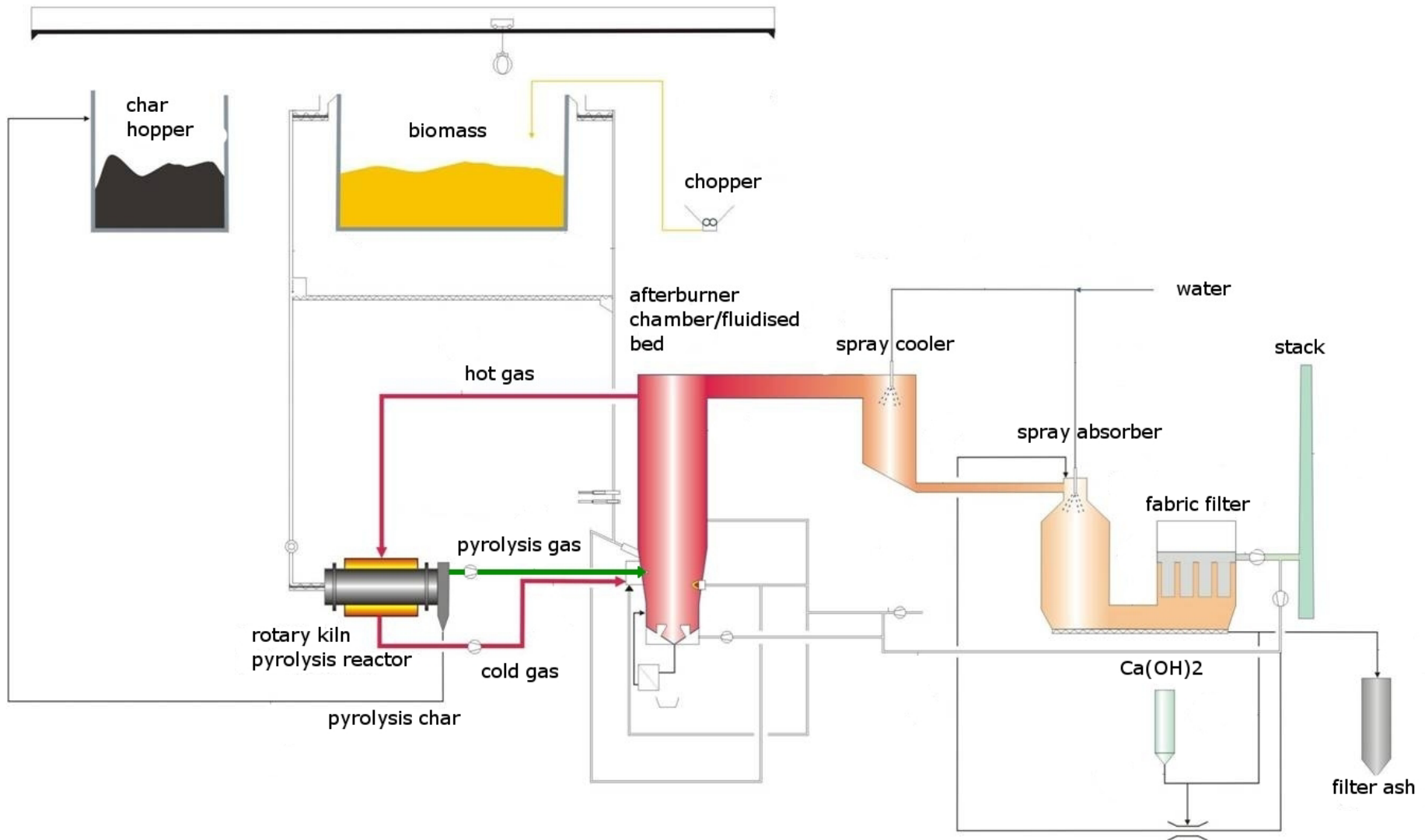


Figure 3-2: Flow sheet of the pyrolysis pilot plant

### 3.1.1 Process description

The delivery and the handling of the ungrinded biomass are carried out by agricultural vehicles. After cutting by a mobile shredder, the material is stored temporarily in a hopper.

The charging of the material for pyrolysis is done by a crane. In an indirectly heated rotary kiln reactor pyrolysis takes place to produce combustible gases and char from biomass.

The combustible gases are burned in a burner muffle located in the freeboard of the fluidised bed combustion chamber implemented as an afterburner. The fluidised bed combustion is not operated simultaneously with pyrolysis gas combustion. For the heating of the rotary kiln reactor flue gas from the afterburner is used. Charcoal is cooled down and stored temporarily in a charcoal hopper. The exhaust gases from the afterburner are cooled down in a spray type cooler by injection of water and cleaned in a spray absorber and the dust is removed in a fabric filter.

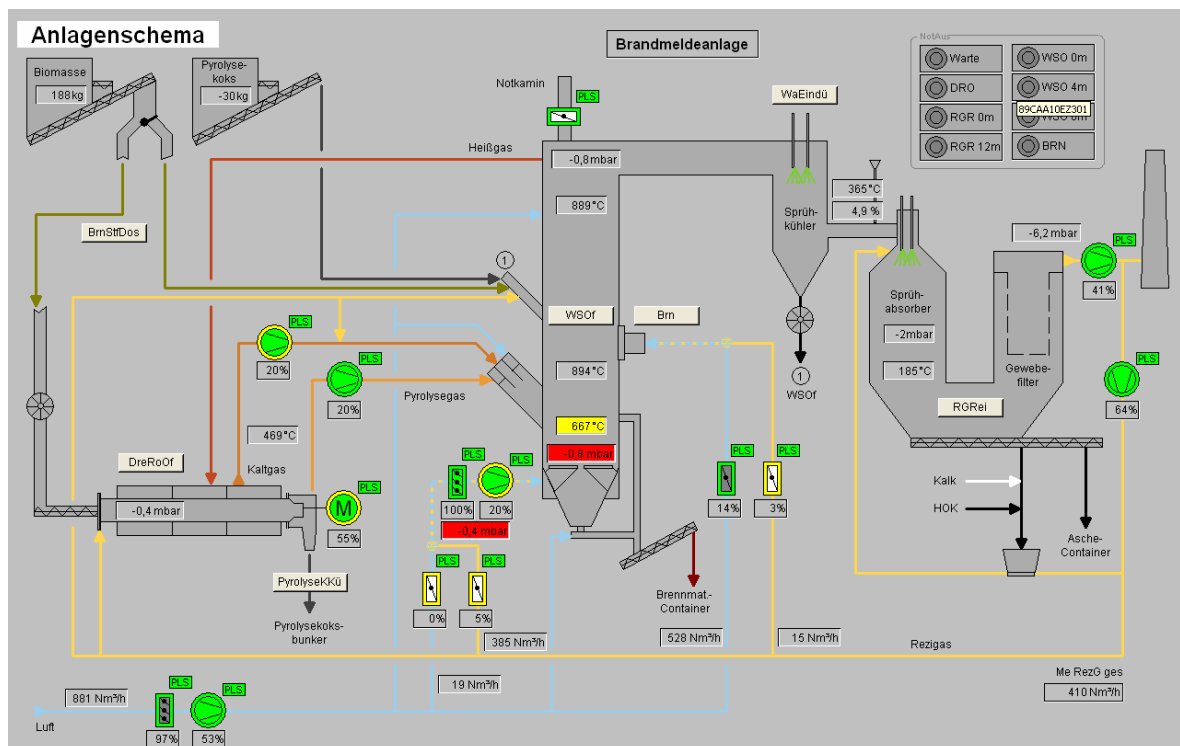


Figure 3-3: Screenshot of the plant scheme from the process control system

Pyrolysis of biomass and burning of the temporarily stored char takes place periodically. If the charcoal hopper is nearly full, the pyrolysis is stopped. The fluidised bed chamber is then used as combustor for charcoal and biomass. The exhaust gases are cooled down in the spray type cooler by injection of



water and cleaned in the spray absorber and the dust is removed using the fabric filter in the same way as described for the exhaust gases from the combustion of the pyrolysis gases.

The majority of the equipment such as fuel dosage, combustion chamber, spray type cooler, spray absorber and fabric filter are used for both operation modes.

### 3.1.2 Pyrolysis operation

The pyrolysis reactor is a jacked rotary kiln reactor that is externally heated. The heating medium is hot gas that is produced in the afterburner by combustion of the pyrolysis gas. The pyrolysis gas temperature at the outlet of the rotary kiln is between 450 and 630 °C. At this temperatures the main amount of undesired components, such as heavy metals, sodium- and potassium salts, stay in the pyrolysis char.

The feedstock is fed in via a lock system at the front wall of the rotary kiln. To transport the pyrolysis gas out of the rotary kiln and to provide optimal process conditions a fan generates a low pressure of a few millibar. To prevent the penetration of air, all locks and seals are pressurised with seal gas. As seal gas, nitrogen, oxygen-deficient recirculation gas or steam can be used.

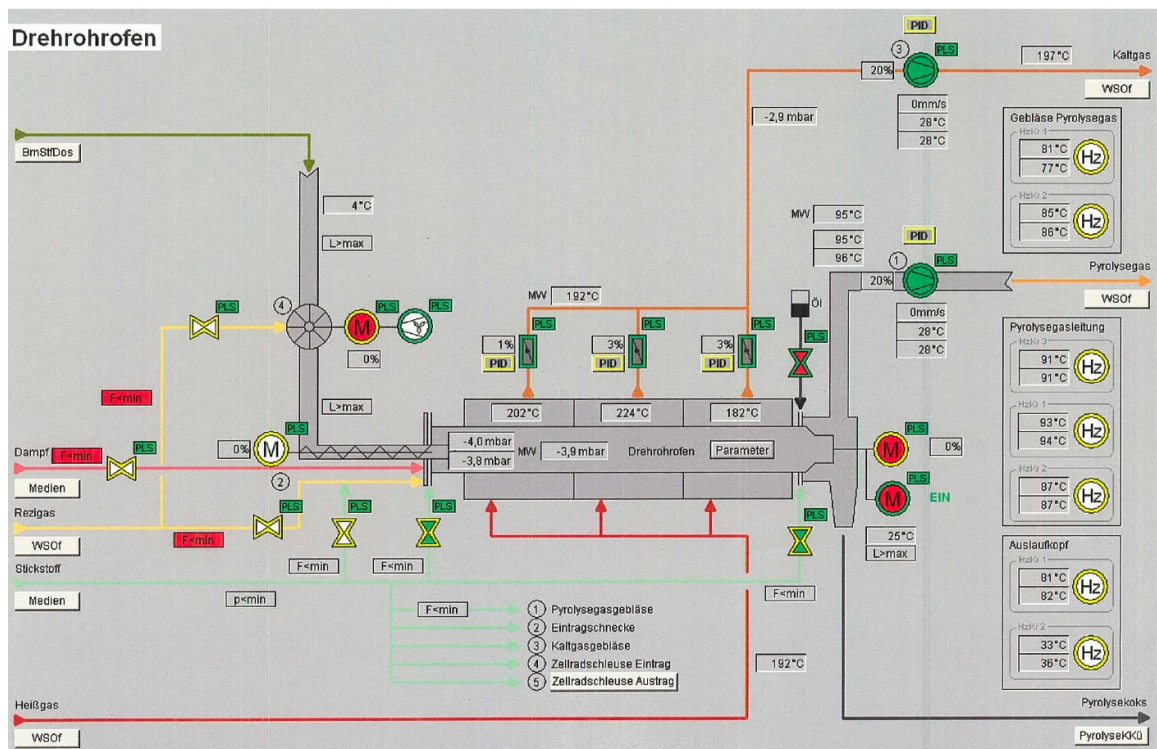


Figure 3-4: Rotary kiln reactor in the process control system

As it can be seen in Figure 3-4, the heating jacket around the reactor is divided in three heating zones. This allows a good adjustment of the temperature and distribution of the heat. The hot gas valves of the rotary kiln are installed to control the hot gas supply depending on the desired pyrolysis gas outlet temperature. The temperature of the hot gas is higher than 800 °C. In this way inner wall of the rotary kiln reactor temperatures of more than 650 °C can be achieved.

Under these conditions the pyrolysis of the biomass takes place. Pyrolysis gases from the rotary kiln reactor are sucked off with a pyrolysis gas fan. In order to avoid condensation from the pyrolysis gas, the gas pipes to the burner muffle are equipped with a trace heating system that uses the heating gas ("cold gas") leaving the rotary kiln reactor as a heating medium. Hot gas and pyrolysis gas pipe lead to the burner muffle in the fluidised bed chamber. In the burner muffle the pyrolysis gas is burned. The mixture of combustion gases, hot gases and regular combustion air, supply the necessary temperature for the heating of the afterburner. The necessary hot gases for the heating of the rotary kiln reactor are taken from the top of the combustion chamber.

At the discharge of the rotary kiln reactor the pyrolysis char has a temperature ranging from 450 to 630 °C. The charcoal is transported via a lock system to an indirectly cooled screw conveyor and a water-cooled chain to cool it down. The cold char coal is conveyed to the charcoal hopper and stored there.

For start-up and shutdown, as well as for necessary auxiliary firing, a gas burner is available. For blow out of exhaust gases during unexpected plant disturbance, an emergency flap at the fluidised bed chamber top cover is provided.

### 3.1.3 Fluidised bed operation

To start up the fluidised bed operation the sand that acts as bed material is heated up by a gas burner. The fuels are injected pneumatically into the combustion chamber. Combustion air is compressed with the forced draft fan.

The recirculation gas is taken after the fabric filter and it is mixed with primary air and compressed in the fluid gas fan. This fluid gas is divided evenly over the nozzles of the distributor.

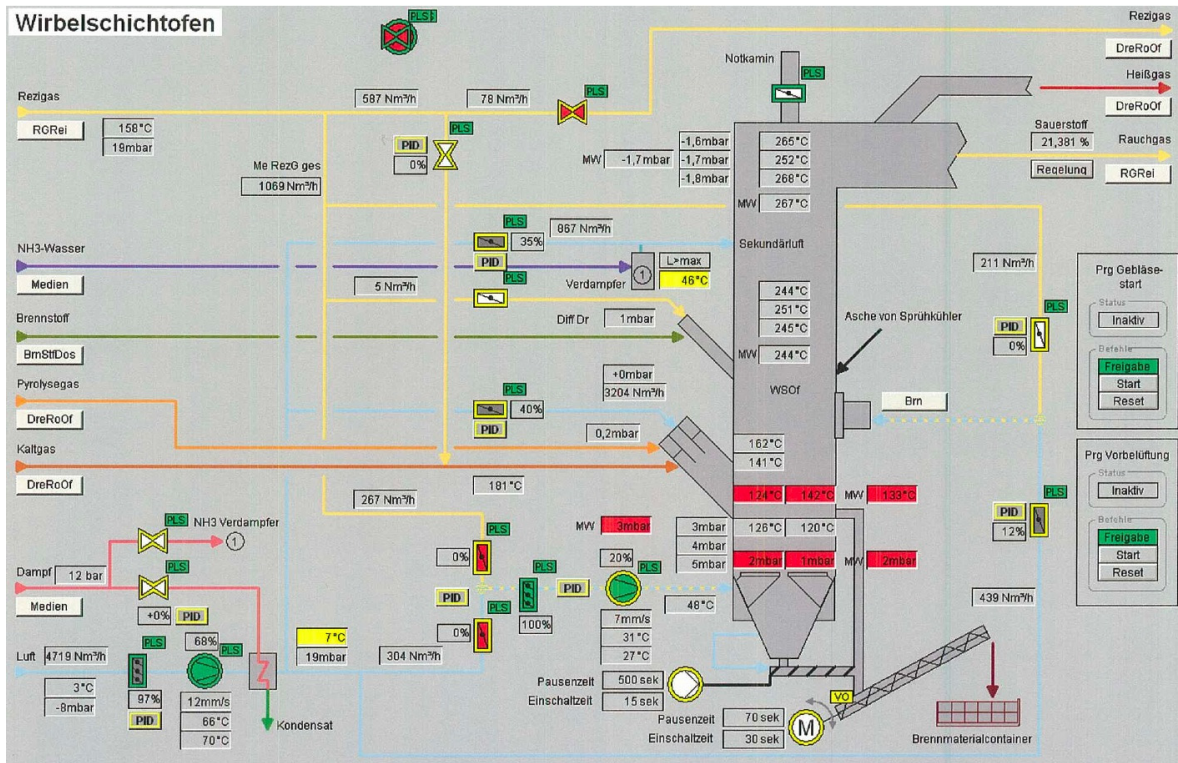


Figure 3-5: Fluidised bed reactor/afterburner

The combustion chamber is un-cooled, refractory lined and constructed as stationary fluidised bed with open nozzle distributor. One afterburning zone with secondary air injection is directly above the stationary fluid bed. The complete burnout of the combustible gases takes place only after addition of the upper secondary air. The solids that seep through the fluid bed are removed over the open nozzle distributor. Figure 3-5 shows a screen shot during operation of the pyrolysis gas combustion

### 3.1.4 Spray type cooler

The pilot plant is not designed for generating energy or heat so the hot flue gas after the combustion chamber has to be cooled down for the gas cleaning section. Therefore, a spray type cooler that injects water into the hot gas stream is used. The water evaporates and the evaporation energy is provided by the hot flue gas. As a result the temperature after the spray type cooler is below 400 °C.



### 3.1.5 Gas cleaning of the pilot plant

For gas cleaning a spray absorber, a selective non-catalytic de-NO<sub>x</sub> and a fabric filter is installed (Figure 3-6).

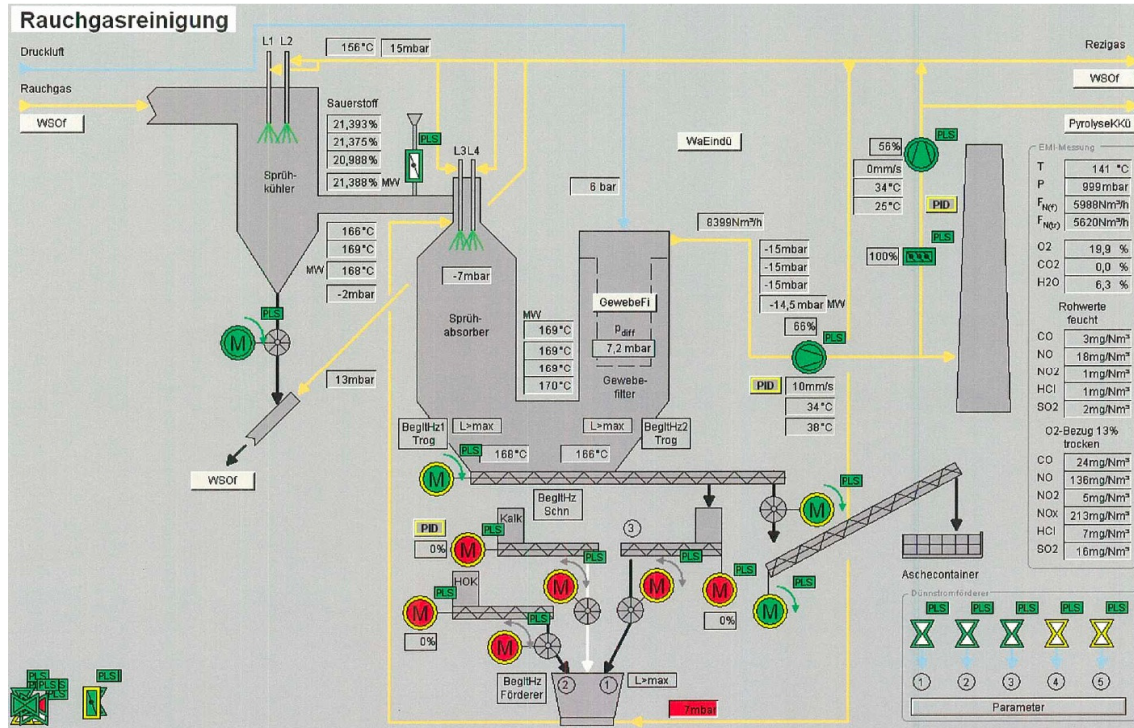
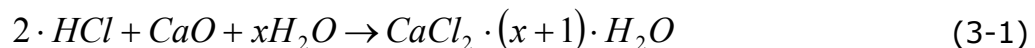


Figure 3-6: Gas cleaning of the pilot plant: spray cooler, spray absorber and fabric filter

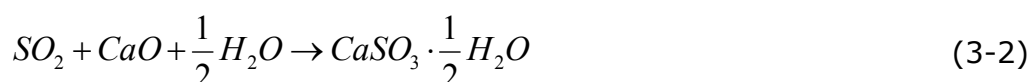
#### Spray absorber

As an adsorbent, calcium hydroxide (Ca(OH)<sub>2</sub>) is used for the cleaning of the gas from sulphur dioxide and hydrochloric acid. The following main reactions of exhaust gas cleaning take place in the spray absorber:

- Hydrochloric acid adsorption:



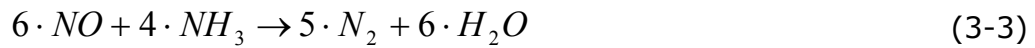
- Desulphurisation:



If the contents of HCl and SO<sub>2</sub> in the flue gas are very low, it is not necessary to use calcium hydroxide. In this case, pure water can be used in the spray absorber.

**De-NO<sub>x</sub>**

For the reduction of nitrogen oxides, an ammonia injection in the freeboard of the fluidized bed is available, a so-called selective non-catalytic de-NO<sub>x</sub> (SNCR). The ammonia water is heated and added to the secondary air, which is injected into the freeboard of the fluidised bed and mixed with the flue gas. At a temperature between 800 and 900 °C, ammonia reacts with nitrogen monoxide as described in the following equation:

**Fabric Filter**

The fly dust in the flue gas is separated by a fabric filter and transported by a screw conveyor to a container.

### 3.1.6 Data logging

The performance data from the pyrolysis pilot plant can be subdivided in three different groups:

- Data from the process control system (Siemens SIMATIC PCS 7)
- Results from analytical measurements at the pilot plant (pyrolysis oil, dust, water content,  $\text{NH}_3$ ,  $\text{HCl}$ ,  $\text{H}_2\text{S}$ )
- Data from external weighing (straw, pyrolysis char)

The data from the process control system comprehend a selection of temperature, pressure, amount and concentration measurement which are stored every minute in a data file.

The second group of measurement data are analytical single measurements in the product (pyrolysis) gas flow. These measurements are carried out in unsteady intervals because they have to be accomplished with great complexity. The characteristic points of measurements are:

- Exit of rotary kiln reactor after pyrolysis gas fan
- Intersection of fluidised bed to spray cooler
- Stack

The third group are external weighing data which are carried out by an industrial weighing machine. Normally only the straw supplies have to be weighted but during the balancing periods every single bale of straw and the produced pyrolysis char, which was collected in a container was exactly weighted.

## 4 Experimental work and chemical analyses

The following chapters give an overview about the used feedstock, the applied measurements and the chemical analyses which have been carried out at the pilot plant.

### 4.1 Feedstock and pyrolysis charcoal characterisation

The composition of the feedstock is the most important factor for the composition of the produced pyrolysis gas. A lot of different types of biomass have been used as a feedstock for the pilot plant. This work focuses on the following feedstock.

- wheat straw (indoor stored)
- straw pellets
- sorghum straw
- miscanthus straw
- reed straw
- palm nut shells
- Waldviertler energy grass (WVE)
- paper residual material

Some of these fuels are only available in very small amounts therefore, the main fuel is straw, especially wheat straw. The information about the availability and potential of straw in the region around the power station Dürnröhr was already collected by Stoifl [Stoifl, 2000].

For the investigations on plant balances in this thesis indoor stored wheat straw was used due to the fact that the properties of the feedstock are constant for all operating points of the plant.

Essential for this work is also the knowledge about the substances in the char that are formed during the pyrolysis process. So the char can be compared with the used feedstock and as a result the enrichment of the undesired substances in the pyrolysis gas (Cl, K, Na) can be checked.

Pyrolysis char and fuel analyses are carried out by the "Testing Laboratory for Combustion Systems" at the Institute of Chemical Engineering, Vienna University of Technology and by the laboratory of the Bioenergy2020+ GmbH according to the DIN and ÖNORM standards.

Table 4-1 shows the applicable DIN and ÖNORM standards for the different analyses.

Table 4-1: Applicable DIN and ÖNORM standards for the different analyses

	Testing Laboratory for Combustion Systems	Laboratory of the Bioenergy2020+ GmbH
Water content	DIN 51718	ÖNORM EN 14774-1
LHV/HHV	DIN 51900 T2	ÖNORM EN 14918
Volatiles	DIN 51720	ÖNORM EN 15148
CHN	not specified	ÖNORM EN 15104
Cl	CEN/TS 15289	ÖNORM EN 15289
S	CEN/TS 15289	ÖNORM CEN/TS 15290 and 15297
Ash	DIN 51719 (550 °C)	ÖNORM EN 14775
Na, K	CEN/TS 15105	ÖNORM CEN/TS 15290 and 15297
Ash melting behaviour	DIN 51730	DIN 51719



## 4.2 Detection of pyrolysis oil

During the pyrolysis process gaseous products are formed. A certain part of the gaseous products condenses at ambient temperatures to a liquid product. The nature of these liquid products is like tar that appears in many other processes like gasification. But for pyrolysis the tar is not undesired in most of the cases, it is a useful product. To accentuate its profit it is called pyrolysis oil instead of tar.

Pyrolysis oils are liquid to semi-solid products that are made by smouldering, carbonisation or gasification of coal, peat or biomass like wood or straw. They are very harmful to health because of the carcinogenic components benzene, toluene, naphthalene, xylene and other polycyclic aromatic hydrocarbons [Hofbauer et al., 2003].

The chemical analysis of the pyrolysis oil is realised by gas chromatography coupled to a mass spectrometer (GC-MS). The pyrolysis oil is quantified by the GC-MS and by a gravimetric method.

But there is a certain limitation for both methods. The applied GC-MS system can only detect components of oil if their boiling point is lower than 450 °C. Components of the oil with a boiling point higher than 450 °C get stuck in the column of the GC-MS system. This causes an error that is depending on the composition of the pyrolysis oil. To make this error smaller there is also a gravimetric method used. The gravimetric method is not able to detect the different compounds and structures in the oil, like the GC-MS, it is only able to detect the amount of oil.

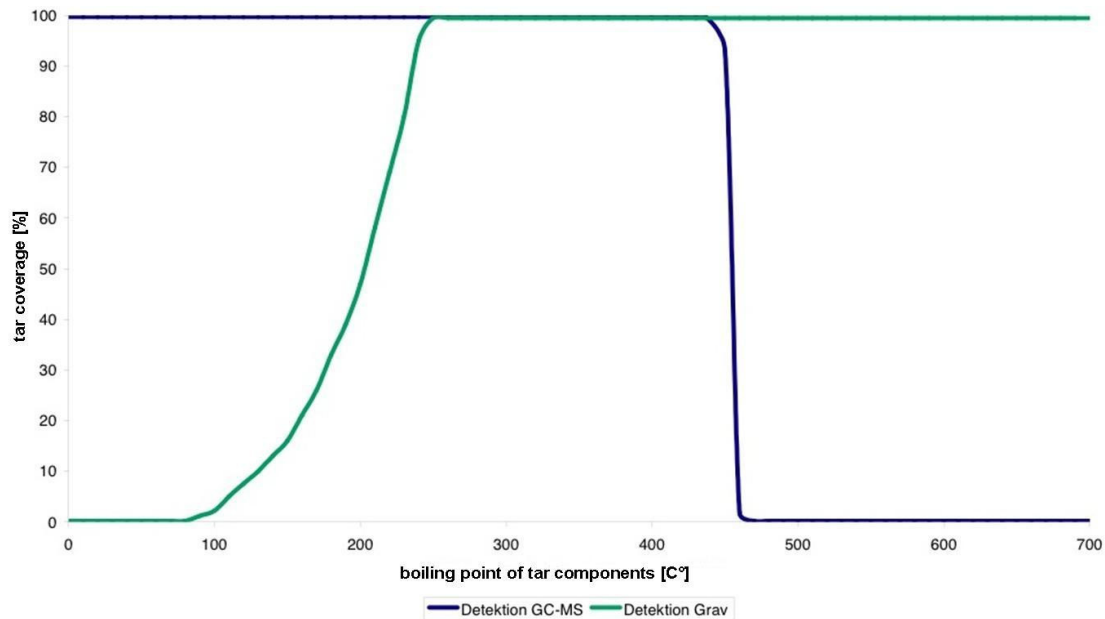


Figure 4-1: Comparison of the detection of pyrolysis oil by GC-MS and gravimetry [Hofbauer et al., 2003]

But there is also a disadvantage in this method. With the gravimetric method there can only be the part of the oil with a boiling point that is higher than 105 °C detected, because this is the temperature where the solvent, that contains the oil, is removed. Furthermore, the absorbing medium is toluene so only components can be absorbed that are heavier than toluene. Figure 4-1 compares the GC-MS method and the gravimetric method for the detection of tar components. There can be seen that a complete detection of the components is not possible. In a temperature range from more than 220 °C to 450 °C both methods record the components, so in this temperature range they overlap.

#### 4.2.1 Gravimetric analysis for pyrolysis oil

The applied method is used to measure the dust, entrained char and pyrolysis oil content in a gas stream together with the water content. For pyrolysis oil measurement a gas stream is isokinetically taken for a certain period of time.

The gas enters the heated sampling line, which consists of a cyclone and a glass wool stuffed filter cartridge, where dust is deposited. Afterwards, the gas is led through six impinger bottles filled with toluene. The impinger bottles are situated in a cooling bath which is cooled down to -10 °C by a cryostat. There the tars and steam condense. A scheme of the pyrolysis oil measuring system is shown in Figure 4-2.

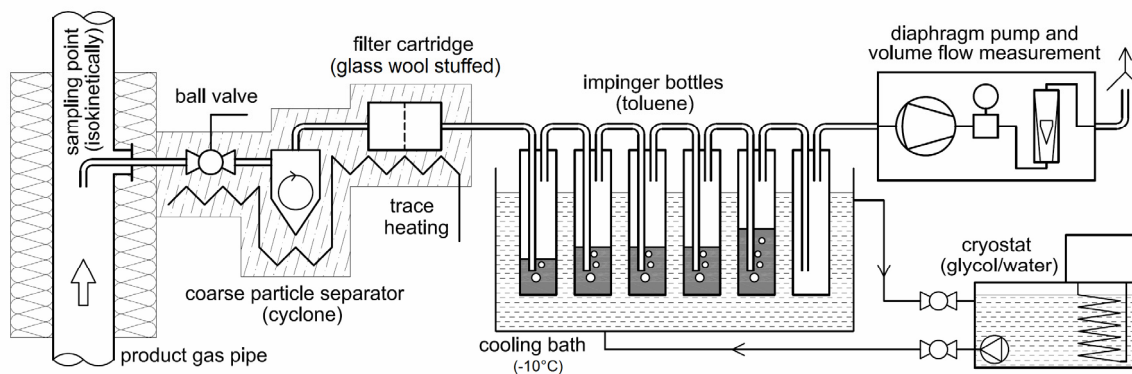


Figure 4-2: Scheme of the tar measuring system, adapted [Hofbauer et al., 2003]

The liquid phases in the impinger bottles are unified and the aqueous phase is separated from the toluene phase. Afterwards, the amount of water is determined to calculate the water content in the gas stream. The amount of toluene is also marked down and a GC-MS sample is taken. Then the main part of the toluene is evaporated from the sample. The residual is transferred to a petri dish and dried for a defined period of time in a drying oven. The petri dish is weighed before and after the analysis [Hofbauer et al., 2003].

To analyse the oil in the filter cartridge it is necessary to carry out a soxhlet extraction with isopropanol (IPA). Again a GC-MS sample of the IPA phase is taken. Afterwards the IPA phase is handled like the toluene phase. The results of the toluene phase and the IPA phase are added, which gives the amount of gravimetric pyrolysis oil in the gas stream [Hofbauer et al., 2003].

The filter cartridge is put into a muffle furnace. By weighing the cartridge before and after the muffle furnace treatment the amount of entrained char and dust can be calculated.

#### 4.2.2 GC-MS/FID analysis for pyrolysis oil

The analyses of the pyrolysis oils were carried out by the Johann Heinrich von Thünen-Institute, Federal Research Institute for Rural Areas, Forestry and Fisheries in Hamburg. A GC-MS/FID (Agilent HP 6890/Agilent HP 5972) system was used for the measurement.

The GC is essentially an oven containing a fused silica capillary. Capillaries are long and fine and have a film of stationary phase coating the inner surface. It is the stationary phase that facilitates the selective binding of analytes to the column due to analytes different physiochemical interactions (dispersion, dipole-dipole interactions and hydrogen bonds). Capillary columns are

available in different dimensions with various stationary phases according to the application. For the measurements of the pyrolysis oils a Factor Four Capillary Column VF-1701ms was used (length = 60m, inner diameter = 0,25mm, film thickness = 0,25 $\mu$ m).

Samples (1 $\mu$ l) are introduced onto the column by a syringe on an auto sampler via a temperature-controlled inlet. This facilitates the vaporization of the sample into the gas phase and allows the sample to be transferred by a carrier gas like helium (mobile phase) onto the front of the column. The column is subjected to a temperature gradient in the oven (oven temperature program: initial temperature 45 °C for 4 min; ramp 3 °C/min to 280 °C; hold for 20 min).

If the analytes have different physiochemical properties they will be separated along the column because they interact differently with the stationary phase.

Molecules with a higher boiling point will elute from the column later than those with a lower boiling point. By optimising the thermal gradient in the gas chromatograph it is possible to separate most of the molecules before they enter the detector.

A mass spectrometer (MS) and a flame ionisation detector (FID) are used as detectors.

### 4.3 Pyrolysis gas characterisation

The pyrolysis gas mainly consists of methane (CH<sub>4</sub>), carbon monoxide (CO), carbon dioxide (CO<sub>2</sub>), hydrogen (H<sub>2</sub>), water (H<sub>2</sub>O) and small amounts of oxygen (O<sub>2</sub>) and nitrogen (N<sub>2</sub>). These gases, except water, are called permanent gases. After cooling down to a certain (mostly ambient) temperature permanent gases are still gaseous. That is why water is not a permanent gas as it condenses to a liquid phase. In the pyrolysis gas methane, carbon monoxide, carbon dioxide and hydrogen are desired, a small content of oxygen and nitrogen occurs due to leaking of the plant. If leaking of the plant appears, it happens at the lock where the feedstock is transported into the rotary kiln reactor. These substances, except nitrogen, can be measured on line in the pyrolysis gas.

The applied device for permanent gas measuring is a gas analyser (model S700, type S710) produced by Sick-Maihak.

These gas analysers detect the concentration (volumetric part) of a certain gas in a gas mix. The gas that has to be analysed flows through the device and by using different modules multiple gases can be detected at the same time. This device is located in a container next to the rotary kiln reactor. The measurement system is also integrated in the process control system, so all the measured values are recorded and can be readout at any time. (cf. Appendix, Table 9-1)

Inside the analyser there are some modules that are detecting the substances by using different technologies.

#### **Module FINOR**

The FINOR operates with the interference filter correlation (IFC) principle. Up to three different gas components can be measured simultaneously. In this application it is used for measuring CO and CH<sub>4</sub>.

#### **Module THERMOR**

The THERMOR uses the different thermal conductivity of gases, to determine the gas concentration of a particular gas in a binary or quasi-binary gas mixture. Here it is used for measuring H<sub>2</sub> and CO<sub>2</sub>.

#### **Module OXOR-P**

This module is used for the detection of oxygen in the pyrolysis gas. Oxygen has a relatively high magnetic susceptibility as compared to other gases and displays a paramagnetic behaviour. The paramagnetic oxygen sensor consists of a cylindrical shaped container inside of which is placed a small glass

dumbbell. The dumbbell is filled with an inert gas such as nitrogen and suspended on a taut platinum wire within a non-uniform magnetic field. The dumbbell is designed to move freely as it is suspended from the wire. When a sample gas containing oxygen is led through the sensor, the oxygen molecules are attracted to the stronger of the two magnetic fields. This causes a displacement of the dumbbell which results in the dumbbell rotating. A precision optical system consisting of a light source, photodiode, and amplifier circuit is used to measure the degree of rotation of the dumbbell.

In fact the pyrolysis gas has a very high load of tar respectively pyrolysis oil that causes fast fouling of tubes and sensors. To provide a reliable operation of the on line permanent gas measurement it is necessary to remove most of the condensing components and to make sure that there is no condensation of gases on the way to the measurement device. The essential device of this gas processing is a scrubber with rapeseed methyl ester that absorbs the pyrolysis oil vapours.

Further important components of the gas are hydrogen sulphide ( $H_2S$ ), ammonia ( $NH_3$ ) and hydrochloric acid ( $HCl$ ). These components are often only trace elements in the range of a few ppm but the load of them give information about the possibility of co-firing of the pyrolysis gas in a high temperature firing.

### 4.3.1 Measurement of NH<sub>3</sub>

Ammonia in the pyrolysis gases is generated during the pyrolysis process in the rotary kiln reactor from the amount of nitrogen in the feedstock. Due to the composition of the pyrolysis gases, the measurement of ammonia is not possible by commercial gas measurement devices. The sampling is also very difficult because ammonia gets lost by condensing pyrolysis gas moisture and it may react with other pollutants in the gas. So, it is often detected less ammonia in the gas than there is effectively present.

The ammonia can be detected in the pyrolysis gas by absorption of the basic nitrogen compounds in sulphuric acid. Therefore, a small part of the gas stream is taken from the pyrolysis gas stream and sucked through several wash bottles, which are filled with diluted sulphuric acid, by a piston pump. After this procedure the concentration of ammonium ions in the sulphuric acid can be detected by a photometric method according to DIN 38 406 part 5 and ÖNORM ISO 7150 part 1.



Four of the six wash bottles are filled with diluted sulphuric acid. The first bottle is filled with 50 ml, the next two bottles each with 100 ml and the fourth bottle is filled with 150 ml. The wash bottles are placed next to the gauge in a glycol/ethanol mix whose temperature is cooled down by a cryostatic temperature controller. The connection to the gauge is heated by an electric trace heating to prevent the pyrolysis oil vapours from condensing. To start the procedure a piston pump sucks the gas through the wash bottles. The volume of the gas is recorded by the pump. After the measurement procedure, the time of the procedure, the volume of pyrolysis gas sucked through the piston pump and the pyrolysis gas temperature is listed. With this data it is possible to calculate the load of ammonia in the pyrolysis gas stream.

### 4.3.2 Measurement of H<sub>2</sub>S

Hydrogen sulphide is also present in the pyrolysis gas and has to be detected.

The sample rig can be separated in four main areas (Figure 4-3):

1. Sensor part with dust separation (sampling probe, cyclone, filter cartridge), 200 °C heated
2. Condensate collector (water cooler + three-neck flask), 50 °C thermostat controlled
3. Pyrolysis oil measurement part (3 wash bottles with 2-propanol),
4. H<sub>2</sub>S measurement part with a pre tar-extraction (5 flasks connected in series)

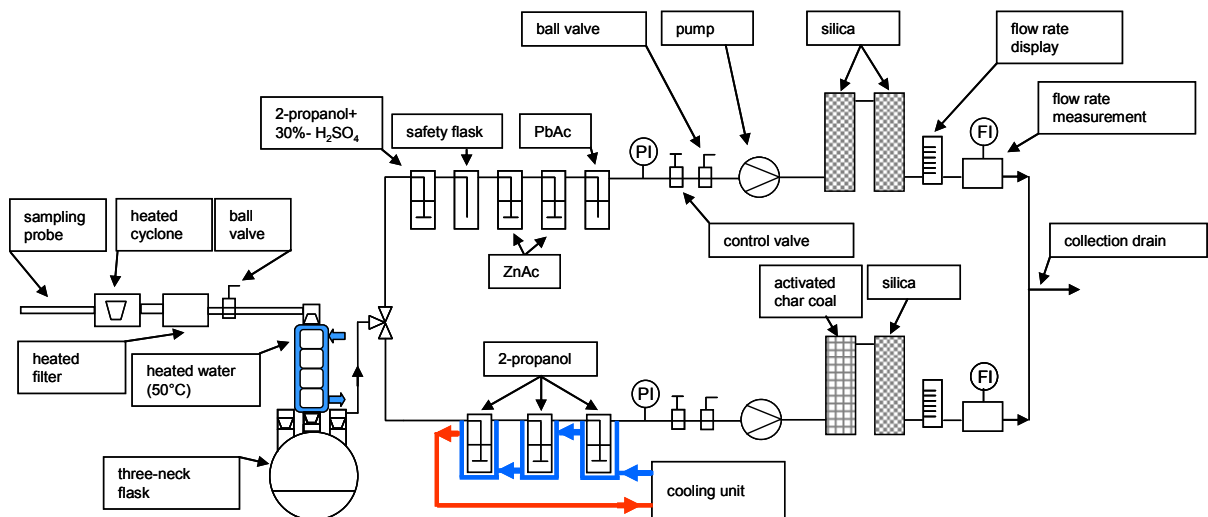


Figure 4-3: Test rig for H<sub>2</sub>S sampling [Kleinhapfl et Zeisler, 2010]

#### Process description

A sampling stream of the dust and tar containing pyrolysis gas is separated from the main gas stream. The dust separation is carried out by a cyclone and a filter cartridge which are heated (200 °C). The flexible tube between the filter cartridge exit and water cooling inlet consist of teflon and is used for gas cooling. The water temperature of the water cooler is kept at a constant temperature of 50 °C by using a cooling aggregate. This ensures that the condensing heavy tars stay pourable.

The three-neck flask has a capacity of two litres and disencumbers the two following wash bottles concerning heavy tars (pyrolysis oils) and condensing water.



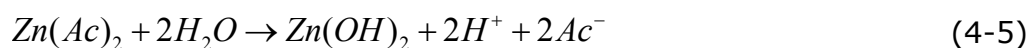
The amount of acetic acid is high enough to get a sour condensate which avoids the recourse of hydrogen sulphide.

Two wash bottles are used before the gas enters the wash bottle with the sampling fluid (zinc acetate). The first bottle contains a mixture of 2-propanol and sulphuric acid. The tar is deposited but the hydrogen sulphide can pass through. The second bottle is a safety bottle which secures that no sulphuric acid reaches the ZnAc – solution, which would lead to a false result. As a control bottle a bottle with lead acetate is used at the end of the sampling line.

Before the gas volume is measured by a diaphragm gas meter it is led through two silica gel columns which are used for gas drying.

### **Sampling of hydrogen sulphide with ZnAc**

This method is based on the precipitation of ZnS (s) by the compound of Zn<sup>2+</sup> - ions with solved S<sub>2</sub> ions following these reaction equations:



A solution of 20 g/l zinc acetate (hydrate) is used. Hydrolyses and formation of carbonate leads to a depot effect (chemical available part) in the solution which results in a very selective sulphide precipitation. Lab scale tests have shown that the retention of the ZnAc solution reaches nearly 100% [Kleinhappl et Zeisler, 2010].

The gained sample is homogenised, filled in a volumetric flask and part of the sample is analysed selective to hydrogen sulphide by using methylene blue according to DIN 38 405-D26. With this method concentrations between 0.1 and 1.500 mg/l can be analysed.

### 4.3.3 Measurement of HCl

Especially HCl is very important for the behaviour concerning high temperature corrosion of the flue gases after co-firing of the pyrolysis gas. To detect hydrochloric acid in the pyrolysis gas there is also an absorption method used.



The hydrochloric acid can be detected in the pyrolysis gas by absorption of chlorine in deionised water. Therefore, a small part of the gas stream is separated from the pyrolysis gas stream and sucked through several wash bottles, which are filled with deionised water, by a piston pump. After this procedure the concentration of hydrochloric acid ions in the deionised water can be detected by IC according to DIN 38 405-D 19/D 20.

Four of the six wash bottles are filled with deionised water. The first bottle is filled with 50ml, the next two bottles each with 100ml and the fourth bottle is filled with 150ml. Wash bottle five and six are empty. The wash bottles are placed next to the gauge in a glycol/ethanol mix whose temperature is cooled down by a cryostatic temperature controller. The connection to the gauge is heated by an electric trace heating to prevent the pyrolysis oil vapours from condensing. To start the procedure a piston pump sucks the gas through the wash bottles. The volume of the gas is recorded by the pump. After the measurement procedure, the time of the procedure, the volume of pyrolysis gas sucked through the piston pump and the pyrolysis gas temperature is listed. With this data it is possible to calculate the load of hydrochloric acid in the pyrolysis gas stream.

## 4.4 Determination of the ash melting behaviour

For the possible usage of straw, as the main feedstock, or the pyrolysis char in a fluidised bed or another combustion system the ash melting behaviour was determined. Ash from biomass and other inorganic compounds do not have a definite melting point but can be described with four characteristic temperatures. Real melting begins after sintering in a more or less large temperature range and before becoming liquid the ash goes through several plastic and viscous states.

The determination of the ash thermal behaviour is standardized in DIN 51730 [DIN 51730, 2007]. The various stages of melting can be described as follows:

### **SIT: beginning of sintering**

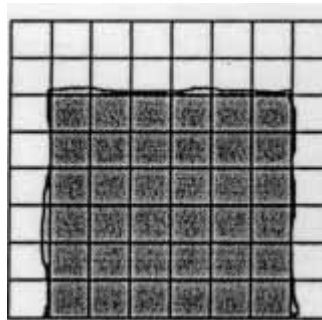


Figure 4-4: Ash melting – beginning of sintering (SIT)

Sintering describes a process, where single ash particles stick together. During this process the sample may change its original dimension without showing characteristics typical at the softening point.

### **SOT: beginning of softening**

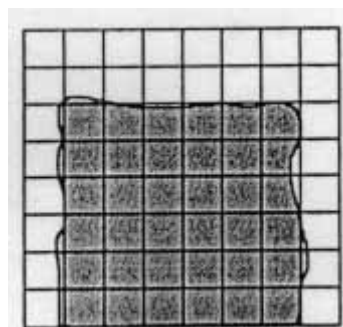


Figure 4-5: Ash melting – beginning of softening (SOT)

At the softening temperature the sample shows the first signs of softening, e.g. surface changes, the rounding of the edges are complete and the sample

starts filling out the gas volume between the particles. If the edges are still sharp, a shrinkage of the sample should not be regarded as softening.

**HT: hemispheric point**

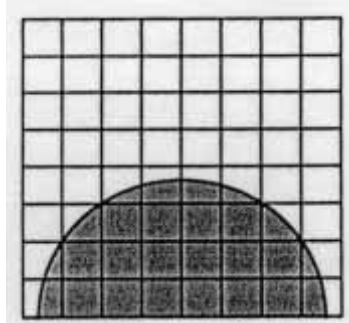


Figure 4-6: Ash melting – hemispheric point (HT)

The hemispheric point gives the temperature, when the sample shows the approximate form of a hemisphere. The height of the melted sample is approximate half the length of the base line.

**FT: flowing point**

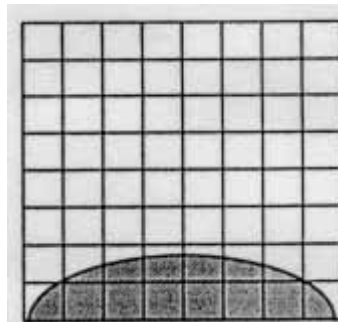


Figure 4-7: Ash melting - flowing point (FT)

At this temperature the sample has shrunk to one third of its original height.

## 5 Overall plant mass and energy balances

There are many measuring points for temperature, pressure and flow at the plant and the composition of pyrolysis gas, feedstock and char is also measured, but there are some parameters that cannot be measured. Such a value is for example the mass flow of the pyrolysis gas. Due to the trace heating of the pyrolysis gas pipe from the rotary kiln reactor to the afterburner, which is implemented by a pipe in pipe construction, the construction of a measuring orifice is not possible. In such a case the value has to be calculated. This can be done by a balance of the plant with the available data [Kern, 2010].

### 5.1 Process simulation

Process simulation is a tool for development and optimisation of technical processes. Process simulation ensures that mass and energy are brought into balance. The most significant advantage here is that unknown data can be calculated from measured values of the system. Simulation allows the prediction of the behaviour of a process based on mathematical models. The model equations are solved numerically by a computer. The quality of the simulation results depends on the model and the quality of the model parameters.

Sequential-modular or equation orientated process simulation programs are the two different options for solving of the numerical system that are in common use.

### 5.1.1 About IPSEpro

For calculation of mass and energy balances the process simulation and balance tool IPSEpro has been used in this work. IPSEpro is a stationary, equation orientated flow sheet simulation tool that has been developed for power systems [Perz, 1990]. Equation-oriented means that the model equations, together with the information from the flow sheet, form a system of equations, which is solved by numerical methods (e.g. Newton-Raphson-algorithm). Many other simulation tools, such as Aspen, solve all units sequentially, which means that material recycling leads to calculation circles and long calculation times. In contrast, the main advantage of the equation-oriented approach is its fast convergence with average calculation times being only a few seconds. This is of great importance when numerous calculation runs must be performed during parameter optimization, or if large and complex systems need to be analyzed. Stationary implies that the simulation result represents a steady state operating point of a plant. Thus, no time dependency is modelled, so dynamic system changes such as start up or shut down or the transition from one stationary state to another cannot be described.

Figure 5-1 shows some functional packages.

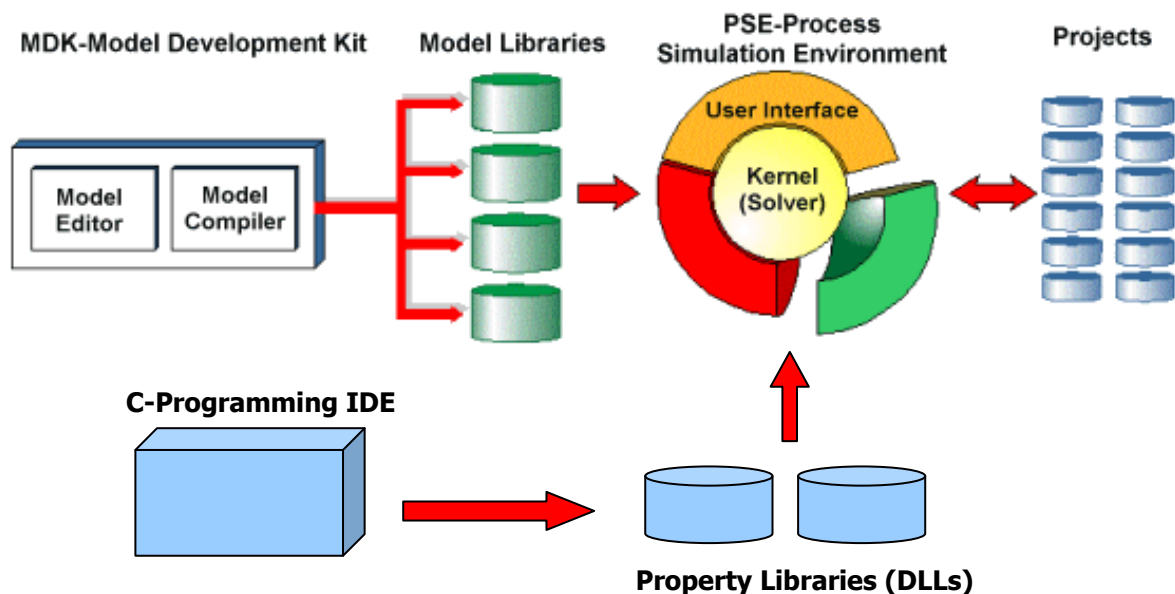


Figure 5-1: Structure of IPSEpro, adapted [SimTech, 2009]

The package PSE (process simulation environment) has a graphical interface for displaying the simulation flow sheet. The structure of the flow diagram, the simulation parameters and the initial values of the variables are stored in project files. The model equations of the individual process components are

available in a model library. Together with the structural parameters of the information and process flow diagram, an equation system can be established. The entire system is broken down into small groups that can be processed. For solving the subsystems there is a multidimensional Newton-Raphson method used. Good starting values are essential for the convergence of the non-linear models. External functions can be recalled from dynamic link libraries (DLL's). The integration of such features in the model equations is already defined in the model editor (MDK). The model development kit (MDK) is a standalone program, in which the base models of the process components can be created and changed. The model libraries are compiled and stored on the disk, ready to be used by PSE [Pröll, 2004].

## 5.2 System modelling

### 5.2.1 General approach

When creating mathematical models generally following steps are necessary:

- Setting of the area that has to be modelled (system boundaries)
- Compilation of relevant parameters for describing the system
- Establish mathematical relationships between the parameters

Thermodynamic processes are a composition of many standard components like heat exchangers, combustion chambers, mixer etc. For the modelling of these processes it is useful to utilise standardised structures for this components. This is why the so-called "units" combine all the mathematical equations that are designed to represent the components of the plant.

The complete model of the plant is a result of globals, units, streams and energetic links.

- Globals are not shown graphically in the diagram. They are present in the background and can be referenced by the other model classes. A typical application for globals is the chemical composition of a material flow. The advantage of using globals is the much smaller number of variables when multiple streams with the same composition in the process occur.
- Units describe the equipment of the plant and are represented by specific icons in the process simulation flow sheet. Mathematically a unit is a collection of all equations that describe a single part of the plant.
- Streams are connections that allow the transport of mass and energy. They define the state between two units (mass flow, thermodynamic properties, composition).
- Energetic links only allow energy transport like a shaft of an engine or a turbine.

A stream takes the information from a unit and provides it to other units. To connect two units by a stream means to set equal their thermodynamic and mass flow properties [Perz, 1990].



## 5.2.2 Modelling of the pyrolysis pilot plant

For modelling of the pilot plant in IPSEPro all the parts of the pilot are placed on a blank sheet in the process simulation environment and are connected by streams and energetic links in the way the piping and instrumentation flow sheets of the pilot plant show it (Figure 5-2).

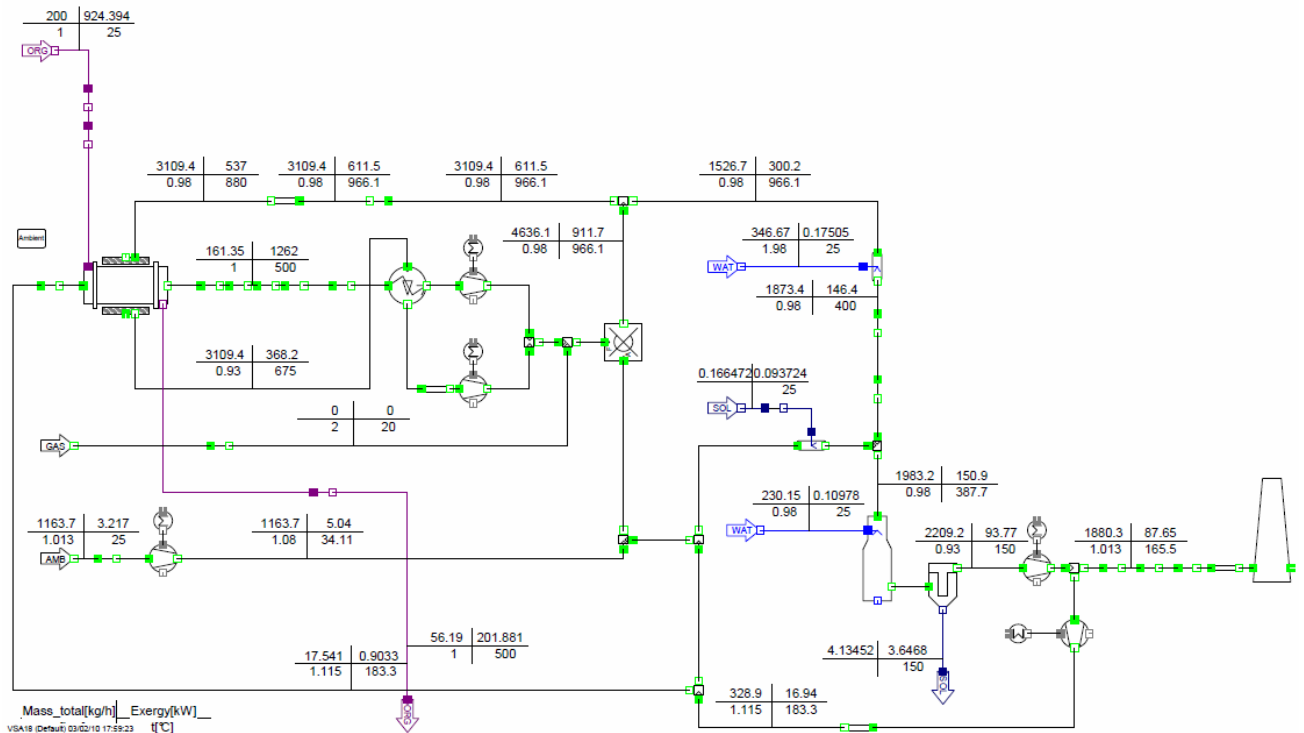


Figure 5-2: Process simulation flow sheet of the pilot plant in IPSEPro

For this work the basis library is the model library BG-LIB. This library has been developed and optimised at the Institute of Chemical Engineering at the Vienna University of Technology and it has been used successfully for several projects.

For creating the process simulation flow sheet of the pyrolysis pilot plant the following units have been used:

- u\_pyrol\_htd\_ - rotary kiln pyrolysis reactor
- u\_comb\_g\_ - fluidised bed combustion chamber that acts as an afterburner during pyrolysis operation
- u\_htex\_gg\_ - gas/gas heat exchanger – represents the trace heating of the pyrolysis gas pipe
- u\_compr\_g\_ - compressor/fan for air/pyrolysis gas/coldgas/recirculation gas, induced draught of off gas
- u\_mot\_el\_ - electric motor for compressor/fan
- u\_inj\_wg\_ - spraycooler
- u\_inj\_sg\_ - injection of  $\text{Ca}(\text{OH})_2$  for FGD
- u\_pipe\_g\_ - pipe element that represents the behaviour of long pipes (losses)
- u\_mixer\_g\_ - mixer, mixes two gas streams
- u\_splitter\_g\_ - splitter, splits a gas stream into two streams
- u\_desulf\_wet\_ - spray absorber for FGD
- u\_sep\_sg\_ - fabric filter for off gas
- u\_sink\_a\_ - stack

Most of the units are used very often in other projects and have been described elsewhere [Pröll, 2004]. One exception is the model for the rotary kiln reactor (u\_pyrol\_htd\_) that has been developed within this project [Kern, 2010] and will be described in more detail.

### Rotary kiln pyrolysis reactor

The unit for the rotary kiln pyrolysis reactor had to be created and integrated into the existing program. This unit is shown in Figure 5-3. The connections are listed and explained in Table 5-1.

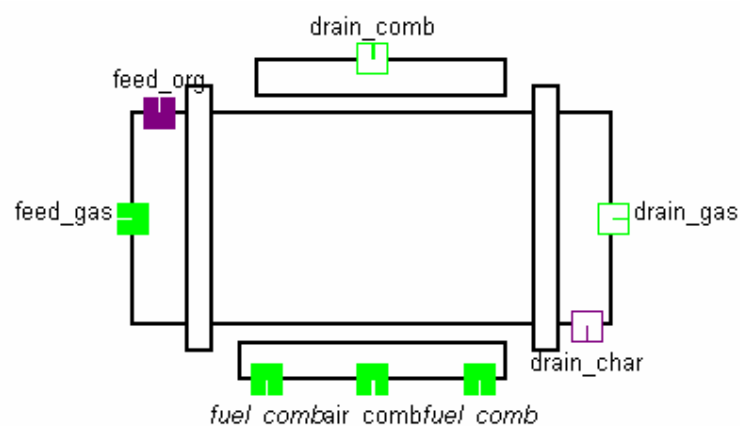


Figure 5-3: IPSEpro model of the rotary kiln pyrolysis reactor

Table 5-1: Connections of the unit u\_pyrol\_htd\_

Connection	used stream	description
drain_gas	c_st_g_	drain for gaseous pyrolysis products including volatile oils/tars/dust/flychar
feed_org	c_st_o_	feed of organic fuel into the pyrolysis reactor (containing inorganic ashes)
feed_gas	c_st_g_	feed for inert or active kiln medium (may be also set to zero)
drain_char	c_st_o_	drain for solid pyrolysis products containing organic char and inorganic ash
Air_comb	c_st_g_	feed of combustion air to external heating burner
fuel_comb	c_st_g_	gas fuel for combustion chamber of external heating
drain_comb	c_st_g_	drain of combustion exhaust gas of external heating

The stream c\_st\_g\_ contains a gas stream and the stream c\_st\_o\_ is a stream of organic matter.

The connection feed\_org is provided with the feedstock (solid biomass). The connection drain\_char is the outlet for the produced pyrolysis char. Drain\_gas is the connection of the rotary kiln reactor where the produced pyrolysis gas that also contains pyrolysis oil vapours, dust and flychar leaves the reactor. Feed\_gas is a connection that is used in the case of the pyrolysis pilot plant for inertisation of screw and lock that feed the biomass into the reactor. Recirculated flue gas is used for this purpose.

The connections air\_comb, fuel\_comb and drain\_comb are designed for heating of the reactor. Usually a fuel like natural gas would be fed trough the connection fuel\_comb into the jacket of the reactor and would be burned there to provide the desired heat. The model of the rotary kiln pyrolysis reactor in the library BG-LIB also allows the supply of heat by a hot medium without combustion in the reactor. Therefore, the inlet for the hot gas is the connection air\_comb and the outlet of the used gas is the connection drain\_comb. This is the way the required energy for pyrolysis is provided at the pilot plant in Dürnröhr.

## Basic data of the model:

- The model solves the mass and energy balances separately for pyrolyser and combustor for external heating.
- feed\_gas and air\_comb are pure gas streams (no dust, char, or tar allowed)
- drain\_gas and feed\_comb contain all of dust, char, and tar
- drain\_comb contains just dust but no char or tar
- feed\_org and drain\_char contain ash and require therefore different objects

Table 5-2 shows the variables which are used for the description of the pyrolysis reactor. Pressure drops, heat losses, mass fractions are for example used to provide a well fitting model.

Table 5-2: Variables of the rotary kiln pyrolysis reactor

Variable	Description
dp_air_comb	Pressure drop for the hotgas
dp_air_rel_comb	Relative pressure drop for the hotgas
dp_fuel_comb	Pressure drop from fuel gas to drain.
dp_fuel_rel_comb	Relative pressure drop for fuel based on feed pressure
P_th_comb	Thermal power of the combustion chamber based on lower heating values of all combustibles entering the reactor.
lambda_comb	Air ratio of the combustion chamber based on the amount of oxygen in air stream needed for stoichiometric combustion of all substances entering the combustion chamber (e.g. also combustibles entering with the air stream).
CO_slip_comb	Molar ratio between CO and CO <sub>2</sub> in flue gas.
Q_loss_comb	Heat loss of the external heating shell.
q_loss_rel_comb	Relative heat loss of the external heating shell in % of thermal fuel power of the combustion chambers.
Q_trans	Heat transfer power from external heating to pyrolyser
dp_feed_org	Pressure drop in pyrolysis reactor: organic feed to gas drain
dp_feed_org_rel	Relative pressure drop in pyrolysis reactor: organic feed to gas drain
dp_feed_gas	Pressure drop in pyrolysis reactor: gas feed to gas drain
dp_feed_gas_rel	Relative pressure drop in pyrolysis reactor: gas feed to gas drain
dp_drain_gas_char	Pressure difference of drain streams: $dp = p_{gas} - p_{char}$
dt_drain_gas_char	Temperature difference between gas and char drain
P_th_pyr	Thermal power of the fuel entering the pyrolyser based on lower heating value.
fract_char_bed	Mass fraction of ash free and water free fuel exiting the pyrolyser as char.
fract_char_pg	Mass fraction of the fuel exiting the pyrolyser as char with the pyrolysis gas (fly char).
fract_tar_pg	Mass fraction of the ash free and water free fuel exiting the pyrolyser as pyrolysis oil in the pyrolysis gas.
fract_fly_ash	Mass fraction of ash introduced with the fuel, which is exiting the pyrolyser as dust in the pyrolysis gas.
unconv_C	Conversion of carbon to gaseous compounds (gas and pyrolysis oil), solid carbon in both fly char and char drain in considered unconverted carbon
E_loss	Exergy loss in the gasifier considering all streams.

### 5.3 Calculating balances with the IPSEpro model

The main purpose of the established IPSEpro model of the pyrolysis pilot plant is to calculate balances of mass and energy at any operating point of the plant. Therefore, the measured values of the operating point that has to be calculated have to be provided. These values are imported into the model of the plant as measured values. An over-determined system of equations is the result of the data upload to the model. IPSEpro is able to calculate a balanced solution that contains the desired balance data of the plant.

Measured data is always afflicted with certain wobbliness. If a system that is already defined gets additional measured data, the system is over determined. In most of the cases this datasets do not coincide with each other exactly. For over determined systems a statement about the quality of the individual measurements is possible by confirmation of plausible values and disagrees of obvious erroneous values with the balance of the plant model. This system of equations is converted by use of the method of Lagrange multipliers into a form that can be solved by the simulation tool. The method for solving this system is described in more detail in a previous work [Pröll, 2004].

$$\sum_i \left( \frac{x_i - \bar{x}_i}{tol_{x_i}} \right)^2 \rightarrow Min \quad (5-1)$$

Needed measured values are the composition of pyrolysis gas, pyrolysis oil, feedstock and char and operating data of streams and devices (temperatures, pressures, flows) that are recorded by the process control system.

Table 5-3 shows the measured values from the pilot plant that are recorded by the process control system. These values are used for the IPSEpro balance. Each measuring point has its own KKS number (power station designation system) that is the identification in the process control system. That means if the KKS number is known the wanted data can be found in the archive. The KKS number is also the name of the measuring points in the piping and instrumentation flow sheet of the plant.

Table 5-3: Measurements used for the IPSEpro balance and their associated KKS number

KKS number	name	unit
89HHG10CF901/89HHG10CF901.OAver	Flow rate natural gas	Nm <sup>3</sup> /h
89ECA20CT001/MES.Oval	Temperature biomass feedstock	°C
89RAA10CT011/MES.Oval	Temperature char after RKR	°C
89HLA10CF001/MES.Oval	Flow rate air before fan	Nm <sup>3</sup> /h
89HLA10CT001/MES.Oval	Temperature air before fan	°C
89HLA20CT001/MES.Oval	Temperature air after fan and preheater	°C
89RHA10CT901/89RHA10CT901.OAver	Temperature pyrolysis gas after RKR	°C
89HBK20CT903/89HBK20CT903.OAver	Temperature combustion fluidised bed outlet	°C
89HRA10CT901/89HRA10CT901.OAver	Temperature after spray type cooler	°C
89HRA10CQ901/89HRA10CQ901.OAver	O <sub>2</sub> content (dry) after spray type cooler	%
89HRA10CT901/MES.Oval	Temperature after spray absorber	°C
89HTE10CT001/MES.Oval	Temperature after fabric filter	°C
89HNF10CT001/MES.Oval	Temperature recirculation gas	°C
Calculated	Flow rate recirculation gas to RKR	Nm <sup>3</sup> /h
Calculated	Flow rate recirculation gas to fb	Nm <sup>3</sup> /h
89HTE10CF001/MES.Oval	Flow rate flue gas after fabric filter	Nm <sup>3</sup> /h
89HNE10CF011/MES.Oval	Flow rate flue gas at stack	Nm <sup>3</sup> /h
89RAN10CT007/MES.Oval	Temperature hotgas to RKR	°C
89RAN10CT008/MES.Oval	Temperature coldgas after RKR	°C
89RAN10CT004/MES.Oval	Temperature coldgas after fan	°C
89HNE10CT001/MES.Oval	Temperature flue gas at stack	°C
89HNE10CQ001/MES.Oval	O <sub>2</sub> content at stack	vol. %
89HNE10CQ002/MES.Oval	CO <sub>2</sub> content at stack	vol. %
89HNE10CQ003/MES.Oval	Water content at stack	vol. %
89HLA20CP001/MES.Oval	Pressure after air fan	mbar
89HBK20CP901/89HBK20CP901.OAver	Pressure at top of fb	mbar
89HRA10CP001/MES.Oval	Pressure after spray type cooler	mbar
89HRB10CP001/MES.Oval	Pressure after spray absorber	mbar
89HTE10CP901/89HTE10CP901.OAver	Pressure after fabric filter	mbar
89HNF10CP001/MES.Oval	Pressure of recirculation gas	mbar
89RAN10CP001/MES.Oval	Pressure coldgas after RKR	mbar
89RAA10CP901/MES.Oval	Pressure inside the RKR	mbar
89HNE20CQ002/MES.Oval	CO <sub>2</sub> content of the pyrolysis gas	%
89HNE20CQ001/MES.Oval	CO content of the pyrolysis gas	%
89HNE20CQ003/MES.Oval	H <sub>2</sub> content of the pyrolysis gas	%
89HNE20CQ004/MES.Oval	CH <sub>4</sub> content of the pyrolysis gas	%
89HNE20CQ005/MES.Oval	O <sub>2</sub> content of the pyrolysis gas	%

## Abbreviations:

RKR ... rotary kiln reactor

fb ... fluidized bed

This dataset can be read out of the process control system for every single day. The values are arithmetic mean values of one, two or five minutes. Every single measurement has a certain tolerance. The knowledge of this tolerance is also necessary for IPSEpro to calculate a balanced solution. A large tolerance means that the corresponding values are adjusted in a larger area.

That means that a huge amount of data has to be transferred to IPSEpro for the calculation of every operating point of the pilot plant.

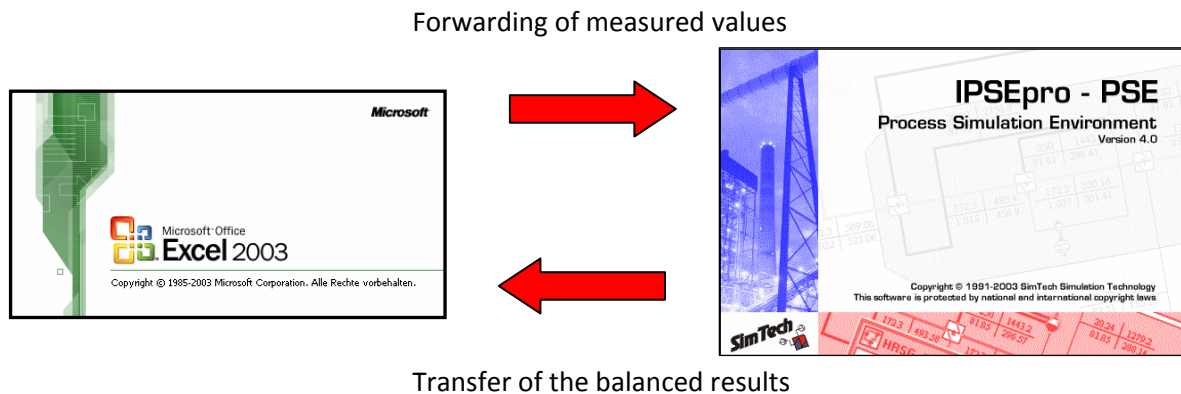


Figure 5-4: Illustration of the communication between IPSEpro PSE and Microsoft Excel [Kern, 2010]

All the data of the process control system and the measured compositions of gas, oil, feedstock and char are imported in an Excel file. In this file there is a sheet where the data has to be chosen that should be transferred to the simulation tool. Using a VBA macro, Excel converts the data into a form IPSEpro can handle. This file can be imported (project/import/validation, Text) to the model file. After calculating a balanced solution the results can be exported (project/export/simple text) from the simulation tool to the Excel file again (Figure 5-4). For every value the balanced solution can be seen in the file, the relative error and if the value was adjusted or not. The balanced solutions can be processed further if it is necessary. A protocol with the results (stream data, etc.) is generated automatically. The protocols for the balanced results (450°C, 500°C, 550°C, 600°C) can be found in the appendix (cf. 9.6).

### 5.3.1 Calculating the pyrolysis oil elemental composition

For an accurate result of the IPSEpro calculation there is also the composition of the pyrolysis oil required. The composition of the pyrolysis oil is analysed by a GC-MS, so the GC-MS measurable part is known.

The results of the GC-MS measurement are the fractions of the different (mostly aromatic) compounds that contain the pyrolysis oil. But the simulation tool needs the composition of the pyrolysis oil given in mass per cent of carbon, oxygen, hydrogen, sulphur, nitrogen and chlorine. So the results of the GC-MS analysis have to be converted in the required form. This happens by an Excel script that is designed for this purpose [Kern, 2010]. The result of the GC-MS analysis can be transferred by copy and paste to this sheet and the elementary composition is calculated (Table 5-4 and Table 5-5).

Table 5-4: Extract of the result from the GC-MS analysis [Kern, 2010]

Probe:	100	Teerkonzentration (mg/Nm3)					
#	Name	Messung 1	Messung 2	Messung 3	Endergebnis	Standardabw	rel. Std.abw
	<b>Teerbestandteile Summe</b>	37450.51	37194.79	37875.73	37475.01	343.96	0.92%
1	<b>1,2,3,4-Tetrahydronaphthal</b>	int. Std.	int. Std.	int. Std.	int. Std.		
2	Phenylacetylen	0.00	0.00	0.00	0.00	0.00	
3	<b>Styrol</b>	1747.97	1760.28	1766.80	<b>1758.35</b>	9.56	0.54%
4	<b>Mesitylen</b>	115.18	135.46	133.29	<b>127.98</b>	11.14	8.70%
5	<b>Phenol</b>	7278.00	6988.24	7333.05	<b>7199.76</b>	185.24	2.57%
6	Benzaldehyd	0.00	0.00	0.00	0.00	0.00	
7	<b>Benzofuran</b>	733.81	744.68	770.03	<b>749.51</b>	18.59	2.48%
8	<b>Inden</b>	1566.87	1561.07	1500.22	<b>1542.72</b>	36.92	2.39%
9	<b>2-Methylphenol</b>	4812.16	4693.36	4946.89	<b>4817.47</b>	126.85	2.63%
10	<b>4-Methylphenol</b>	5294.60	5343.14	5350.38	<b>5329.38</b>	30.33	0.57%
11	<b>2-Methylbenzofuran</b>	350.61	327.43	362.92	<b>346.99</b>	18.02	5.19%
12	Guajacol	0.00	0.00	0.00	0.00	0.00	
13	<b>2,6-Dimethylphenol</b>	947.51	968.52	996.77	<b>970.93</b>	24.72	2.55%
14	<b>2,5-Dimethylphenol</b>	1265.52	1178.59	1122.81	<b>1188.97</b>	71.92	6.05%
15	<b>2,4-Dimethylphenol</b>	1869.66	1884.88	2016.72	<b>1923.75</b>	80.87	4.20%
16	<b>3,5-Dimethylphenol</b>	4583.97	4582.52	4649.17	<b>4605.22</b>	38.07	0.83%
17	2,3-Dimethylphenol	0.00	0.00	0.00	0.00	0.00	
18	<b>3,4-Dimethylphenol</b>	813.50	832.33	831.61	<b>825.81</b>	10.67	1.29%
19	2-Methoxy-4-Methylphenol	0.00	0.00	0.00	0.00	0.00	
20	<b>Naphthalin</b>	933.75	956.93	987.35	<b>959.34</b>	26.88	2.80%
21	1-Benzothiophen	0.00	0.00	0.00	0.00	0.00	
22	<b>2-Methylnaphthalin</b>	1484.29	1453.86	1435.03	<b>1457.72</b>	24.86	1.71%
23	Isochinolin	0.00	0.00	0.00	0.00	0.00	
24	<b>1-Methylnaphthalin</b>	1021.40	1027.92	1027.92	<b>1025.74</b>	3.76	0.37%
25	Eugenol	0.00	0.00	0.00	0.00	0.00	
26	<b>Indol</b>	494.04	528.81	512.87	<b>511.91</b>	17.41	3.40%
27	<b>Biphenyl</b>	354.23	350.61	352.06	<b>352.30</b>	1.82	0.52%
28	Isoeugenol	0.00	0.00	0.00	0.00	0.00	
29	<b>Acenaphthylen</b>	770.03	766.41	770.76	<b>769.07</b>	2.33	0.30%
30	<b>Acenaphthen</b>	299.90	299.90	296.28	<b>298.69</b>	2.09	0.70%

Table 5-5: Result of a conversion to elemental pyrolysis oil composition

C	H	O	N	S	Cl
80.867	7.174	10.868	0.163	0.000	0.000



## 6 Experimental and simulation results

The main fuel for the pyrolysis pilot plant at coal fired power station Dürnröhr is straw but due to the fact that there is also a broad range of different other biomasses available the following chapters do not only focus on the usage of wheat straw but also consider different biomasses which have been under investigation.

Following biomasses are considered in this work:

- wheat straw (indoor stored)
- straw pellets
- sorghum straw
- miscanthus straw
- reed straw
- palm nut shells
- Waldviertler energy grass (WVE)
- paper residual material

For the balancing considerations indoor stored wheat straw was chosen because of the fact that it was available in huge amounts and its elemental composition and water content stays nearly constant.

The elemental composition of the different pyrolysis char samples was also an important point. Attention was also given to the composition of the pyrolysis oils and the pyrolysis gas.

Ammonia, hydrogen chloride and hydrogen sulphide analysis have been carried out to get an insight in the quality of the pyrolysis gas. For a further thermal usage of the pyrolysis char the ash melting behaviour was also determined.

The distribution of the chemical elements of the feedstock in pyrolysis gas, oil and char is an important point within the following chapters.

Furthermore, the amounts of gas, oil and char for different pyrolysis temperatures are also of great interest.

At last the results, gained from the measurements and the balancing, were used to calculate the efficiency of the pilot plant and the pyrolysis process.

## 6.1 Fuel and pyrolysis char analysis

Under the aspect of a possible energy production from agricultural residues a broad range of different lignocellulosic biomass was selected. Figure 6-1 shows the selected biomasses and for comparison reasons also a paper residual material.



Figure 6-1: Different fuel samples:(1) palm nut shells, (2) reed straw, (3) sorghum straw, (4) straw pellets, (5) miscanthus, (6) Waldviertler energy grass, (7) paper residual material



Figure 6-2 shows the different biomass samples after the pyrolysis process – the so called pyrolysis char.



Figure 6-2: Different pyrolysis char samples from the pilot plant:(1) palm nut shells, (2) reed straw, (3) sorghum straw, (4) straw pellets, (5) miscanthus, (6) Waldviertler energy grass, (7) paper residual material

As already mentioned the knowledge about the substances in the char that are formed during the pyrolysis process is of great importance. So the pyrolysis char can be compared with the used feedstock and as a result the enrichment of the undesired substances in the pyrolysis gas (Cl, K, Na) can be checked.

A whole overview about the results of the fuel and pyrolysis char analyses (dry matter) can be found in the appendix (Table 9-8 and Table 9-9).

For the composition of the pyrolysis char which is produced in the pilot plant two plant settings are of major importance, the pyrolysis temperature and the residence time which is controlled by the rotational speed.

Table 6-1 shows the settings of the pilot plant which have the most influence on the composition of the pyrolysis char. The values are mean values which have been calculated from data which was collected during the sampling period.

Table 6-1: Plant settings during the sampling period of the different pyrolysis char samples

	Pyrolysis temperature [°C]	Speed of the rotary kiln [%]
palm nut shells char	574	36
reed straw char	540	24
sorghum char	555	30
straw pellets char	573	54
miscanthus char	563	42
Waldviertler energy grass char 560°C	560	59
paper residual char	555	28
Waldviertler energy grass char 500°C	500	32

### 6.1.1 Carbon content and LHV

Cellulose, hemicellulose and lignin mainly consist of carbon, oxygen and hydrogen, which are the most important elements in thermochemical utilisation processes. Figure 6-3 shows the carbon content and the lower heating value referred to dry matter (dm) of different fuel samples. The carbon content is between 315900 mg/kg (paper residual) and 530400 mg/kg (palm nut shells). For the gramineous types of biomass the carbon content is in the range of 463200 to 504200 mg/kg. The only exception within the observed gramineous fuel samples is reed straw. This sample was already affected from biological decomposition and also contained various types of non specified biomass and waste, therefore, the content of carbon is lower (423700 mg/kg). Due to the fact that higher carbon content means higher heating value the lower heating value (LHV) follows the trend of the carbon content. The highest LHV is in the range of 19 MJ/kg (palm nut shells) and the lowest is in the range of 9.8 MJ/kg (paper residual).

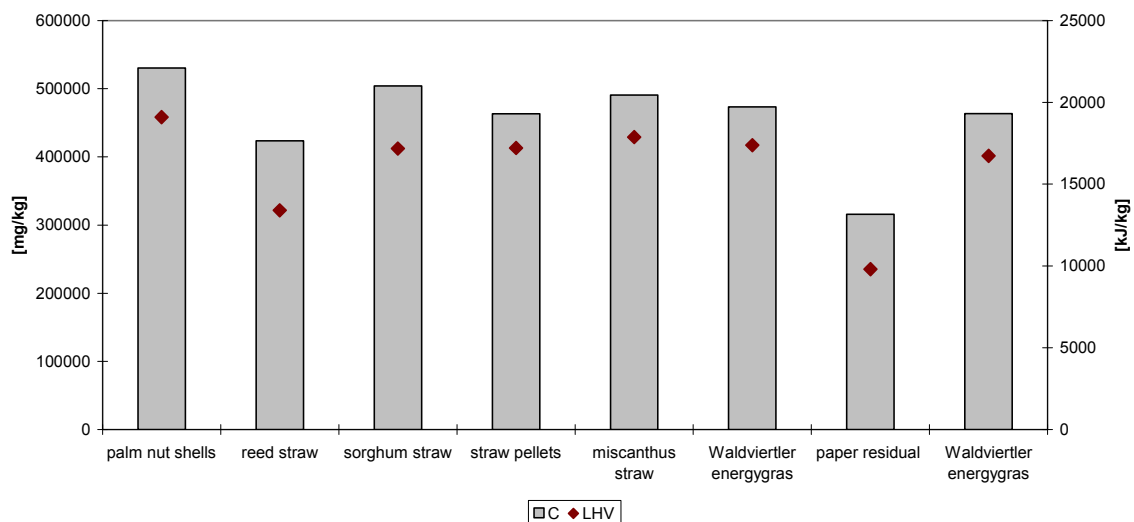


Figure 6-3: Carbon content and LHV of different fuel samples (dm)

Figure 6-4 shows the carbon content and LHV of samples of char for the same fuels as shown in Figure 6-3. Comparing Figure 6-3 and Figure 6-4 it is obvious that the fuel samples have a lower heating value than the pyrolysis char samples. The reason for this is that the lower heating value is linked with the carbon content by the combustion reaction.



Figure 6-4: Carbon content and LHV of different pyrolysis char samples (dm)

Due to the pyrolysis process the carbon content in the pyrolysis char samples is enriched and rises up to 845000 mg/kg (palm nut shells). This corresponds with the measured LHV which is in the range of 31.4 MJ/kg. For the gramineous types the carbon content ranges from 70000 to 770000 mg/kg this fits with the LHV which is in the range of 26.8 to 30 MJ/kg. Due to the above mentioned facts the carbon content of the reed straw sample only rises to 459600 mg/kg and the LHV to 16.5 MJ/kg. The carbon content and the LHV of the paper residual material char does not really differ from the fuel sample this means that paper residual material is not appropriate for a usage in the present pyrolysis process.

Figure 6-5 shows the correlation of the carbon content and the LHV of the different pyrolysis char samples. It is obvious that with increasing carbon content the LHV is also increasing because of the fact that higher carbon content means higher heating value. Therefore the lower heating value (LHV) follows the trend of the carbon content.

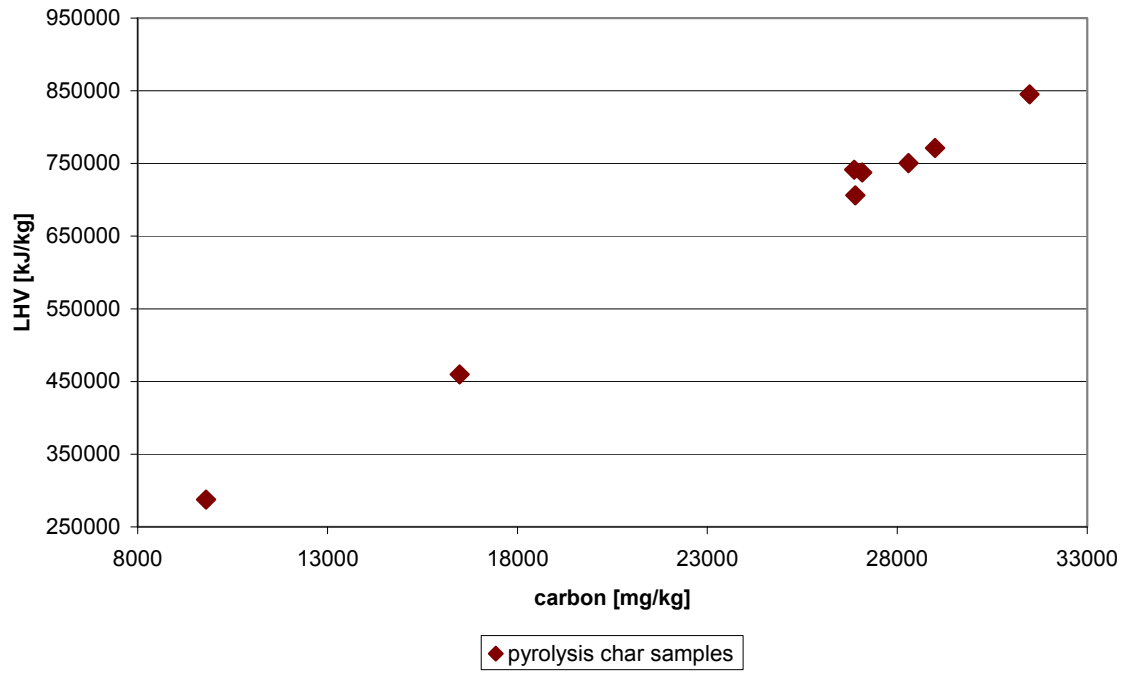


Figure 6-5: Correlation of carbon content and LHV of pyrolysis char samples

### 6.1.2 Volatiles

Volatiles are products of decomposition of the organic matter. The percentage of the volatiles from the total of lignocellulosic based fuels is in the range of 74 to 83 % dry matter [Hofbauer, 2006].

The content of volatiles concerning the fuel samples (dm) is shown in Figure 6-6. The fuel samples have a content of volatiles ranging from 62.9 wt. % (reed straw) to 84.3 wt. % (miscanthus straw).

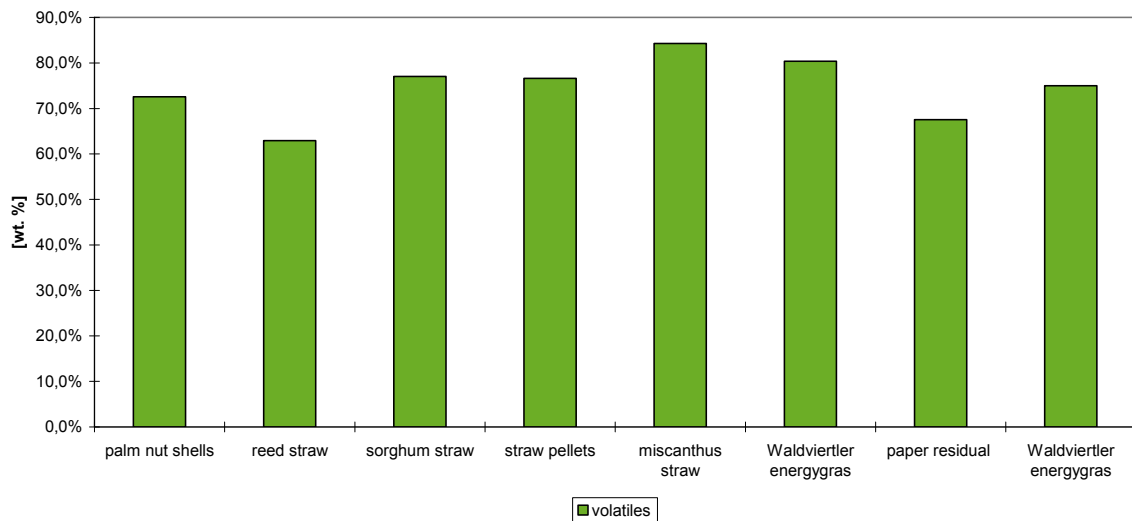


Figure 6-6: Content of volatiles of different fuels (dm)

Figure 6-7 shows the content of volatiles of the different pyrolysis char samples. The volatiles are ranging from 8.6 to 17.1 wt. % depending on the type of fuel and degree of devolatilisation by the pyrolysis process.

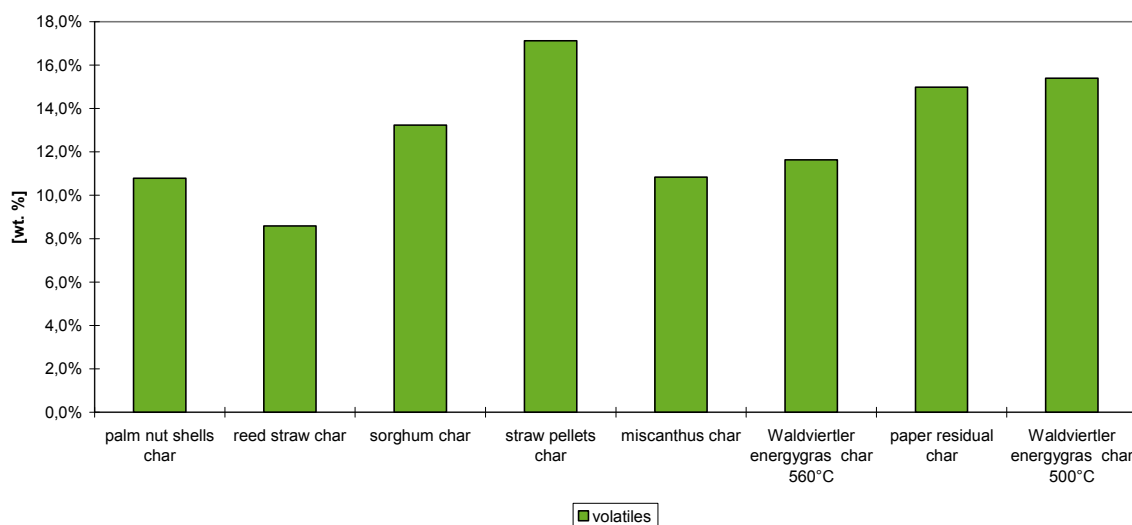


Figure 6-7: Content of volatiles of different pyrolysis char samples (dm)



### 6.1.3 Ash content

The ash content of reed straw is in the range of 27.3 wt. % This is high value is due to the fact that this sample was already affected from biological decomposition and also contained various types of non specified biomass and waste. The paper residual material shows also a very high ash content (41.3 wt. %) because of the used fillers and pigments. The ash content of the other fuels is in the range of 2.7 to 6.9 wt. %. For two fuel samples (straw pellets, miscanthus straw) the ash content was not analysed.

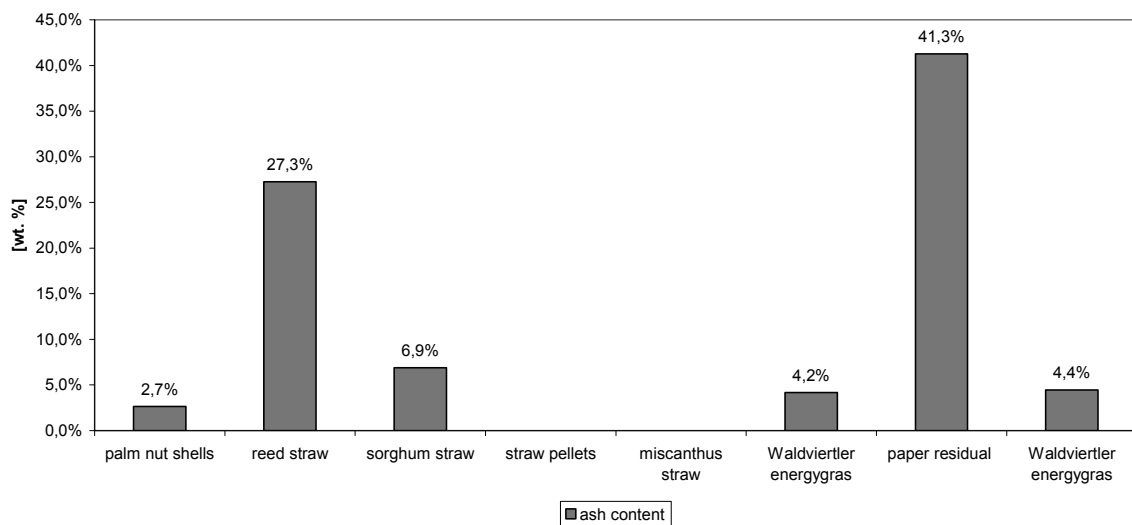


Figure 6-8: Ash content of different fuels (dm)

Figure 6-8 shows the ash content of the different pyrolysis char samples.

For two pyrolysis char samples (straw pellets, miscanthus straw) the ash content was not analysed due to problems with the measurement system.

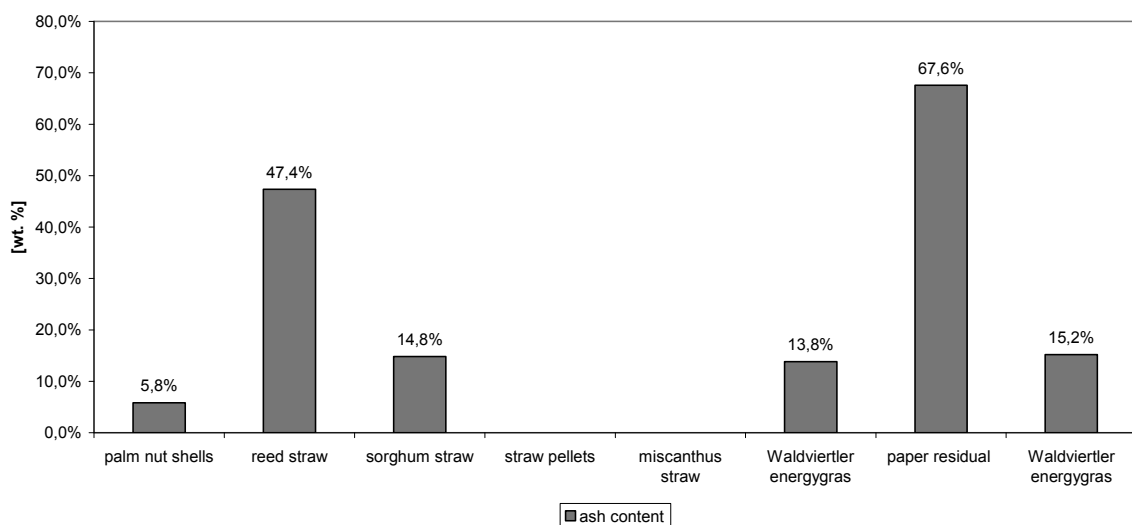


Figure 6-9: Ash content of different pyrolysis char samples (dm)

The ash content in char is higher than in the fuel samples because of the enrichment of the mineral compounds in the char. The high ash values of the two fuels (reed straw, paper residual) are reflected in the pyrolysis char samples.

### 6.1.4 Elemental analysis

The pyrolysis process causes an enrichment of potassium, chlorine, sulphur, sodium and nitrogen in the char. This enrichment is wanted because in this way those elements are partly avoided to be released to the pyrolysis gas. Especially chlorine, sodium, potassium and sulphur can lead to corrosion in the gas pipes as well as in the reactor and heat exchanger surfaces (cf. 2.6.3). The elemental analysis of the different feedstock's and pyrolysis char samples is displayed and discussed in the following chapters. Hydrogen (H), nitrogen (N), sulphur (S), chlorine (Cl), potassium (K), and sodium (Na) were analysed.

#### 6.1.4.1 Hydrogen

Hydrogen is an essential component of the biomass which is used during reactions (photosynthesis) and part of a wide variety of structures (cellulose, hemicellulose, lignin). Figure 6-10 shows the content of hydrogen for the different fuel samples (dm). The hydrogen content is in the range of 37400 mg/kg to 59200 mg/kg and differs not very much among the different fuel samples.

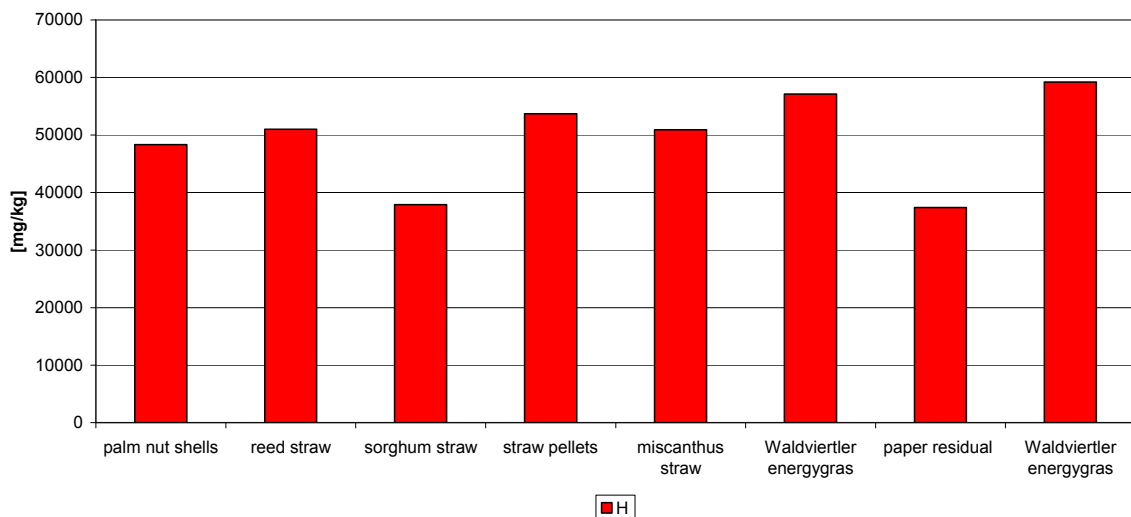


Figure 6-10: Hydrogen content of different fuel samples (dm)

Hydrogen decreases in the pyrolysis char samples because of separation reactions during depolymerisation and can be found in the pyrolysis gas.

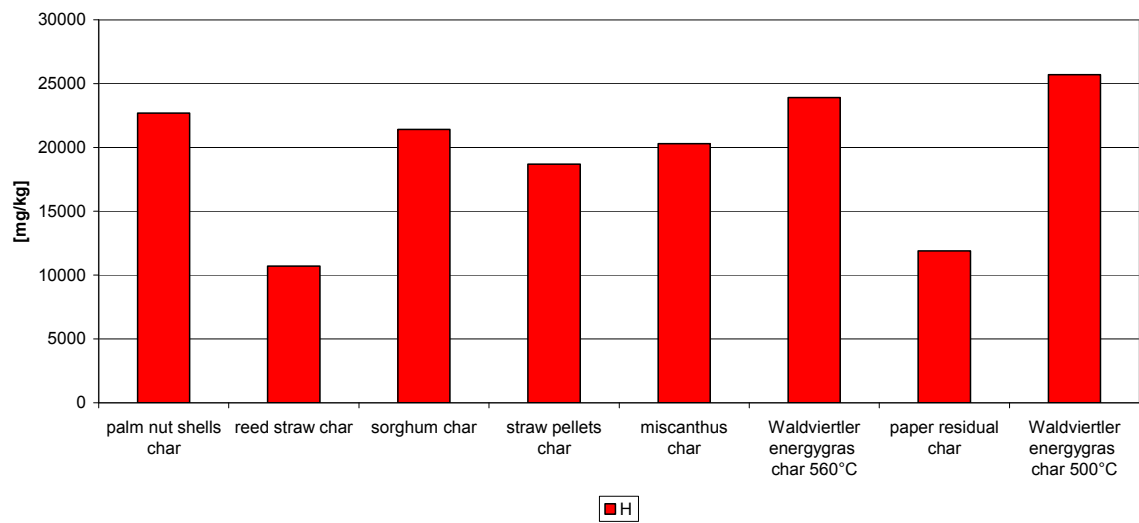


Figure 6-11: Hydrogen content of different pyrolysis char samples (dm)

Figure 6-11 shows the hydrogen content of different pyrolysis char samples (dm). Hydrogen decreases and, therefore, the content ranges from 10700 to 25700 mg/kg. Most of the hydrogen is released into the volatiles. Hrbek [Hrbek, 2005] showed that after the biomass pyrolysis at a temperature of about 800 °C only very small amounts of hydrogen were detected in the pyrolysis char.

#### 6.1.4.2 Nitrogen

Figure 6-12 shows the content of nitrogen for the different fuel samples (dm). The nitrogen content is in the range of 1000 mg/kg to 8500 mg/kg. The concentration of nitrogen varies widely with the biomass type. Nitrogen is an essential nutrient for the biomass growth. It is incorporated in biomass as biopolymers, in a wide variety of structures such as proteins, DNA, RNA, alkaloids, porphyrin and chlorophyll [Tian et al., 2004].

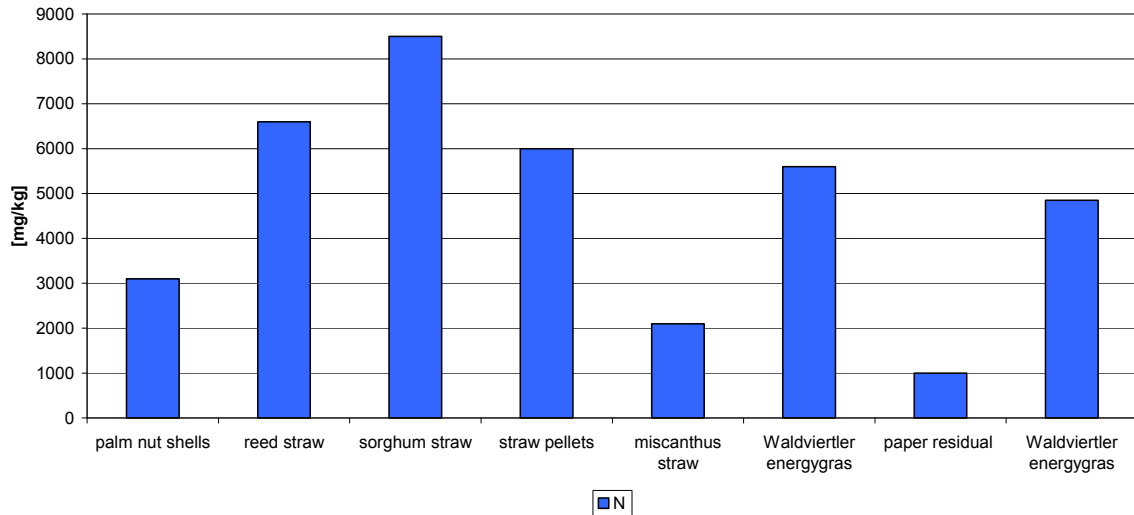


Figure 6-12: Nitrogen content of different fuel samples (dm)

Both the aliphatic and the heteroaromatic N-containing structures may be found in biomass. Plants or part of plants with high protein content have generally higher nitrogen content than typical lignocellulosic materials like wood or straw [Hofbauer, 2006].

Figure 6-13 shows the content of nitrogen for the different pyrolysis char samples. The nitrogen content is in the range of 1000 mg/kg to 12600 mg/kg.

Compared to Figure 6-12 nitrogen is increasing in the pyrolysis char samples. The biggest enrichment, from 5600 to 12600 mg/kg, could be seen for Waldviertler energy grass at a pyrolysis temperature of 560°C.

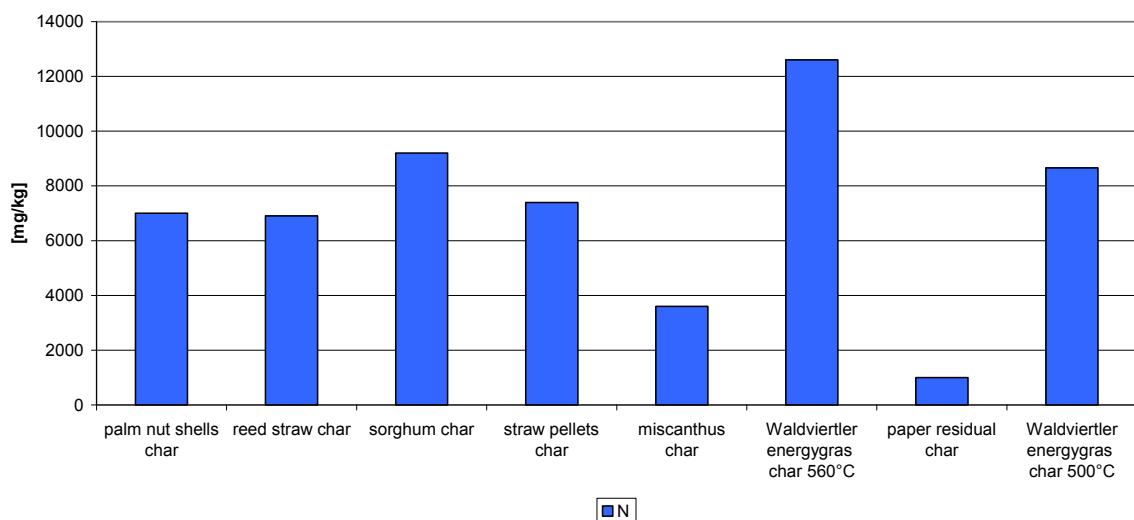


Figure 6-13: Nitrogen content of different pyrolysis char samples (dm)

Nitrogen in the volatiles is bond mostly as HCN and NH<sub>3</sub>, these are two important gaseous NO<sub>x</sub> precursors formed during the pyrolysis of biomass. The

formation of  $\text{NH}_3$  requires the presence of a condensed phase (s) formed by carbonaceous materials rich in hydrogen. The thermally less stable N-containing structures are mainly responsible for the formation of HCN, the thermally more stable N-containing structures may be slowly hydrogenated by the H radicals to  $\text{NH}_3$ . The formation of HCN and  $\text{NH}_3$  are controlled by the local availability of the radicals, particularly the H radicals, in the pyrolysis solid. [Li et Tan, 2000]

### 6.1.4.3 Sulphur

Sulphur is a macronutrient required for plant growth and is increasingly being recognized as the fourth major plant nutrient after nitrogen, phosphorus and potassium [Tandon, 1991]. Sulphur is a component of essential amino acids and plays an important role in the formation of proteins and glucosinolates. Figure 6-14 shows the content of sulphur for the different fuel samples (dm). The sulphur content is in the range of 200 mg/kg to 1300 mg/kg. For two fuel samples (straw pellets, miscanthus straw) the sulphur content was not analysed due to problems with the measurement system. The concentration of the sulphur based proteins (methionin, cystin, cystein) and the glucosinolates (e.g. mustard oil) is responsible for the difference in the sulphur content [Kaltschmitt et al., 2009].

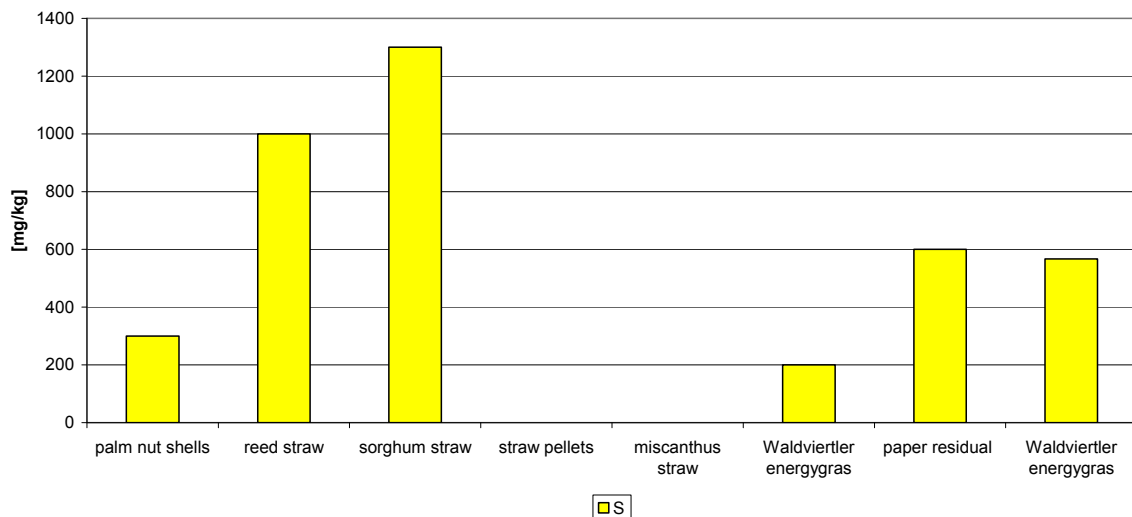


Figure 6-14: Sulphur content of different fuel samples (dm)

Figure 6-15 shows the content of sulphur for the different pyrolysis char samples. The sulphur content is in the range of 300 mg/kg to 1500 mg/kg. For two pyrolysis char samples (straw pellets, miscanthus straw) the sulphur content was not analysed due to problems with the measurement system. Compared with Figure 6-14 the char shows a slight increase in sulphur content. Two samples (reed straw, Waldviertler energy grass 560 °C) show a decreasing of the sulphur content. A significantly decrease could be recognized for reed straw which could be explained by the fact that this sample was already affected from biological decomposition and also contained various types of non specified biomass and waste.

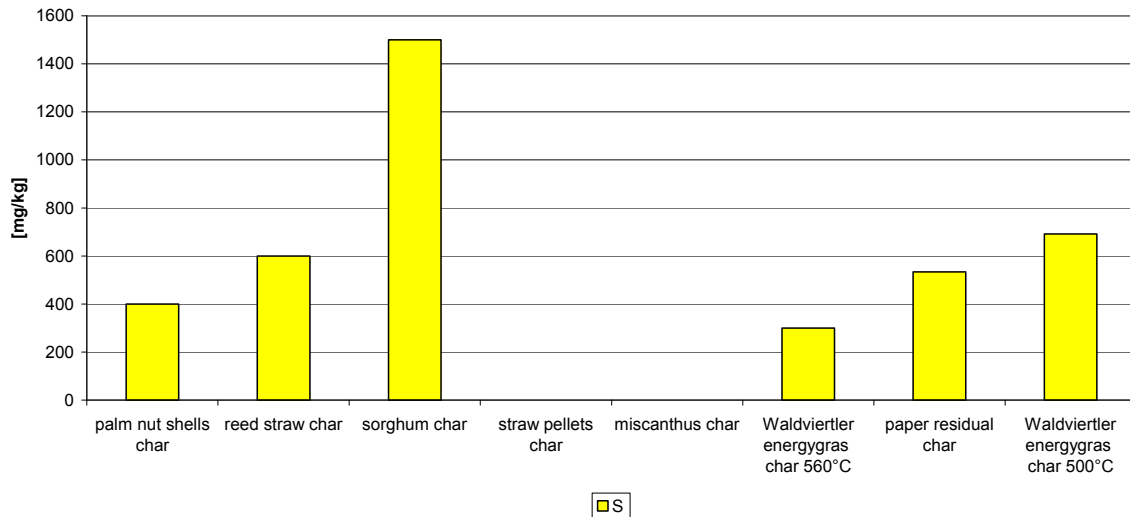


Figure 6-15: Sulphur content of different pyrolysis char samples (dm)

Lang et al recorded that up to 50 per cent of total S from eight biomass types was lost during pyrolysis at 500°C [Lang et al., 2005]. At higher temperatures (500 °C to 700 °C), the residual S contents of biochar did not change significantly.

#### 6.1.4.4 Chlorine

Chlorine is a naturally abundant element and is taken up by plants in the form of chloride ion,  $\text{Cl}^-$ . Chlorine in plants occurs mainly as a free anion or is loosely bound to exchange sites. In addition, a number of chlorinated organic compounds have been found in plants, however, the functional requirement for plant growth of most of these compounds is not known. Chlorine plays an essential role in a number of processes, including the opening and closure of stomata. Similar to potassium, chloride has high mobility within the plant, and average chlorine content in plants ranges from 0.2 - 2.0 % of dry plant weight. The supply of chlorine can be from a variety of sources including irrigation water, rain, fertilizers, and air pollution generally exceeds the plant's growth requirements, and therefore concerns exist about chlorine toxicity in plants rather than chlorine deficiency [Marschner, 1993].

Figure 6-16 shows the content of chlorine for the different fuel samples (dm). The chlorine content is in the range of 100 mg/kg to 3500 mg/kg. For two fuel samples (straw pellets, miscanthus straw) the chlorine content was not analysed. The difference of chlorine content between the fuels is due to the above mentioned broad variety of chlorine sources.



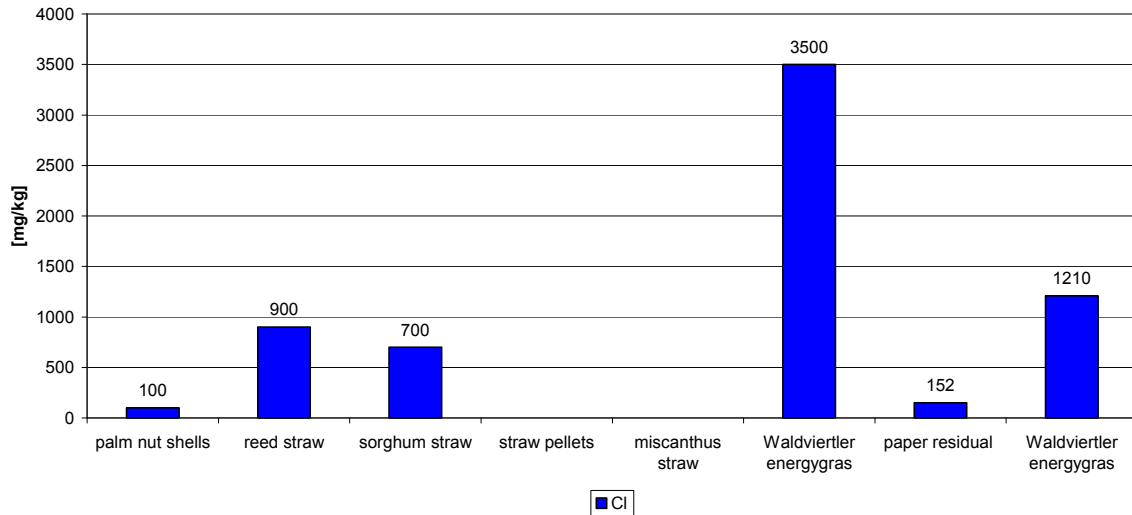


Figure 6-16: Chlorine content of different fuel samples (dm)

Figure 6-17 shows the content of chlorine for the different pyrolysis char samples (dm). The chlorine content is in the range of 100 mg/kg to 4100 mg/kg. For two pyrolysis char samples (straw pellets, miscanthus straw) the chlorine content was not analysed. As it can be seen from Figure 6-17 the chlorine content in char increases.

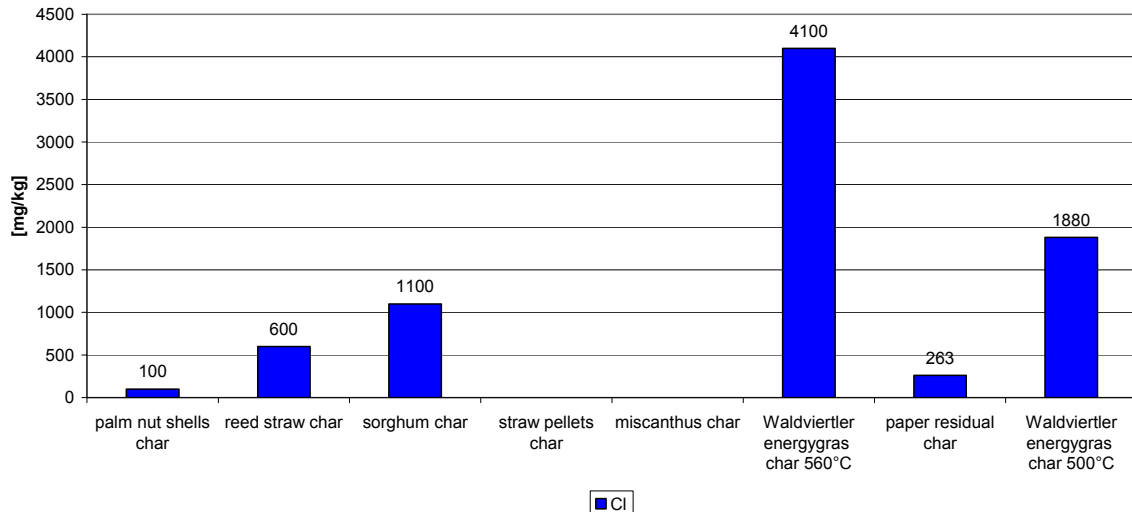


Figure 6-17: Chlorine content of different pyrolysis char samples (dm)

The chlorine in the biomass strongly influences the behaviour of other elements. In the presence of Cl and S the volatilisation temperatures of some heavy metals, especially Cd, Cu, and Pb are lower than in the absence of these elements and their species. The evaporation test performed by Lindt et Kauppinen [Lindt et Kauppinen, 1999] showed that without chlorine, virtually no evaporation of the heavy metals was observed, whereas the tests with

chlorine clearly showed a significant evaporation following the behaviour of the ashes.

Investigations have shown that the first amount of chlorine is released between 200 °C and 400 °C, and most of the residual chlorine is released when temperatures increase from 700 °C to 900 °C (cf. Figure 6-50) [Wei et al., 2002], [Wei et al., 2005], [Jensen et al., 2000], [Björkman et Strömberg, 1997].

Figure 6-18 shows a comparison of chlorine release during pyrolysis of different biomass samples. It can be seen, that the results measured by Hrbek [Hrbek, 2005] correspond well with the data from literature.

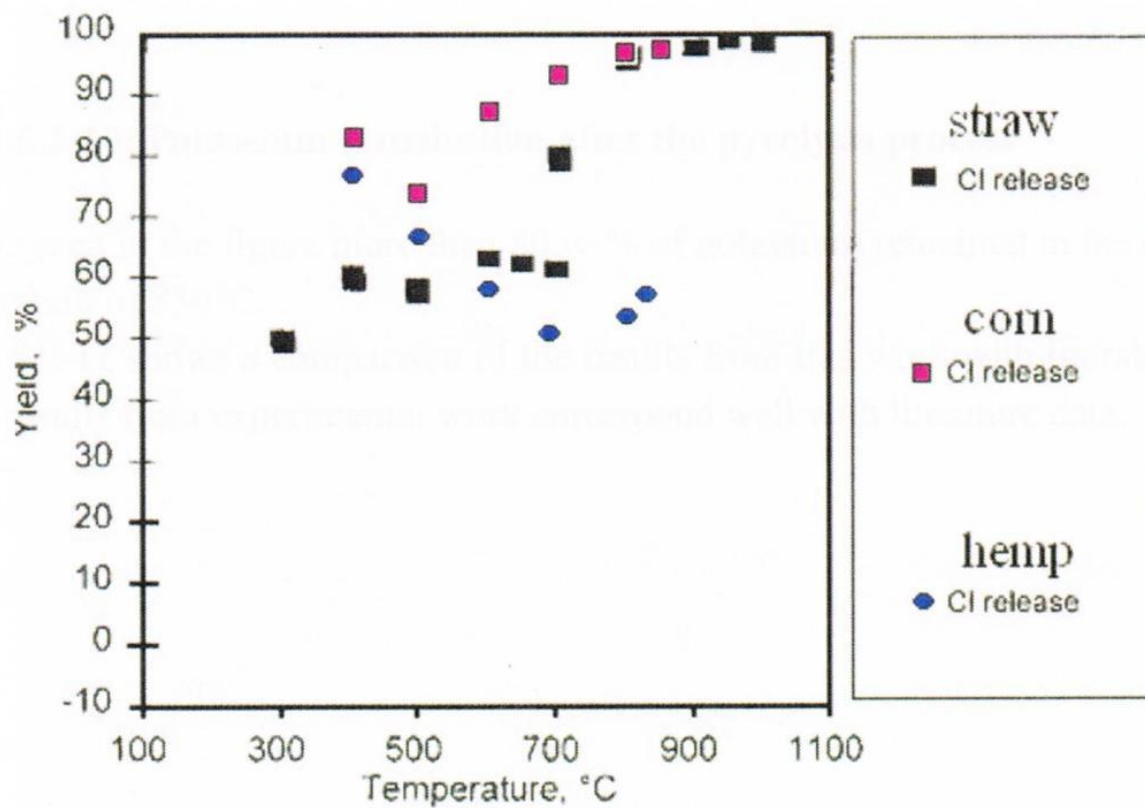


Figure 6-18: Comparison of chlorine release during the pyrolysis of different types of biomass [Hrbek, 2005]

Chlorine can also cause corrosion problems because of the HCl formation during the conversion process. Furthermore, HCl emissions have to be reduced as far as possible.

### 6.1.4.5 Potassium

Potassium is the macronutrient required by plants in the largest amount after nitrogen [Wallingford, 1980]. The potassium requirement for optimum plant growth is in the 1-5% dry matter weight range, depending on species, while the potassium concentration in mature plants generally does not exceed 2 % of dry matter. Potassium is characterized by its high mobility in plants at all levels, including between individual cells, between tissues, and in long-distance transport within the plant [Marschner, 1993]. Figure 6-19 shows the content of potassium for the different fuel samples (dm). The potassium content is observed in the range of 384 mg/kg to 11700 mg/kg. There are also big differences among the fuel samples analysed. The reason for this could be a difference in the bio-availability of potassium or the application of fertilisers.

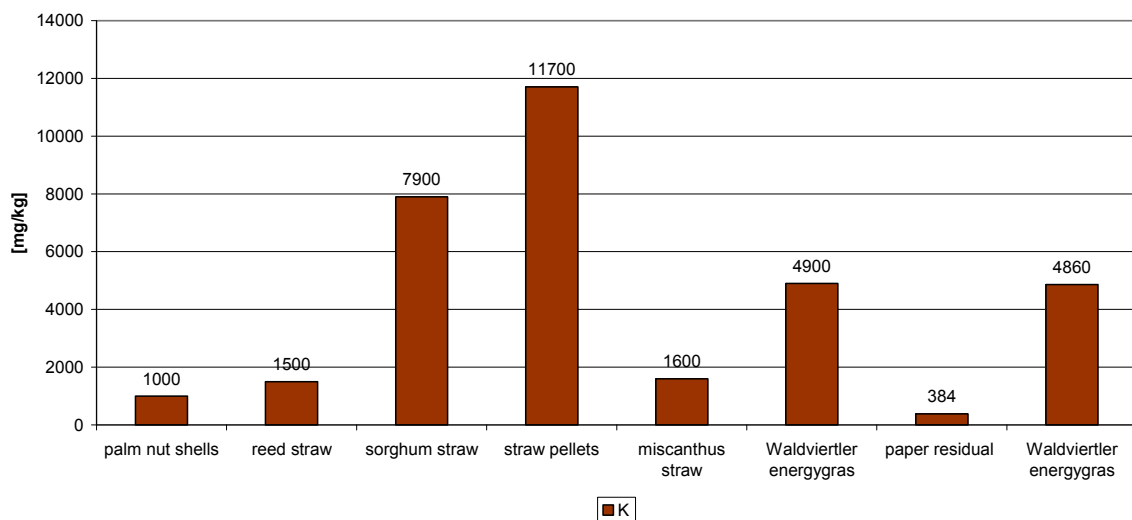


Figure 6-19: Potassium content of different fuel samples (dm)

Figure 6-20 shows the content of potassium for the different pyrolysis char samples (dm). The potassium content is in the range of 1060 mg/kg to 37100 mg/kg. Comparing the content in the fuel and in the char no clear trend could be derived. The potassium content in pyrolysis char samples (reed straw, Waldviertler energy grass 560 °C) is decreasing whereas for the other samples the potassium content is significantly increasing.

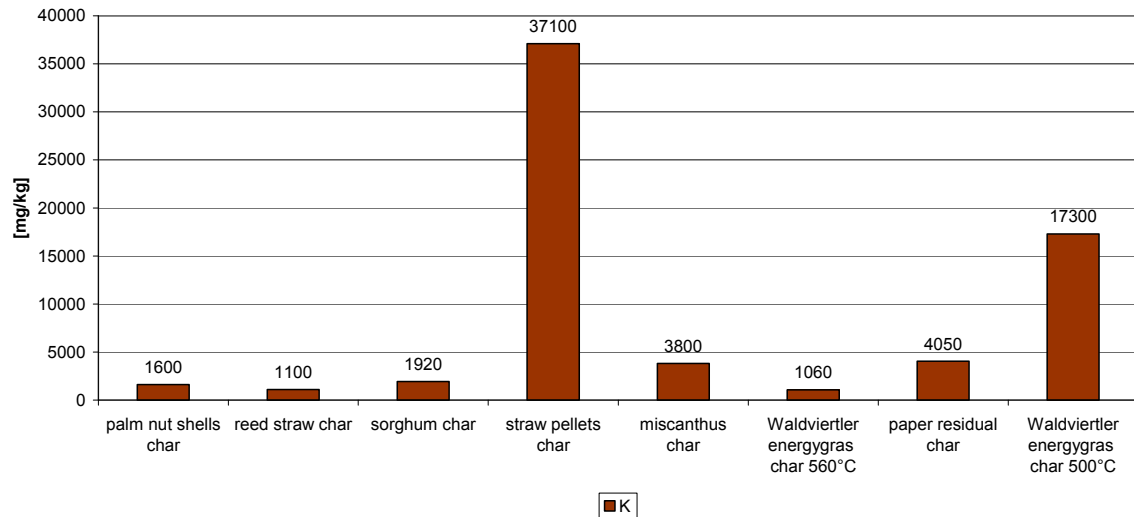


Figure 6-20: Potassium content of different pyrolysis char samples (dm)

During straw pyrolysis at temperatures between 200 to 400 °C potassium is bond as KCl and  $K_2CO_3$  and at temperatures between 400 to 700 °C no significant amounts of potassium were released to the gas phase (cf. Figure 6-50). From 700 °C all KCl evaporated. At this temperature, K also reacts with silicon and potassium silicates are generated. From 830 to 1000 °C  $K_2CO_3$  is decomposed and potassium is released as KOH or as free potassium atoms. Possibly, potassium can also be released from the char matrix. Above 1000 °C, potassium may be released to the gas phase from the char matrix and from potassium silicates. [Jensen et al., 2000]

On the contrary, Yu et al. [Yu et al., 2005] studied the chemical forms and the release of K and Na during pyrolysis of rice straw between 400 °C and 1372 °C. Between 473 °C and 673 °C, about half of the total metal content (48 and 55 per cent, respectively, for K and Na) was lost by vaporization.

Figure 6-21 shows the changes in K contents of rice straw biochar as a function of temperature during pyrolysis [Yu et al., 2005].

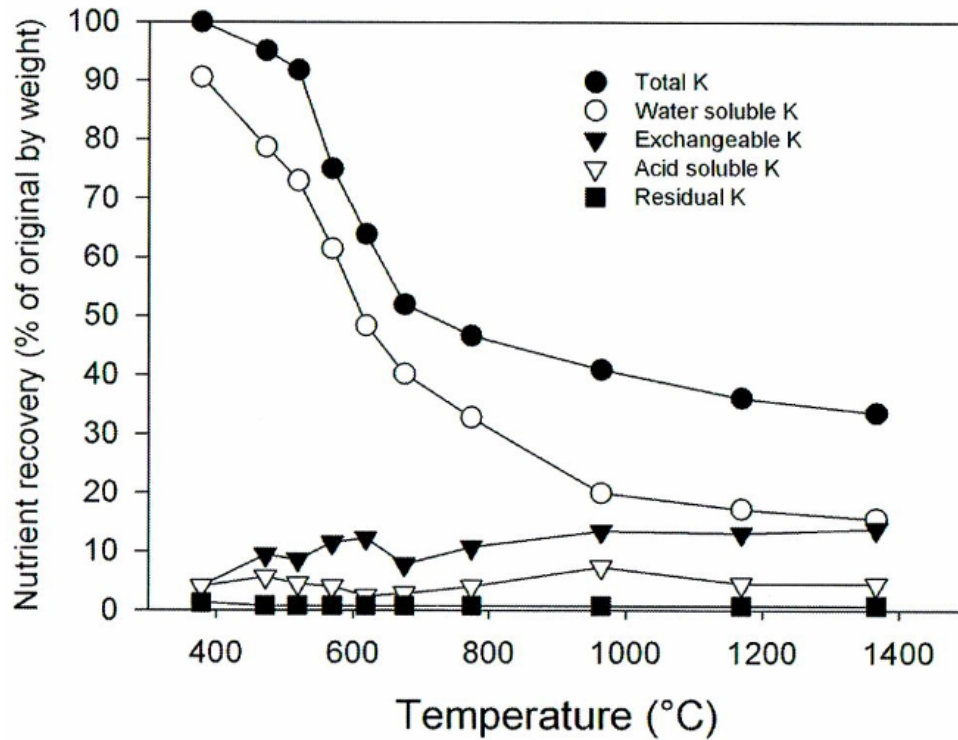


Figure 6-21: Changes in K contents of rice straw biochar as a function of temperature during pyrolysis [Yu et al., 2005]

About 90 per cent of total K in rice straw was in water-soluble form, exactly this form of K was lost when heating up to 673 °C.

#### 6.1.4.6 Sodium

Figure 6-22 shows the content of sodium for the different fuel samples (dm). The sodium content is in the range of 20 mg/kg to 1050 mg/kg. As it can be seen from Figure 6-22 there are big differences in sodium content. The reason for this are in most cases differences in the soil composition or habitat, however sodium plays a minor role for plants.

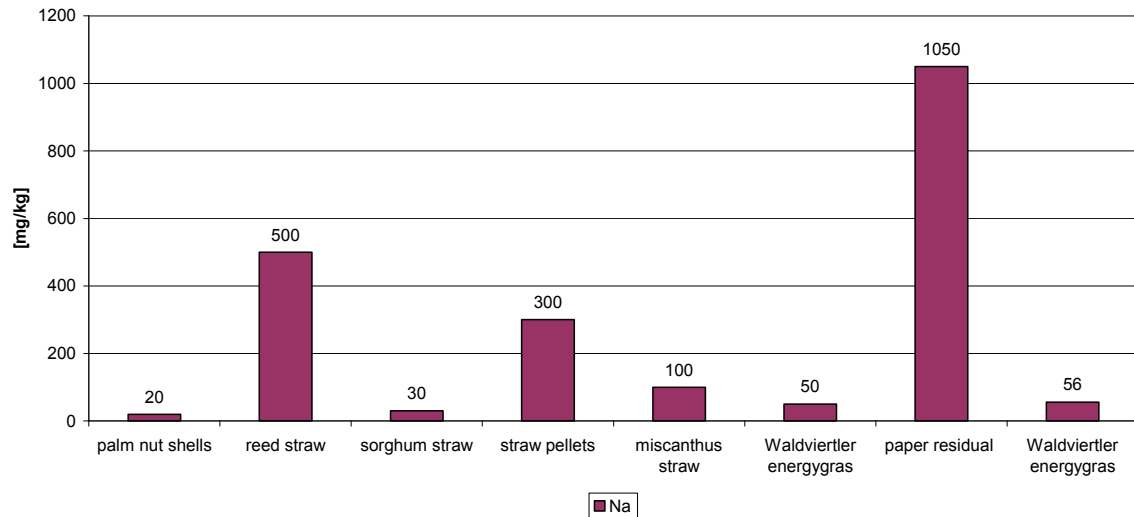


Figure 6-22: Sodium content of different fuel samples (dm)

Figure 6-23 shows the content of sodium for the different pyrolysis char samples (dm). The sodium content is in the range of 10 mg/kg to 2900 mg/kg. It can be seen that sodium is completely enriched in the pyrolysis char. For palm nut shells and sorghum straw the amount is decreasing but this could also be because of an inaccuracy at the sampling.

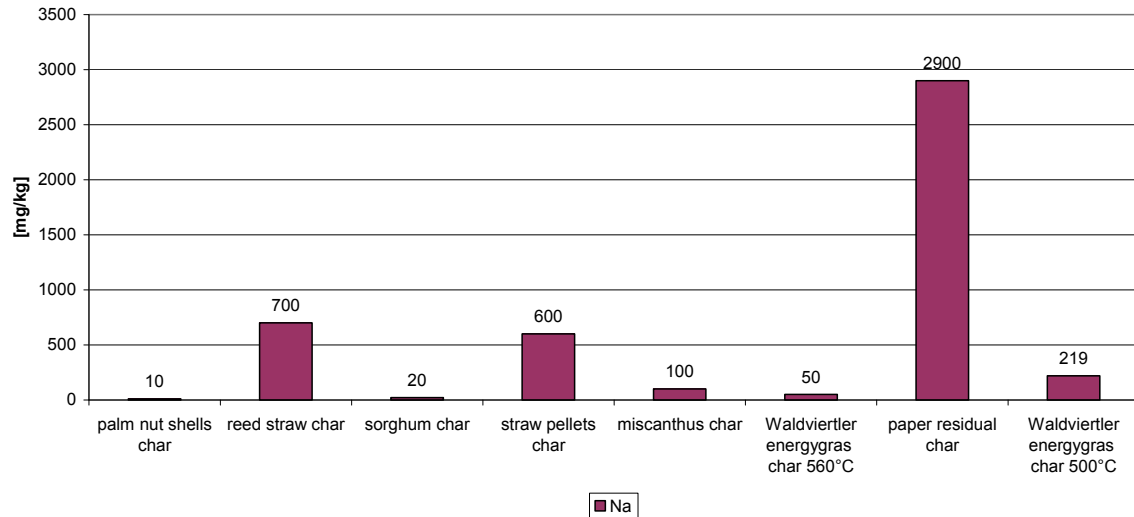


Figure 6-23: Sodium content of different pyrolysis char samples (dm)

The sodium content in most of the biomass samples is more than ten times lower than the potassium content therefore, less attention could be given to the release of sodium because these amounts are insignificant.

## 6.2 Results of the gravimetric detection of pyrolysis oils from pyrolysis pilot plant

In this work pyrolysis oil refers only to the organic condensable but water is not included. Following figures relate the pyrolysis gas temperature and the pyrolysis oil content of the different fuels. A decreasing amount of pyrolysis oil at higher pyrolysis gas temperatures is expected but not observed in all cases. The lower content of pyrolysis oil at higher pyrolysis gas temperatures is explained by the increasing emergence of small gaseous molecules from the cellulose-based tars (alcohols, aldehydes, ketones and carbon acids). The reactions to mention are dehydration, decarboxylation and decarbonylation.

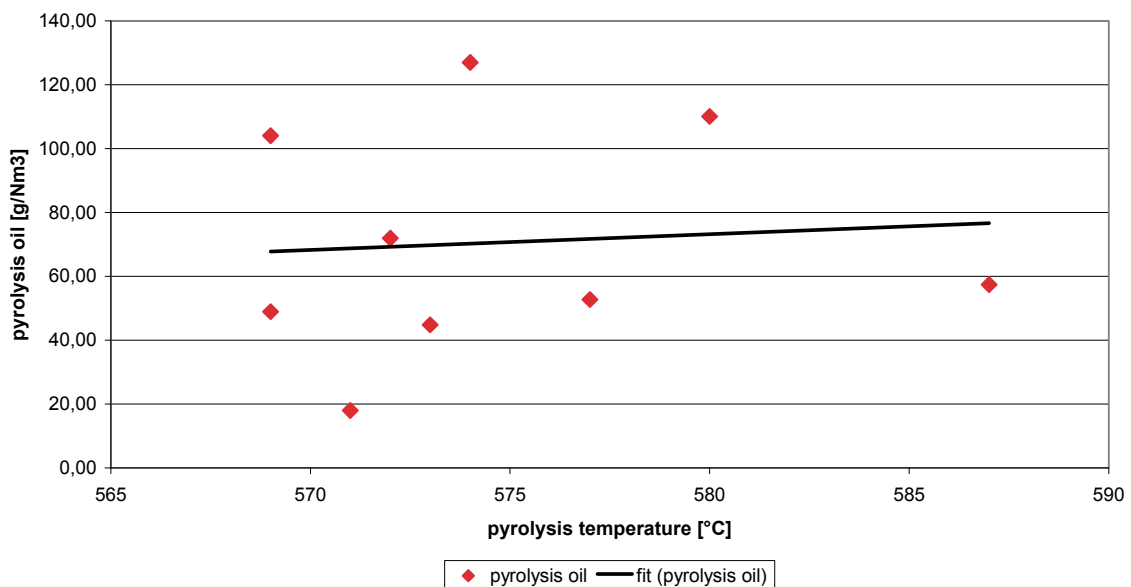


Figure 6-24: Gravimetric pyrolysis oil content of palm nut shells

The detected amount of pyrolysis oil for palm nut shells varies between 17.99 to 126.96 g/Nm<sup>3</sup>. A temperature dependency concerning a decrease of pyrolysis oils at higher temperatures could not be approved because of the very small pyrolysis temperature range and the discontinuous operation while using palm nut shells as fuel.

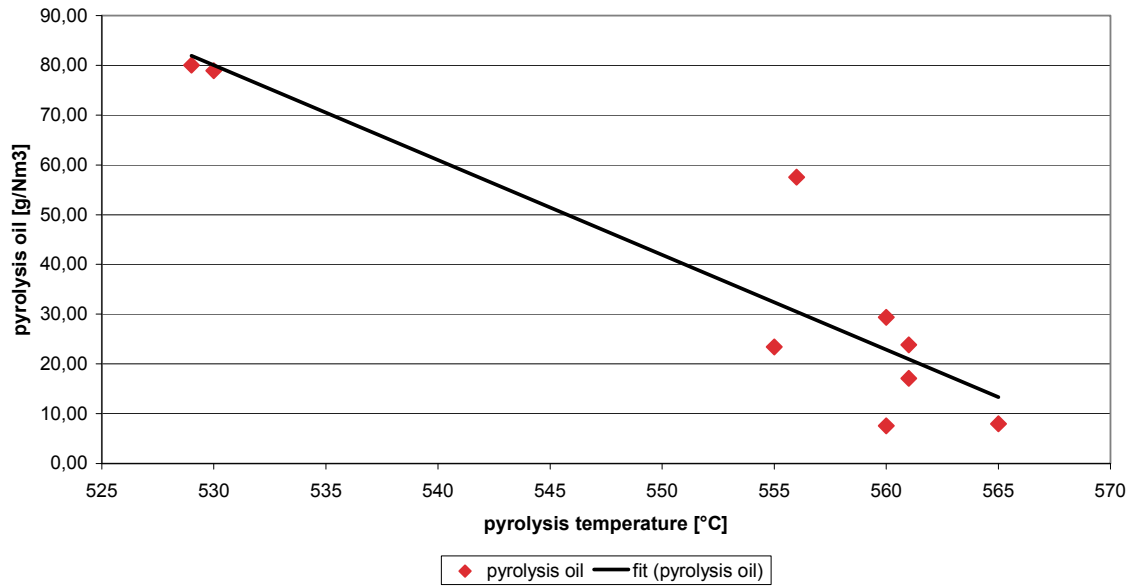


Figure 6-25: Gravimetric pyrolysis oil content of reed straw

The detected amount of pyrolysis oil for reed straw varies between 8.0 to 80.5 g/Nm<sup>3</sup>. A decreasing amount of pyrolysis oil at higher pyrolysis gas temperatures could be approved although only few samples were taken at lower temperatures.

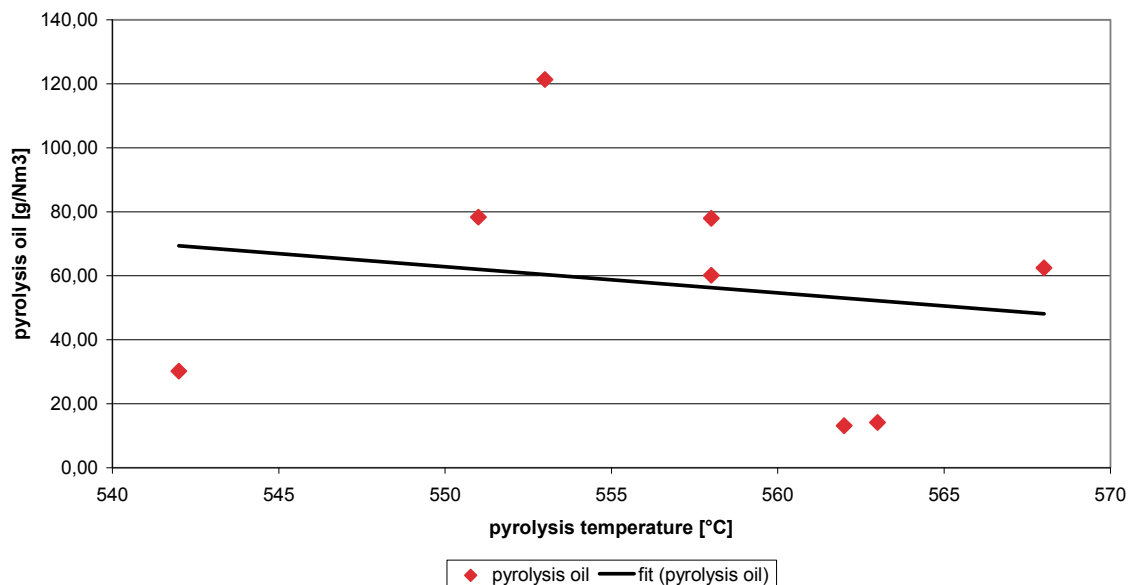


Figure 6-26: Gravimetric pyrolysis oil content of sorghum straw

The detected amount of pyrolysis oil in case of sorghum straw varies between 13.14 to 121.35 g/Nm<sup>3</sup>. A temperature dependency could not clearly be observed although there is a slight decrease at higher temperatures.



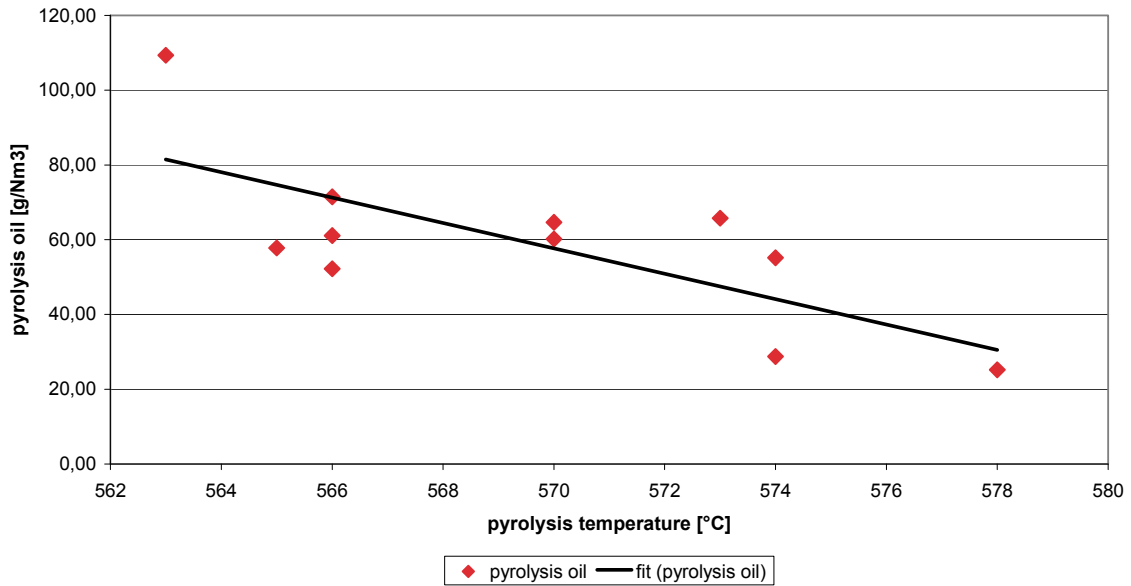


Figure 6-27: Gravimetric pyrolysis oil content of straw pellets

The detected amount of pyrolysis oil for straw pellets varies between 25.18 to 109.33 g/Nm<sup>3</sup>. A decreasing amount of pyrolysis oil at higher pyrolysis gas temperatures could be clearly seen.

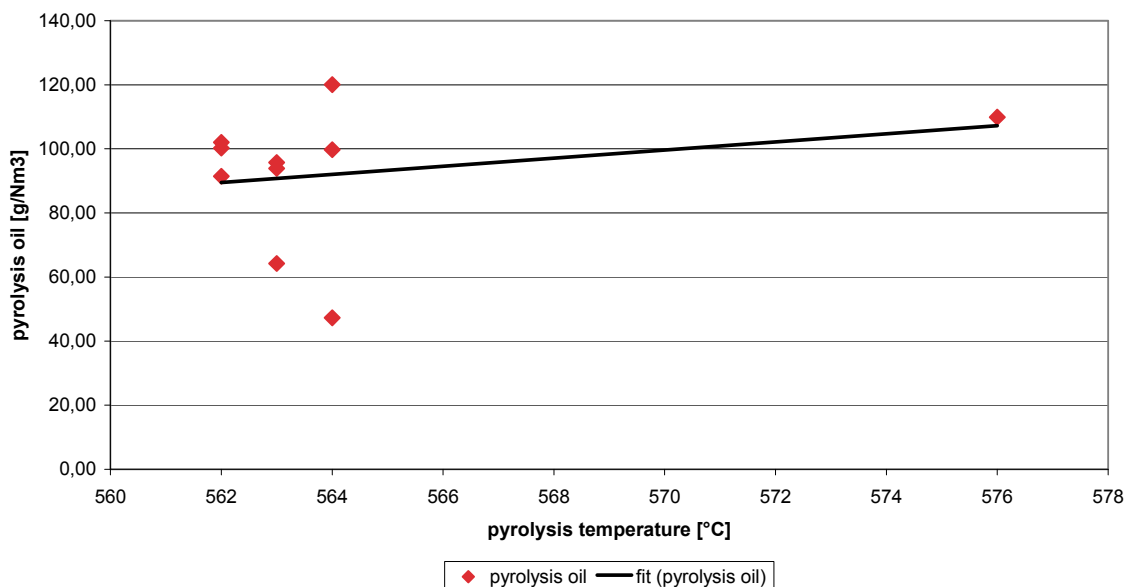


Figure 6-28: Gravimetric pyrolysis oil content of miscanthus straw

The detected amount of pyrolysis oil for miscanthus straw pyrolysis varies between 47.23 to 120.02 g/Nm<sup>3</sup>. A temperature dependency concerning a decrease of pyrolysis oils at higher temperatures could not clearly be

observed, however, there was only one sample taken at higher pyrolysis temperatures.

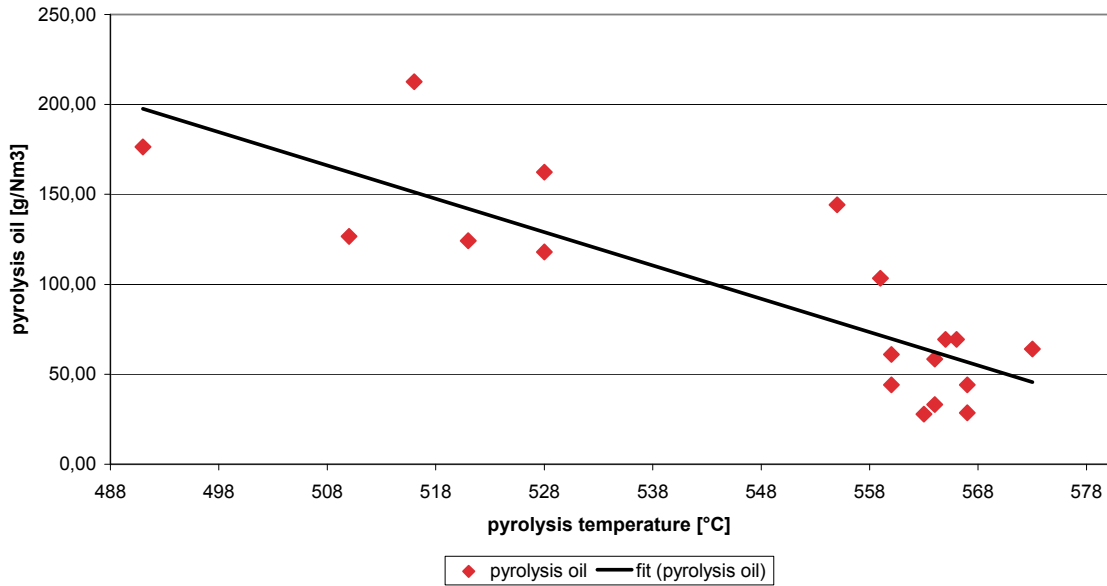


Figure 6-29: Gravimetric pyrolysis oil content of Waldviertler energy grass

The detected amount of pyrolysis oil from Waldviertler energy grass varies between 28.62 to 212.67 g/Nm<sup>3</sup>. Concerning Waldviertler energy grass as fuel a huge number of samples were taken, therefore, a decreasing amount of pyrolysis oil at higher pyrolysis gas temperatures could be clearly approved.

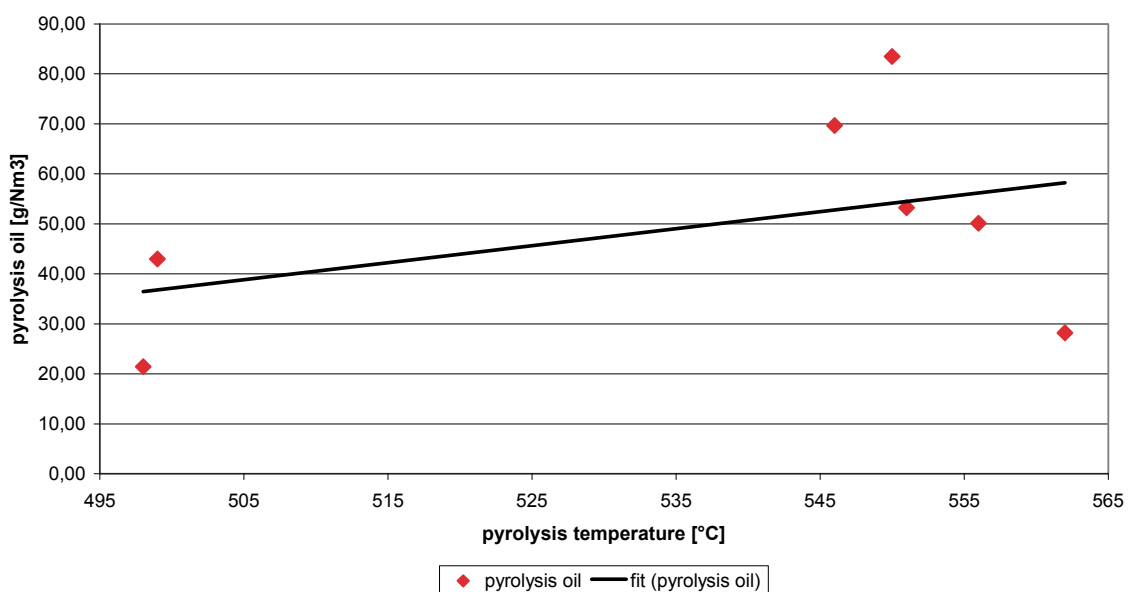


Figure 6-30: Gravimetric pyrolysis oil content of paper residual material

The detected amount of pyrolysis oil from paper residual material varies between 21.41 to 83.48 g/Nm<sup>3</sup>.

A temperature dependency concerning a decrease of pyrolysis oils at higher temperatures did not appear because of the small sample numbers.

Brownsort [Brownsort, 2009] gives an overview about collected data from different pyrolysis process technologies, also concerning the yields of liquid, gas and char. Liquid yields are higher with increased pyrolysis temperatures up to a maximum value, usually at 400 to 550 °C but dependent on equipment and other conditions. Above this temperature secondary reactions causing vapour decomposition become more dominant and the condensed liquid yields are reduced. Gas yields are generally low with irregular dependency on temperature below the peak temperature for liquid yield; above this gas yields are increased strongly by higher temperatures, as the main products of vapour decomposition are gases. For fast pyrolysis the peak liquid yields are generally obtained at a temperature of around 500 °C [Toft, 1996], [Bridgwater et al., 1999]. Peak liquid yields for slow pyrolysis are more variable. Demirbas [Demirbas, 2001] reports peak liquid yields of 28 to 41 % at temperatures between 377 °C and 577 °C, depending on feedstock, when using a laboratory slow pyrolysis technique. The Haloclean process yields a peak of 42 to 45 % liquid at temperatures of 385 to 400 °C with different straw feeds [Hornung et al, 2006].

The effects of peak pyrolysis temperature for fast and intermediate pyrolysis are shown in Figure 6-31, Figure 6-32 and Figure 6-33.

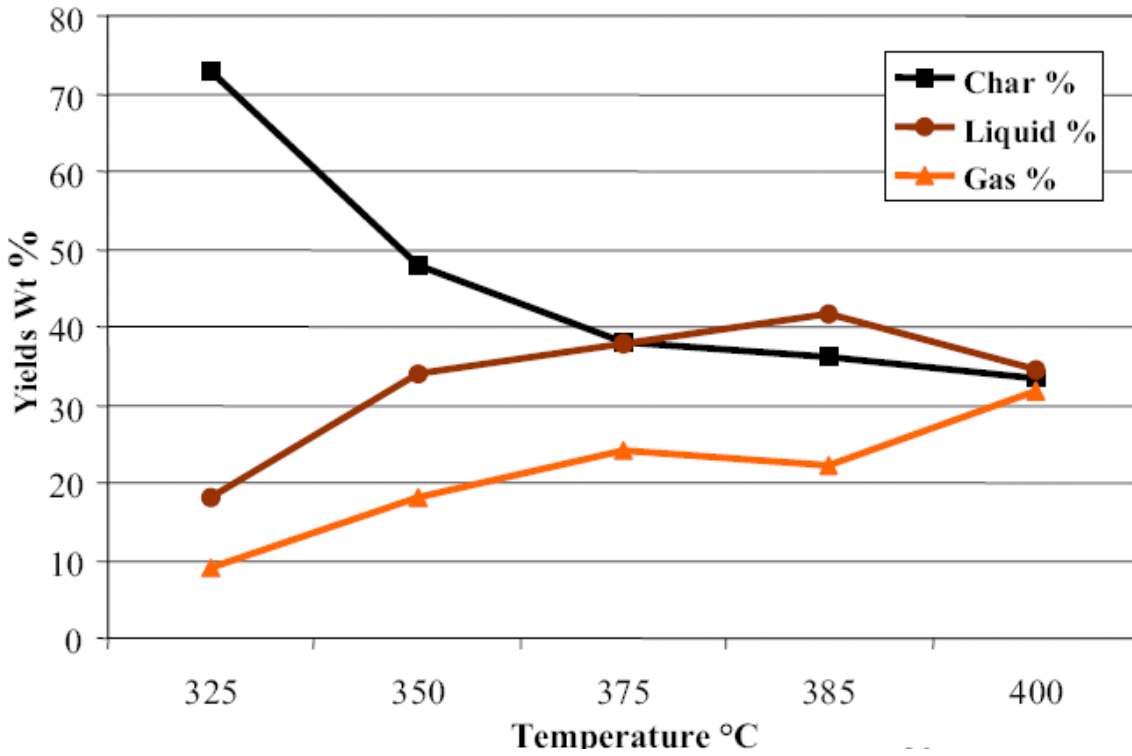


Figure 6-31: Intermediate pyrolysis of powdered straw: Haloclean process yields [Hornung, 2008]

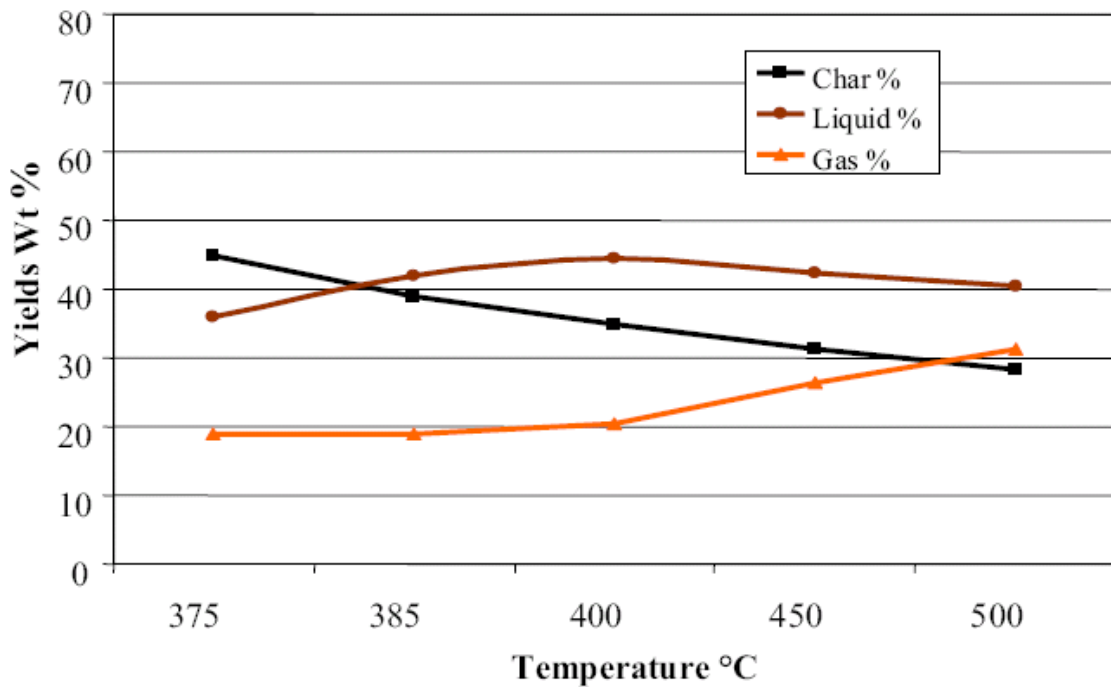


Figure 6-32: Intermediate pyrolysis of straw pellets: Haloclean process yields [Hornung, 2008]

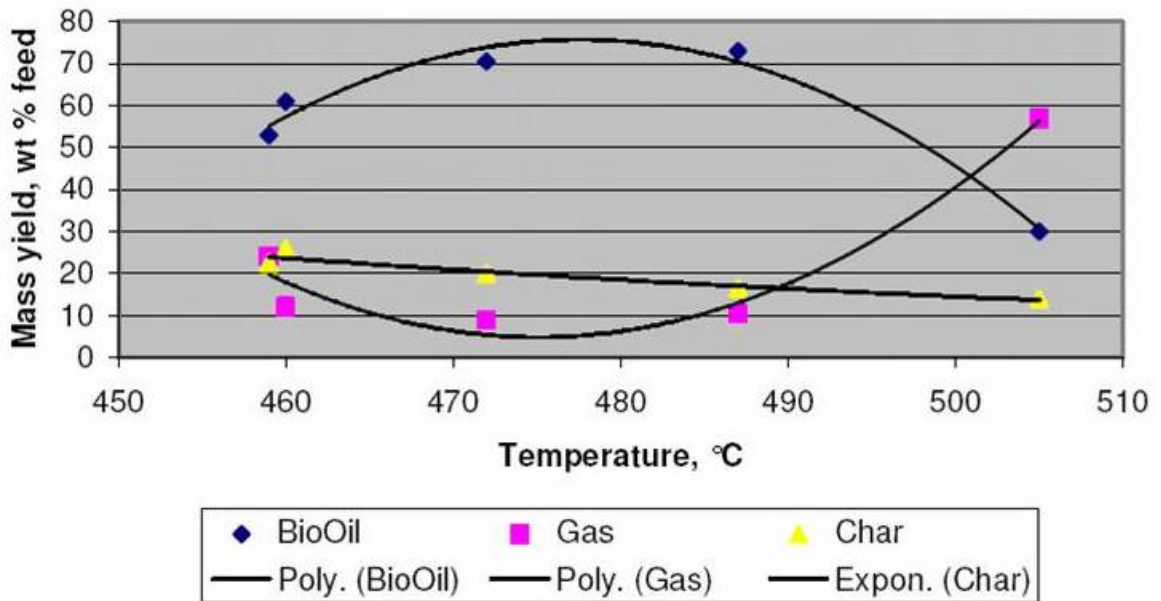


Figure 6-33: Fast pyrolysis of pine/spruce: Biotherm process yields [Brownsort, 2009]

The trends for typical slow pyrolysis processes are similar to intermediate pyrolysis.

### 6.3 Water content of pyrolysis gas and fuel samples

Following chapter focuses on the water content of the pyrolysis gas and the fuel samples. The definition of pyrolysis gas comprehends gas and condensable liquids which also includes the water content. It is of major interest if the water content of the fuel has an influence on the water content of the pyrolysis gas.

Figure 6-34 shows the water content of the pyrolysis gas and the fuel samples. The water content of the pyrolysis gas ranges from 36.92 to 74.51 % and consists of the reaction water as well as the water content of the used biomass. The water content of the different fuels ranges from 4.06 to 50 %. The very high water content of reed straw (50 %) could be explained by the already mentioned effects that the sample was affected from biological decomposition responsible for that could be an unsuitable storage or harvest time. Comparing the measured water content of the different fuels with literature values [Kaltschmitt et al., 2009] the low water content indicates a well suited storage as well as a good harvest time with natural low water contents or forced drying of the fuel. Although the water content of the different fuels varies from 4.06 to 26.22 % (excluding reed straw) the water content in the pyrolysis gas stays nearly constant in the range of 36.92 to 54.37 %.

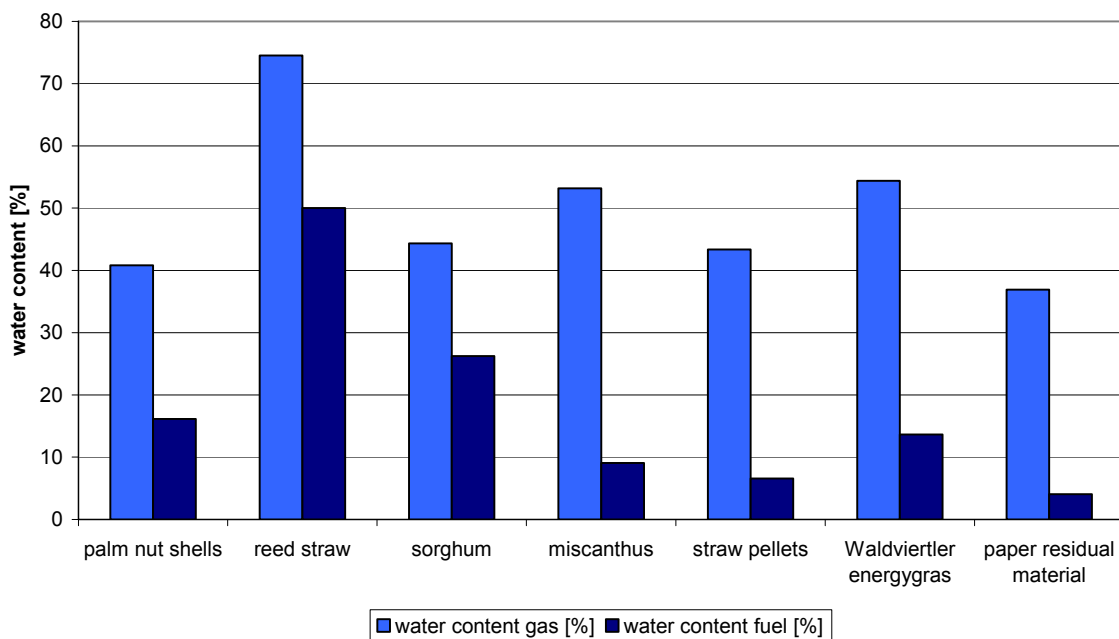


Figure 6-34: Water content of pyrolysis gas and fuel samples

Figure 6-35 shows the correlation of the water content of the different fuel samples and the water content of the pyrolysis gas. As already mentioned the water content of the pyrolysis gas consists of the reaction water and the water content of the used biomass. It seems that a big part (18.11 to 44.1 %) of the water content in the pyrolysis gas is formed by the reaction water.

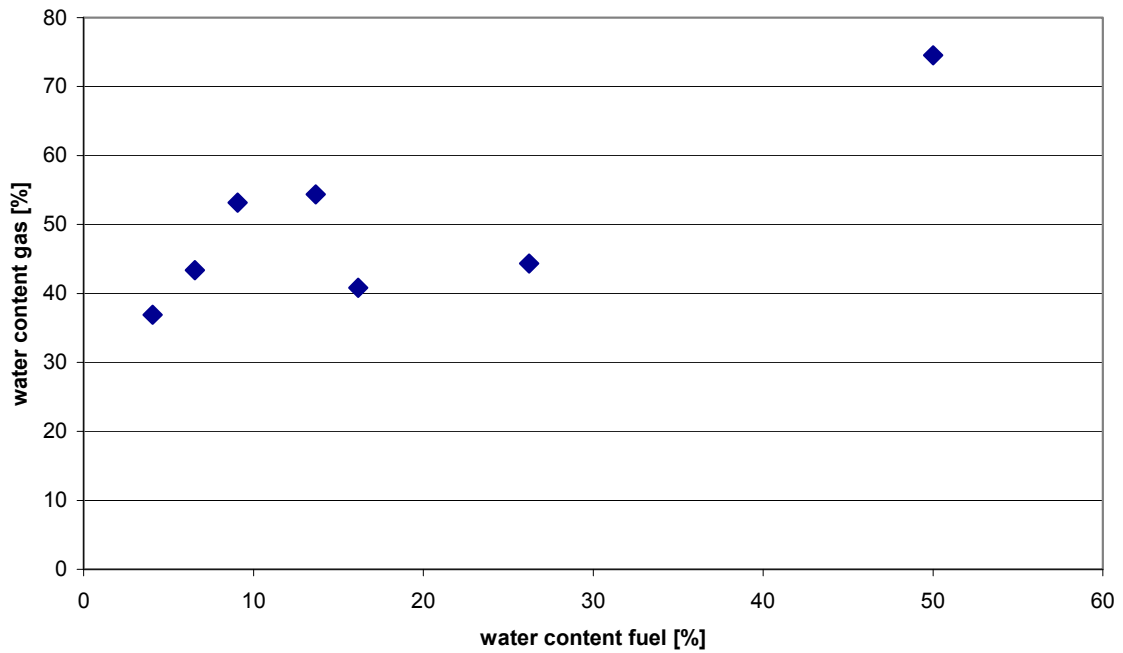


Figure 6-35: Correlation of water content gas and water content fuel

## 6.4 Dust and entrained char

Figure 6-36 shows the dust and entrained char content from the test runs with different fuel samples. The difference between dust and entrained char is that dust is the inorganic part of the particles and the entrained char the organic part of the overall particle load of the pyrolysis gas. The particle load of the pyrolysis gas ranges from 8.52 to 30.7 g/Nm<sup>3</sup> excluding the paper residual material which has a very high content of 197.34 g/Nm<sup>3</sup>.

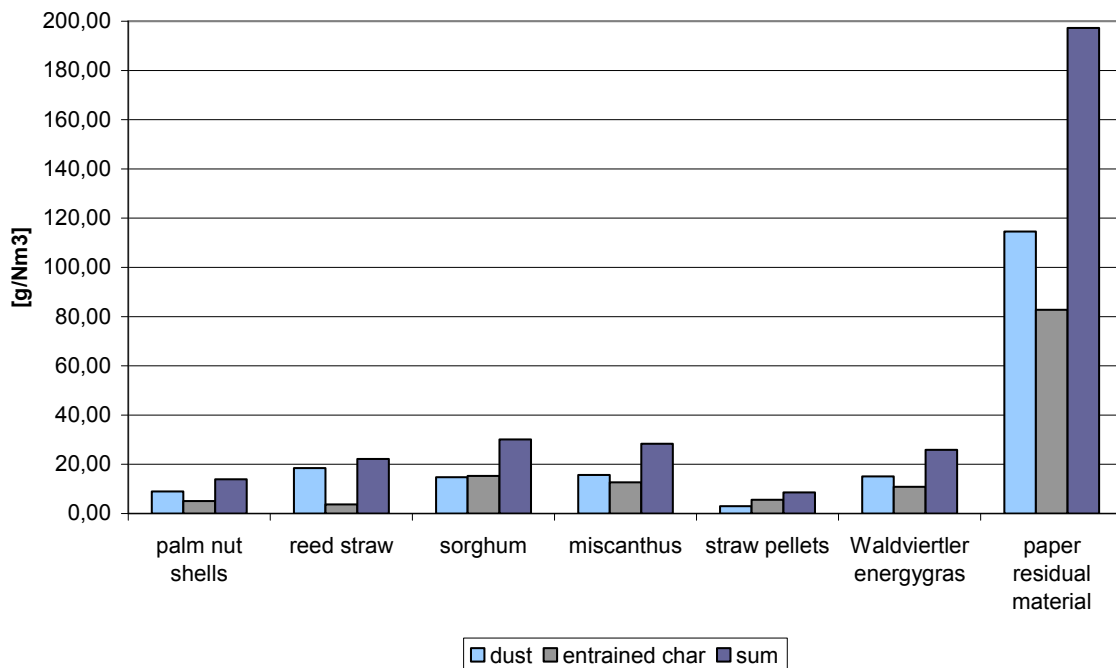


Figure 6-36: Dust and entrained char of different fuel samples

The values of the dust and entrained char measurements have to be considered carefully. The measuring probe is located above the pyrolysis char screw conveyer, which can influence the actual dust and entrained char concentration of the pyrolysis gas, due to dust, which is dispersed by the screw conveyer. This could lead to an over detection of the particle load in the pyrolysis gas.



## 6.5 Ash melting behaviour of fuel and pyrolysis char samples

For the usage of different types of biomass in the fluidised bed combustion the ash melting behaviour was determined. Ash from biomass does not have a definite melting point but melting range. Four temperatures are defined to characterize this behaviour (see chapter 4.4). Real melting begins after sintering in a more or less large temperature range and before becoming liquid the ash goes through several plastic and viscous states. Figure 6-37 shows the ash melting behaviour of different biomass samples. The data for maize is taken from the database Biobib [Reisinger et al., 2010] because of a failure in preparing the maize sample.

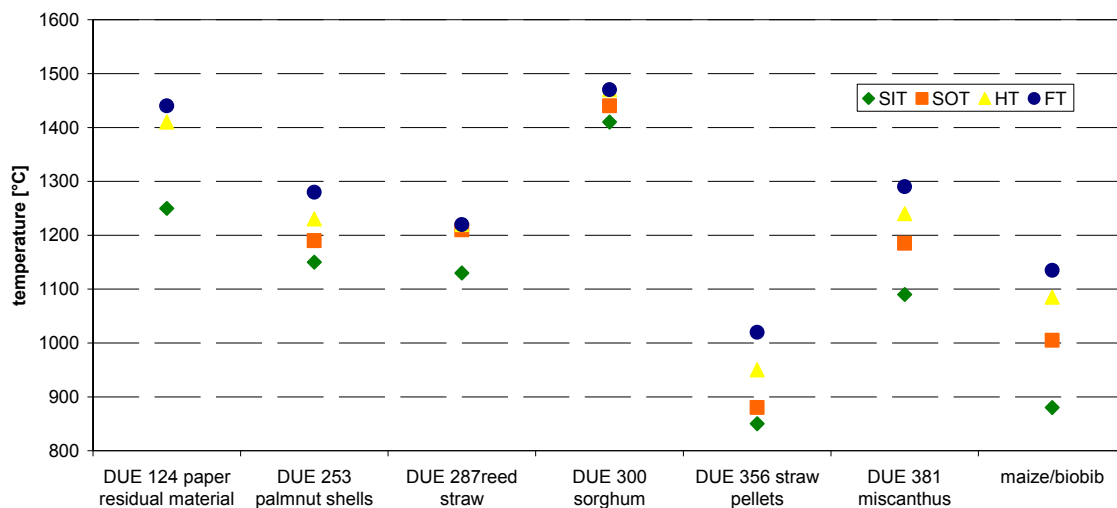


Figure 6-37: Ash melting behaviour of different biomass samples

Figure 6-38 shows the ash melting behaviour of two wheat straw samples compared with the data for wheat straw from the database Biobib [Reisinger et al., 2010]. As it can be seen the melting ranges are different depending on the fuel. The lowest temperature for the softening point (SOT) is in the range of 950 °C and the highest is in the range of 1050 °C.

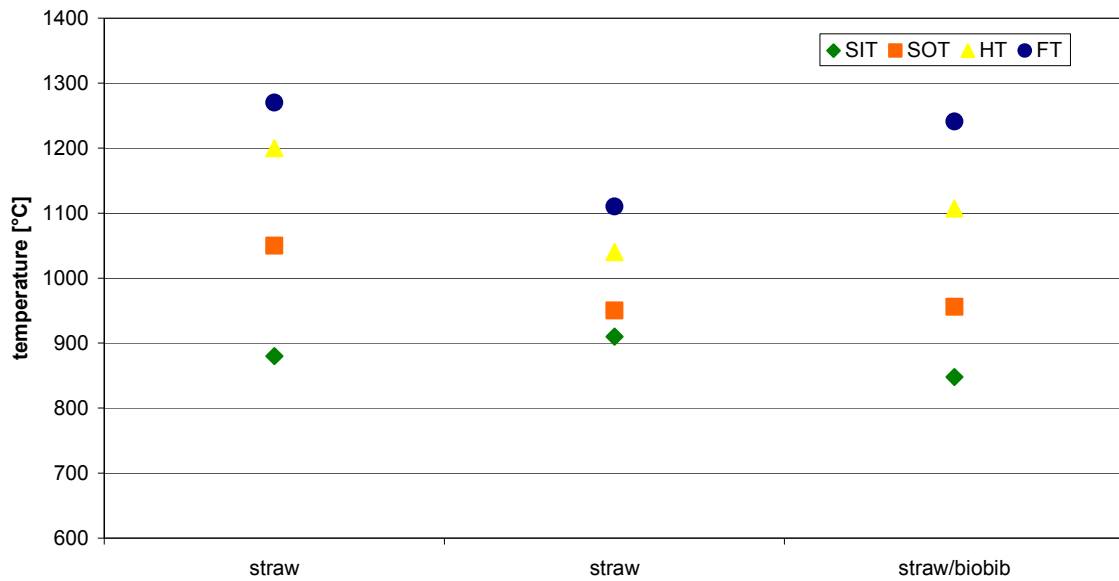


Figure 6-38: Ash melting behaviour of two straw samples compared with the data from the database Biobib

Figure 6-39 shows the ash melting behaviour of the different pyrolysis char samples.

The pyrolysis char is an excellent fuel for combustion systems, as fluidised bed combustion systems do not operate at such high temperatures like the pulverized coal combustion of the Dürnrrohr power station. Therefore, for the operation of a fluidised bed system it is important that the operation temperature (normally 800 to 850 °C) is below the softening temperature (SOT) which is the case for all char samples.

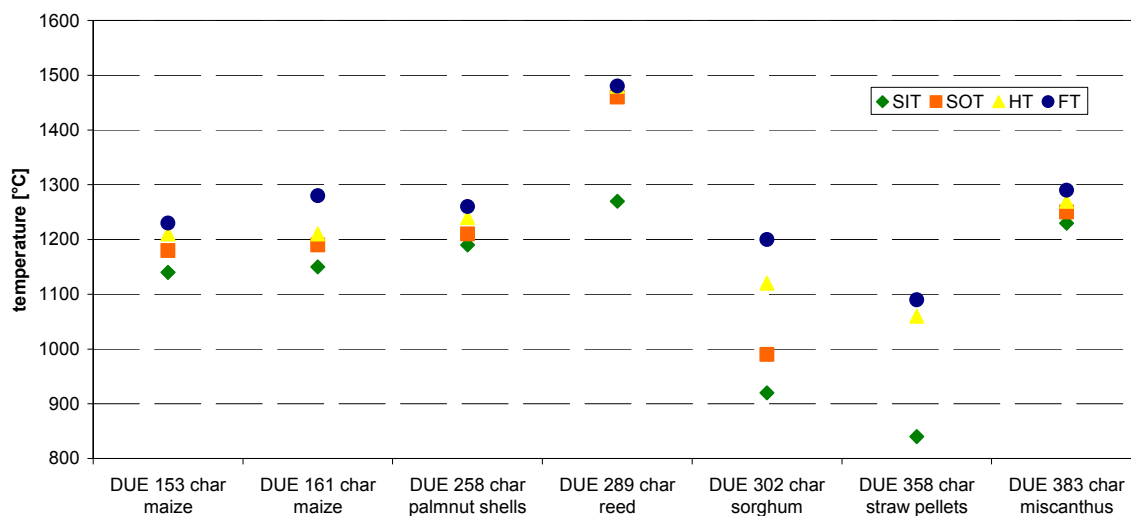


Figure 6-39: Ash melting behaviour of the different pyrolysis char samples

Figure 6-40 shows the ash melting behaviour of four pyrolysis char samples from wheat straw as this fuel shows the lowest SOT. The softening point of the pyrolysis char is about 1000 °C or higher. For a further usage of this char in a combustion system it will be important to keep the operation temperature below the softening point otherwise this will lead to slagging and fouling problems.

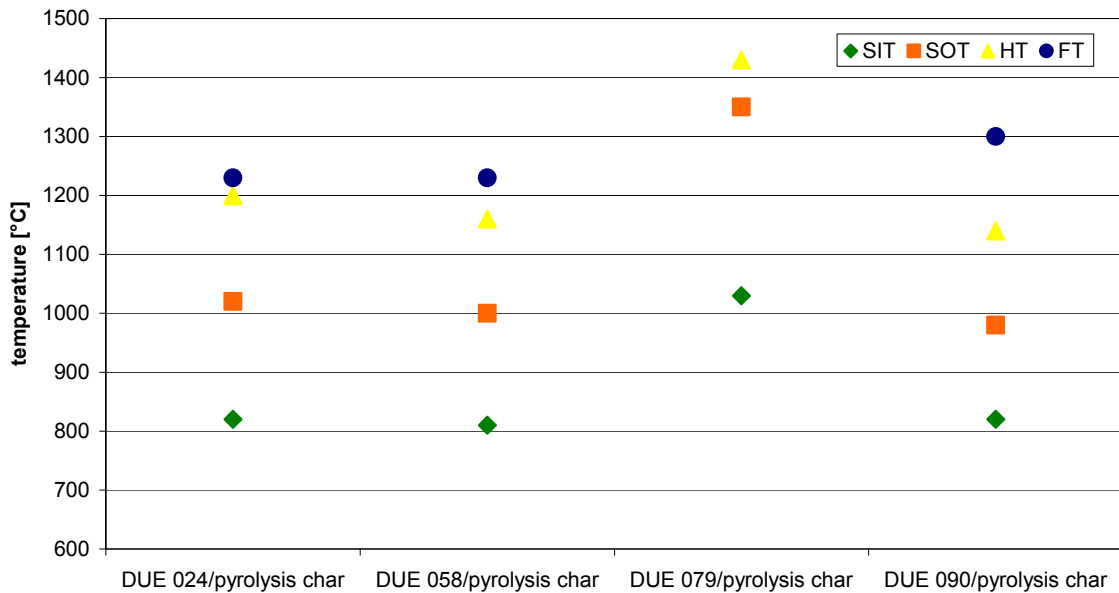


Figure 6-40: Ash melting behaviour of four pyrolysis char samples from wheat straw

An important point is also the content of alkaline earths (not yet analysed) especially calcium (Ca) because these elements can lead to a higher ash melting behaviour and also cause that large parts of the sulphur are captured in the ash and are not released as  $\text{SO}_2$  to the flue gas [Kaltschmitt et al., 2009].

## 6.6 Operation with indoor stored wheat straw

Indoor stored wheat straw was used as the main feedstock. For the balancing considerations indoor stored wheat straw was chosen because of the fact that it was available in huge amounts and its elemental composition and water content stays nearly constant.

To get reliable results an on-site balancing was carried out. This means that the bales of straw were weighted by an industrial weighing machine and after the pyrolysis process the produced pyrolysis char was collected in a container and exactly weighted. The second data for the balancing considerations are data from the balancing model which was programmed in IPSEpro.

Ammonia, hydrogen chloride and hydrogen sulphide analyses had been carried out to get an insight in the quality of the pyrolysis gas. The distribution of selected chemical elements of the feedstock in pyrolysis gas, oil and char is an important point within the following chapters. Also important is the yields of gas, oil and char for the different pyrolysis temperatures. Finally, the results, gained from the measurements and the balancing, were used to calculate the efficiency of the pilot plant and the pyrolysis process.

Table 6-2 shows the conditions which have been chosen for the balancing considerations. During the temperature variation (450, 500, 550, 600 °C) the rotation of the kiln was set to 20% whereas during the residence time variation (20, 40, 100%) the rotation of the kiln was kept constant in the range of 20 %.

Table 6-2: Conditions for investigations with wheat straw

	Pyrolysis Temperature [°C]	Rotation of kiln [%] (Residence Time)
Temperature variation	450, 500, 550, 600	20
Residence time variation	560	20, 40, 100

### 6.6.1 Characterization of feedstock

For the balance of the operating points with the used feedstock, indoor stored wheat straw from Lassee, the following composition of straw was used. The values are arithmetic mean values of four straw samples (DUE 508, DUE 510, DUE 512, DUE 513).

Table 6-3: Elemental analysis of straw

Water content	wt. %	7.1%
<b>Dry matter (dm)</b>		
Ash content (550 °C)	wt. %	4.1%
Carbon content	mg/kg	468250
Hydrogen content	mg/kg	63700
Nitrogen content	mg/kg	4992.5
Sulphur content	mg/kg	900.5
Chlorine content	mg/kg	1682.5
Sodium content	mg/kg	47
Potassium content	mg/kg	9555
LHV	kJ/kg	17150



Figure 6-41: A typical straw sample (Lassee) which was used for plant balancing

### 6.6.2 Pyrolysis char from wheat straw

After pyrolysis the elemental composition of the produced char was analysed. To get reliable results four different samples were taken during the balancing operation on-site. For the balancing model the arithmetic mean value was taken.

Table 6-4: Elemental analysis of pyrolysis char from straw at different pyrolysis temperatures

Sample number		DUE 518	DUE 516	DUE 514	DUE 519
Pyrolysis temperature	°C	450	500	550	600
Water content	wt.%	12.4%	7.0%	11.2%	14.5%
<b>Dry matter (dm)</b>					
Ash content (550 °C)	wt.%	12.6%	14.0%	14.5%	16.4%
Carbon content	mg/kg	659700	681500	713400	745300
Hydrogen content	mg/kg	31100	25200	19100	14400
Nitrogen content	mg/kg	8590	11000	11200	11400
Sulphur content	mg/kg	1300	2030	2015	2000
Chlorine content	mg/kg	3700	3820	3760	3290
Sodium content	mg/kg	218	480	549	619
Potassium content	mg/kg	27700	34100	31000	29200
LHV	kJ/kg	23760	24520	25790	27060
Volatiles	wt.%	28.6%	23.8%	17.1%	15.4%



Figure 6-42: A typical pyrolysis char from the feedstock straw

The bulk density of the pyrolysis char from indoor stored wheat straw is about 90 kg/m<sup>3</sup>.

Figure 6-43 shows the pyrolysis char yield during the on-site balancing operation in 2010 and the pyrolysis char yield which was calculated from the IPSE model. The simulation shows that the amount of pyrolysis char slightly decreases with higher pyrolysis temperatures. This trend could also be proven by the on-site balancing operation which was carried out in January 2010.

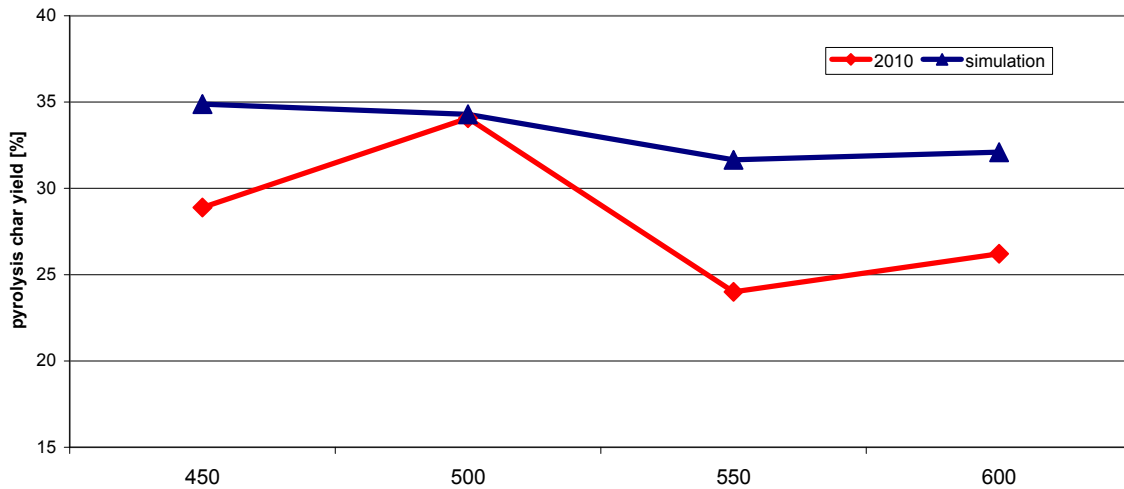


Figure 6-43: Pyrolysis char yield during the on-site balancing 2010 and the yield which was calculated from the model

The pyrolysis char yield is in the range of 24.00 to 34.07 % for the on-site balancing operation and between 31.65 to 34.89 % for the calculated yields from the model.

The quantity of these products depends upon the composition of the biomass and the conditions under which pyrolysis occurs [Shafizadeh, 1982]. Table 6-5 gives an overview about the typical product yields for different modes of pyrolysis published in literature. For the slow pyrolysis, which is comparable with the operation in the pilot plant, the pyrolysis char yield is recorded with 35 % that is in good agreement with the data obtained in this work.

Table 6-5: Typical product yields (dry basis) for different modes of pyrolysis [Bridgwater, 2007]

Mode	Conditions	Liquid (%)	Char (%)	Gas (%)
Fast	Moderate temperature ~ 500°C short vapour residence time ~ 1sec	75	12	13
Moderate	Moderate temperature ~ 500°C Moderate vapour residence time ~ 10–20sec	50	20	30
Slow	Moderate temperature ~ 500°C Very long vapour residence time ~ 5–30min	30	35	35
Gasification	High temperature >750°C Moderate vapour residence time ~ 10–20sec	5	10	85

### 6.6.3 Elemental analysis of pyrolysis char from wheat straw

Figure 6-44 shows that due to the pyrolysis process the carbon content in the pyrolysis char samples is enriched and rises from 659700 mg/kg to 745300 mg/kg compared to the original straw with a value of 468250 mg/kg.

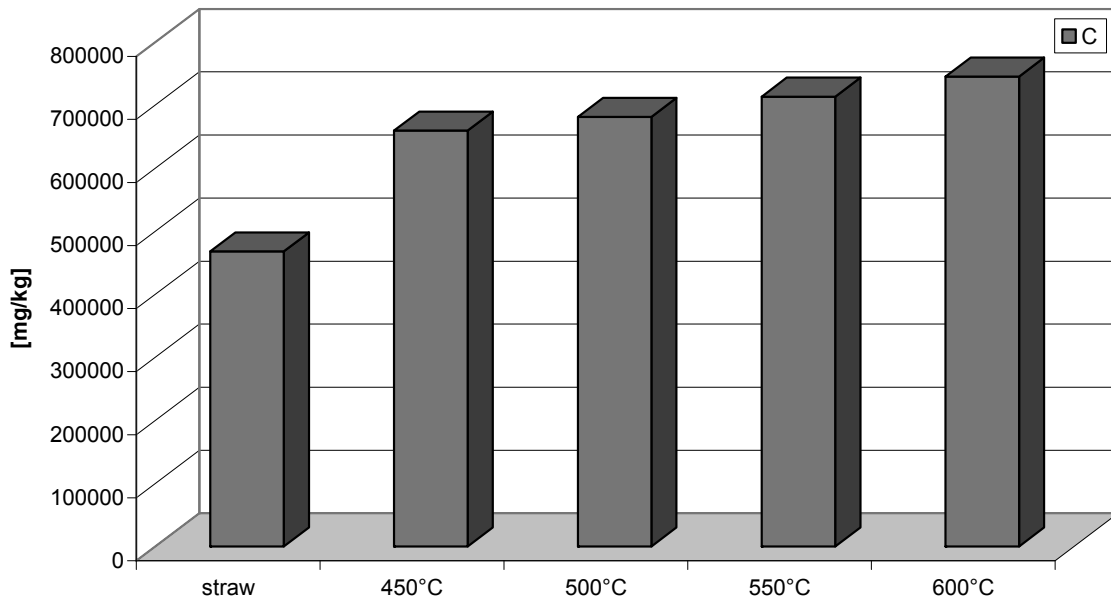


Figure 6-44: Carbon content of pyrolysis char at different pyrolysis temperatures

Lang et al shows that the release of C, H, and O with rising temperature is similar for all biomass fuels. An increasing enrichment of carbon in the char as temperature increases is also an obvious fact. Simultaneously, a steady preferential loss of H and O occurs, such that at 1100 °C, H and O are essentially fully depleted [Lang et al., 2005]. The same effects were already shown by Ahlhaus [Ahlhaus, 1995] for spruce wood. As the determining parameter for the pyrolysis char composition the pyrolysis end temperature was defined.

Figure 6-45 shows the changes in elements with increasing temperature during the charring process of wood, as well as data from fast pyrolysis products and biochar: here, the differences are illustrated between low-temperature biochars and those produced at high-temperature fast pyrolysis (Pyrolysis products) as well as biochar (BC, black locust wood) produced at 350 °C [Lehmann et Joseph, 2009].



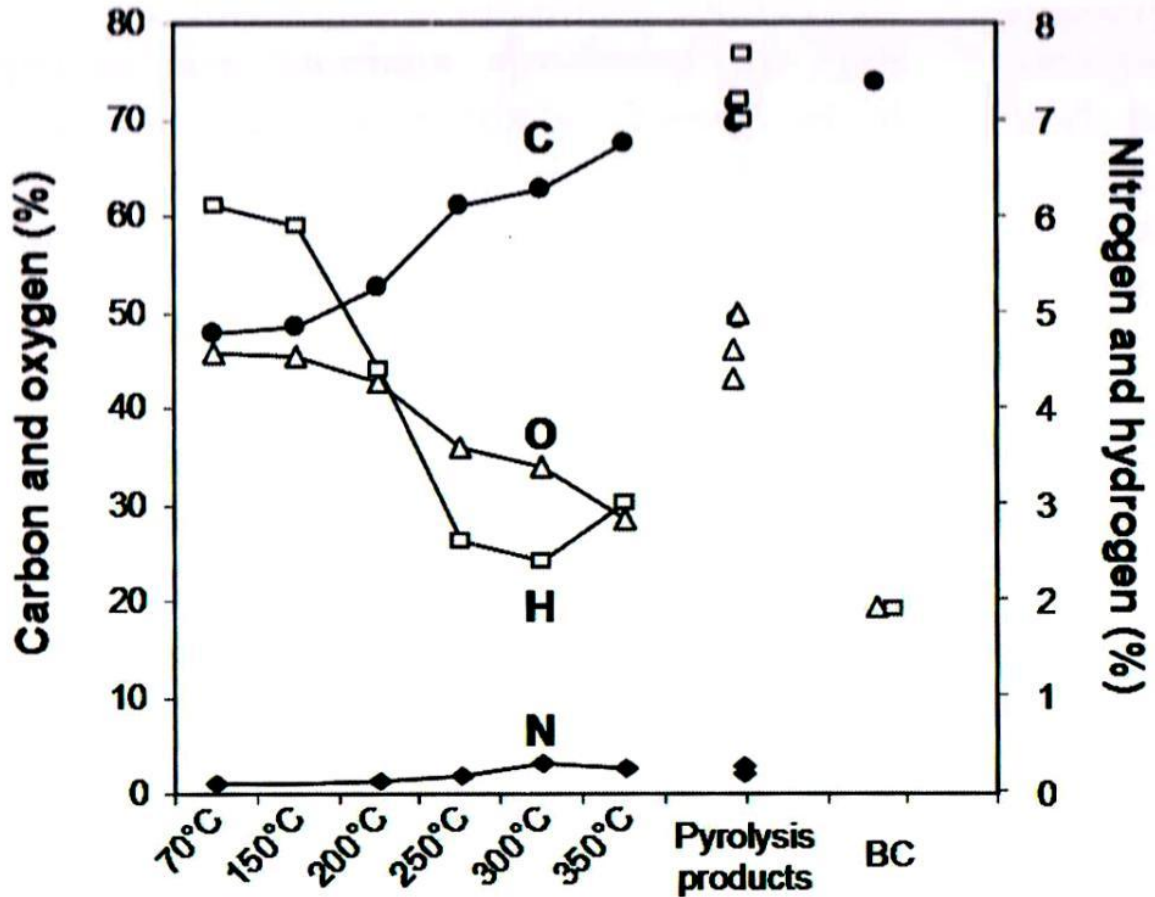


Figure 6-45: Changes in elements with increasing temperature during the charring process of wood [Baldock et Smernik, 2002], Pyrolysis products ... Fast pyrolysis products [Tsai et al., 2006], BC ... biochar [Cheng et al., 2006]

Figure 6-46 shows the content of hydrogen for four pyrolysis char samples at different pyrolysis temperatures.

Hydrogen decreases in the pyrolysis char samples because of separation reactions during depolymerisation and can be found in the pyrolysis gas.

Hydrogen decreases and therefore the content decreases from 31100 to 14400 mg/kg. The original fuel sample contained 63700 mg/kg hydrogen. Hydrogen is one of the most volatile elements released into the volatiles during the thermochemical process. Hrbek [Hrbek, 2005] showed that after the biomass pyrolysis at a temperature of about 800 °C only very small amounts of hydrogen were detected in the char. These results are strengthened by the results shown in Figure 6-46 which show a steady decrease of hydrogen by increasing pyrolysis temperatures.

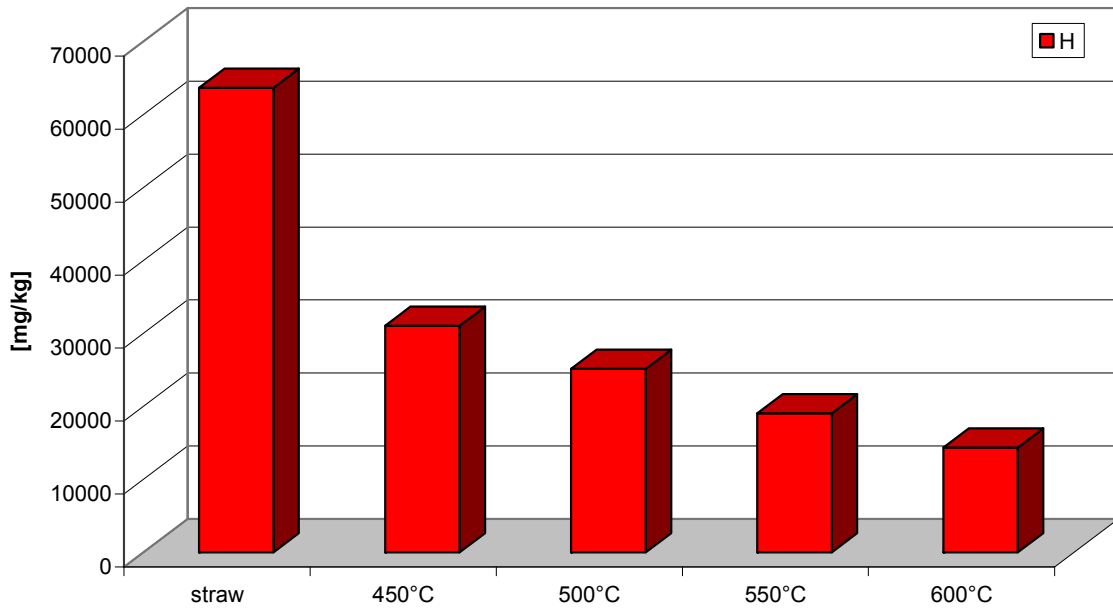


Figure 6-46: Hydrogen content of pyrolysis char at different pyrolysis temperatures

Figure 6-47 shows the content of nitrogen for four pyrolysis char samples at different pyrolysis temperatures. The nitrogen content is in the range of 8590 mg/kg to 11400 mg/kg. It is increased essentially compared to the original fuel with a value of 4992 mg/kg

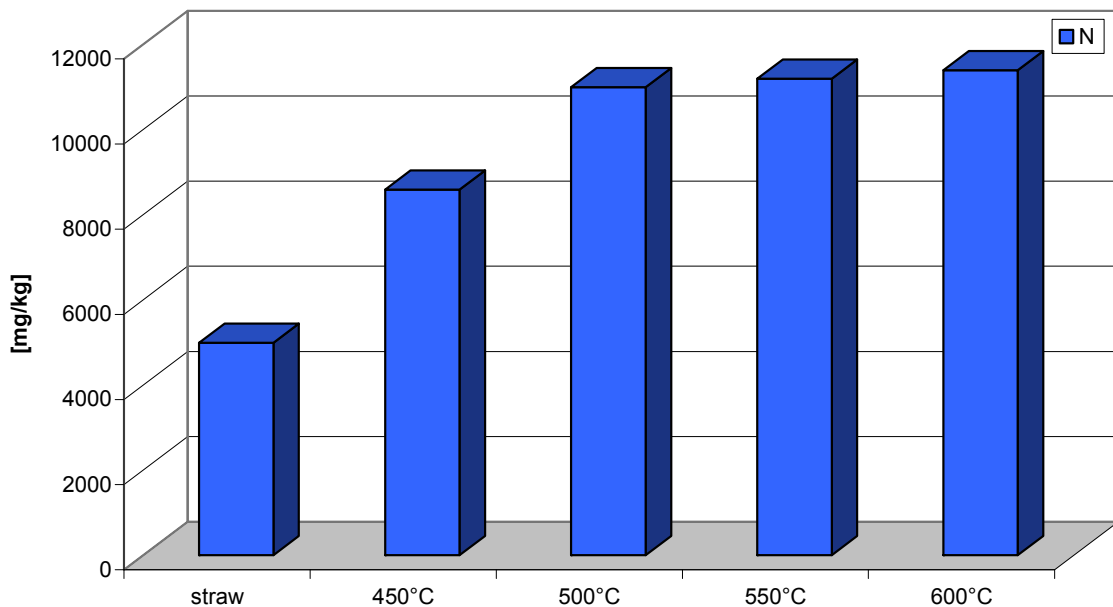


Figure 6-47: Nitrogen content of pyrolysis char at different pyrolysis temperatures

Lang et al shows that all of the investigated biomass types lost at least half of their nitrogen as volatiles at 400 °C. The loss of total N at higher temperatures was also accompanied by a change in the chemical structure of the remaining N in the biochar. According to Bagreev et al [Bagreev et al., 2001], organic N, probably present as amine functionalities in the material at low temperature, was gradually transformed into pyridine-like compounds with increased basicity of the surface at higher temperatures (>600 °C). The change results in reduced availability of N present in biochar. Significantly, this conversion occurred between 400 °C and 600 °C.

Figure 6-48 shows the content of sulphur for four pyrolysis char samples at different pyrolysis temperatures. The sulphur content is in the range of 1300 to 2030 mg/kg and shows a higher value compared to the original fuel with 900 mg/kg.

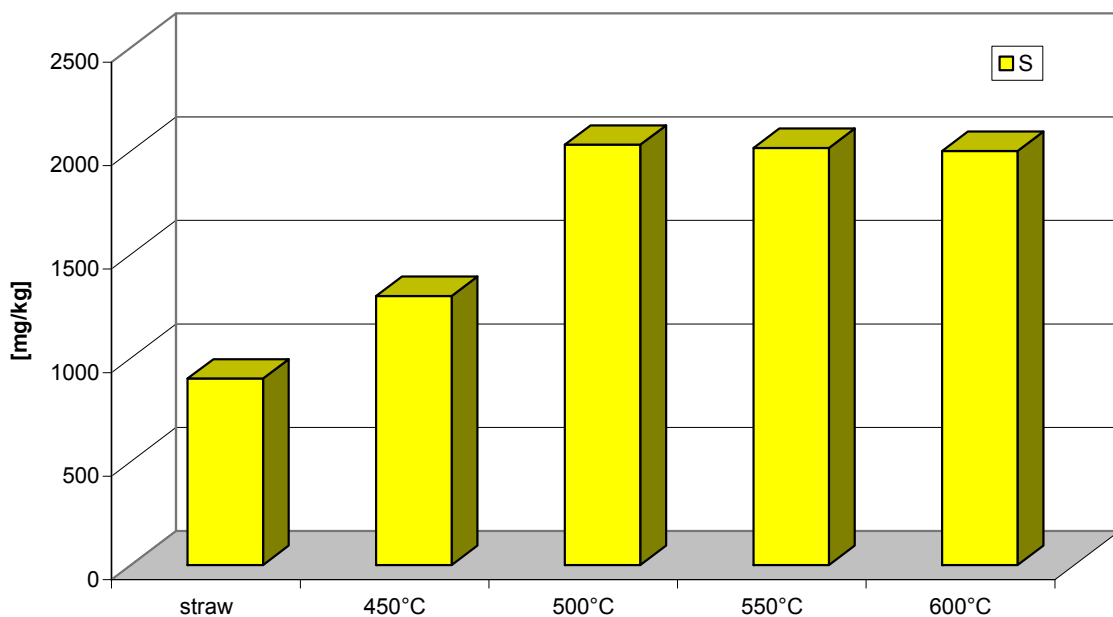


Figure 6-48: Sulphur content of pyrolysis char at different pyrolysis temperatures

Lang et al recorded that up to 50 per cent of total S from eight biomass types was lost during pyrolysis at 500 °C [Lang et al., 2005]. Knudsen et al [Knudsen et al., 2004] studied S transformation during pyrolysis of typical Danish wheat straw. Before pyrolysis, S was found to be associated partly as inorganic sulphate (40 to 50 per cent of total S) and partly proteins (50 to 60 per cent). Results indicated that 35 to 50 per cent of the total S was released to the gas phase during pyrolysis at 400 °C as a result of thermal decomposition of organic S. The latter commenced at 178 °C to 283 °C. At

higher temperatures (500 °C to 700 °C), the residual S contents of biochar did not change significantly.

Figure 6-49 shows the content of chlorine for four pyrolysis char samples at different pyrolysis temperatures. The chlorine content is in the range of 3290 mg/kg to 3820 mg/kg. The original fuel contained 1682.5 mg/kg.

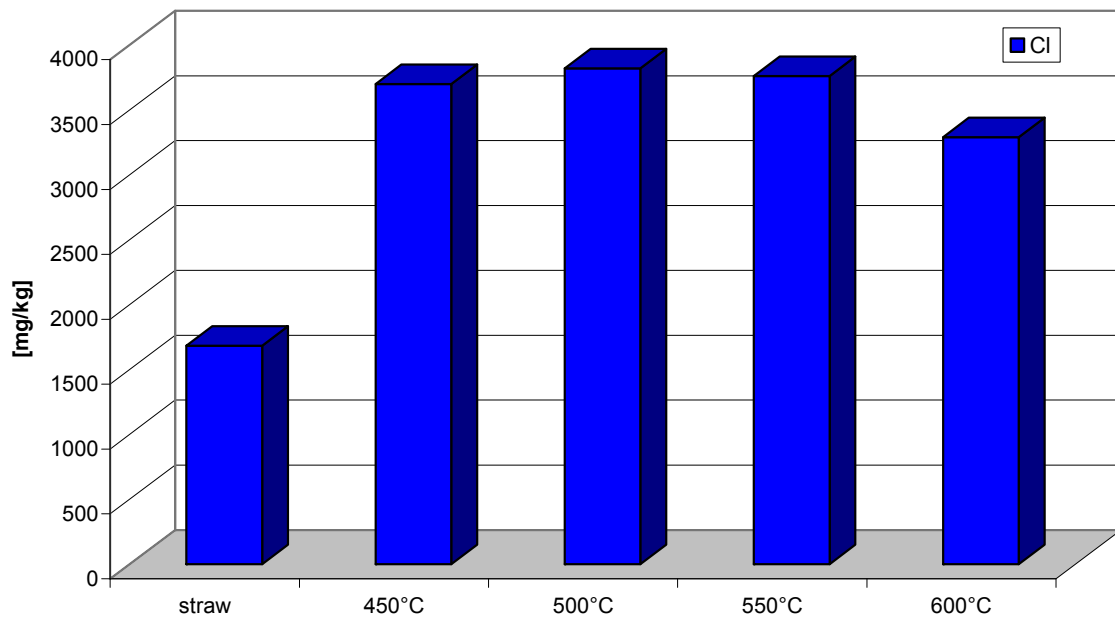


Figure 6-49: Chlorine content of pyrolysis char at different pyrolysis temperatures

The chlorine in the biomass strongly influences the behaviour of other elements. In the presence of Cl and S the volatilisation temperatures of some heavy metals, especially Cd, Cu, and Pb are lower than in the absence of these elements and their species. The evaporation test performed by Lindt et Kauppinen [Lindt et Kauppinen, 1999] showed that without chlorine, virtually no evaporation of the heavy metals was observed, whereas the tests with chlorine clearly showed a significant evaporation.

Investigations have shown that the first amount of chlorine is released between 200 °C and 400 °C, and most of the residual chlorine is released when temperatures increase from 700 °C to 900 °C [Wei et al., 2002], [Wei et al., 2005], [Jensen et al., 2000], [Björkman et Strömberg, 1997].

Below 200 °C no significant release of chlorine was observed. At 400 °C between 20 and 50 wt. % of the chlorine was released [Björkmann, 1996].

Figure 6-50 shows the release of chlorine and potassium during the pyrolysis of straw.

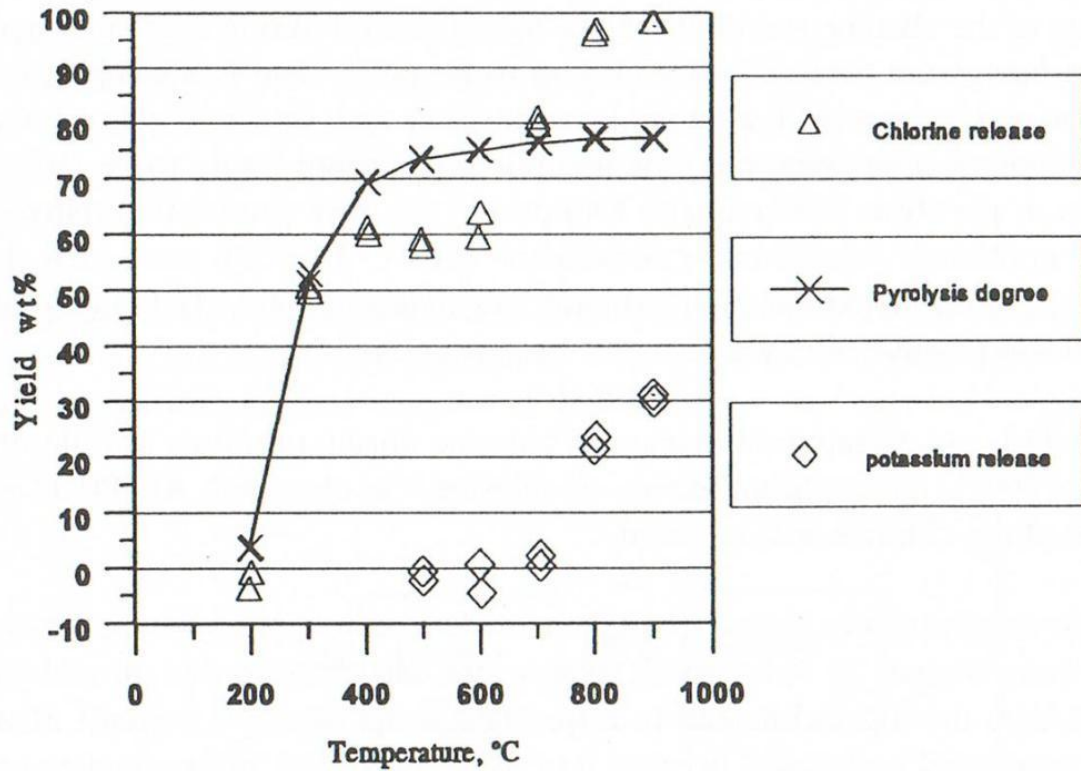


Figure 6-50: Release of chlorine and potassium during pyrolysis of straw [Dam-Johansen et al., 1997]

The chlorine was released in two steps, about 60 % was released between 200 and 400 °C, and the residual chlorine was released between 600 and 900 °C.

Chlorine can also cause corrosion problems because of the HCl formation during the conversion process.

Figure 6-51 shows the content of potassium for four pyrolysis char samples at different pyrolysis temperatures. The potassium content is in the range of 27700 mg/kg to 34100 mg/kg. The original fuel contained 9555 mg/kg.

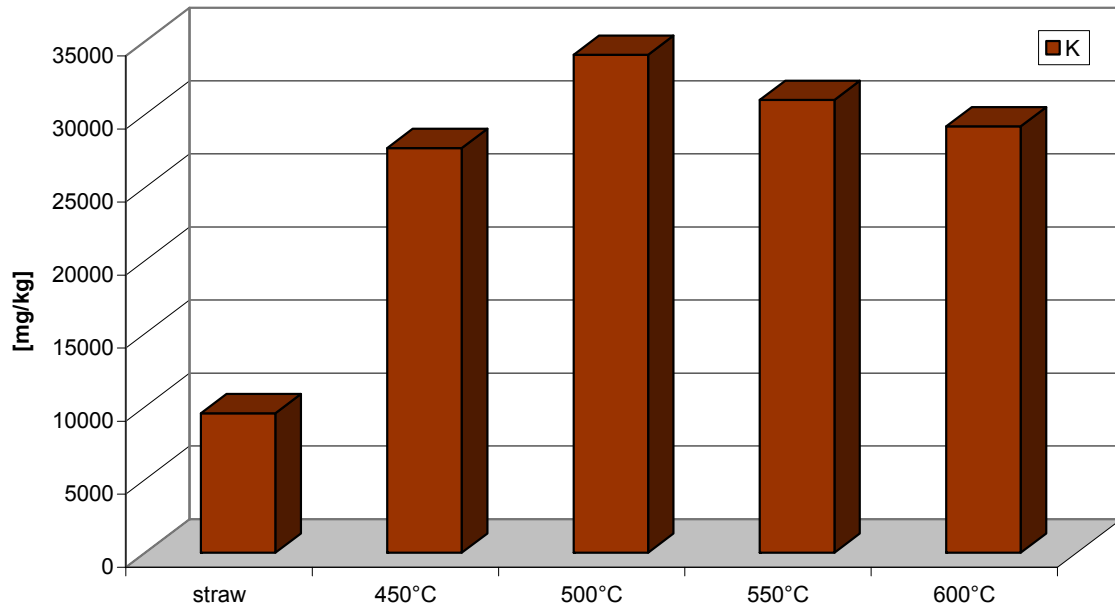


Figure 6-51: Potassium content of pyrolysis char at different pyrolysis temperatures

From literature it is known that during straw pyrolysis at temperatures between 200 to 400 °C potassium is bond as KCl and  $K_2CO_3$  and at temperatures between 400 to 700 °C no significant amounts of potassium were released to the gas phase (cf. Figure 6-50 and Figure 6-52). [Jensen et al., 2000].

Figure 6-52 shows the release of potassium during straw and wood pyrolysis. This figure is taken from literature [Jensen et al., 2000]. In the temperature range of 450 to 630 °C nearly all the potassium stays in the char. This value is approved by the simulation results which also show that nearly 100 per cent stay in the pyrolysis char.

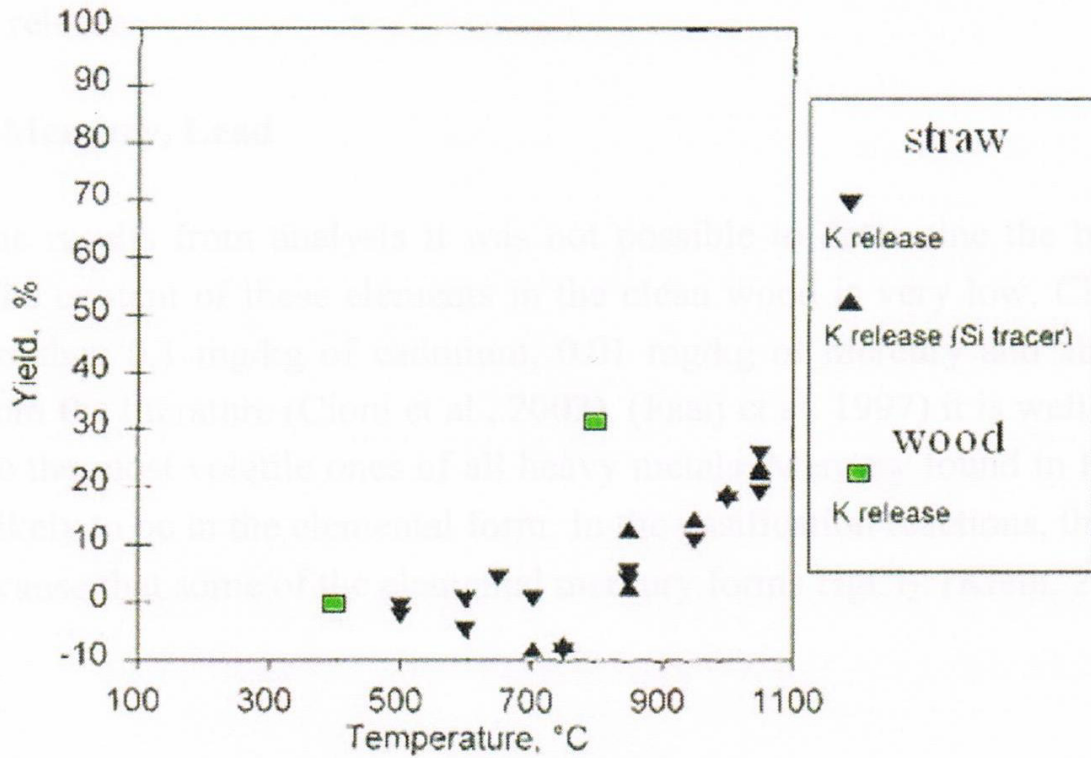


Figure 6-52: Comparison of K release to the gas phase; straw and wood pyrolysis [Jensen et al., 2000]

Figure 6-53 shows the content of sodium for four pyrolysis char samples at different pyrolysis temperatures. The sodium content is in the range of 218 mg/kg to 619 mg/kg. The original fuel contained 47.025 mg/kg.

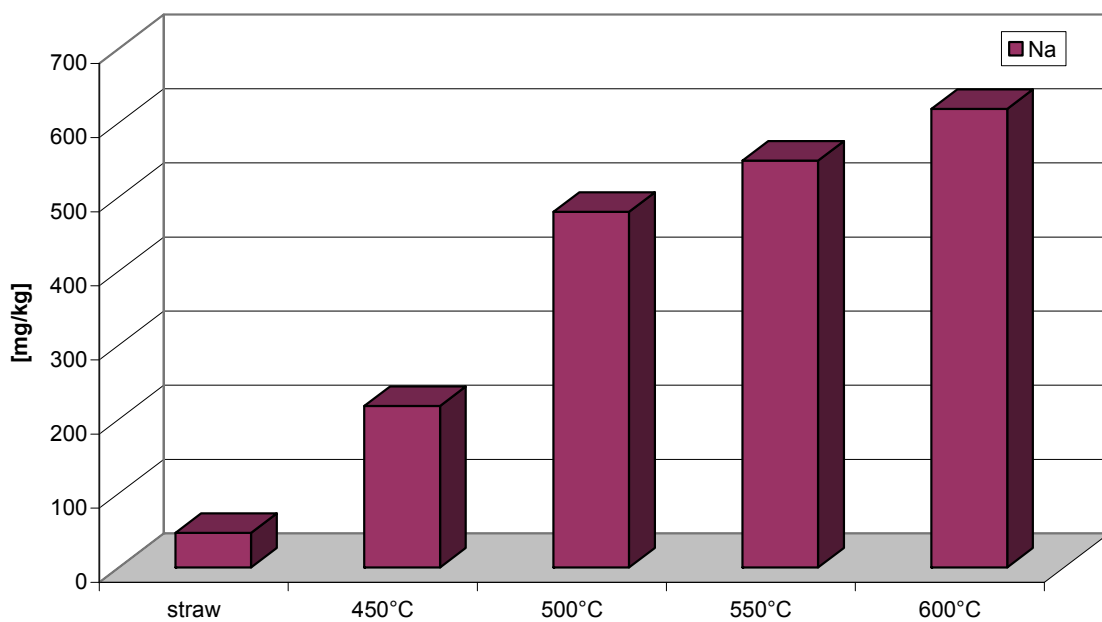


Figure 6-53: Sodium content of pyrolysis char at different pyrolysis temperatures

As already mentioned the sodium content in most of the biomass samples is more than ten times lower than the potassium content, therefore, less attention could be given to the release of sodium because these amounts are nearly insignificant. In the case of higher sodium contents it has to keep in mind that sodium is known for lowering the sintering temperatures.

The analysed LHVs correspond with the enrichment of carbon by increasing pyrolysis temperatures and rises from 23760 kJ/kg to 27060 kJ/kg by increasing the pyrolysis temperature. The original LHV of straw was 17150 kJ/kg.

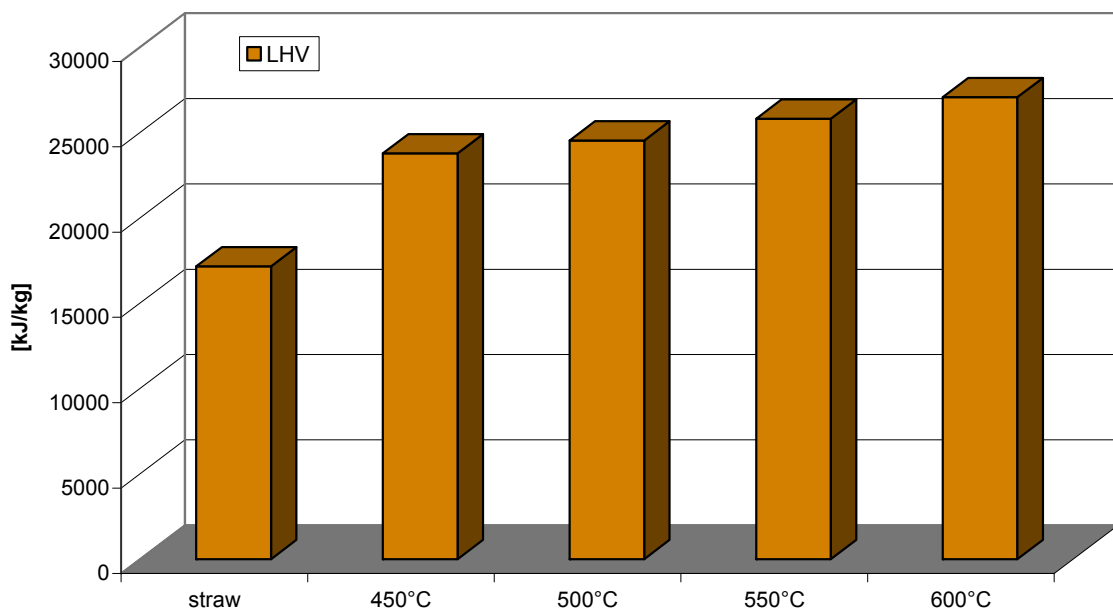


Figure 6-54: Lower heating value of and original straw and pyrolysis char (dm) at different pyrolysis temperatures

Figure 6-55 shows the residual content of volatiles for four pyrolysis char samples at different pyrolysis temperatures. The volatiles are decreasing from 28.6 to 15.4 wt. % by increasing the pyrolysis temperature.

This trend is obvious because of the fact that higher pyrolysis temperature favours the production of gaseous products by decomposition processes. The volatiles consist of a condensable and a non-condensable fraction.



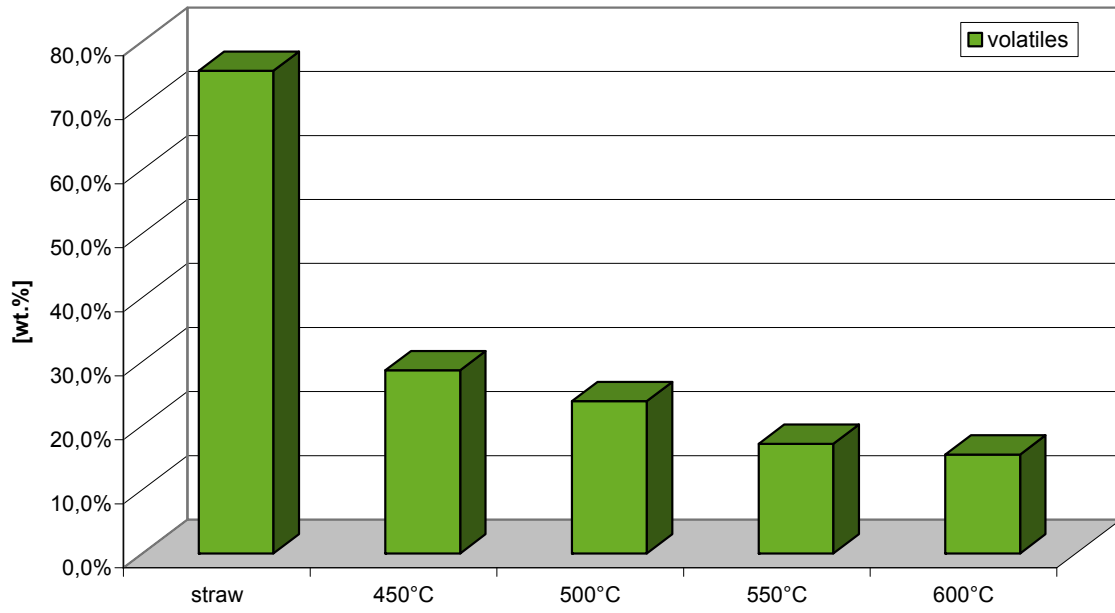


Figure 6-55: Fraction of volatiles of pyrolysis char at different pyrolysis temperatures

### 6.6.4 Pyrolysis gas composition

The pyrolysis gas composition is a very important parameter because the gas is intended to be used for co-firing in the coal fired power plant. Table 6-6 shows a typical pyrolysis gas composition concerning the permanent gases from indoor stored wheat straw at a pyrolysis gas temperature of 550 °C.

Apparently, the composition of the gas fraction versus temperature between 450 and 600 °C does not vary a lot for the tested wheat straw (cf. appendix, 9.6 Balanced results).

Ethene, ethane, propane were not measured because of the limitation of the measurement system.

Zanzi et al. [Zanzi et al., 2001] measured at a lab-scale slow pyrolysis reactor for miscanthus straw 1.6 wt. % (maf – moisture and ash free) and for wheat straw pellets 1.8 wt. % (maf) C<sub>2</sub>-gases. Ruiz et al. in [Kaltschmitt et Bridgwater, 1997] measured yields of 0.63 to 3.38 (% of feed) of C<sub>2</sub>-gases for the pyrolysis of straw pellets at which the yield of C<sub>2</sub>H<sub>6</sub> captured the highest part (0.22 to 3.11 % of feed).

Table 6-6: Pyrolysis gas composition concerning permanent gases at a pyrolysis temperature of 550°C

	unit	pyrolysis gas	pyrolysis gas (db)
LHV	[MJ/Nm <sup>3</sup> ]	7,20	14,57
CH <sub>4</sub>	[vol%]	12,67	25,64
CO	[vol%]	16,79	33,97
CO <sub>2</sub>	[vol%]	13,35	27,01
H <sub>2</sub>	[vol%]	4,97	10,06
H <sub>2</sub> O	[vol%]	50,57	---
N <sub>2</sub>	[vol%]	0,76	1,55

Figure 6-56 shows the permanent gas composition in relation to the pyrolysis temperatures, it can be seen that the composition of the gas did not change significantly in the operated temperature range. For straw CO was present at a concentration of about 34 vol. %<sub>db</sub>, CO<sub>2</sub> at 27 vol. %<sub>db</sub>, CH<sub>4</sub> at 25.5 vol. %<sub>db</sub> and H<sub>2</sub> at 10 vol. %<sub>db</sub>. The lower heating value for dry pyrolysis gas without pyrolysis oil from straw ranges between 14.44 MJ/Nm<sup>3</sup> at 450 °C and 14.97 MJ/Nm<sup>3</sup> at 600 °C.

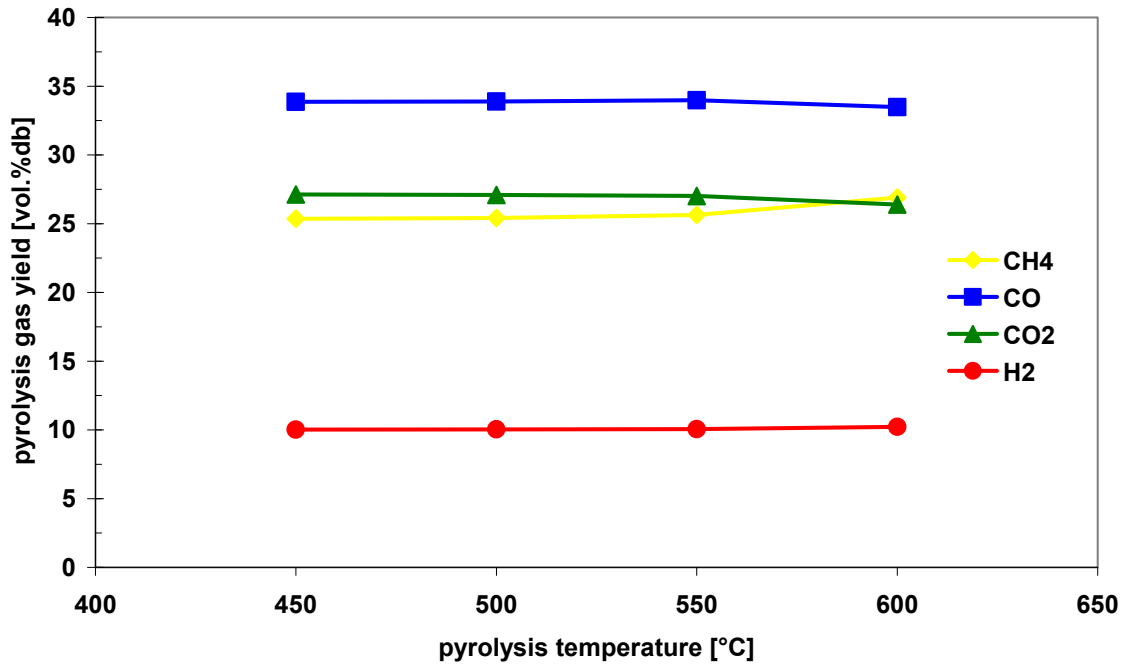


Figure 6-56: Pyrolysis gas composition of straw

CO had the highest concentration in the analysed samples. The CO is thought to mainly come from the decomposition of cellulose. Wannapeera et al. [Wannapeera et al., 2008] show that CO is the main product of cellulose decomposition; while the majority of product gases from lignin is H<sub>2</sub>. Previous studies have shown that CO is formed during the primary decomposition of hemicellulose and cellulose with a smaller proportion of CO coming from lignin by the cracking of carbonyl (C-O-C) and carboxyl (C=O) in biomass [Yang et al., 2007].

Fagbemi et al analysed three different materials (wood, straw, coconut shells) and recorded the composition of the gas fraction versus temperature between 500 and 900 °C, as indicated on Table 6-7.

A regular decrease in CO<sub>2</sub> concentration with temperature occurs with a simultaneous increase in CO and H<sub>2</sub> concentration. High temperatures are known to favour the production of H<sub>2</sub> to the detriment of higher hydrocarbons (in C<sub>2</sub>, C<sub>3</sub>) which are dehydrogenated by thermal cracking. The evolution of CO and CO<sub>2</sub> concentrations are consistent particularly when considering the heterogeneous gas-solid reaction at thermodynamic equilibrium (reaction equation 6-2), an increase in temperature results in a higher concentration in carbon monoxide [Fagbemi et al., 2001].



Table 6-7: Yields of the major gases (in % volume; A, wood; B, coconut shell; C, straw) [Fagbemi et al., 2001]

		<i>T</i> (°C)					
		400	500	600	700	800	900
CO	A	34.2	39.7	42.5	44.3	50.2	53.5
	B	31	35.0	38.1	40.1	44.2	–
	C	–	35.0	37.7	41.0	48.1	53.3
CO <sub>2</sub>	A	51.9	36.6	23.0	16.7	9.1	5.0
	B	53.1	42.2	28.7	17.9	9.8	–
	C	–	40.7	30.0	15.8	8.4	4.5
H <sub>2</sub>	A	1.3	7.6	10.8	15.5	20.8	25.3
	B	1.0	5.4	12.4	18.5	23.5	–
	C	–	7.4	12.8	19.2	23.4	24.6
CH <sub>4</sub>	A	9.3	12.8	16.5	16.1	14.2	12.1
	B	10.2	13.2	16.8	17.2	15.8	–
	C	–	11.8	13.0	15.3	13.7	12.1
C <sub>2</sub> H <sub>x</sub>	A	3.3	3.3	7.2	7.4	5.8	4.1
	B	4.7	4.2	4	6.3	5.3	–
	C	–	5.1	5.5	8.7	6.5	5.5

A big difference to the literature is the concentration of methane (CH<sub>4</sub>) in the pyrolysis gas of the pilot plant which is about 25 vol. % for the pyrolysis of indoor stored wheat straw, whereas Fagbemi et al mentioned that the concentrations of CH<sub>4</sub> and C<sub>2</sub>H<sub>x</sub> reach a maximum value at about 750 °C, that is in accordance with the results of other investigators [Deglise et al., 1980], [Sanchez et Simmons, 1981], who found values of CH<sub>4</sub> content of about 13 to 15 % between 700 and 800 °C.

#### 6.6.4.1 Water content

The average water content of the used straw (indoor stored wheat straw) is about 7 wt. %. The water content of the pyrolysis gas decreases from 62.67 to 44.65 % with increasing pyrolysis temperature. This obvious trend is also confirmed by Figure 6-78 [Fagbemi et al., 2001].

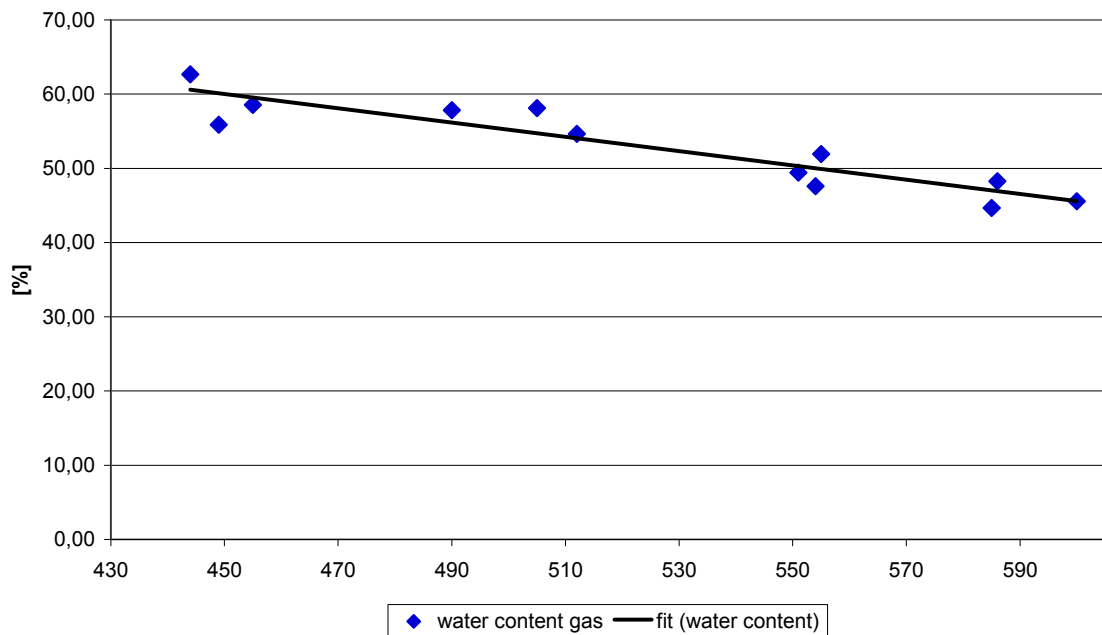


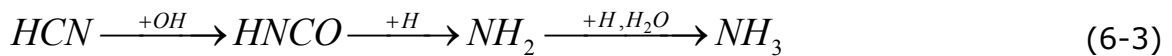
Figure 6-57: Correlation of water content of pyrolysis gas and pyrolysis temperature

The water content of the pyrolysis gas consists of the reaction water as well as the water content of the used biomass. At the operation temperatures (400 – 600 °C) the whole water is evaporated.

#### 6.6.4.2 NH<sub>3</sub> in the pyrolysis gas

Pyrolytic decomposition is one of the main steps which favour the production of nitrogenous gas components. During pyrolytic decomposition pyrolysis gases like methane (CH<sub>4</sub>) are formed from methyl groups, carbon monoxide (CO) from ether compounds, hydrogen (H<sub>2</sub>) from ring condensations and nitrogenous compounds (as gases NH<sub>3</sub> and HCN) are formed out of ring structures [Solomon et al., 1992]. So this highly volatile nitrogen could be detected as NH<sub>3</sub> and HCN [Baumann et Möller, 1991], [Solomon et Colket, 1978], [Bassilakis et al., 1993] after they are formed during the devolatilisation process.

Hämäläinen et al. [Hämäläinen et al., 1994] found in experiments with different model substances that the NH<sub>3</sub> / HCN - ratio does not depend on the nitrogen compounds instead of oxygen compounds and their relative position to the nitrogen atom. Only amino groups, which occur mainly in biomass, crack to NH<sub>3</sub>. Peck et al. [Peck et al., 1991] stated that NH<sub>3</sub> is present in the pyrolysis gas is due to a multi-step reaction in the gas phase of HCN to NH<sub>3</sub>.



Bassilakis et al [Bassilakis et al., 1993] mentioned three possible mechanisms for the release of HCN and NH<sub>3</sub> during devolatilisation (Figure 6-58):

1. Release of HCN directly from the fuel and reaction with fuel-hydrogen to NH<sub>3</sub> inside the pores.
2. Homogenous reaction from HCN with hydrogen in the gas phase.
3. Release of HCN and NH<sub>3</sub> directly from the fuel.

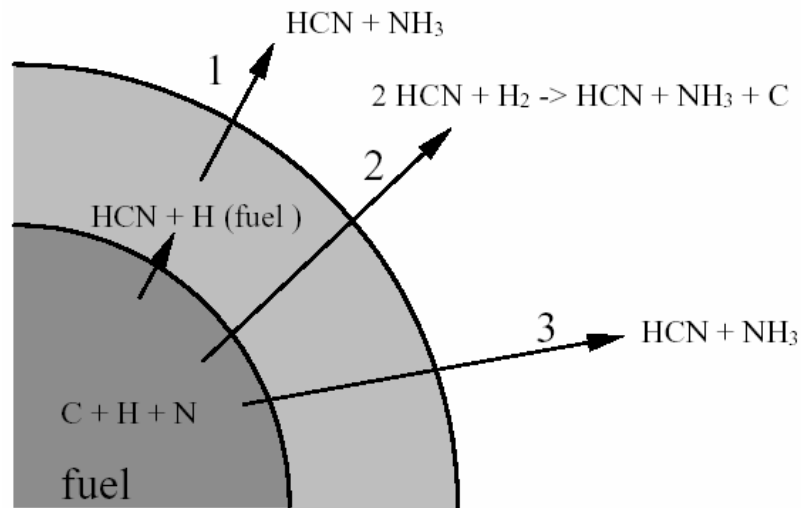


Figure 6-58: Mechanism of NH<sub>3</sub> and HCN disposal during devolatilisation [Bassilakis et al., 1993]

NH<sub>3</sub> measurements were carried out on three days focusing on three different pyrolysis temperatures. On the first day the pyrolysis temperature was set on 550 °C.

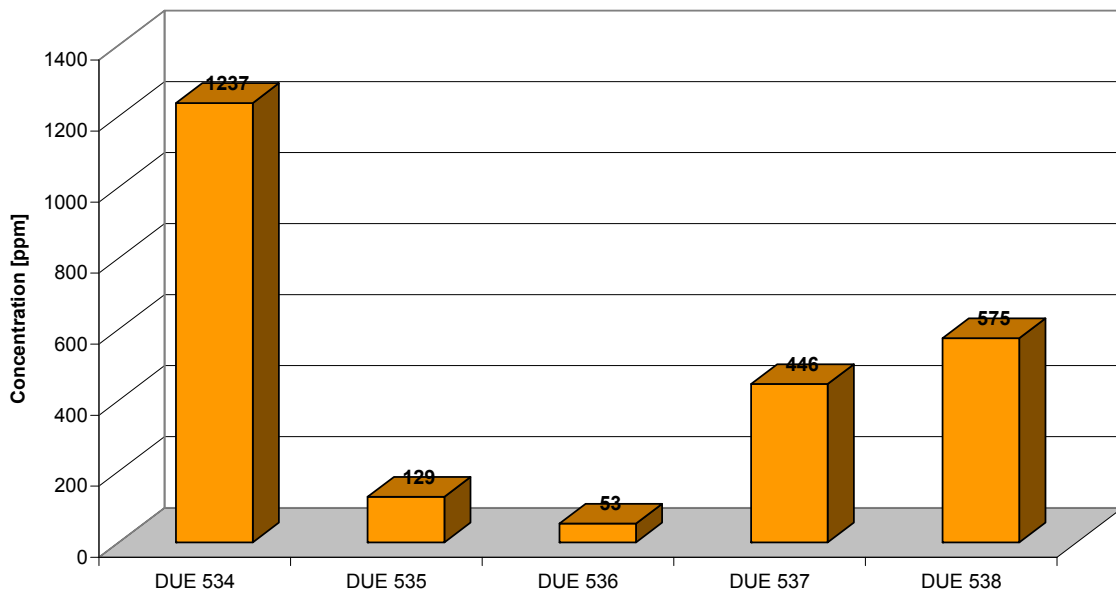


Figure 6-59: Concentration of NH<sub>3</sub> in the pyrolysis gas (pyrolysis gas temperature 550 °C)

Figure 6-59 shows the whole sampling of the first day. The concentration of NH<sub>3</sub> for a pyrolysis temperature of 550 °C is between 53 and 1237 ppm. The second part of the NH<sub>3</sub> measurements were carried out on a second day and the pyrolysis temperature was set on 500 °C.

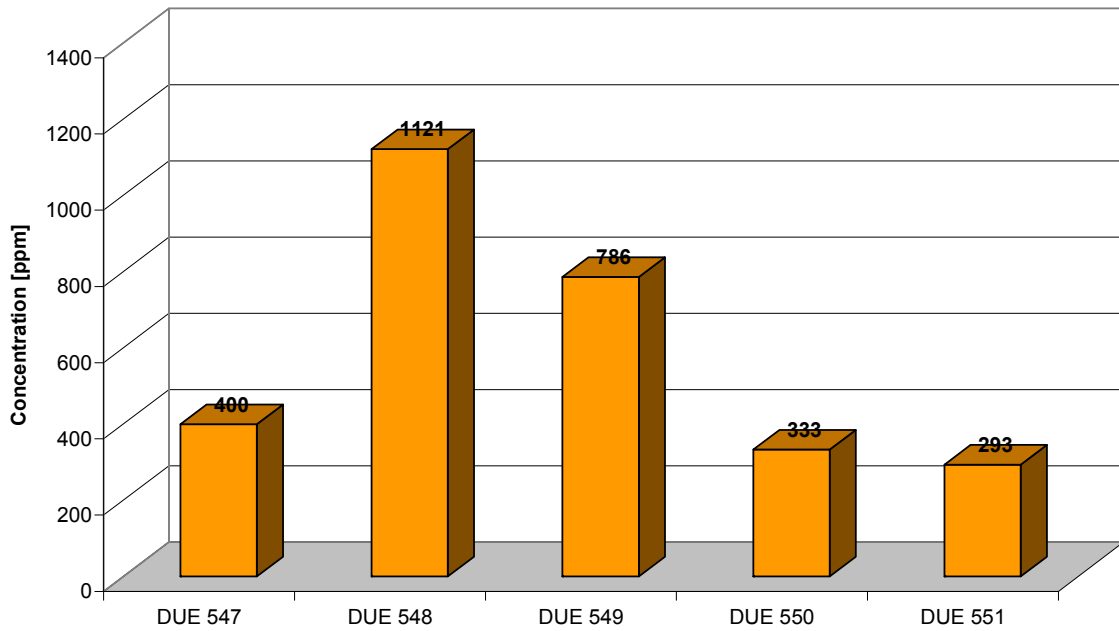


Figure 6-60: Concentration of NH<sub>3</sub> in the pyrolysis gas (pyrolysis gas temperature 500 °C)

Figure 6-60 shows the whole sampling of the second day. The concentration of NH<sub>3</sub> for a pyrolysis temperature of 500 °C is between 293 and 1121 ppm.

The third part of the NH<sub>3</sub> measurements was carried out again on another day and the pyrolysis temperature of 450 °C. Figure 6-61 shows the whole sampling of the third day. The concentration of NH<sub>3</sub> for a pyrolysis temperature of 450 °C is between 97 and 489 ppm.

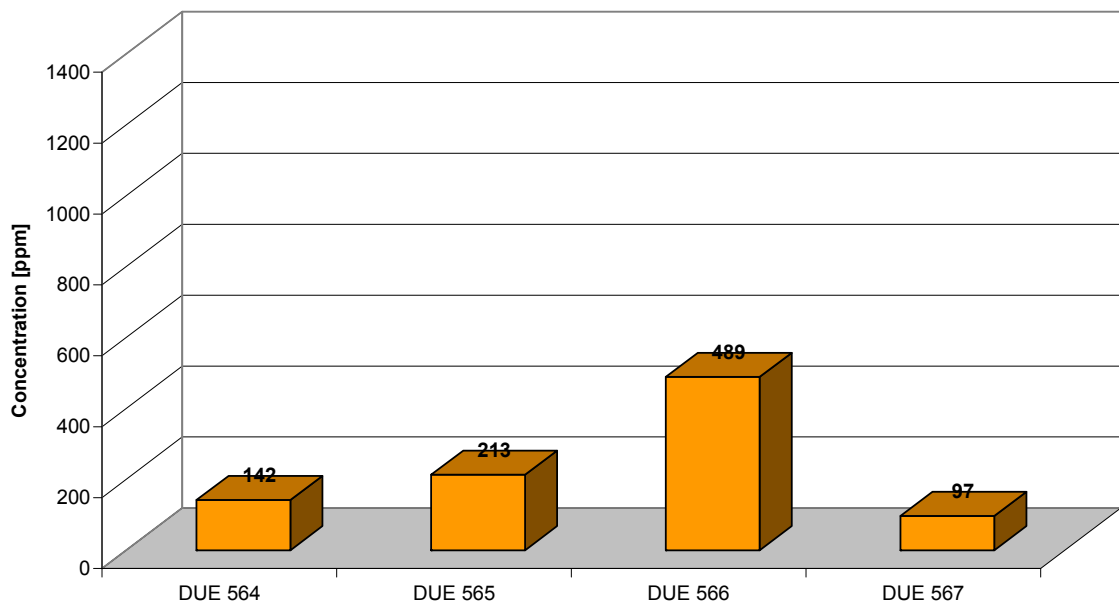


Figure 6-61: Concentration of NH<sub>3</sub> in the pyrolysis gas (pyrolysis gas temperature 450 °C)



Although the measurements were carried out with a great accuracy the results vary a lot and a temperature dependency could not be derived. Because of the fact that the operation of the pilot plant was stationary the only conclusion can be that the applied measurement method is not feasible for pyrolysis gases.

The overall mean value of  $\text{NH}_3$  in the pyrolysis gas is 451 ppm and there is no significant temperature dependency observable.

#### 6.6.4.3 HCl in the pyrolysis gas

Hydrogen chloride (HCl) measurements were carried out at a pyrolysis temperature of 550 °C. Figure 6-62 shows that the measured concentration of HCl for a pyrolysis temperature of 550 °C is between 2.3 and 4.8 ppm.

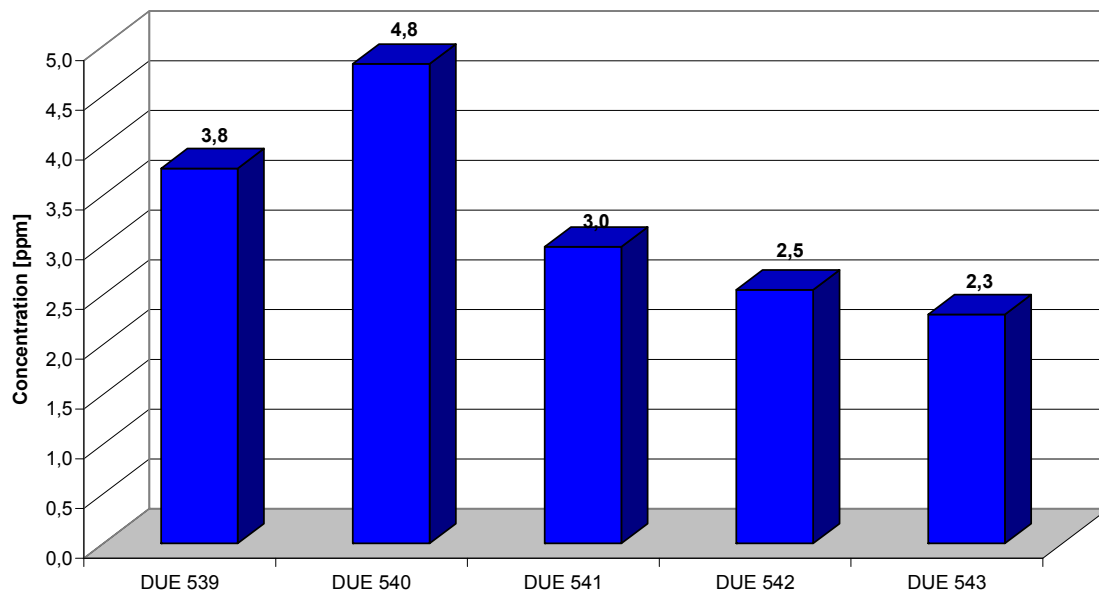


Figure 6-62: Concentration of HCl in the pyrolysis gas (pyrolysis gas temperature 550°C)

Jensen et al [Jensen et al., 2000] published data about straw pyrolysis. The release of Cl is gradually increasing and at temperatures of about 550 °C about 55 % of Cl was released to the gas phase. Above 800 °C all the chlorine from the char is released to the gas phase. This release to the gas phase is shown in Figure 6-63.

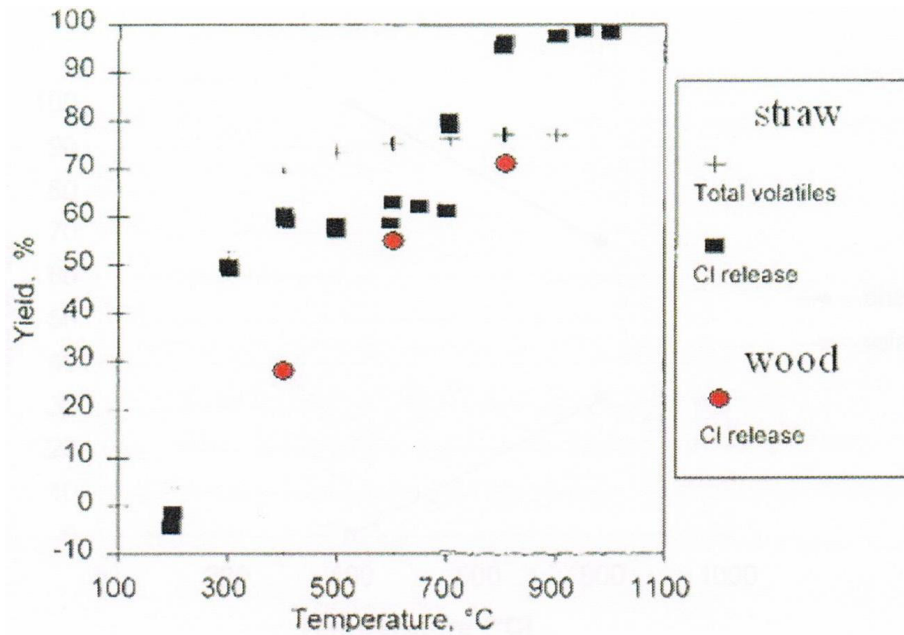


Figure 6-63: Comparison of Cl release to the gas phase; straw and wood pyrolysis [Jensen et al., 2000]

Björkmann and Strömberg [Björkmann et Strömberg, 1997] investigated the release of chlorine during pyrolysis of different types of biomass. Below 200 °C no significant release of chlorine was observed, but at 400 °C between 20 and 50 per cent of the chlorine was released. At higher temperatures residual Cl is remaining in the char. This is a different result to that shown in Figure 6-63.

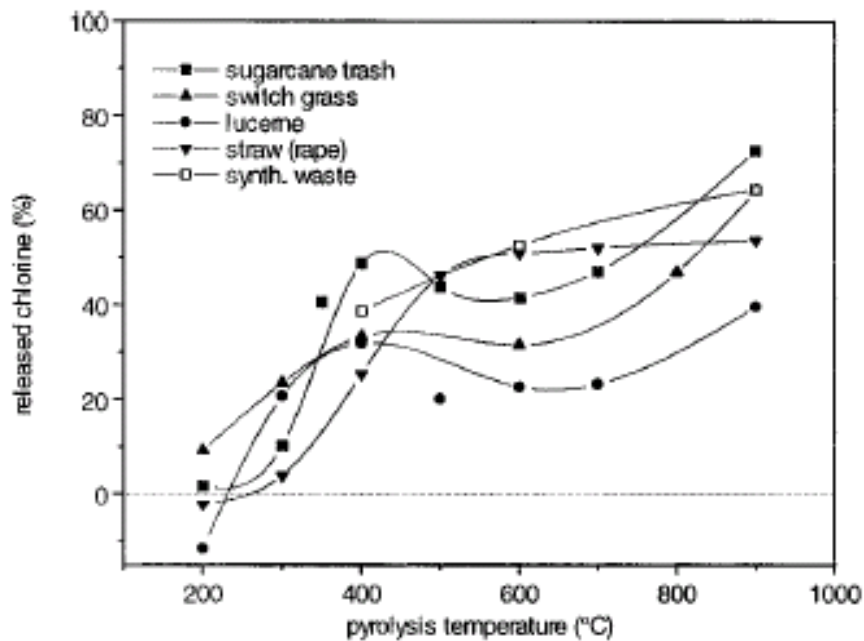


Figure 6-64: Percentage of released chlorine as a function of the pyrolysis temperature for different biomass [Björkmann et Strömberg, 1997]

Release of a significant amount of chlorine, however, cannot be avoided. The chlorine will be transported into the boiler as HCl. However, the increased level of HCl is not expected to induce a seriously increased corrosion [Nielsen et al., 1998]

#### 6.6.4.4 H<sub>2</sub>S in the pyrolysis gas

The high sulphur content in the biomass results on the one hand from the amino acids and the formed polymers (proteins) and on the other hand from already oxidised sulphur. Due to the fact that sulphur is very often a component of fertilizers used in agriculture the amount of sulphur found in biomass growing in agricultural areas is significantly higher than in forest areas.

Obernberger [Obernberger, 1998] describes that during thermo-chemical conversion most of the bound sulphur descends to the gas phase, but no chemical mechanisms are mentioned. Ma et al [Ma et al., 1989] and Stahlberg [Stahlberg et al., 1998] stated that it has to be expected that H<sub>2</sub>S, COS, mercaptanes, and CS<sub>2</sub> are formed.

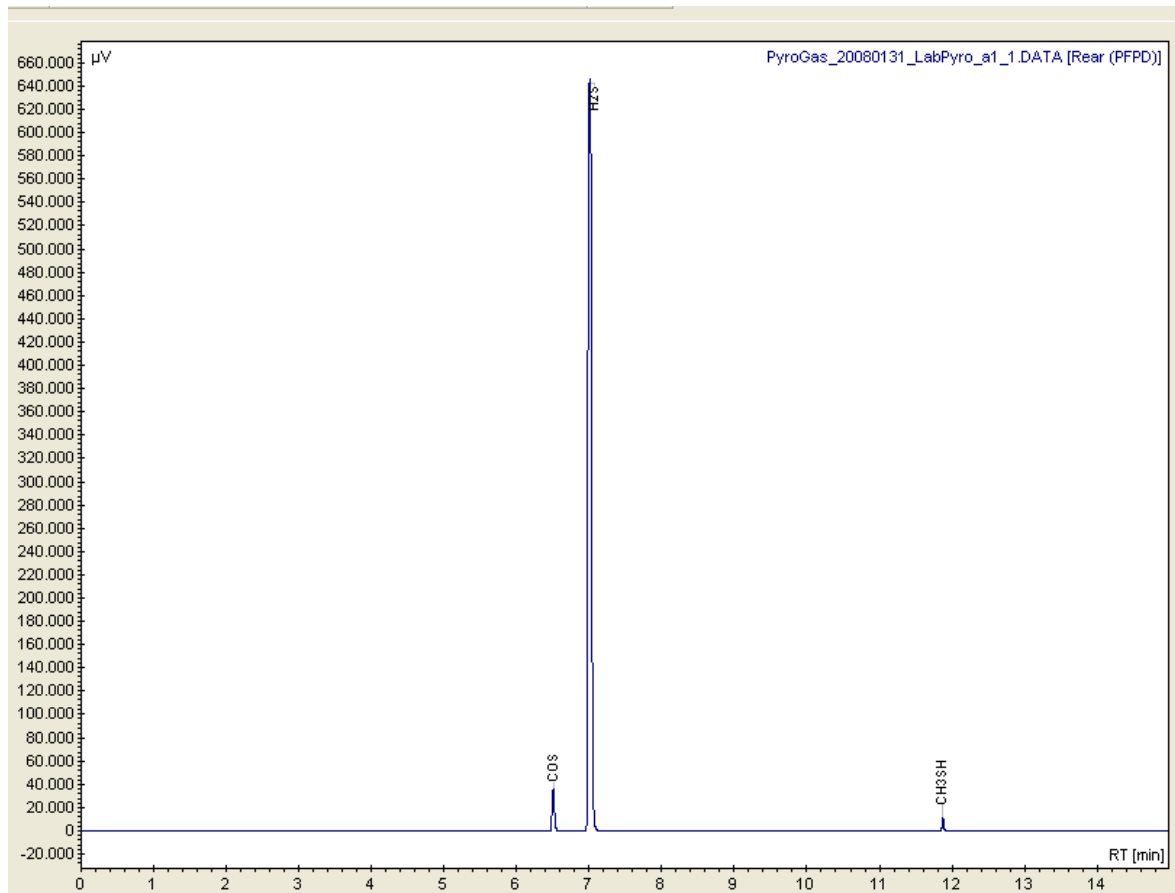


Figure 6-65: Chromatogram of sulphur sampling (permanent gases) at a pyrolysis temperature of 650°C and wheat straw as fuel [Lettner et al., 2008]

Figure 6-65 shows a chromatogram of the sulphur sampling which was carried out at the TU Graz. The main sulphur compound is H<sub>2</sub>S. The detected amount is in the range of 240 ppm at a pyrolysis temperature of 650 °C [Lettner et al., 2008].

As already mentioned in case of the formation of  $\text{NH}_3$  the pyrolytic decomposition is also the main step which favours the production of sulphurous gas components.

Following reactions are mentioned in literature [Ma et al., 1989], [Sasaoka et al., 1995]:



It could be assumed that the primarily organic bond sulphur (amino acids and proteins) in the biomass is completely released to the gas phase. The already oxidised sulphur will also be completely released to the gas phase but not as  $\text{H}_2\text{S}$  but as volatile alkali sulphates [Obernberger, 1998].

$\text{H}_2\text{S}$  measurements were carried out on two days focusing on three different pyrolysis temperatures. On the first day the pyrolysis temperature was set on 550 °C.

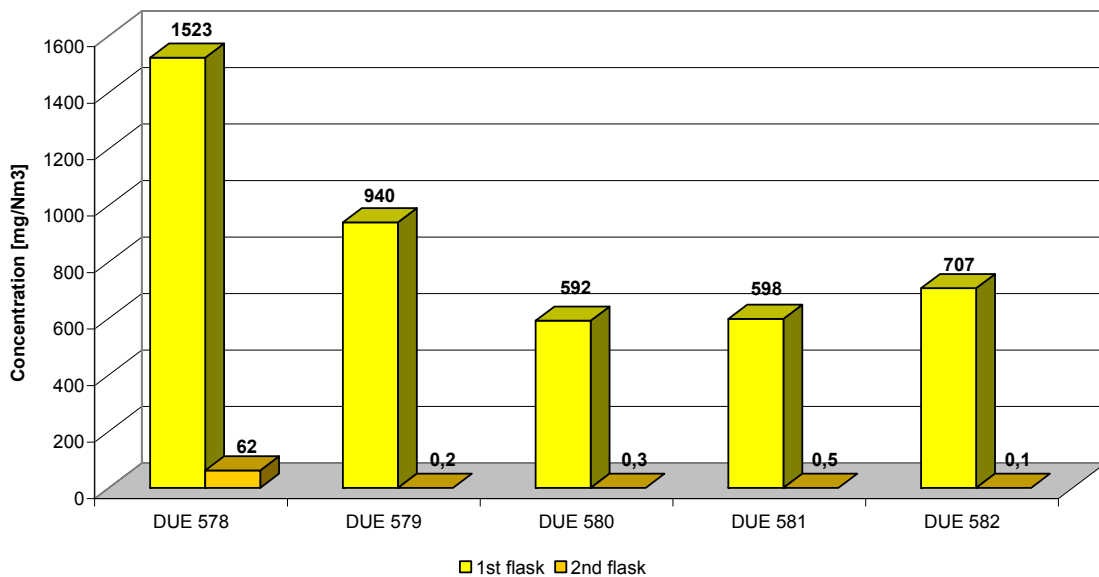


Figure 6-66:  $\text{H}_2\text{S}$  sampling at a pyrolysis temperature of 550 °C

Figure 6-66 shows all samples from the first day. The first two measurements show compared with the following measurements relatively high H<sub>2</sub>S values. After these two measurements the test rig was adjusted and an intermediate cleaning of the sampling probe and the cyclone was carried out. For the overall consideration the first two measurements are excluded.

On the second day the measurements where carried out at a pyrolysis temperature of 500 °C and 600 °C. Because of the already discussed problems with the gas filter the measurement was carried out only three times with the cyclone. After that an intermediate cleaning was carried out.

Figure 6-67 and Figure 6-68 show the results of the H<sub>2</sub>S measurements on the second day with pyrolysis temperatures of 500 and 600 °C.

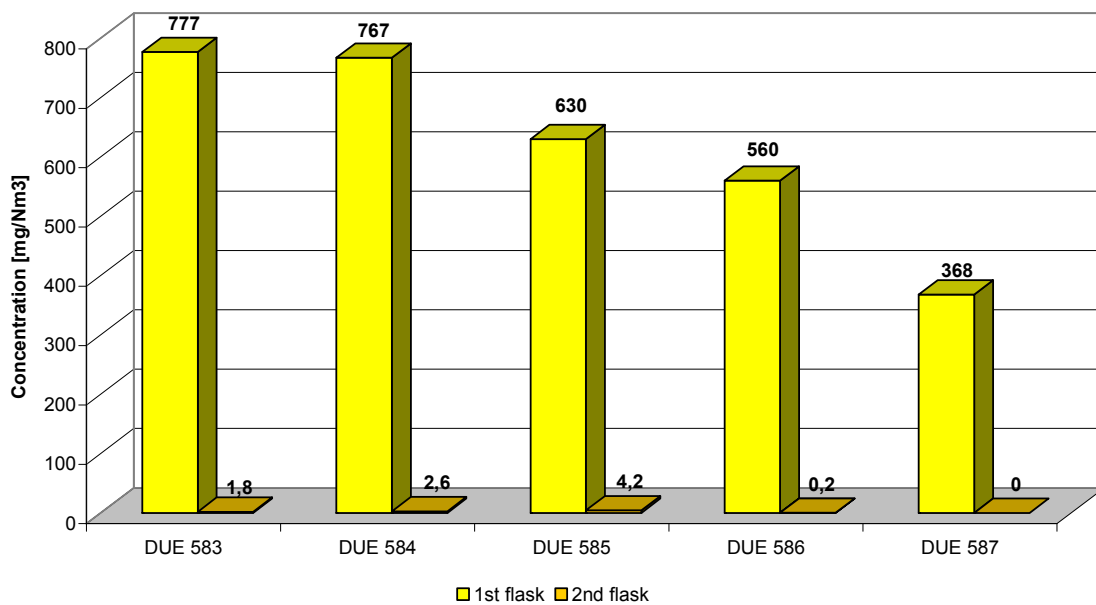


Figure 6-67: H<sub>2</sub>S sampling at a pyrolysis temperature of 500 °C

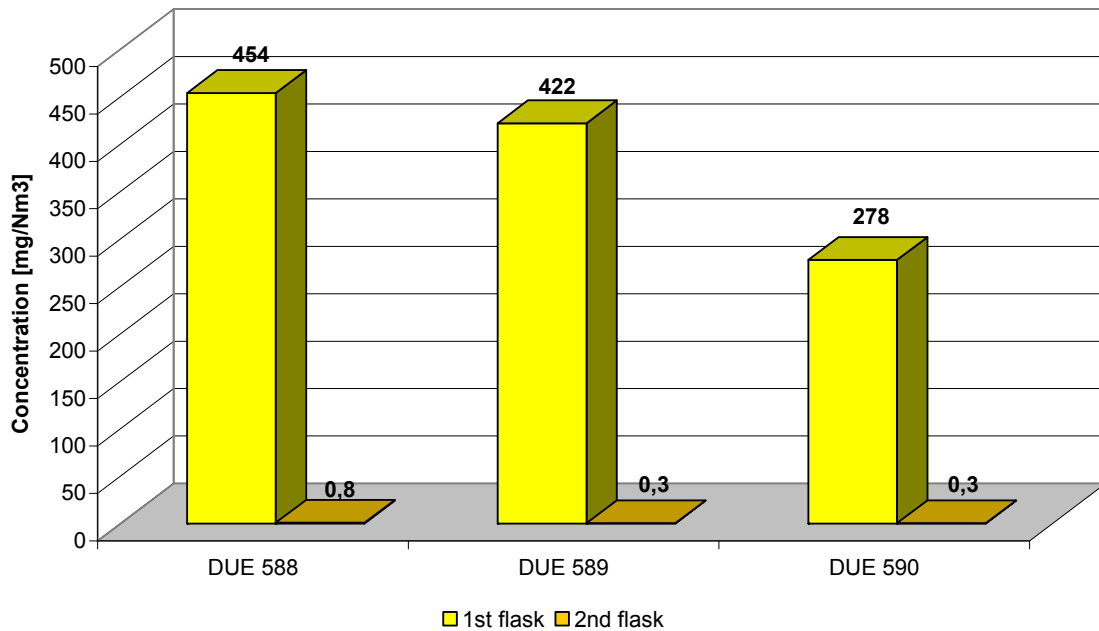


Figure 6-68: H<sub>2</sub>S sampling at a pyrolysis temperature of 600 °C

In principle the sampling was very selective (99 % in the 1<sup>st</sup> flask) this leads to the assumption that the whole amount of H<sub>2</sub>S was collected. Concerning the first two measurements, which have been carried out with the same adjustments, a big difference ranging from 1586 mg/Nm<sup>3</sup> to 940 mg/Nm<sup>3</sup> can be noticed.

An explanation for this discrepancy could be given by the lesser sampling volume or the lesser saturation of the drying columns with CO<sub>2</sub> at the beginning (both leads to deficits in the volume). Another explanation could be the adsorptive retention capacity of the dust (physi- and chemi-sorption).

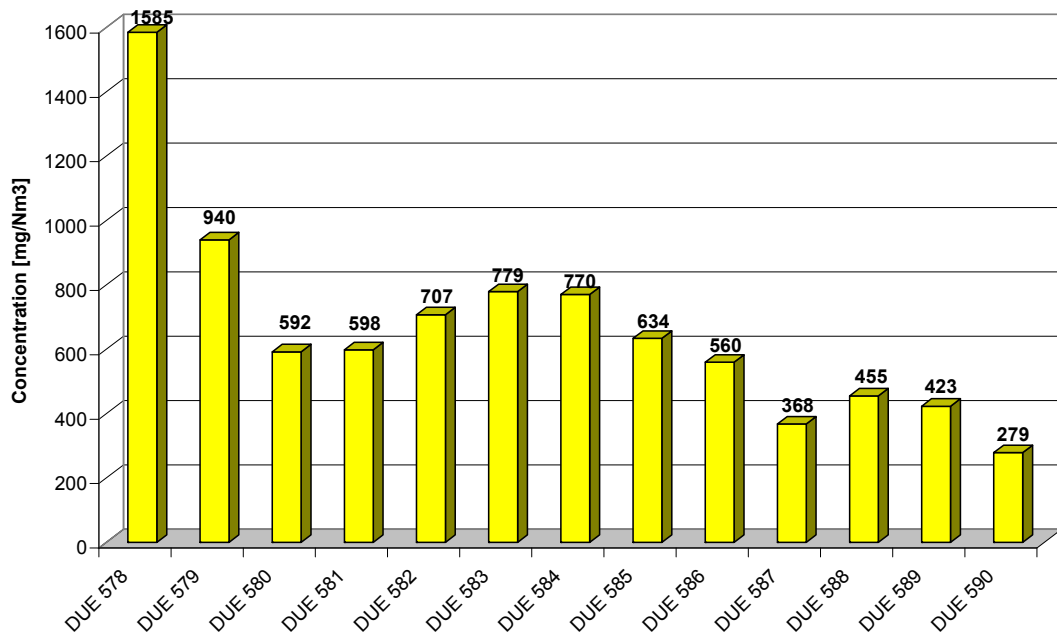


Figure 6-69: All measured H<sub>2</sub>S concentrations during the sampling period

Looking at Figure 6-69 a decrease of the concentration during the sampling period can be recognised. The average is in the range of 560 mg/Nm<sup>3</sup>. A small decrease of the concentration by increasing temperature can also be noticed.



### 6.6.5 Pyrolysis oil composition

Essentially pyrolysis oil consists of a mixture of alcohols, furans, aldehydes, phenols, organic acids as well as oligomer carbohydrates and lignin products. From the chemical point of view pyrolysis oil consists of a few hundreds single components with following functional groups: organic acids, aldehydes, ester, acetal, hemiacetal, alcohols, olefins, aromatic hydrocarbons and phenols [Kaltschmitt et al., 2009].

A typical composition of pyrolysis oil separated in GC-detectable components, polar components, oligomer (pyrolysislignin) and water is shown in Figure 6-70. The composition is dependent on feedstock, pyrolysis process, separator system and storage conditions. In this work pyrolysis oil refers only to the organic condensable but water is not included.

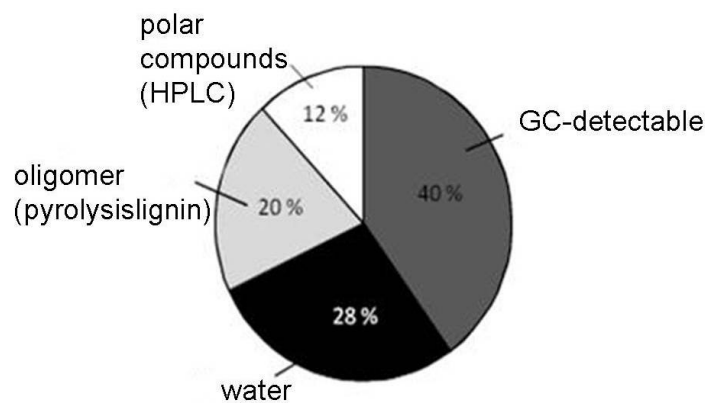


Figure 6-70: Typical distribution of main fractions of pyrolysis oil [Kaltschmitt et al., 2009]

A first overview about the detected single components is given in the master thesis of Wolfesberger [Wolfesberger, 2008]. The relative proportion of the substance groups is based on the sum of single compounds of GC/MS tars and is displayed in Figure 6-71.

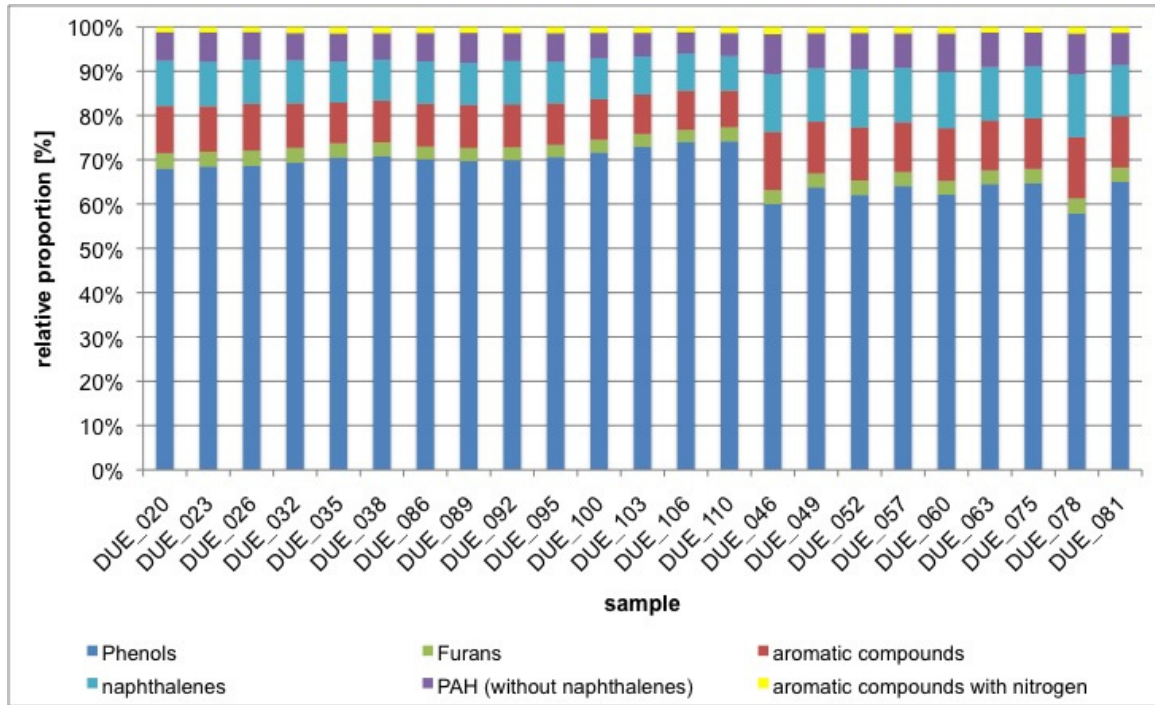


Figure 6-71: Relative proportions of group compounds of GC/MS tar [Wolfsberger, 2008]

To get more detailed information about the single components four pyrolysis oil samples were collected during the H<sub>2</sub>S measurement (c.f. 4.3.2) and analysed by using GC-MS/FID. Table 6-8 shows the detected substance groups found in the pyrolysis oil samples.

Table 6-8: Detected substance groups in the pyrolysis oil by GC-MS/FID

substance groups	
acids	catechols
nonaromatic aldehydes	aromatic aldehydes
nonaromatic ketones	aromatic ketones
furans	lignin derived phenols
pyrans	guaiacols (methoxy phenols)
sugars	syringols (dimethoxy phenols)
benzenes	miscellaneous

Detailed information about the detected single components (appendix, Table 9-10) in the pyrolysis oil samples by using GC-MS/FID and chromatograms could be found in the appendix (cf. Appendix, 9.7).

### 6.6.6 Detection of gravimetric pyrolysis oil

Figure 6-72 shows the detected amount of pyrolysis oil during using the gravimetric method described in chapter 4.2.1. The amount of pyrolysis oil varies between 53.63 – 214.19 g/Nm<sup>3</sup>.

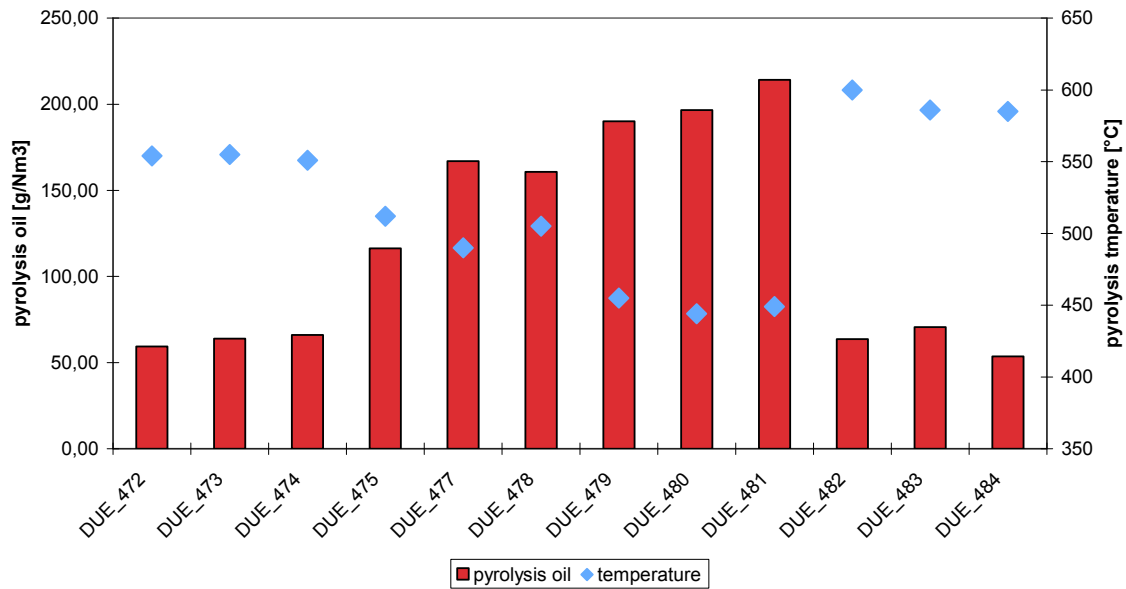


Figure 6-72: Measured amounts of pyrolysis oil by the gravimetric method

Figure 6-73 relates the pyrolysis gas temperature and the pyrolysis oil content of the different fuels investigated in this work.

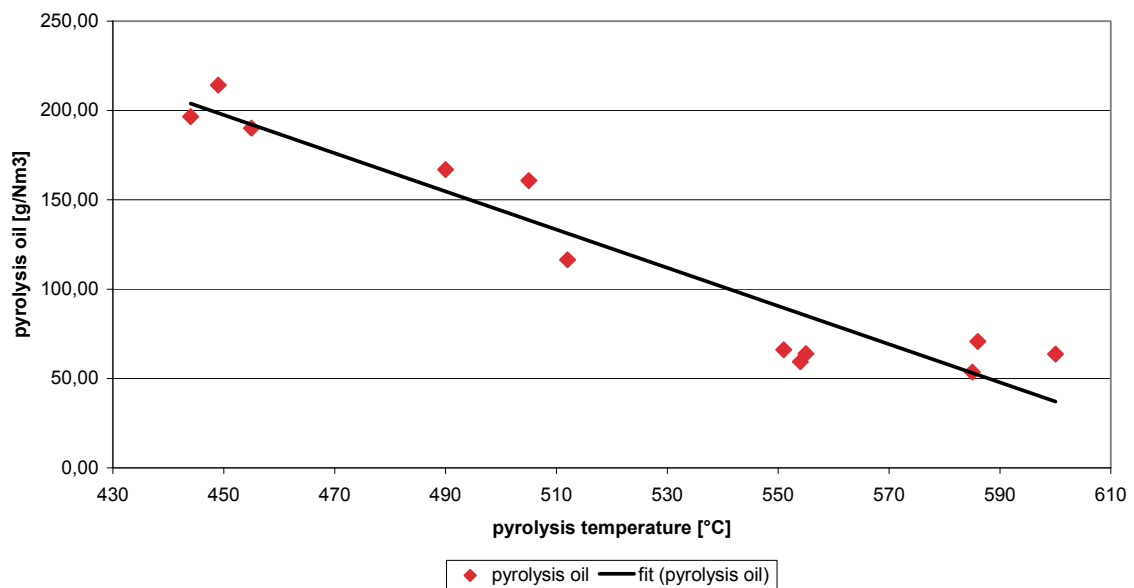


Figure 6-73: Temperature dependency of pyrolysis oil

A decreasing amount of pyrolysis oil at higher pyrolysis gas temperatures could be clearly approved.

The lower content of pyrolysis oil at higher pyrolysis gas temperatures is explained by the increasing emergence of small gaseous molecules from the cellulose-based tars (alcohols, aldehyds, ketons and carbon acids). The reactions to mention are dehydration, decarboxylation and decarbonylation.

### 6.6.7 Dust and entrained char

Figure 6-74 and Figure 6-75 show the dust and entrained char content during the sampling period over three days.

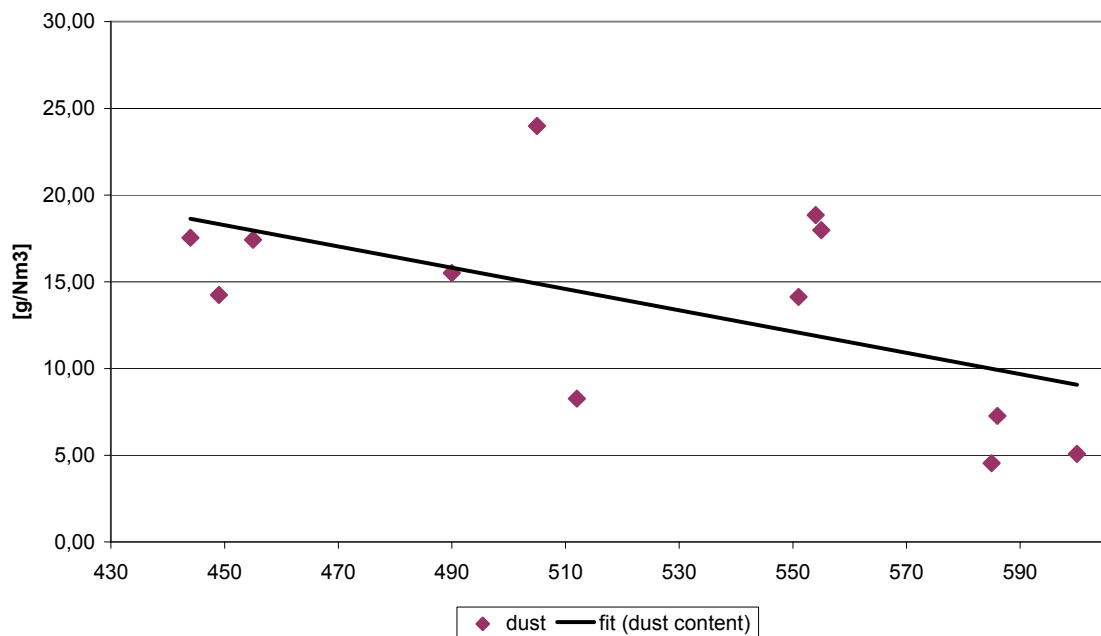


Figure 6-74: Temperature dependency of dust

The dust content varies between 4.53 – 23.99 g/Nm<sup>3</sup>. The entrained char content varies between 3.64 – 19.64 g/Nm<sup>3</sup>. An obvious temperature dependency of the dust and char content could not be approved.

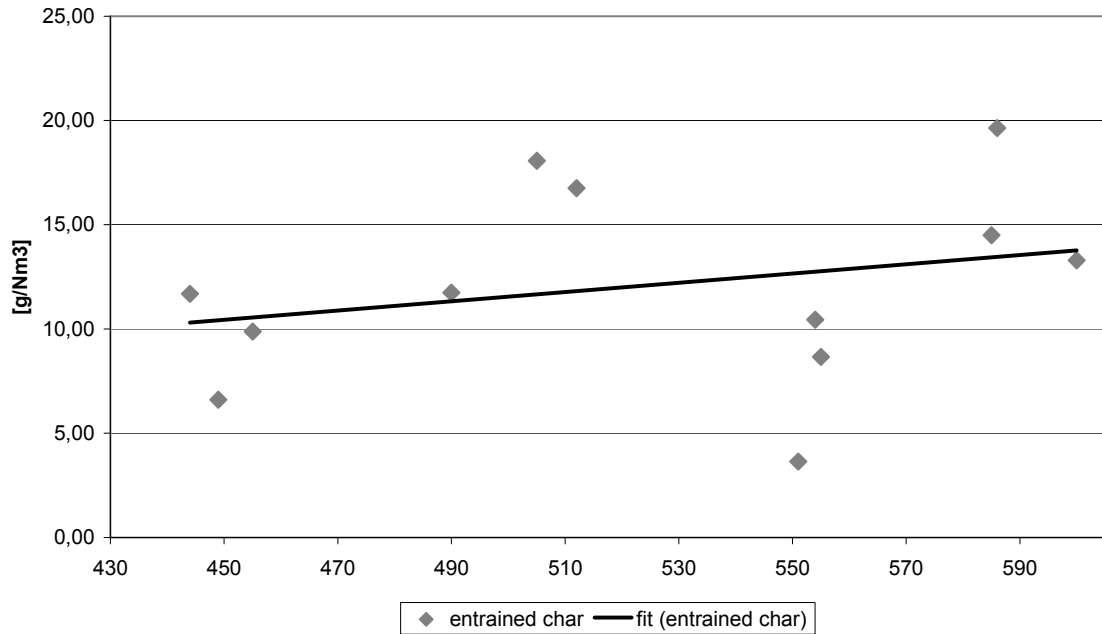


Figure 6-75: Temperature dependency of entrained char

As already mentioned, the representativeness of the dust and entrained char measurements has to be questioned. The measuring probe is located above the pyrolysis char screw conveyer, which can influence the actual dust and entrained char concentration of the pyrolysis gas, due to dust, which is dispersed by the screw conveyer. This could lead to an over detection of the particle load in the pyrolysis gas.

### 6.6.8 Variation of the pyrolysis temperature

To get more detailed insight the results from the test runs with pyrolysis temperatures of 450, 500, 550 and 600 °C have been used for the following balances.

An important point is the yield of gas, oil and char at different pyrolysis temperatures. For comparing the four operating points the energy and mass contents of those three fractions were each converted to the reference of the sum of the energy or mass contents of gas (containing the whole amount of water), oil and char (=100 %).

Figure 6-76 and Figure 6-77 show that by increasing pyrolysis temperature, the amount of pyrolysis gas increases significantly whereas the amount of char slightly goes back and the mass of pyrolysis oil is reduced heavily.

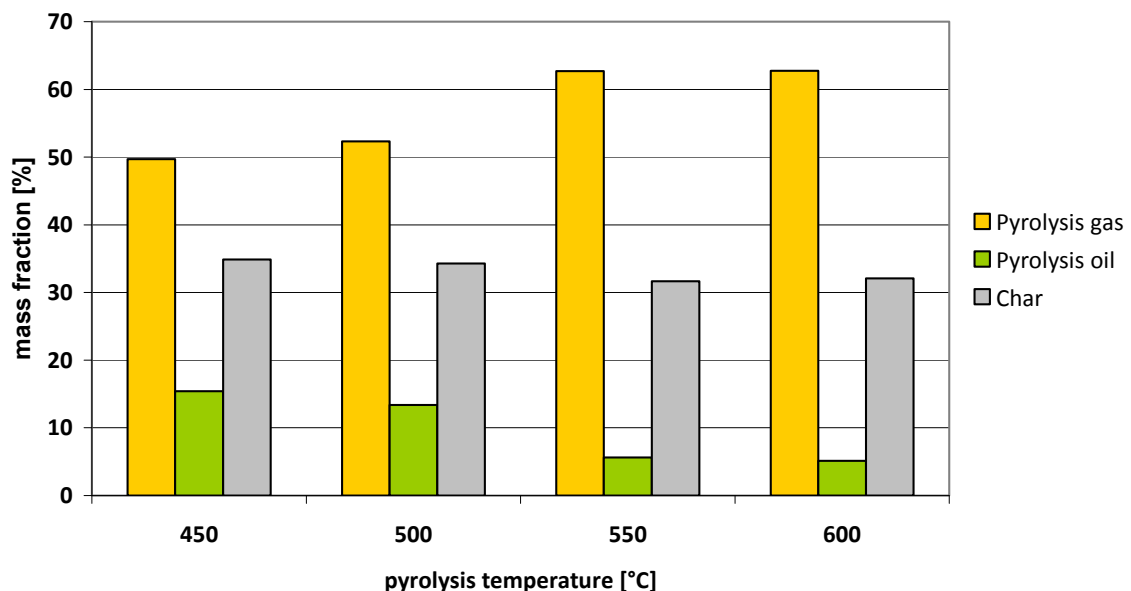


Figure 6-76: Mass fractions of the pyrolysis products for temperature variation during pyrolysis of straw

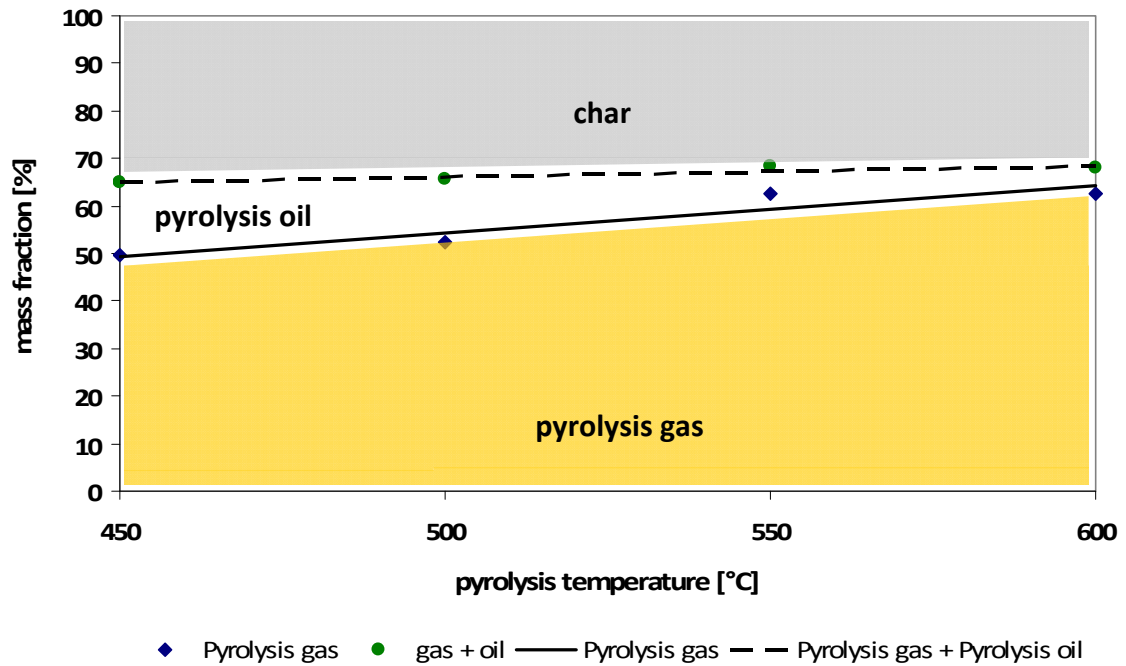


Figure 6-77: Trends of the mass fractions of the pyrolysis products for temperature variation during pyrolysis of straw

This strengthens the already known fact that a higher pyrolysis temperature forces the production of gas at the expense of the formation of pyrolysis oil. The higher temperature causes the decomposition of oil to gas. Slightly less mass of char results in the fact, that more volatile compounds are used to be stripped due to higher temperatures. Figure 6-78 shows the effect of temperature on the decomposition products found by Fagbemi et al [Fagbemi et al., 2001].

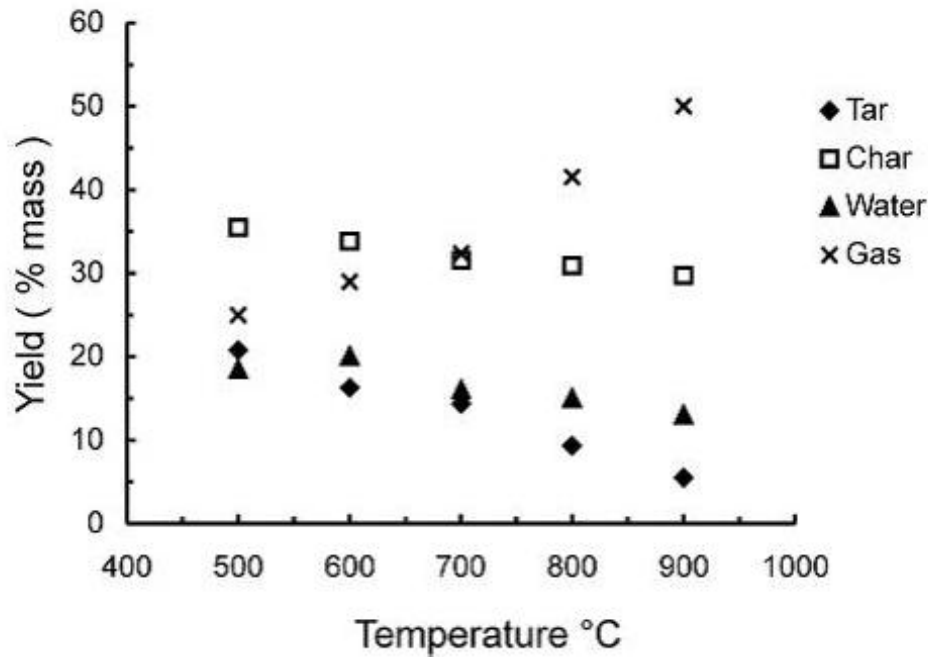


Figure 6-78: Straw pyrolysis: effect of temperature on the decomposition product [Fagbemi et al., 2001]

Fagbemi et al. state that by increasing the pyrolysis temperature, the produced amount of pyrolysis gas increases significantly. The water content and the pyrolysis oil/tar content decreases heavily (c.f. Figure 6-57 and Figure 6-73). The amount of pyrolysis char slightly decreases (c.f. Figure 6-43). These results correspond well with the measured and balanced data in this work.

Figure 6-79 and Figure 6-80 show that increasing pyrolysis temperature causes a raise of energy delivered by pyrolysis gas and char and a drop of the energy delivered by pyrolysis oil. Most of these effects are caused by the different amounts of the products that are obtained. A further reason is that due to different pyrolysis temperatures the chemical composition of the products is slightly different. So, in the rotary kiln reactor there are more polyaromatic compounds with a high heating value at lower temperatures.



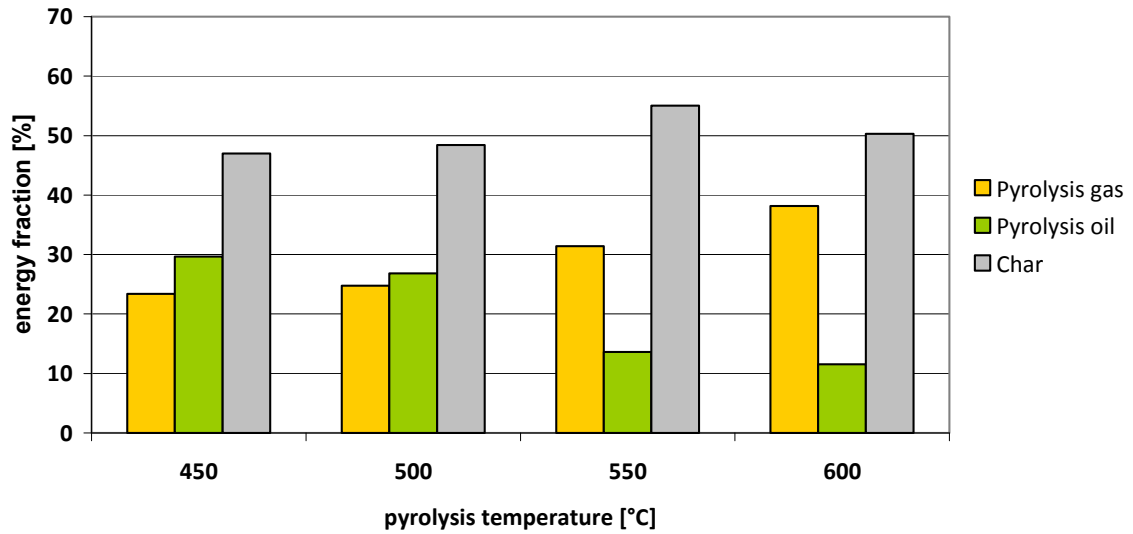


Figure 6-79: Fractions of the pyrolysis products for temperature variation during pyrolysis of straw

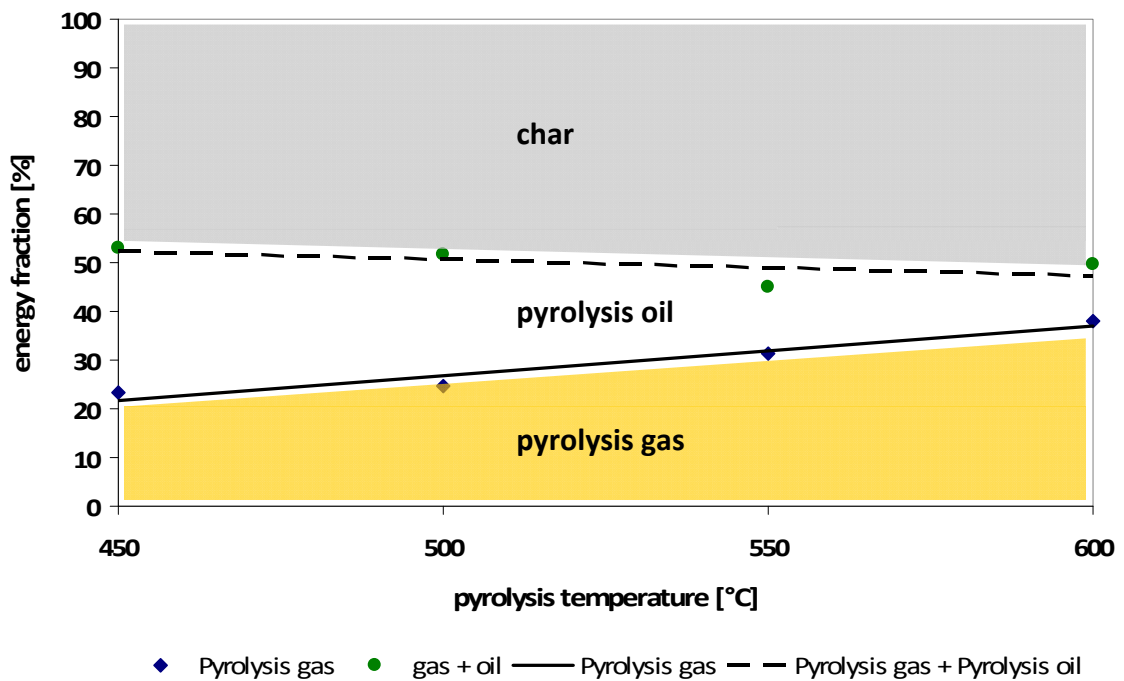


Figure 6-80: Trends of the energy fractions of the pyrolysis products for temperature variation during pyrolysis of straw

During the temperature variation the rotating speed was always set to the nominal value of 100 %. In the following chapter the influence of the residence time which corresponds to the rotating speed of the rotary kiln at constant feed rate is investigated.

### 6.6.9 Variation of the residence time

A balance of the plant for variation of the residence time has been carried out for 20 and 40 % of the speed of the rotary kiln reactor. This means that the feed rate of the rotary kiln stays constant but the amount of feedstock which is in the pyrolysis reactor increases because of the decreasing rotational speed. An additional operating point for a value of 100 % was also calculated to show trends. The temperature for residence time variation was set to 560 °C.

The mass of the products is also influenced by the residence time of the feedstock in the pyrolysis reactor. Figure 6-81 shows the mass fractions of the pyrolysis products for residence time variation of straw and Figure 6-82 shows the trends of the mass fractions of the pyrolysis products for residence time variation of straw.

There is not a straight trend for the amount of gas and char evident but a decent trend can be seen at the produced mass of pyrolysis oil. The yield of oil increases by an increase of the residence time of the feedstock in the rotary kiln reactor. Also the sum of pyrolysis gas and pyrolysis oil defines a trend. So the mass fraction of the gaseous products (pyrolysis oil + pyrolysis gas) which are intended to be co-fired in the coal power station increases by extending the residence time in the rotary kiln reactor.

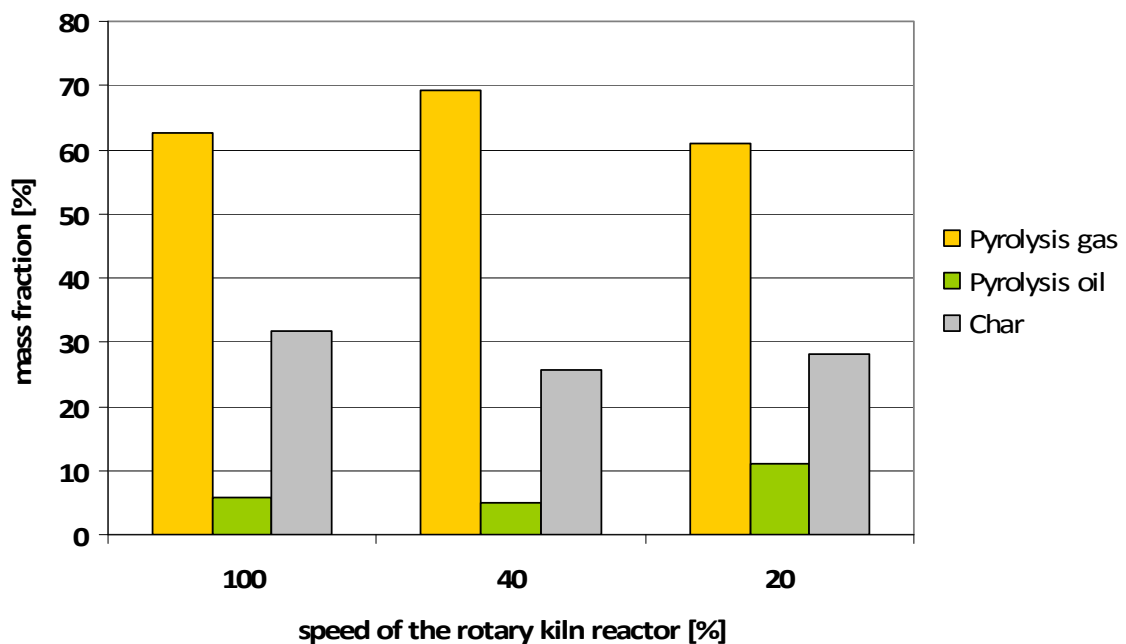


Figure 6-81: Mass fractions of the pyrolysis products for residence time variation during pyrolysis of straw at 560 °C

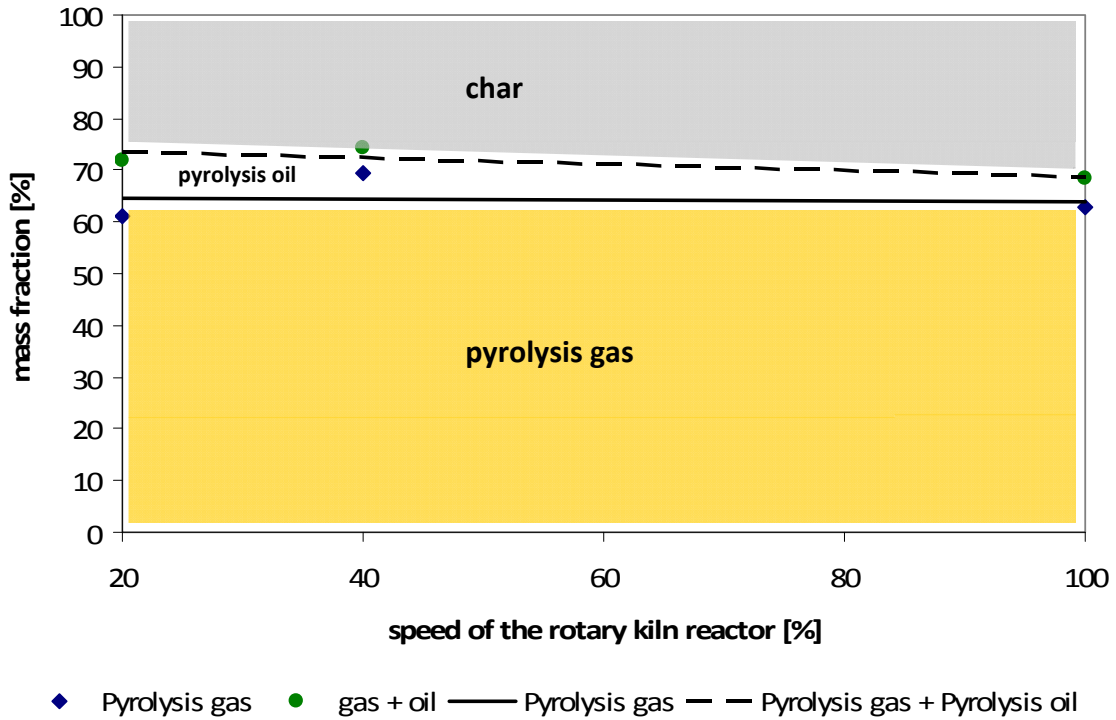


Figure 6-82: Trends of the mass fractions of the pyrolysis products for residence time variation during pyrolysis of straw at 560 °C

The chemical energy that is delivered by the pyrolysis gas drops slightly by slowing down the speed of the rotary kiln (increase of the residence time), but the energy contained in the pyrolysis oil clearly increases (Figure 6-83 and Figure 6-84).

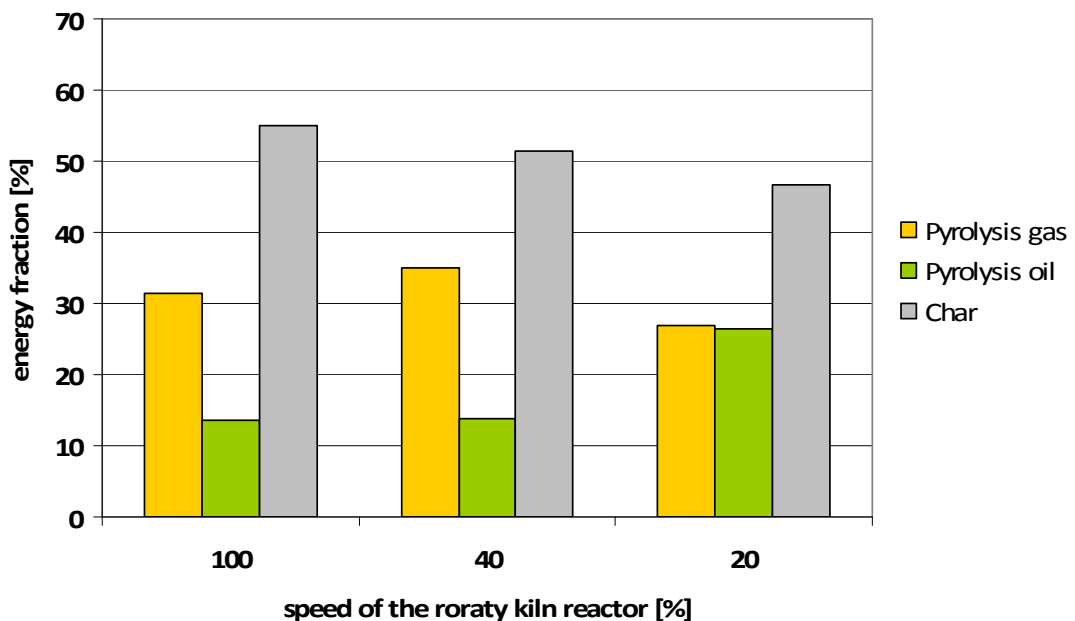


Figure 6-83: Energy fractions of the pyrolysis products for residence time variation during pyrolysis of straw at 560 °C

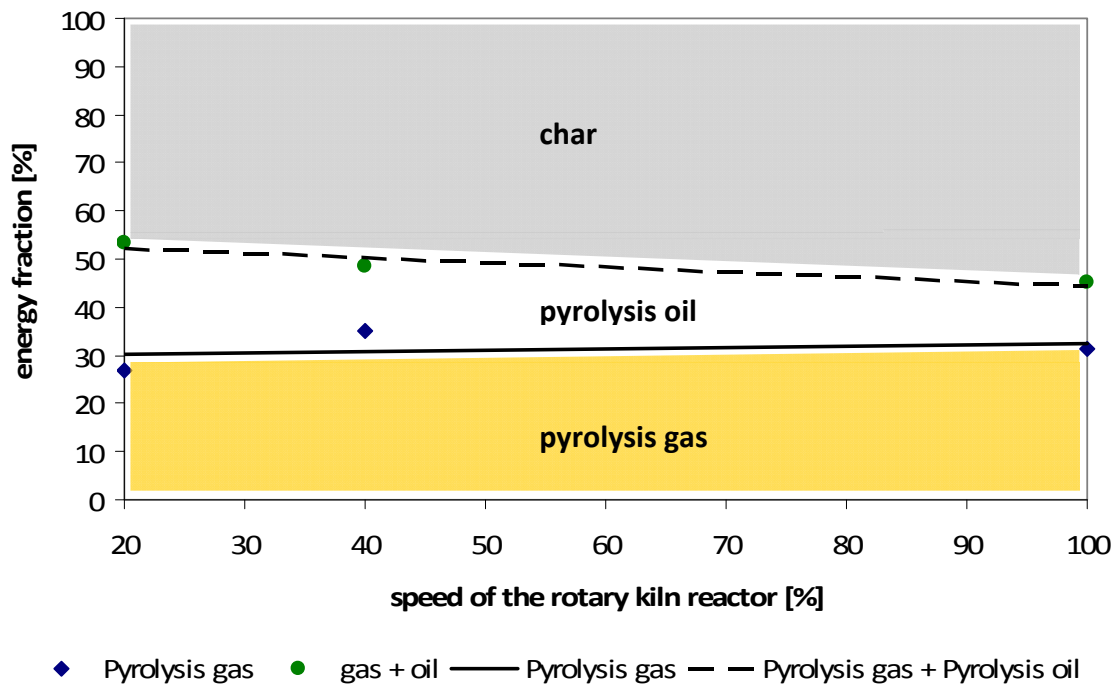


Figure 6-84: Trends of the energy fractions of the pyrolysis products for residence time variation during pyrolysis of straw at 560 °C

## 6.7 Distribution of chemical elements in the pyrolysis products

The distribution of chemical elements of the feedstock in pyrolysis gas, oil and char is an important point within this work. As already mentioned before, it is of major significance that the pyrolysis process is operated in a way that prevents the undesired components, which could lead to high temperature corrosion in the boiler, to enter the evaporated pyrolysis products. So elements like chlorine and potassium should be enriched in the pyrolysis char.

Table 6-9 shows, for comparison reasons, the results of the straw pyrolysis at different pyrolysis temperatures which have been carried out by Soukup [Soukup, 2005].

Table 6-9: Remaining fractions of elements in the pyrolysis char of straw at different pyrolysis temperatures [Soukup, 2005]

Temperature	C	H	N	S	Cl	K	Na
450 °C	54.8	22.0	56.4	48.9	78.3	78.8	72.6
550 °C	47.9	13.9	41.6	47.6	90.5	79.7	46.9
650 °C	42.6	7.4	35.1	47.0	66.5	72.2	37.5

Following figures (Figure 6-85, Figure 6-86, Figure 6-87) show the distribution of the chemical elements analysed in pyrolysis gas, oil and char for indoor stored wheat straw at pyrolysis temperatures ranging from 450 °C to 550 °C.

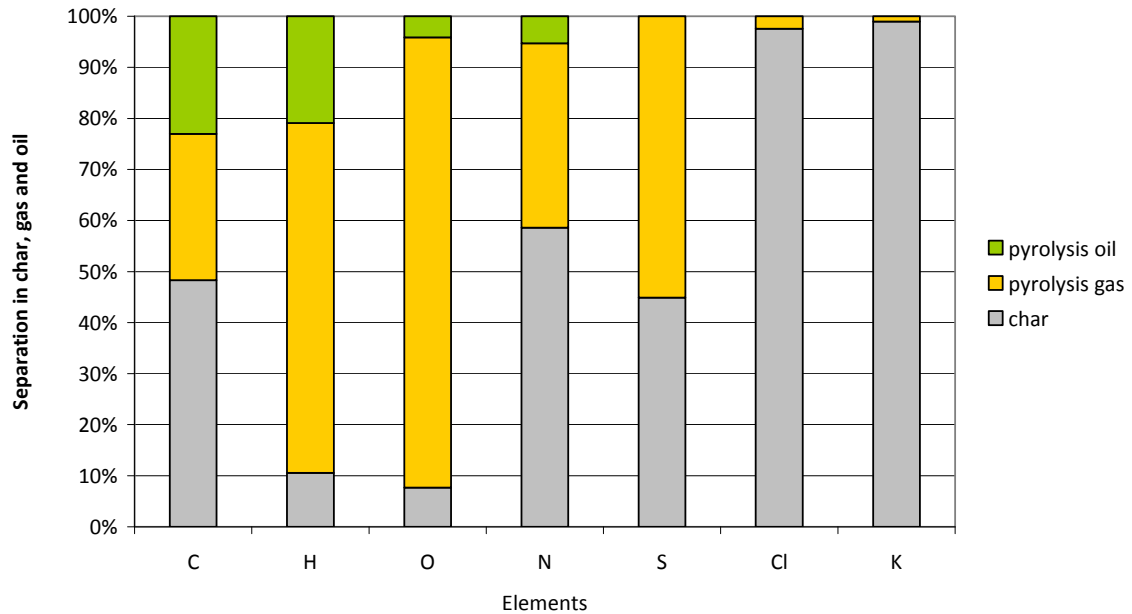


Figure 6-85: Distribution of the chemical elements in the pyrolysis products for indoor stored straw at a pyrolysis temperature of 450 °C

Undesired substances (Cl, N, S, and K) should be concentrated in the pyrolysis char. Almost 100 per cent of potassium and chlorine are concentrated in the pyrolysis char, approximately 45 per cent of sulphur and nearly 60 per cent of nitrogen are also enriched in the char. So the much higher chlorine content in the biomass should be no problem if the process is linked to the coal fired power station because no significant amount could be found in the pyrolysis gas. The experienced problems due to high potassium content [Michelsen et al., 1998] should also be no problem because no significant amount of potassium could be found in the pyrolysis gas. Most of the oxygen and hydrogen can be found in the pyrolysis gas as CO, CO<sub>2</sub>, CH<sub>4</sub> and H<sub>2</sub>. Approximately 20 per cent of carbon and hydrogen can be found in the pyrolysis oil which is due to the nature of the pyrolysis oil. Small amounts of oxygen and nitrogen can also be found in the pyrolysis oil (c.f. Table 9-10).

Results from Knudsen et al [Knudsen et al., 2004] indicated that 35 to 50 per cent of the total S was released to the gas phase during pyrolysis at 400 °C as a result of thermal decomposition of organic S. At higher temperatures (500 °C to 700 °C), the residual S contents of biochar did not change significantly any more.

The distribution of sulphur fits very well with the already mentioned figures from Lang et al who recorded that up to 50 per cent of total S from eight biomass types was lost into the volatiles during pyrolysis at 500 °C [Lang et al., 2005].

Jensen et al [Jensen et al., 2000] published that during straw pyrolysis at temperatures of 200 to 400 °C about 20 to 60 per cent of chlorine were released to the gas phase (c.f. Figure 6-63). The same was investigated by Björkmann and Strömberg [Björkmann et Strömberg, 1997] who researched on the release of chlorine during pyrolysis of different types of biomass. They found that below 200 °C no significant release of chlorine was observed, but at 400 °C between 20 and 50 per cent of the chlorine was released (c.f. Figure 6-64).

These figures could not be approved for the applied pyrolysis process, as nearly 100 per cent of the chlorine is captured in the pyrolysis char.

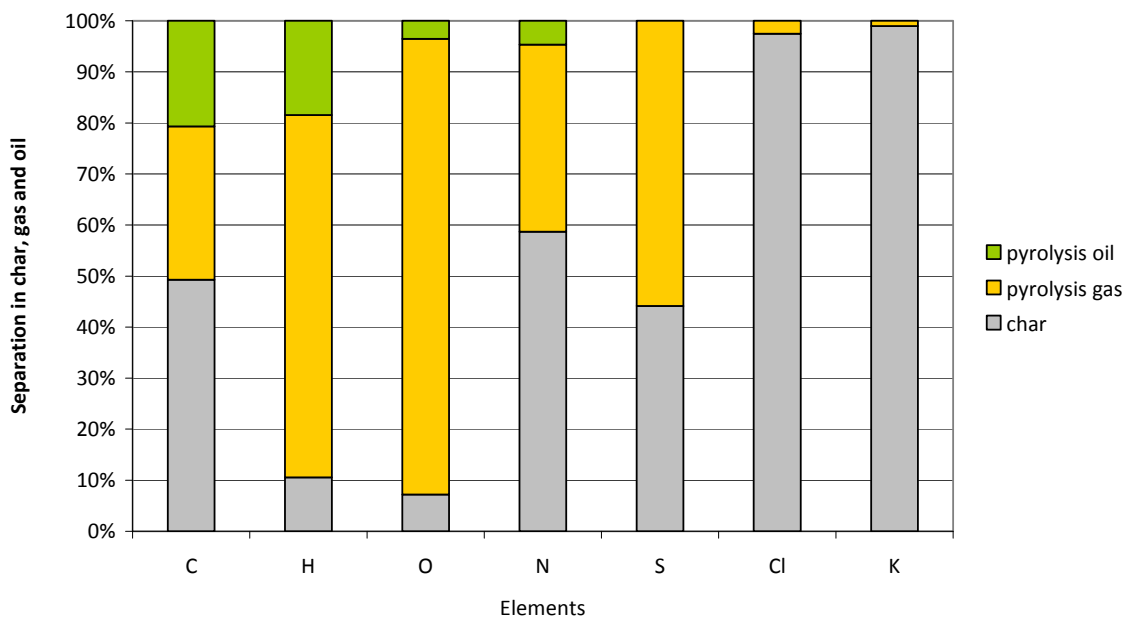


Figure 6-86: Distribution of the chemical elements in the pyrolysis products for indoor stored straw at a pyrolysis temperature of 500 °C

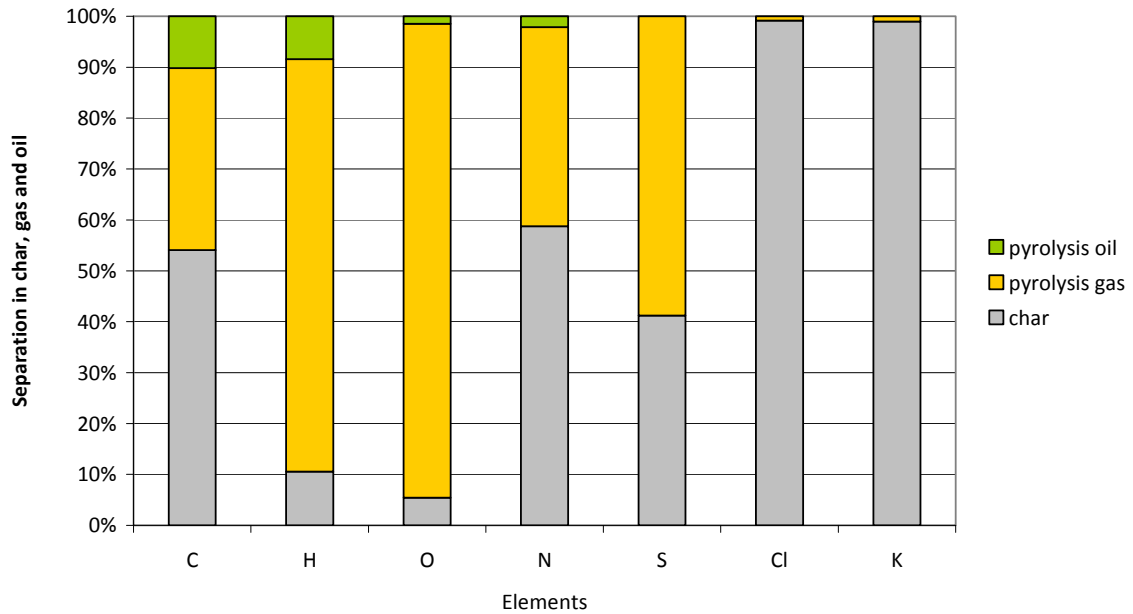


Figure 6-87: Distribution of the chemical elements in the pyrolysis products for indoor stored straw at a pyrolysis temperature of 550 °C

In accordance with Jensen et al, who have shown that during straw pyrolysis at temperatures between 200 to 400 °C potassium is bound as  $KCl$  and  $K_2CO_3$  and at temperatures between 400 to 700 °C no significant amounts of potassium were released to the gas phase (c.f. Figure 6-52), nearly 100 per cent of potassium is captured in the pyrolysis char.

It can be seen that the chemical composition of the pyrolysis products vary only in very small range depending on the pyrolysis temperature. One of the most important results is that chlorine and potassium that have a significant fraction in the feedstock (indoor stored wheat straw), are enriched nearly completely in the char. This is a proof that the used technology is suitable for producing a burnable gas that is almost free of corrosion causing elements and can be used in the Dürnröhr coal fired power station without any danger.



## 6.8 Efficiency

The efficiency of a plant concept is a very important factor for every process. Two efficiencies are of importance, the chemical efficiency of the produced gaseous (evaporated) products  $\eta_{ch}$  and the efficiency of the whole pyrolysis process  $\eta_p$ .

### 6.8.1 Chemical efficiency

The chemical efficiency is the ratio of the chemical energy of the product to the chemical energy of the feedstock.

$$\eta_{ch} = \frac{E_{product,ch}}{E_{feed,ch}} \quad (6-7)$$

$\eta_{ch}$  .....chemical efficiency

$E_{product,ch}$  ...chemical energy of the products

$E_{feed,ch}$  ....chemical energy of the feedstock

In this work the feedstock in the pyrolysis process is biomass. The products are the gaseous products of the pyrolysis process that are used for co-firing. In this case the gaseous products contain the pyrolysis gas and the pyrolysis oil. Entrained char and entrained dust are unaccounted here because these are only minor amounts and the loading of solid fines depends very much on the design of the gas outlet.

Figure 6-88 shows the distribution of the chemical energy obtained by pyrolysis of indoor stored wheat straw as feedstock at a pyrolysis temperature of 560 °C.

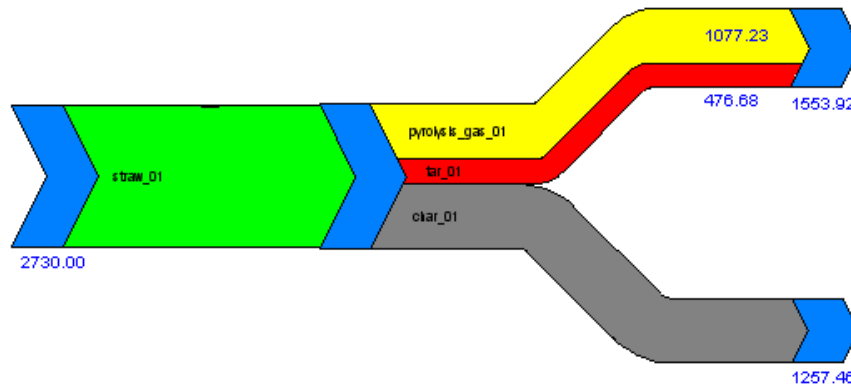


Figure 6-88: Sankey-diagram of dividing the feedstock's chemical energy by the pyrolysis reactor for pyrolysis of straw at a pyrolysis temperature of 560 °C, values in [kW]

The chemical energy of the feedstock (straw) is split up in a in a volatile fraction poor in undesired substances (Cl, N, S, Na and K) and a char fraction where these substances are concentrated. The difference of the chemical energy from the reactant to the products could be explained by endothermic reactions which occur during pyrolysis. These reactions have the ability to form compounds which have higher heating values than the starting materials.

Figure 6-89 shows that the chemical efficiencies for pyrolysis of indoor stored wheat straw dependent on temperature are about 50 %.

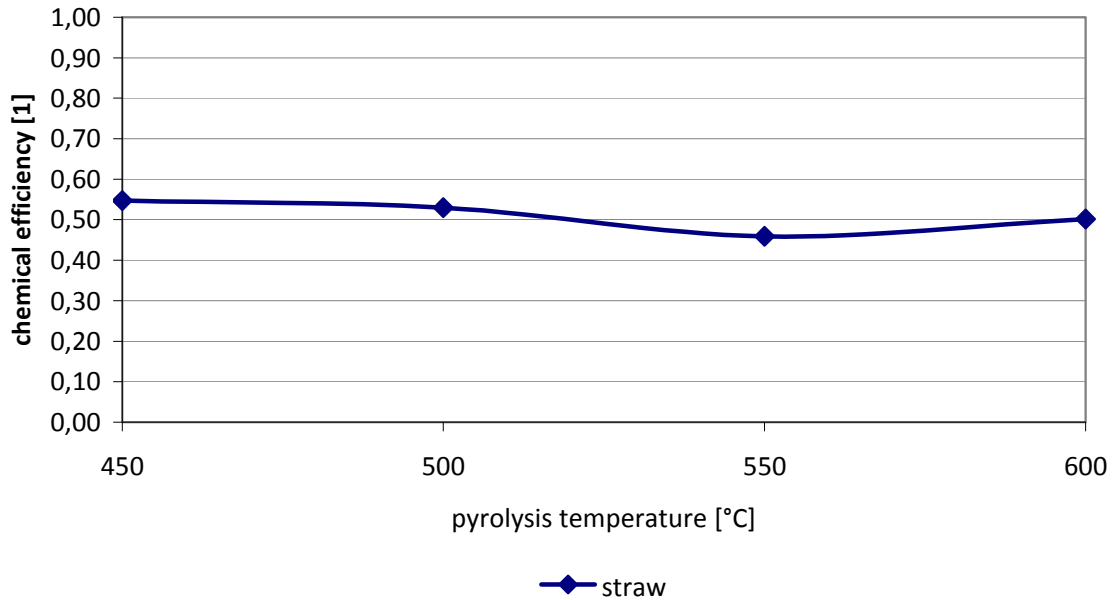


Figure 6-89: Chemical efficiencies for indoor stored wheat straw at different pyrolysis temperatures

### 6.8.2 Plant efficiency

The calculation of the efficiency of the whole plant concept is not as easy as for the chemical efficiency because the energy that is needed to run the process has also to be considered.

$$E = E_{ch} + E_{th} \tag{6-8}$$

$$\eta_P = \frac{E_{product}}{E_{feed}} \tag{6-9}$$

E .....energy

E<sub>ch</sub> .....chemical energy

E<sub>th</sub> .....thermal energy

η<sub>P</sub> .....plant efficiency

E<sub>product</sub> .....energy of the products

E<sub>feed</sub> .....energy of the feedstock

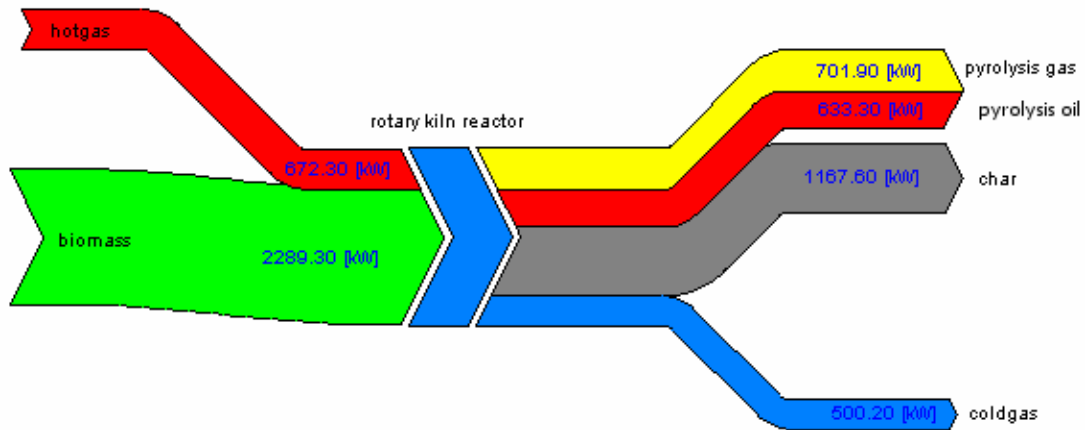


Figure 6-90: Typical energy balance of the pyrolysis reactor for pyrolysis of straw at a temperature of 550 °C

Figure 6-90 shows that a certain energy amount delivered by the hotgas is needed for the process. In the actual pyrolysis pilot plant there is the whole pyrolysis gas burned in the afterburner/fluidised bed or a mixture of natural gas and pyrolysis gas. If the process would be used for producing burnable gas for co-firing, the thermal energy for the rotary kiln has to be produced externally. This could happen by firing a part of the produced gas in a separate combustion chamber, by firing straw or another feedstock in a fluidised bed combustion or extraction of hot flue gas from the coal fired power plant.

Figure 6-91 focuses on the first case, burning a part of the produced gas to provide the required thermal energy. This is the concept for scaling up the results from the pilot plant to the industrial scale. For this purpose an IPSEpro model has been established [Kern, 2010].

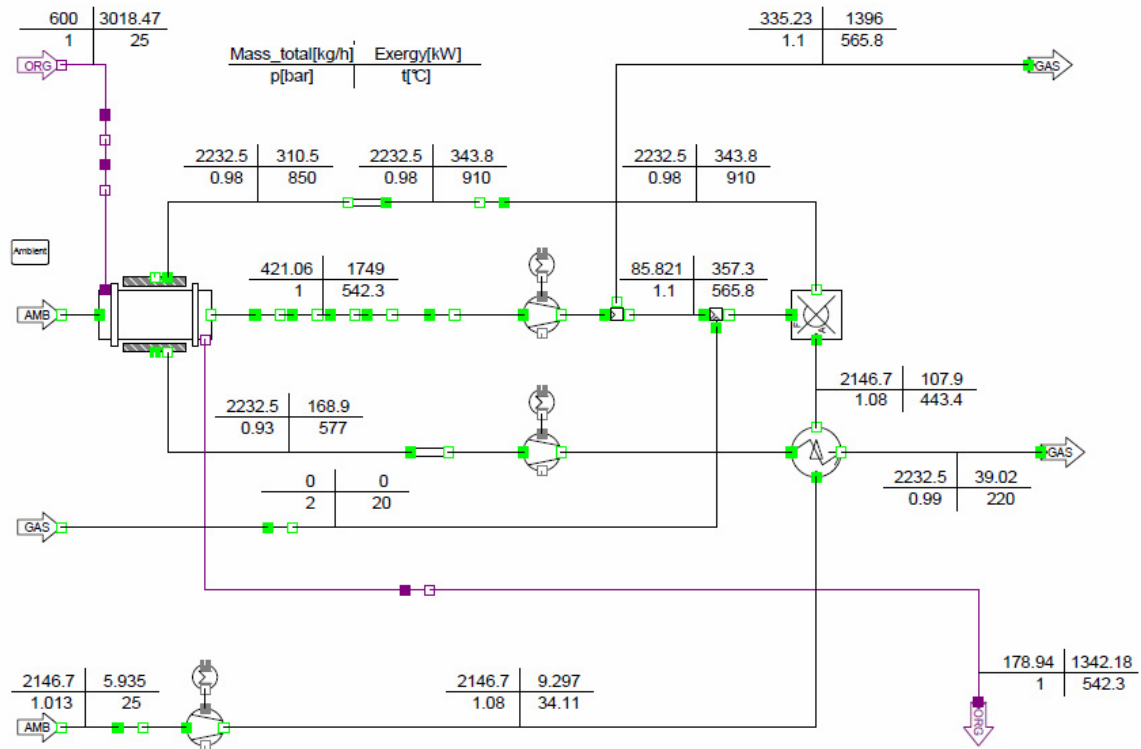


Figure 6-91: IPSEpro model for the case of energy supply by pyrolysis gas, values are for the size of the pilot plant (about 3 MW) [Kern, 2010]

For this IPSEpro calculation the feedstock and pyrolysis parameter (pyrolysis temperature, residence time) have been set to the standard values, so the feedstock is indoor stored straw, the pyrolysis temperature is set to 550 °C and the speed of the rotary kiln (residence time) is the nominal power of 100 %.

The results of this balance can be found in the appendix and the energy flows are shown in the following Sankey-diagram (Figure 6-92).

One big step to improve the efficiency is to use the energy in the coldgas that exits the jacket of the rotary kiln reactor with more than 550 °C, for preheating the air that enters the combustion chamber/afterburner. This is already included in the calculated case by using an economizer, so, the flue gas that is released to the stack has a temperature of about 200 °C or less. In the Sankey-diagram in Figure 6-91 the temperature at the end of the pipe has been set to 220 °C, which is a high level, but there has to be kept in mind that there are no losses of pipes etc. included. The heat loss of the hotgas on the way from the afterburner to the pyrolysis reactor is known from the pilot plant, so that loss is already included.

The dataset for this balance is from pyrolysis operation of straw with a pyrolysis temperature of 550 °C. For this case the net pyrolysis efficiency is 0.48.

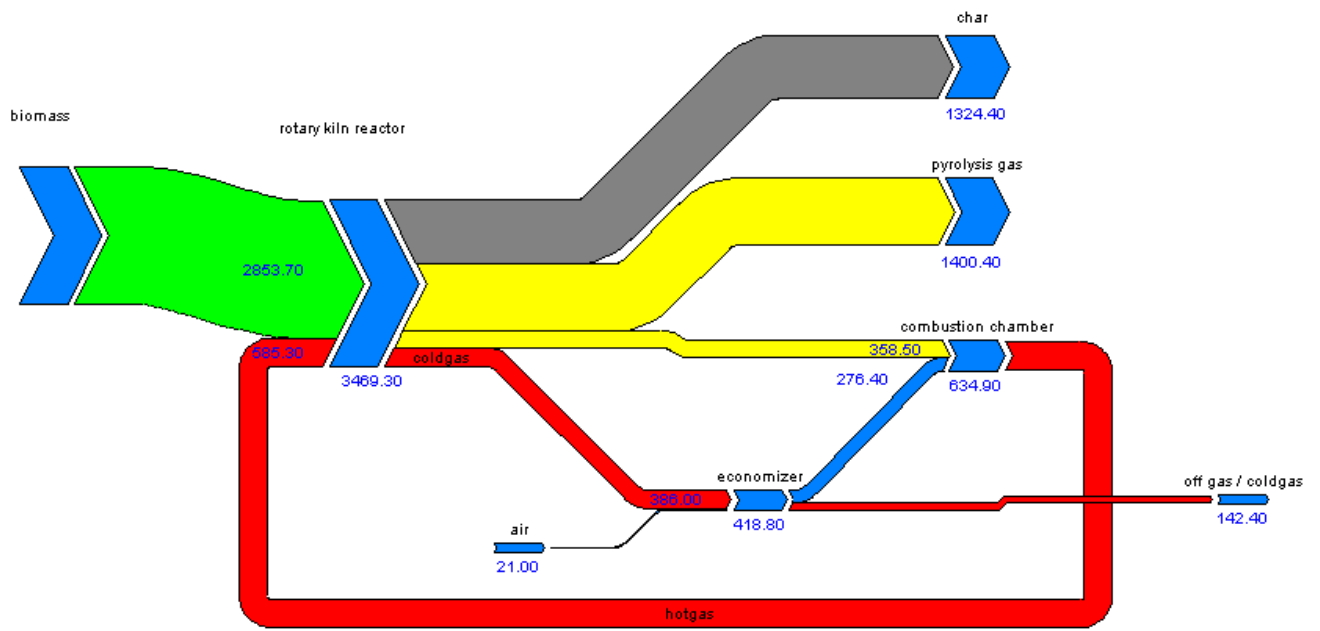


Figure 6-92: Sankey-diagram for the pilot plant size and straw pyrolysis for the case of energy supply by pyrolysis gas, energy flows, values in [kW]

## 7 Conclusion and outlook

### 7.1 Conclusion

Pyrolysis of agricultural residues in an externally heated rotary kiln pyrolysis reactor is a prospective technology which has been investigated in this thesis. Based on the fact that a lot of research in the field of pyrolysis is done in lab-scale facilities a pyrolysis pilot plant (3 MW) was built and scientifically accompanied over a period of two years. One of the main points of interest was whether the applied process technology is suitable to produce gaseous pyrolysis products (gas and evaporated oil) that can be used for co-firing at coal fired power plants. Another point was to keep as much as possible of undesired components, like chlorine, potassium or sodium, back in the pyrolysis char to prevent the boiler and other plant parts from high temperature corrosion.

The main fuel for the pyrolysis pilot plant at coal fired power station Dürnröhr is straw but due to the fact that there is also a broad range of different other biomasses available in huge amounts the focus was not only set on the usage of wheat straw but also different other biomasses have been considered.

It turned out that the operation, handling and control of the pilot plant, especially the pyrolysis reactor is possible without serious problems with the current state of knowledge. The ruggedly designed rotary kiln reactor is also insusceptible for a contamination of the feedstock with soil or other inorganic particles.

For calculation of mass and energy balances the process simulation and balance tool IPSEpro has been used in this work. The unit for the rotary kiln pyrolysis reactor had to be created and integrated into the existing program.

The elemental composition of the different pyrolysis char samples was also an important point. Attention was also given to the composition of the pyrolysis oils and the pyrolysis gas. Ammonia, hydrogen chloride and hydrogen sulphide analysis have been carried out to get an insight in the quality of the pyrolysis gas. For a further thermal usage of the pyrolysis char the ash melting behaviour was also determined.

For the balancing considerations indoor stored wheat straw was chosen because of the fact that it was available in huge amounts and its elemental composition and water content stays nearly constant.

The distribution of the chemical elements of the feedstock in pyrolysis gas, oil and char is an important point. Furthermore, the amounts of gas, oil and char for different pyrolysis temperatures are also of great interest.

To get more detailed insight the results from the test runs with pyrolysis temperatures of 450, 500, 550 and 600 °C and a variation of residence time for 20 and 40 % of the speed of the rotary kiln reactor has been carried out.

It turned out that a higher pyrolysis temperature forces the production of gas at the expense of the formation of pyrolysis oil. The higher temperature causes the decomposition of oil to gas. Slightly less mass of char results in the fact, that more volatile compounds are used to be stripped due to higher temperatures.

The mass of the products is also influenced by the residence time of the feedstock in the pyrolysis reactor. There is not a straight trend for the amount of gas and char evident but a decent trend can be seen at the produced mass of pyrolysis oil. The yield of oil increases by an increase of the residence time of the feedstock in the rotary kiln reactor. Also the sum of pyrolysis gas and pyrolysis oil defines a trend. So the mass fraction of the gaseous products which are intended to be co-fired in the coal power station increases by extending the residence time in the rotary kiln reactor.

It is of major significance that the pyrolysis process is operated in a way that prevents the undesired components, which could lead to high temperature corrosion in the boiler, to enter the evaporated pyrolysis products. So elements like chlorine and potassium should be enriched in the pyrolysis char.

The chemical energy of the feedstock (straw) is split up in a in a volatile fraction poor in undesired substances (Cl, N, S, Na and K) and a char fraction where these substances are concentrated. It can be seen that the chemical composition of the pyrolysis products vary only in very small range depending on the pyrolysis temperature. One of the most important results is that chlorine and potassium that have a significant fraction in the feedstock (indoor stored wheat straw), are enriched nearly completely in the char.

The results, gained from the measurements and the balancing, were used to calculate the efficiency of the pilot plant and the pyrolysis process. The chemical efficiencies for pyrolysis of indoor stored wheat straw dependent on temperature are about 50 %.

The plant efficiency is calculated for the case that the thermal energy that runs the pyrolysis process is provided by combustion of a part of the pyrolysis gas in a separate combustion chamber. The rest of the produced gas can be used in the power plant. In this case and for the pyrolysis of indoor stored



wheat straw a net efficiency of 0.48 would be reached. The Dürnrrohr power station has an electrical efficiency of 0.42 [Böhmer et al., 2003] so if the pyrolysis process would be connected to the power station there would be an electrical efficiency of 0.20 (20 %) for the generation of electrical energy of straw. This efficiency is significantly higher than the electrical efficiency of smaller biomass fired power stations or CHP systems.

The results clearly show that the used technology is suitable for producing a burnable gas that is almost free of corrosion causing elements and can be used in the Dürnrrohr coal fired power station without any danger.

## 7.2 Outlook – Scale up of pilot plant

The pyrolysis pilot plant will be the basis for a scale up to a plant that delivers the produced gas directly to the coal fired power plant. Currently there are two stages of expansion investigated. Stage one (Figure 7-1) is a scale up of one pyrolysis reactor to a fuel power of 30 MW. Stage two (Figure 7-2) would be the parallel operation of three rotary kiln reactors with a fuel power each of 30 MW. That means stage two has a total fuel power of 90 MW. An important point to look at is the heating of the pyrolysis reactors. For stage two the produced pyrolysis char and straw could be fired in a combustion chamber to provide the heat.

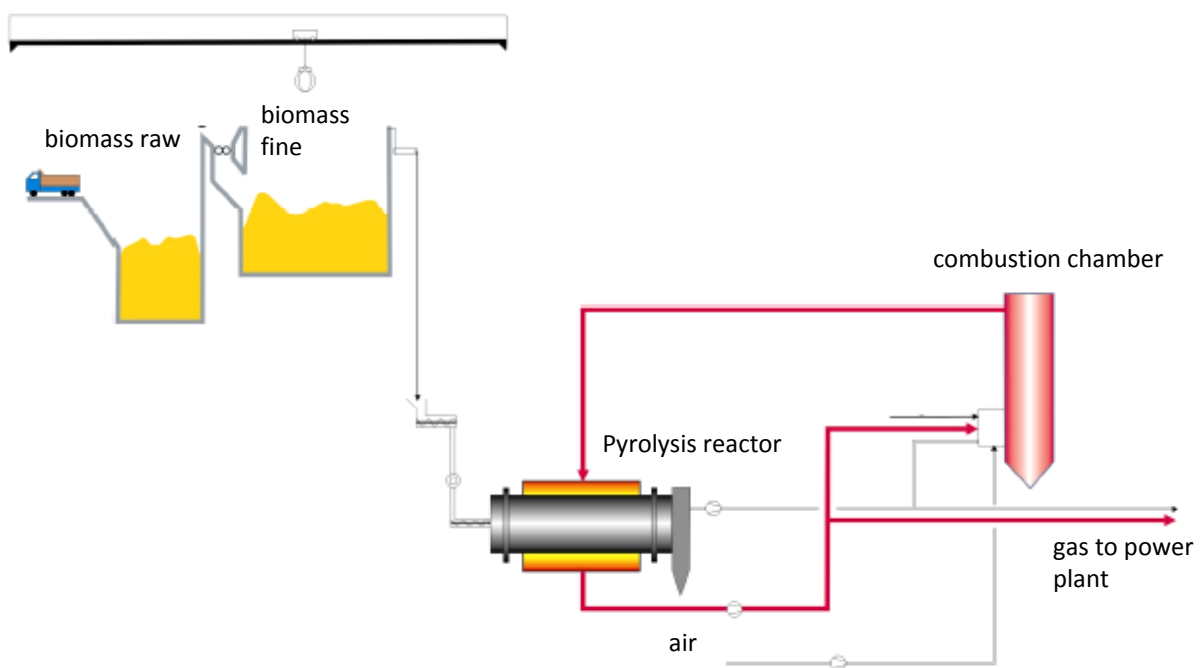


Figure 7-1: Scenario one: One 30 MW pyrolysis reactor, supply of pyrolysis energy by combustion of pyrolysis gas

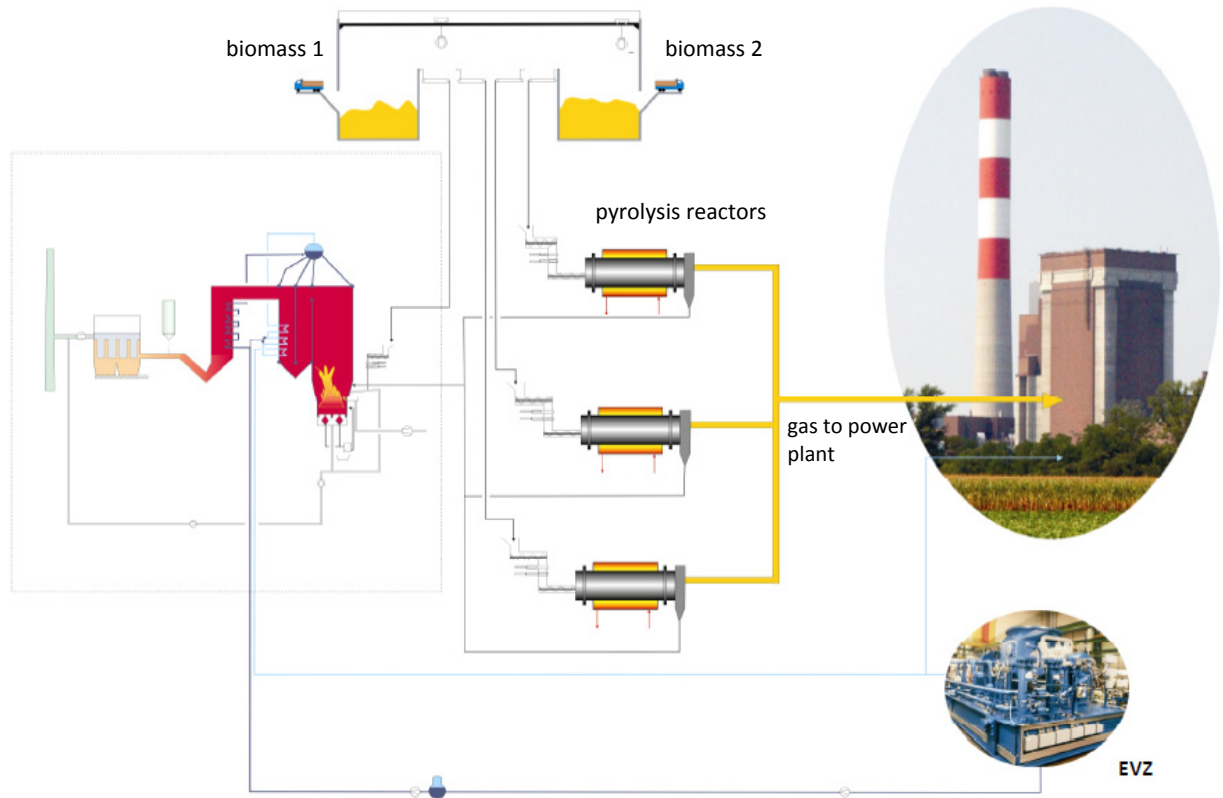


Figure 7-2: Scenario two: Three parallel operating pyrolysis reactors, supply of pyrolysis energy by combustion of char and biomass

### 7.3 Outlook – Biochar production

A second pathway for the biochar after the scale up would be the application as a soil amendment and as a sustainable carbon sequestration technology.

So far, only less attention was given to the solid pyrolysis product, pyrolysis char or so called biochar. The pyrolysis char has a very high heating value and is nearly free of any water content. So the pyrolysis char is considered to be an excellent fuel for combustion systems, like fluidised bed combustion systems that do not operate at such high temperatures like the pulverized coal combustion of the Dürnrrohr power station. Biochar could also be restored to the fields where the feedstock came from. Biochar is excellently suitable for the improvement of soil and therefore could be used as a soil amendment. Using the pyrolysis char as reducing agent in the non-ferrous metallurgy is also under investigation [Griessacher et Antrekowitsch, 2010] [Griessacher et al., 2010].

The pyrolysis char could also be used for providing the thermal energy to run the pyrolysis process. At the moment the plant efficiency is calculated for the case that the thermal energy that runs the pyrolysis process is provided by combustion of a part of the pyrolysis gas in a separate combustion chamber.

The application of biochar techniques to soil has rarely been investigated to date. The effectiveness of applications of composts, animal manure or mineral fertilizers are known to vary significantly whether they are incorporated or surface applied, banded or broadcast [Jarvis and Bolland, 1991][Gherardi and Rengel, 2003], and similar responses can be expected to the method of biochar application.

The purpose of applying biochar to soil mainly falls into four broad categories:

- Agricultural profitability
- Management of pollution and eutrophication risk to the environment
- Restoration of degraded land
- Sequestration of carbon from the atmosphere

A very important point for the near future will be the sequestration of carbon. Biochar application to soil places C originating from atmospheric CO<sub>2</sub> into the soil to protect it from surface combustion by fires and to maintain it in relatively stable forms for a long period of time with opportunities for C trading. A better contact with soil minerals enhances biochar stability and increases its mean residence time. Sequestration in subsoils may be an especially effective way to increase stability. A deeper application method may

therefore be useful for increasing the C trading value of biochar [Lehmann and Joseph, 2009].

Figure 7-3 shows that the carbon in biochar resists degradation and can hold carbon in soils for hundreds to thousands of years.

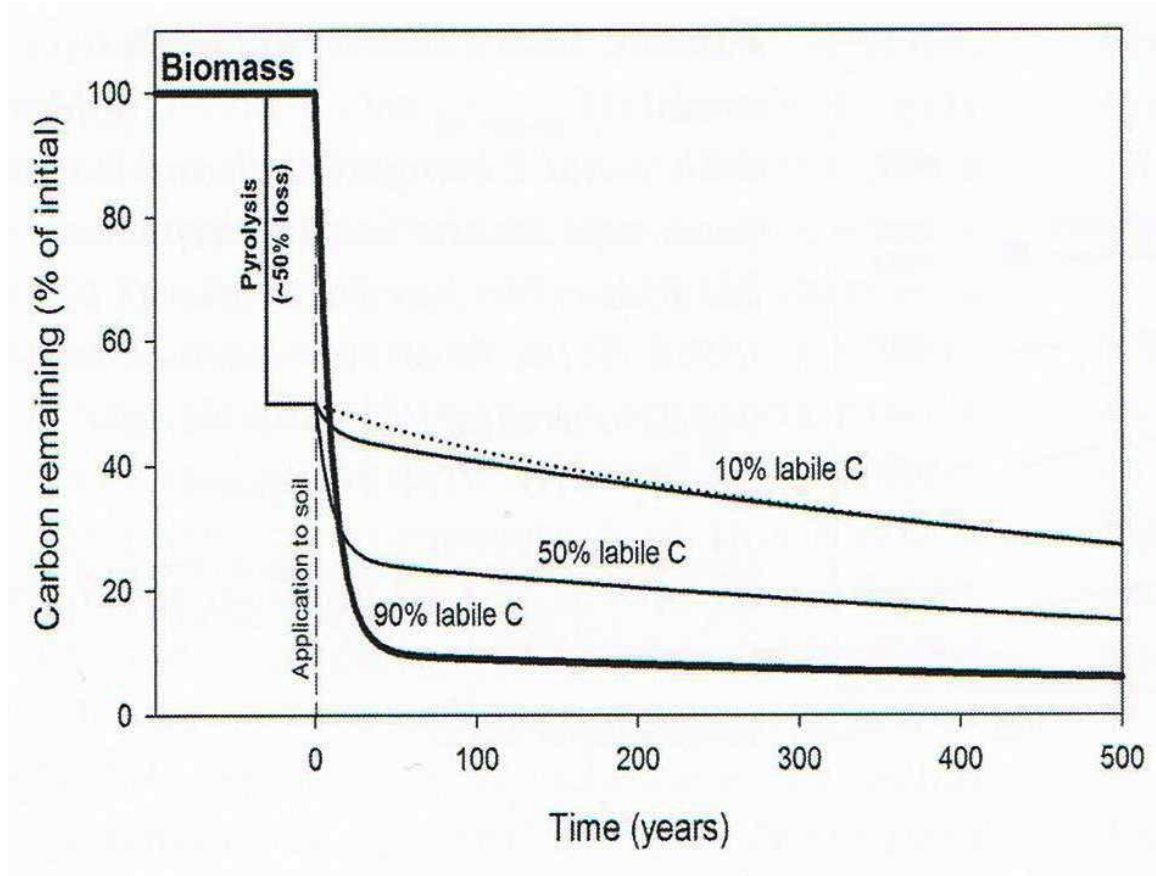


Figure 7-3: Conceptual model of C remaining from biomass using a double-exponential decay model with a mean residence time of 10 years for the labile C pool and 1000 years for the stable C pool but different proportions of labile C [Lehmann and Joseph, 2009]

The line lines in Figure 7-3 represent the conversion of biomass into biochar, the thick line represents decomposition of uncharred biomass. The dotted line shows decomposition with 10 per cent labile C using 100 years as a mean residence time of the labile pool. The carbon losses by pyrolysis average approximately 50 per cent, but can vary significantly depending upon feedstock and production conditions [Lehmann and Joseph, 2009].

Sustainable biochar systems can be carbon negative because they hold a substantial portion of the carbon in soil. The result is a net reduction of carbon dioxide in the atmosphere. Whereas fossil fuels are carbon positive, they add more carbon to the atmosphere and other ordinary biomass fuels are carbon neutral because the carbon captured in the biomass by photosynthesis would

have eventually returned to the atmosphere through natural processes, combust biomass for energy only accelerates this process.

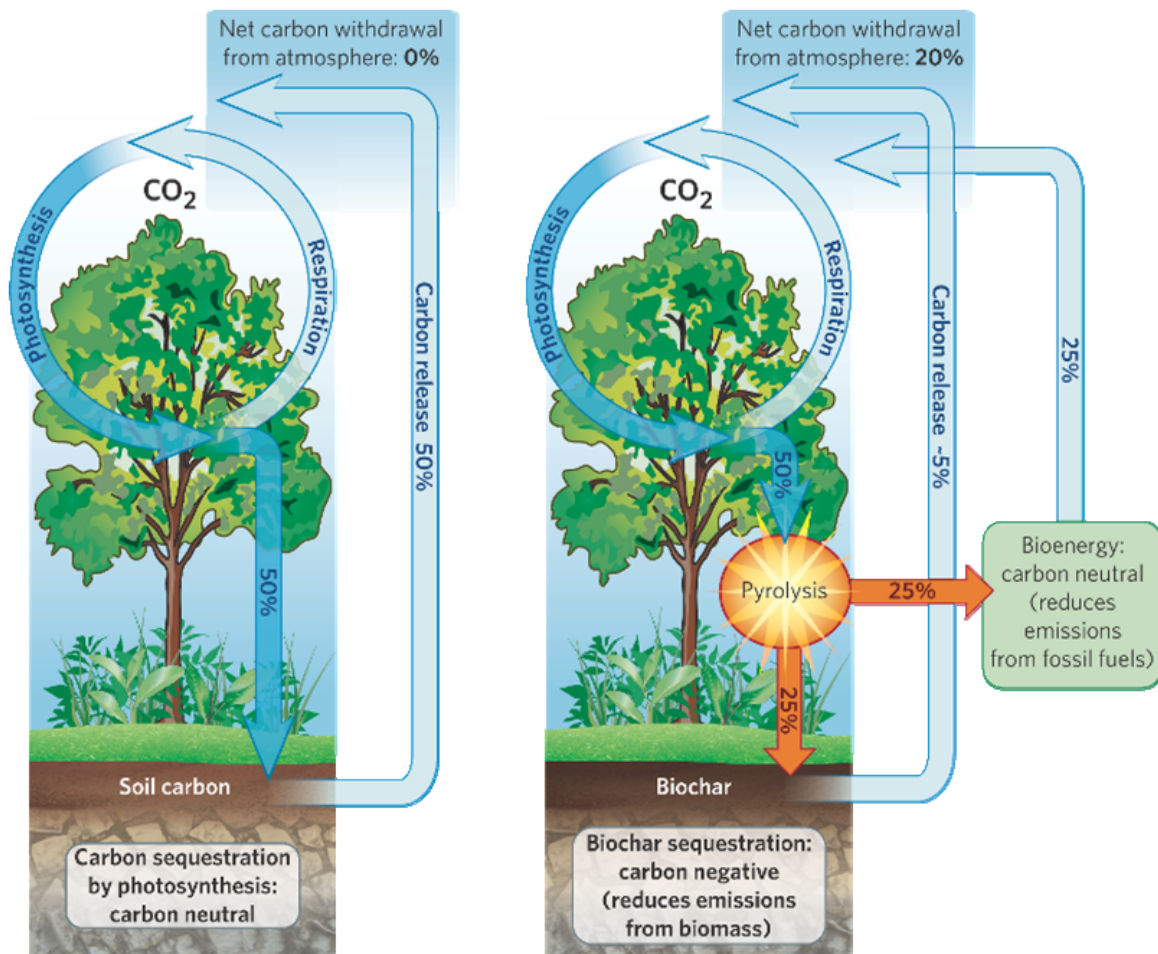


Figure 7-4: Carbon sequestration by photosynthesis and biochar sequestration [IBI, 2011]

I want to finish this outlook with a quotation from Mr. Al Gore (Vice President of the United States and 2007 Nobel Peace Prize Co-recipient) who said: "One of the most exciting new strategies for restoring carbon to depleted soils and sequestering significant amounts of CO<sub>2</sub> for 1000 years and more, is the use of biochar." "The principle barrier to the use of this strategy is the lack of a price on carbon that would drive the economy toward the most effective ways to sequester it. There is presently no formalized network of biochar distribution channels or commercial scale production facilities. But a stable price on carbon would cause them to quickly emerge - because biochar holds such promise as an inexpensive and highly effective way to sequester carbon in soil."

## 8 Bibliography

- Ahlhaus, M., 1995**, Die Pyrolyse als Vorstufe der energetischen Nutzung lignocellulosischer Roh- und Abfallstoffe, Dissertation, Fachbereich 06 – Verfahrenstechnik, Umwelttechnik, Werkstoffwissenschaften, TU Berlin
- Antal, M.J., Grønli, M., 2003**, The art, science and technology of charcoal production. *Industrial and Engineering Chemistry Research*, 42, (8), 1619-1640
- Antal, M.J, Varhegyi, G., 1995**, Cellulose pyrolysis kinetics: The current state of knowledge. *Industrial and Engineering Chemistry Research*, 34(3):703–717
- Bagreev, A., Bandosz, T.J., and Locke D.C., 2001**, Pore structure and surface chemistry of adsorbents obtained by pyrolysis of sewage-derived fertiliser, *Carbon*, vol 39, pp 1971-1979
- Baldock, J.A., Smernik, R.J., 2002**, Chemical composition and bioavailability of thermally altered *Pinus resinosa* (red pine) wood, *Organic Geochemistry*, vol 33, pp1093-1109
- Banyasz, J.L., Li, S., Lyons-Hart, J.L., Shafer, K.H., 2001**, Cellulose pyrolysis: the kinetics of hydroxyacetaldehyde evolution, *J Anal Appl Pyrol*, 57:223–248
- Banyasz, J.L., Li, S., Lyons-Hart, J.L., Shafer, K.H., 2001**, Gas evolution and the mechanism of cellulose pyrolysis, *Fuel*, 80:1757–1763
- Bassilakis, R., Zhao, P., Solomon, P. R. and Serio, M. A., 1993**, Sulphur and Nitrogen Evolution in the Argonne Coals: Experiment and Modelling, *Energy & Fuels*, Vol. 7, pp. 710-720

- Basu, P., 2010,** Biomass Gasification and Pyrolysis - Practical Design and Theory, Academic Press
- Baumann, H., Möller, P., 1991,** Pyrolysis of Hard Coals under Fluidised Bed Combustor Conditions, Erdöl, Kohle, Erdgas, Petrochemie, Vol. 44, pp. 29-33
- Baxter, L., 2005,** Biomass-coal co-combustion: opportunity for affordable renewable energy, Fuel 84, pp1295-1302
- Baxter, L., Koppejan, J., 2004,** Biomass-coal Co-combustion: Opportunity for Affordable Renewable Energy. Published in EuroHeat and Power 1/2004
- Björkmann, E., 1996,** Release of chlorine from biomass at gasification conditions, Developments in Thermochemical Biomass Conversion, Banff, Canada, 20-24 May 1996
- Björkman, E., Strömberg, B., 1997, Release of Chlorine from Biomass at Pyrolysis and Gasification Conditions, Energy & Fuels 1997, 11, 1026-1032**
- Bradbury, A., Sakai, Y., Shafizadeh, F., 1979,** A kinetic model for pyrolysis of cellulose, Journal of Applied Polymer Science, 23:3271–3280
- Bridgwater, A. V., 2003,** Renewable fuels and chemicals by thermal processing of biomass, Chemical Engineering Journal (91), 87-102
- Bridgwater, A., Czernik, S., Diebold, J., Meier, D., Oasmaa, A., Peacocke, C., Piskorz, J. and Radlein, D. 2003,** Fast Pyrolysis of Biomass: A Handbook. 1, CPL Press, UK
- Bridgwater, A. V., Grassi, G., 1991,** Biomass pyrolysis liquids upgrading and utilization, Essex, Elsevier Science Publishers LTD, ISBN 1-85166-565-X



- Bridgwater, A., Meier, D., Radlein, D., 1999**, An overview of fast pyrolysis of biomass. *Organic Geochemistry* (30), 1479-1493
- Bridgwater, A.V., Peacocke, G.V.C., 1999**, Fast pyrolysis processes for biomass, *Sustainable and Renewable Energy Reviews*, Elsevier, pp. 1-72
- Bridgwater, A.V., Peacocke, G.V.C., 2000**, Fast pyrolysis processes for biomass, *Renewable and Sustainable Energy Reviews* 4, 1-73
- Bridgwater, A.V., 2007**, IEA Bioenergy Update 27, Biomass Pyrolysis, *Biomass and Bioenergy*, vol 31, ppI-V
- Brown, R., 2009**, Biochar Production Technology, Chapter 8 in J. Lehmann, J. and Joseph, S. (eds) *Biochar for Environmental Management*, Earthscan, London
- Brownsort, P.A., 2009**, Biomass pyrolysis processes: Performance parameters and their influence on biochar system benefits, Master Thesis, University of Edinburgh
- Buranov, A. U., Mazza, G., 2008**, Lignin in straw of herbaceous crops, *Industrial crops and products*, 28 (3), pp. 237-259
- Böhmer, S., Schindler, I., Szednyj, I., Winter, B., 2003**, Stand der Technik bei kalorischen Kraftwerken und Referenzanlagen in Österreich, Wien, Umweltbundesamt GmbH, ISBN 3-85457-682-X
- Canadell, J., Le Quere, C., Raupach, M., Field, C., Buitehuis, T., Ciais, P., Conway, T., Gillet, N., Houghton, R., Marland, G., 2007**, Contributions to accelerating atmospheric CO<sub>2</sub> growth from economic activity, carbon intensity, and efficiency of natural sinks, *Proceedings of the National Academy of Sciences*, vol 104, pp18866-18870

**Cheng, C.H., Lehmann, J., Thies, J.E., Burton, S.D., Engelhard, M.H., 2006,** Oxidation of black carbon by biotic and abiotic processes, *Organic Geochemistry*, vol 37, pp1477-1488

**Chiaramonti D., Oasmaa A., Solantausta Y., 2005,** Power generation using fast pyrolysis liquids from biomass, *Renewable and Sustainable Energy Reviews*

**Cremers, M.F.G., 2009,** IEA Bioenergy Task 32, Deliverable 4, Technical status of biomass co-firing, KEMA, The Netherlands

**Czernik S, Bridgwater A.V., 2004,** Overview of applications of biomass fast pyrolysis oil. *Energy & Fuels*, 18(2):590–598

**Dam-Johansen, K., Hu, G., Sander, B., Laerkedahl, L., Jensen, P.A., 1997,** Pretreatment of straw by pyrolysis and char wash, published in: *Biomass Gasification and Pyrolysis*, eds. Kaltschmitt et Bridgwater, CPL Press, UK

**Davidsson K.O., Koresgren J.G., Pettersson J.B.C., Jaglid U., 2002,** The effects of fuel washing techniques on alkali release from biomass, *Fuel* 81, pp137-142

**Defra (UK Department for Environment, Food and Rural Affairs), 2003,** The Scientific Case for Setting a Long-Term Emission Reduction Target, Defra,  
[www.defra.gov.uk/Environment/climatechange/pubs/pdf/ewp\\_targetscience.pdf](http://www.defra.gov.uk/Environment/climatechange/pubs/pdf/ewp_targetscience.pdf)

**Deglise. X., Richard, C., Rolin, A., Francois, H., 1980,** Influence de la température et du taux d'humidité sur la pyrolyse éclair des déchets ligno-cellulosiques. *Revue Generale de Thermique* 1980, 19:871–80.

**Demirbas, A., 2000,** Mechanisms of liquefaction and pyrolysis reactions of biomass, *Energy Conversion and Management* (41), 633-646

**Demirbas, A., 2001,** Carbonization ranking of selected biomass for charcoal, liquid and gaseous products, *Energy Conversion and Management*, 42, 1229-1238

**Demirbas, A., 2007,** Progress and recent trends in biofuels, *Progress in Energy and Combustion Science*, 33(1):1 – 18

**DIN EN 38406,** Bestimmung von Gesamtstickstoff in Kohlenwasserstoffen

**DIN 38405,** Bestimmung von Chlorid; Argentometrische Methode

**DIN 51730, 2007,** Prüfung fester Brennstoffe- Bestimmung des Asche-Schmelzverhaltens

**Encinar, J.M, Beltrán, F.J., Ramiro, A., González, J.F., 1998,** Pyrolysis/gasification of agricultural residues by carbon dioxide in presence of different additives: influence of variables, *Fuel Processing Technology*, 55, 219-233

**European Commission, 2000,** Addressing the constraints for successful replication of demonstration technologies for co-combustion of biomass/waste, booklet DIS 1743/98-NL

**Faij, A. P., 2006,** Bio-energy in Europe: changing technology choices. *Energy Policy* (34), 322-342

**Fagbemi, L., Khezami, L., Capart, R., 2001,** Pyrolysis products from different biomasses: application to the thermal cracking of tar, *Applied Energy* 69, 293–306

**Faix, O., Meier, D., Fortmann, I., 1988,** Pyrolysisgas chromatography-mass spectrometry of two trimeric lignin model compounds with alkyl-aryl ether structure, *J. Anal. Appl. Pyrolysis* 14, pp115-148

- Forster, P., Ramaswamy, V., Artaxo, P., Bernsten, T., Fahey, D.W., Haywood, J., Lean, J., Lowe, D.C., Myhre, G., Nganga, J., Prinn, R., Raga, G., Schulz, M., Van Dorland, R., 2007, Climate Change 2007, The Physical Science Basis. Contribution of Working Group I to the Fourth Assessment Report of the Intergovernmental Panel on Climate Change, Cambridge University Press, Cambridge, UK**
- Funino, J., Yamaji, K., Yamamoto, H., 1999, Biomass - balance table for evaluating bioenergy resources. Applied Energy, 63:75–89**
- Gercel, H.F., 2002, Production and characterization of pyrolysis liquids from sunflower pressed bagasse. Bioresource Technol., 85:113–7.**
- Gherardi, M.J., Rengel, Z., 2003, Deep banding improves residual effectiveness of manganese fertilisers for bauxite residue revegetation, Australian Journal of Soil Research, vol 41, pp1273-1282**
- Goyal, H., Seal, D., Saxena, R., 2008, Biofuels from thermochemical conversion of renewable resources: A review. Renewable and Sustainable Energy Reviews, 12, 504-517**
- Griessacher, T., Antrekowitsch, J., 2010, Charcoal from Biomass - A Sustainable Reductant. Proceedings of 3rd International Conference on Engineering for Waste and Biomass Valorisation (2010), Peking, China**
- Griessacher, T., Antrekowitsch, J., Offenthaler, D., 2010, Bio-char respectively Bio-coke from Agricultural Wastes for Metallurgical Uses. Proceedings of 18th European Biomass Conference and Exhibition - From Research to Industry and Markets (2010), Lyon, Frankreich, 1475 - 1480**
- Gullu, D., Demirbas, A., 2001, Biomass to methanol via pyrolysis process, Energy Convers Manage, 42(11): 1349–1356**

**Haslinger, W., Wopienka, E., 2009**, Versorgung von Industriebetrieben mit Wärme aus erneuerbaren Quellen im kleinen und mittleren Leistungsbereich, Neue Brennstoffe für den Wärmemarkt, Thermische und fermentative Verwertung von Biomasse, TechnoScope Workshop, Tulln, 23. Juni 2009, BIOENERGY 2020+

**Heitmann, H. G., 2000**, Chemie und Korrosion in Kraftwerken, Essen, Vulkan Verlag, ISBN 3 8027-2921-8

**Hofbauer, H., 2008**, Thermische Biomassenutzung I und II. Vorlesungsunterlagen 2008, Technische Universität Wien

**Hofbauer, H., 2006**, Brennstoff- und Energietechnologie, Vorlesungsunterlagen 2006, Technische Universität Wien

**Hofbauer, H., Rauch, R., & Siefert, I. G., 2003**, Endbericht Analytik III. Renet

**Hornung, A., 2008**, Fast, intermediate or slow pyrolysis for fuels production, power generation from various biomasses or as pre-conditioning unit for gasifiers, Presentation to Imperial College, Aston University, <http://www3.imperial.ac.uk/pls/portallive/docs/1/44315696.PDF>

**Hornung, A., Apfelbacher, W., Koch, W., Linek, A., Sagi, S., Schoner, J., Stohr, J., Seifert, H., Tumiatti, V., Lenzi, F., 2006**, Thermo-chemical conversion of straw - Haloclean intermediate pyrolysis, 17th International Symposium on Analytical and Applied Pyrolysis, 2006

**Hrbek, J., 2005**, Experimental investigations of selected elements behaviour during biomass pyrolysis and gasification, Dissertation, Institut für Verfahrenstechnik, Technische Universität Wien

**Hämäläinen, J., Aho, M. J. and Tummavori, J. L., 1994**, Formation of Nitrogen Oxides from Fuel-N through HCN and NH<sub>3</sub>: A Model Compound Study, Fuel, Vol. 73, pp. 1894-1898

**IBI, International Biochar Initiative, 2011,** Climate Change and Carbon Sequestration, <http://www.biochar-international.org/biochar/carbon>

**IEA, 2011,** Co-firing database, <http://www.ieabcc.nl/database/cofiring.php>

**IPCC, 2007,** IPCC Fourth Assessment Report , Climate Change, Cambridge University Press, Cambridge, UK

**Jarvis, R.J., Bolland, M.D.A., 1991,** Lupin grain yields and fertilisers effectiveness are increased by banding superphosphate below the seed, Australian Journal of Experimental Agriculture, vol 31, pp357-366

**Jensen, P.A. Frandsen, F.J, Dam-Johansen, K., Sander, B., 2000,** Experimental investigation of the transformation and release to gas phase of potassium and chlorine during straw pyrolysis, Energy & Fuel, 14(6) 1280-1285

**Jensen P.A., Sander B., Dam-Johansen K., 2001,** Pretreatment of straw for power production by pyrolysis and char wash, Biomass & Bioenergy, 20, pp431-446

**Kaltschmitt, M., Hartmann, H., Hofbauer, H. (Hrsg.), 2009,** Energie aus Biomasse. Grundlagen, Techniken und Verfahren, 2. Auflage - Berlin u.a., Springer Verlag, ISBN 978-3-540-85095-3.

**Kaltschmitt, M. et Bridgwater, A.V., 1997,** Biomass Gasification & Pyrolysis, State of the Art and Future Prospects, CPL Press, Newbury, UK

**Kern, St., 2010,** Niedertemperatur Drehrohrpyrolyse als Vorschaltprozess für die Co-Verbrennung von unkonventionellen Brennstoffen in thermischen Anlagen, Diplomarbeit, Institut für Verfahrenstechnik, Technische Universität Wien

- Kiel J., 2005**, Co-utilization of coal, biomass and other fuels, Presented at JRC-Integration & Enlargement Workshop on the Perspectives for Cleaner Fossil Fuel Energy Conversion Technologies in an Enlarging EU, Petten, the Netherlands, 10-11 November 2005, ECN
- Klemm, D., Heublein, B., Fink, H.-P., Bohn, A., 2005**, Cellulose: faszinierendes Biopolymer und nachhaltiger Rohstoff. *Angewandte Chemie* (117), 3422-3458.
- Kleinhappl, M., Zeisler, J., 2010**, Beprobungen von H<sub>2</sub>S in Pyrolysegas, Analysenbericht, Bioenergy 2020+GmbH
- Knudsen, J.N., Jensen P.A., Lin, W., Frandsen, F.J., Dam-Johnson, K. , 2004**, Sulfur transformations during thermal conversion of herbaceous biomass, *Energy and Fuels*, vol 18. pp810-819
- Kopetz, H., G., 2010**, Die vermeidbare Energiekrise, Mit erneuerbaren Energien zu sicherer Energieversorgung und wirksamem Klimaschutz in Österreich, Österreichischer Biomasseverband (Hrsg.), Weishaupt Verlag
- Koppejan, J., 2004**, Overview of experiences with co-firing biomass in coal power plants, IEA Bioenergy Task 32: Biomass Combustion and co-firing
- Kostamo, J., 1999**, Co-firing tests at Naantali-3 Power Plant. Presented in Swedish-Finnish Flame Day 1999
- Lang, T., Jensen, A.D., and Jensen, P.A., 2005**, Retention of organic elements during solid fuels pyrolysis with emphasis on the peculiar behaviour of nitrogen, *Energy and Fuels*, vol 19, pp 1631-1643
- Lehmann, J., Joseph, St., (Hrsg.), 2009**, Biochar for environmental management, Science and Technology, Earthscan, UK

- Lettner, F., Haselbacher, P., Timmerer, H., 2008,** Wissenschaftliche Begleitung des Projekts Pyrolysevorschaltanlage KW Dürnrrohr, Endbericht, TU Graz, IWT
- Li, C.Z., Tan L.L., 2000,** Formation of NO<sub>x</sub> and SO<sub>x</sub> precursors during the pyrolysis of coal and biomass, part III, Further discussions on the formation of HCN and NH<sub>3</sub> during pyrolysis, *Fuel*, 79, 1899-1906
- Lind, T., Kauppinen, E.I., 1999,** Heavy metals behaviour during circulation fluidized bed combustion of willow, *Proceedings of 15<sup>th</sup> International Conference on Fluidized Bed Combustion*, May 16-19, Savannah, Georgia
- Livingston W.R., 2005,** A review of the recent experience in Britain with the co-firing of biomass with coal in large pulverised coal-fired boilers, Mitsui Babcock, Renfrew, Scotland, Presented at IEA Exco Workshop on Biomass Co-firing, Copenhagen
- Luo, Z., Wang, S., Liao, Y., Cen, K., 2004,** Mechanism study of cellulose rapid pyrolysis, *Ind Eng Chem Res*, 43:5605–5610
- Ma R., P., Felder R. M., Ferrel J. K., 1989,** Evolution of Hydrogen Sulfide in a Fluidized Bed Coal Gasification Reactor, *Ind. Eng. Chem. Res.*, 28, 27-33
- Maciejewska, A., Veringa, H., Sanders, J., Peteves, S.D, 2006,** Co-firing of biomass with coal: Constraints and role of biomass pre-treatment, DG JRC, Institute for Energy
- Marschner, H., 1993,** Mineral Nutrition of Higher Plants, 2nd edition; Academic Press, London, United Kingdom
- Michelsen, H. P., Frandsen, F., Dam-Johansen, K., Larsen, O., 1998,** Deposition and high temperature corrosion in a 10 MW straw fired boiler, *Fuel Processing Technology* 54, 1998, 95–108



- Mohan, D., Pittman, Jr., C.U. and Steele, P.H., 2006**, Pyrolysis of wood/biomass for bio-oil: A critical review, *Energy and Fuels*, vol 20 (3) pp848-889
- Mok, W.S.L, Antal, M.J, 1983**, effects of pressure on biomass pyrolysis. II Heats of reaction of cellulose pyrolysis, *Thermochimica Acta*, vol 68, pp165-186
- Nielsen, H. P., Frandsen, F., Dam-Johansen, K., Larsen, O., 1998**, Deposition and high temperature corrosion in a 10 MW straw fired boiler, *Fuel Processing Technology* 54, 1998, 95–108
- NEWAG NIOGAS, Verbundkraft, 1987**, Der sanfte Weg, Kraftwerk Dürrohr, Die neue Generation der Wärmekraftwerke, Wien-Berlin , A.F. Koska, ISBN 385-334-0377
- Obernberger, I., 1998**, Nutzung fester Biomasse in Verbrennungsanlagen, dbv – Verlag
- Oravainen, H., 2008**, Experiences of biomass co-firing in Finland, IEA Biomass Combustion and Cofiring, Workshop on October 21st 2008 in the Netherlands, VTT Technical Research Centre of Finland)
- Orjala, M., Heiskanen, V.-P., 2004**, Technologies for co-firing of biomass and fossil fuels, OPET CHP and DHP Conference 26-27 April 2004, Gdansk, Poland
- Pakdel, H., Roy, H., Kalkreuth, W., 1999**, Oil production by vacuum pyrolysis of canadian oil shales and fate of the biological markers. *Fuel*, 78:365–75.
- Peck, R. E., Glarborg, P., Johnsson, J. E., 1991**, Kinetic Modeling of Fuel-Nitrogen Conversion in One-Dimensional, Pulverized- Coal Flames, *Combust. Sci. Tech.*, Vol. 76, pp. 81-109

**Perz, E., 1990,** A computer method for thermal power cycle calculation. ASME-Paper IGTI GT-351

**Piskorz, J., Radlein, D., Scott, D.S., Czernik, S., 1988,** Liquid products from the fast pyrolysis of wood and cellulose, In: Bridgwater AV, Kuester JL, editors, Research in thermochemical biomass conversion, London, New York, Elsevier Applied Science, pp557-571.

**Prins, M.J., Ptasinski, K.J, Janssen, F.J.J.G, 2006,** Torrefaction of wood, Part 1. Weight loss kinetics, J. Anal. Appl. Pyrolysis 77, 28-34

**Pröll, T., 2004,** Potenziale der Wirbelschichtdampfvergasung fester Biomasse – Modellierung und Simulation auf Basis der Betriebserfahrungen am Biomassekraftwerk Güssing, Dissertation, Technische Universität Wien

**Radlein, D., Piskorz, J., Scott, D.S., 1991,** Fast pyrolysis of natural polysaccharides as a potential industrial process, J. Anal. Appl. Pyrolysis, 19, pp41-63

**Reisinger, K., Haslinger, C., Herger, M., Hofbauer, H., 2010,** BIOBIB - A database for biofuels, Institute of Chemical Engineering, Fuel and Environmental Technology, University of Technology Vienna, Getreidemarkt 9, 1060 Wien, Austria, <http://www.vt.tuwien.ac.at/biobib/biobib.html>

**Richards, G.N., 1988,** Glycolaldehyde from pyrolysis of cellulose, J. Anal. Appl. Pyrolysis 10, 251-255

**Rösch, Ch., Wintzer, D., 1997,** Gasification and pyrolysis of biomass, TAB report no. 049, Berlin

**Rutherford, D.W., Wershaw, R.L., Cox, L.G., 2004,** Changes in composition and porosity occurring during the thermal degradation of

wood and wood components, US Geological Survey, Scientific Investigation Report 2004, Reston, VA

**Rüdiger, H., 1997**, Pyrolyse von festen biogenen Brennstoffen zur Erzeugung eines Zusatzbrennstoffes für Feuerungsanlagen, Berichte aus der Energiewirtschaft D93, Shaker, Aachen

**Sanchez, M., Simmons, G., 1981**, High temperature gasification kinetics of biomass pyrolysis, Journal of Analytical and Applied Pyrolysis 1981;3:161-71

**Sasaoka, E., Taniguchi, K., Hirano, S., Uddin, A., Kasaoka, S., Sakata, Y., 1995**, Catalytic Activity of ZnS Formed from Desulfurization Sorbent ZnO for Conversion of COS to H<sub>2</sub>S, Ind. Eng. Chem. Res., 34, 1102-1106

**Savolainen, K., Nyberg, K. and Dernjatin, P., 2003**, Co-firing biomass in the pulverised fuel boiler. BIOENERGY2003, International Nordic Bioenergy Conference, Jyväskylä, Finland, From 2nd to 5th September 2003

**Savolainen, K., Sormunen, R., 2001**, Co-firing of biomass and coal: a means to reducing greenhouse gas emissions. Presented in PowerGen '01, Bryssel, Belgium, 29. - 31.5. 2001

**Schreiner, M., Boblenz, K., Meyer, B., Krzack, St., 2009**, Biomassepyrolyse im Drehrohr als Vorschaltanlage für das Kraftwerk Dürnrrohr, Enbericht, Institut für Energieverfahrenstechnik und Chemieingenieurwesen (IEC), TU Bergakademie Freiberg

**Shafizadeh, F., 1982**, Introduction to pyrolysis of biomass, Journal of Analytical and Applied Pyrolysis, 3(4):283 - 305

- Shafizadeh, F., 1982**, Chemistry of pyrolysis and combustion of wood, In: Sarkanen, K.V.; Tillman, D.A.; Jahn, E.C. (Hrsg.): Progress in Biomass Conversion; Academic press, New York, 1982, vol 3, pp51-76
- Shafizadeh, F., Fu, Y.L., 1973**, Pyrolysis of cellulose, Carbohydrate Research, 29(1):113 – 122
- Simader, G.R, Moritz, G., 2002**, The analysis report of plant No. 20: Cofiring of biomass - evaluation of fuel procurement and handling in selected existing plants and exchange of information (COFIRING) - Part 2, Zeltweg, Austria
- SimTech Homepage, 2009**, IPSEpro system description, <http://www.simtechnology.com/IPSEpro/english/IPSEpro.php>
- Soukup, G., 2005**, Grundlagenuntersuchung zur Pyrolyse von Biomasse, Diplomarbeit, Institut für Verfahrenstechnik, Technische Universität Wien
- Solomon, P. R., Serio, M. A., and Suuberg, E.M., 1992**, Coal Pyrolysis: Experiments, Kinetic Rates and Mechanisms, Prog. Energy Combust. Sci., Vol. 18, p. 133-220
- Solomon, P. R. and Colket, M. B., 1978**, Evolution of Fuel Nitrogen in Coal Devolatilization, Fuel, Vol. 57, pp. 749-755
- Stahlberg, P., Lappi, M., Kurkela, E., Simell, P., Oesch, P., Nieminen, M., 1998**, Sampling of contaminants from product gases of biomass gasifiers, VTT Tiedotteita 1903 VTT Research Notes ESPOO
- Steen, C., 2011**, Holz ein vielseitiger Rohstoff, <http://www.uni-duesseldorf.de/MathNat/Biologie/Didaktik/Holz/dateien/index.html>
- Stoifl, B., 2000**, Energetische Nutzung von Stroh in kalorischen Kraftwerken anhand eines konkreten Beispiels – Wärmekraftwerk Dürnrrohr,

Diplomarbeit, Institut für Angewandte Botanik, Technische Mikroskopie und Organische Rohstofflehre, Technische Universität Wien

**Sturzl, R., 1997**, The commercial co-firing of RTP bio-oil at the Manitowoc Public Utilities power generation station, available at <http://www.ensyn.com>

**Sun, R., Lawther, J.M., Banks, W.B., 1997**, A tentative chemical structure of wheat straw, Industrial Crops and Products 6

**Tandon, H.L.S., 1991**, Sulphur research and Agricultural Production in India, 3rd revised edition, The Sulphur Institute, Washington D.C.

**The Perkin Elmer Corporation, 1997**, TurboMass GC Mass Spectrometer Hardware Guide.

**Tian, F.-J., Yu, J.-I., McKenzie, L.J., Hayashi, J.-I., Chiba, T., Li, C.-Z., 2004**, Formation of NO<sub>x</sub> precursors during the pyrolysis of coal and biomass, Part VII, Pyrolysis and gasification of cane trash with steam, Fuel, 84, 371-376

**Toft, A., 1996**, A Comparison of Integrated Biomass to Electricity Systems, PhD Thesis, Aston University, Birmingham, UK

**Tsai, W.T., Lee, M.K., Chang, Y.M., 2006**, Fast pyrolysis of rice husk: Product yields and composition, Bioresource Technology, vol 98, pp22-28

**Unger, C., Ising, M., 2002**, Mechanismen und Bedeutung der Teerbildung und Teerbeseitigung bei der thermochemischen Umwandlung fester Kohlenstoffträger. DGMK-Tagungsbericht . 2, pp. 131-142. Velen/Westf.: DGMK.

**Van Loo, S., Koppejan, J., 2002**, Handbook of biomass combustion and co-firing, IEA Bioenergy Task 32, Twente University Press, The Netherlands

**Vattenfall, 2007**, The Climate Threat: Can Humanity Rise to the Greatest Challenge of our Times?, <http://www.rockwool.com/files/rockwool.com/Energy%20Efficiency/PDF%20-%20Energy%20efficiency/P0273929.pdf>

**Verbund AG Homepage, 2004**, Pressefotos, <http://www.verbund.at>

**Vorher, W., 1976**, Entwicklung eines kontinuierlichen Pyrolyseverfahrens zum Abbau von Phenollignin mit dem Ziel der Ligninverwertung unter besonderer Berücksichtigung der Rückgewinnung von Phenol aus Ablaugen eines Phenolzellstoffprozesses, Dissertation, Universität Hamburg

**Wagenaar, B.M., Gansekoele, E., Florijn, J., Venderbosch, R.H., Penninks, F.W.M., Stellingwerf A., 2004**, Bio-oil as natural gas substitute in a 350 MWe power station, In: Second world conference on biomass for energy, industry and climate protection, 10–14 May 2004, Rome, Italy

**Wagenaar, B.M., Venderbosch, R.H., Prins, W., Penninks, F.W.M., 2002**, Bio-oil as a coal substitute in a 600 MWe Power Station. In: 12th European conference and technology exhibition on biomass for energy, industry and climate protection, 17–21 June 2002, Amsterdam, The Netherlands

**Wallingford, W., 1980**. Functions of Potassium in Plants, In: Potassium for Agriculture, Potash and Phosphate Institute, Atlanta, Georgia

**Wannapeera, J., Worasuwanarak, N, Pipatmanomai, S., 2008**, Product yields and characteristics of rice husk, rice straw and corncob during fast pyrolysis in a drop-tube/fixed-bed reactor, Songklanakarin J. Sci. Technol., 30 (3), 393-404

**Wei, X., Lopez, C., Puttkamer, T., Schnell, U., Unterberger, S., Hein, K.R.G., 2002**, Assessment of Chlorine- Alkali-Mineral interactions

during co-combustion of coal and straw, *Energy & Fuels*, 16(5):1095–1108

**Wei, X., Schnell, U., Hein, K.R.G., 2005**, Behaviour of gaseous chlorine and alkali metals during biomass thermal utilisation. *Fuel*, 84(7-8):841 – 848

**Weinwurm, F., 2010**, Heißwasservorbehandlung von Stroh, Diplomarbeit, Institut für Verfahrenstechnik, Technische Universität Wien

**Wiest, W., 1998**, Zur Pyrolyse von Biomasse im Drehrohreaktor, Dissertation, Fachbereich 15 – Maschinenbau, Universität Gesamthochschule Kassel

**Wolfesberger, U., 2008**, First test runs and tar analyses of a low temperature pyrolysis biomass pilot plant, Masterarbeit, Institut für Verfahrenstechnik, Technische Universität Wien

**Wu, Y., Zhao, Z., Li, H., He, F., 2009**, Low temperature pyrolysis characteristics of major components of biomass, *Journal of fuel chemistry and technology*, 37(4), pp427-432

**Yaman S., Sahan M., Haykiri-Acma H., Sesen K., Kucukbayrak S., 2000**, Production of fuel briquettes from olive refuse and paper mill waste, *Fuel Processing Technology* 68, 23–31

**Yang, H., Yan, R., Chen, H., Lee, D.H., Zheng, C., 2007**, Characteristics of hemicellulose, cellulose and lignin pyrolysis, *Fuel* (86), 1781-1788

**Yu, C., Tang, Y., Fang, M., Luo, Z., Cen, K., 2005**, Experimental study on alkali emission during rice straw pyrolysis, *Journal of Zhejiang University (Engineering Science)*, vol 39, pp1435-1444

**Zanzi, R., Bai, X., Capdevila, P., Bjornbom, E., 2001**, Pyrolysis of biomass in the presence of steam for preparation of activated carbon, liquid and

gaseous products, 6<sup>th</sup> World Congress of Chemical Engineering, September 23-28, 2001, Melbourne, Australia

**Zuwala J., Sciazko M., 2005,** Co-firing based energy systems – modelling and case studies, Paper presented at the 14th European Biomass Conference & Exhibition Biomass for Energy, Industry and Climate Protection, Paris, 17-21 October 2005



## 9 Appendix

### 9.1 Measured values and name of their measuring points in the process control system

Table 9-1: Measured values and the name of their measuring points in the process control system

CO	89HNE20CQ001
CO <sub>2</sub>	89HNE20CQ002
H <sub>2</sub>	89HNE20CQ003
CH <sub>4</sub>	89HNE20CQ004
O <sub>2</sub>	89HNE20CQ005

### 9.2 Design data of the pyrolysis pilot plant Dürnrrohr

Table 9-2: Design data of the pilot plant for pyrolysis operation

Fuel thermal output	3-5 MW
Biomass amount	600-1100 kg/h
Pyrolysis gas amount	500-850 kg/h
Pyrolysis charcoal amount	140-300 kg/h
Combustion air amount	2000-3000 Nm <sup>3</sup> /h
Flue gas amount combustion total	7300-12800 Nm <sup>3</sup> /h
Heating gas amount for rotary kiln reactor	2500-5900 Nm <sup>3</sup> /h
Flue gas amount over fabric filter	6600-10800 Nm <sup>3</sup> /h
Exhaust gas amount over stack	4300-6600 Nm <sup>3</sup> /h
Recirculation gas for combustion	1000-4200 Nm <sup>3</sup> /h
Water injection total	1.4-2.4 m <sup>3</sup> /h
Absorber addition	2-4 kg/h
Amount fabric filter ash	5-8.5 kg/h
Heating temperature	800-1000° C
Pyrolysis gas temperature	350-650° C
Flue gas temperature stack	150-200° C
O <sub>2</sub> -content combustion	2.5-3.5 %

Table 9-3: Design data of the pilot plant for fluidised bed operation

---

Fuel thermal output	3-5 MW
Pyrolysis charcoal amount	0-300 kg/h
Combustion air amount	1200-2600 Nm <sup>3</sup> /h
Flue gas amount combustion total	4000-8500 Nm <sup>3</sup> /h
Flue gas amount over fabric filter	5600-11200 Nm <sup>3</sup> /h
Exhaust gas amount over stack	2800-5700 Nm <sup>3</sup> /h
Recirculation gas for combustion	2800-5600 Nm <sup>3</sup> /h
Water injection total	1.4-2.4 m <sup>3</sup> /h
Absorber addition	2-4 kg/h
Amount fabric filter ash	28-67 kg/h
Combustion chamber temperature	800-850° C
Flue gas temperature stack	150-200° C
O <sub>2</sub> -content combustion	3-4 %

---

## 9.3 Analyses of black coal

Table 9-4: Black coal Murcki

Immediat-Analyse			Ascheanalyse (Schmelztablette_uni)			
	analysefeucht	wasserfrei	Konz.		Konz.	
			Ma.-%		Ma.-%	
W [Ma.-%]	5,58		CO2		C	
A [Ma.-%]	10,65	11,28			O	47,150
VM [Ma.-%]	32,10	34,00	Na2O	0,350	Na	0,260
Cfix [Ma.-%]	51,67	54,72	MgO	2,690	Mg	1,622
Elementar-Analyse			Al2O3	28,380	Al	15,020
	analysefeucht	wasserfrei	SiO2	46,190	Si	21,590
C [Ma.-%]	68,30	72,34	P2O5	0,604	P	0,264
H [Ma.-%]	4,19	4,44	SO3	5,318	S	2,130
N [Ma.-%]	1,18	1,25	K2O	2,324	K	1,930
S [Ma.-%]	0,71	0,75	CaO	4,562	Ca	3,260
O [Ma.-%]	9,54	10,10	TiO2	1,074	Ti	0,644
Brenn- und Heizwert			Fe2O3	7,801	Fe	5,456
	analysefeucht	wasserfrei	BaO	0,250	Ba	0,224
Hu [MJ/kg]	26,037	27,720	Cl	0,006	Cl	0,006
Ho [MJ/kg]	27,087	28,688	Schwermetalle (Orientierungswerte)			
Ascheschmelzverhalten			Cu			0,017
Veraschungstemperatur [°C]		815	Zn			0,018
Erweichungstemperatur [°C]		1.230	Sr			0,094
Sphärischtemperatur [°C]		1.460	Sn			
Halbkugeltemperatur [°C]		1.470	Pb			0,019
Fließtemperatur [°C]		1.500	Cr			0,013
			Mn			0,077
			Ni			0,022

Table 9-5: Black coal Centrum

Immediat-Analyse			Ascheanalyse (Schmelztablette_uni)			
	analysefeucht	wasserfrei	Konz.		Konz.	
			Ma.-%		Ma.-%	
W [Ma.-%]	3,91		CO2		C	
A [Ma.-%]	12,05	12,54			O	46,760
VM [Ma.-%]	32,95	34,29	Na2O	0,500	Na	0,371
Cfix [Ma.-%]	51,09	53,17	MgO	4,641	Mg	2,798
Elementar-Analyse			Al2O3	24,740	Al	13,090
	analysefeucht	wasserfrei	SiO2	45,380	Si	21,210
C [Ma.-%]	69,35	72,17	P2O5	0,406	P	0,177
H [Ma.-%]	4,24	4,41	SO3	6,267	S	2,510
N [Ma.-%]	1,18	1,23	K2O	2,364	K	1,962
S [Ma.-%]	0,75	0,28	CaO	6,994	Ca	4,999
O [Ma.-%]	8,83	9,19	TiO2	0,952	Ti	0,571
Brenn- und Heizwert			Fe2O3	7,275	Fe	5,089
	analysefeucht	wasserfrei	BaO	0,200	Ba	0,179
Hu [MJ/kg]	26,586	27,768	Cl	0,005	Cl	0,005
Ho [MJ/kg]	27,607	28,730	Schwermetalle (Orientierungswerte)			
Ascheschmelzverhalten			Cu			0,014
Veraschungstemperatur [°C]		815	Zn			0,019
Erweichungstemperatur [°C]		1240	Sr			0,088
Sphärischtemperatur [°C]		1275	Sn			
Halbkugeltemperatur [°C]		1295	Pb			0,012
Fließtemperatur [°C]		1340	Cr			0,018
			Mn			0,072
			Ni			0,019

Table 9-6: Black coal Rydultowy

Immediat-Analyse			Ascheanalyse (Schmelztablette_uni)			
	analysefeucht	wasserfrei	Konz.		Konz.	
			Ma.-%		Ma.-%	
W [Ma.-%]	1,54					
A [Ma.-%]	6,51	6,61				
VM [Ma.-%]	33,90	34,43				
Cfix [Ma.-%]	58,05	58,96				
Elementar-Analyse						
	analysefeucht	wasserfrei				
C [Ma.-%]	79,48	80,72	CO2		C	
H [Ma.-%]	4,92	5,00			O	45,350
N [Ma.-%]	1,52	1,54	Na2O	1,300	Na	0,964
S [Ma.-%]	0,63	0,64	MgO	4,441	Mg	2,678
O [Ma.-%]	5,60	5,69	Al2O3	25,650	Al	13,580
Brenn- und Heizwert			SiO2	37,580	Si	17,560
	analysefeucht	wasserfrei	P2O5	1,601	P	0,699
Hu [MJ/kg]	31,323	31,851	SO3	6,742	S	2,700
Ho [MJ/kg]	32,434	32,941	K2O	1,892	K	1,571
Ascheschmelzverhalten			CaO	8,630	Ca	6,168
Veraschungstemperatur [°C]		815	TiO2	0,704	Ti	0,422
Erweichungstemperatur [°C]		1253	Fe2O3	10,300	Fe	7,201
Sphärischtemperatur [°C]		1300	BaO	0,490	Ba	0,439
Halbkugeltemperatur [°C]		1316	Cl	0,016	Cl	0,016
Fließtemperatur [°C]		1346	Schwermetalle (Orientierungswerte)			
			Cu			0,037
			Zn			0,020
			Sr			0,354
			Sn			
			Pb			0,049
			Cr			0,013
			Mn			0,103
			Ni			0,032

Table 9-7: Black coal Kru Trade

Immediat-Analyse			Ascheanalyse (Schmelztablette_uni)			
	analysefeucht	wasserfrei	Konz.		Konz.	
			Ma.-%		Ma.-%	
W [Ma.-%]	4,40					
A [Ma.-%]	15,69	16,41				
VM [Ma.-%]	32,08	33,56				
Cfix [Ma.-%]	47,83	50,03				
Elementar-Analyse						
	analysefeucht	wasserfrei				
C [Ma.-%]	65,37	68,38	CO2		C	
H [Ma.-%]	4,24	4,44			O	49,220
N [Ma.-%]	2,03	2,12	Na2O	0,137	Na	0,101
S [Ma.-%]	0,31	0,32	MgO	1,015	Mg	0,612
O [Ma.-%]	7,97	8,34	Al2O3	21,330	Al	11,290
Brenn- und Heizwert			SiO2	66,950	Si	31,290
	analysefeucht	wasserfrei	P2O5	0,636	P	0,277
Hu [MJ/kg]	25,208	26,481	SO3	0,175	S	0,070
Ho [MJ/kg]	26,240	27,448	K2O	2,352	K	1,953
Ascheschmelzverhalten			CaO	0,992	Ca	0,709
Veraschungstemperatur [°C]		815	TiO2	0,945	Ti	0,567
Erweichungstemperatur [°C]		1270	Fe2O3	5,128	Fe	3,587
Sphärischtemperatur [°C]		>1500	BaO	0,160	Ba	0,143
Halbkugeltemperatur [°C]			Cl	0,005	Cl	0,005
Fließtemperatur [°C]			Schwermetalle (Orientierungswerte)			
			Cu			0,009
			Zn			0,013
			Sr			0,068
			Sn			
			Pb			0,013
			Cr			0,009
			Mn			0,046
			Ni			0,007

Table 9-8: Elemental analysis of different fuel samples

	water content wt. %	ash content (550°C) wt. % (dm)	volatiles wt. % (dm)	C	H	N	S	Cl	K	Na	LHV kJ/kg
						dry matter (dm)					
palm nut shells	16,16	2,7%	72,6%	530400	48300	3100	300	100	1000	20	19094
reed straw	50	27,3%	62,9%	423700	51000	6600	1000	900	1500	500	13395
sorghum straw	26,22	6,9%	77,1%	504200	37900	8500	1300	700	7900	30	17174
straw pellets	6,55	n.d.	76,6%	463200	53700	6000	n.d.	n.d.	11700	300	17216
miscanthus straw	9,06	n.d.	84,3%	490700	50900	2100	n.d.	n.d.	1600	100	17873
Waldviertler energy grass	11,36	4,2%	80,4%	473400	57100	5600	200	3500	4900	50	17381
paper residual	4,06	41,3%	67,6%	315900	37400	1000	600	152	384	1050	9800
Waldviertler energy grass	15,97	4,4%	75,0%	463600	59200	4850	567	1210	4860	56	16730

Table 9-9: Elemental analysis of different pyrolysis char samples

	ash content (550°C) wt. % (dm)	volatiles wt. % (dm)	C	H	N	S	Cl	K	Na	LHV kJ/kg
					dry matter (dm)					
palm nut shells char	5,8%	10,8%	845000	22700	7000	400	100	1600	10	31484
reed straw char	47,4%	8,6%	459600	10700	6900	600	600	1100	700	16480
sorghum char	14,8%	13,2%	741300	21400	9200	1500	1100	1920	20	26865
straw pellets char	n.d.	17,1%	706300	18700	7400	n.d.	n.d.	37100	600	26897
miscanthus char	n.d.	10,8%	750300	20300	3600	n.d.	n.d.	3800	100	28298
Waldviertler energy grass char 560°C	13,8%	11,6%	771200	23900	12600	300	4100	1060	50	28991
paper residual char	67,6%	15,0%	287400	11900	1000	534	263	4050	2900	9800
Waldviertler energy grass char 500°C	15,2%	15,4%	737500	25700	8660	692	1880	17300	219	27080

n.d. ... not detected

## 9.4 Process simulation flow sheet

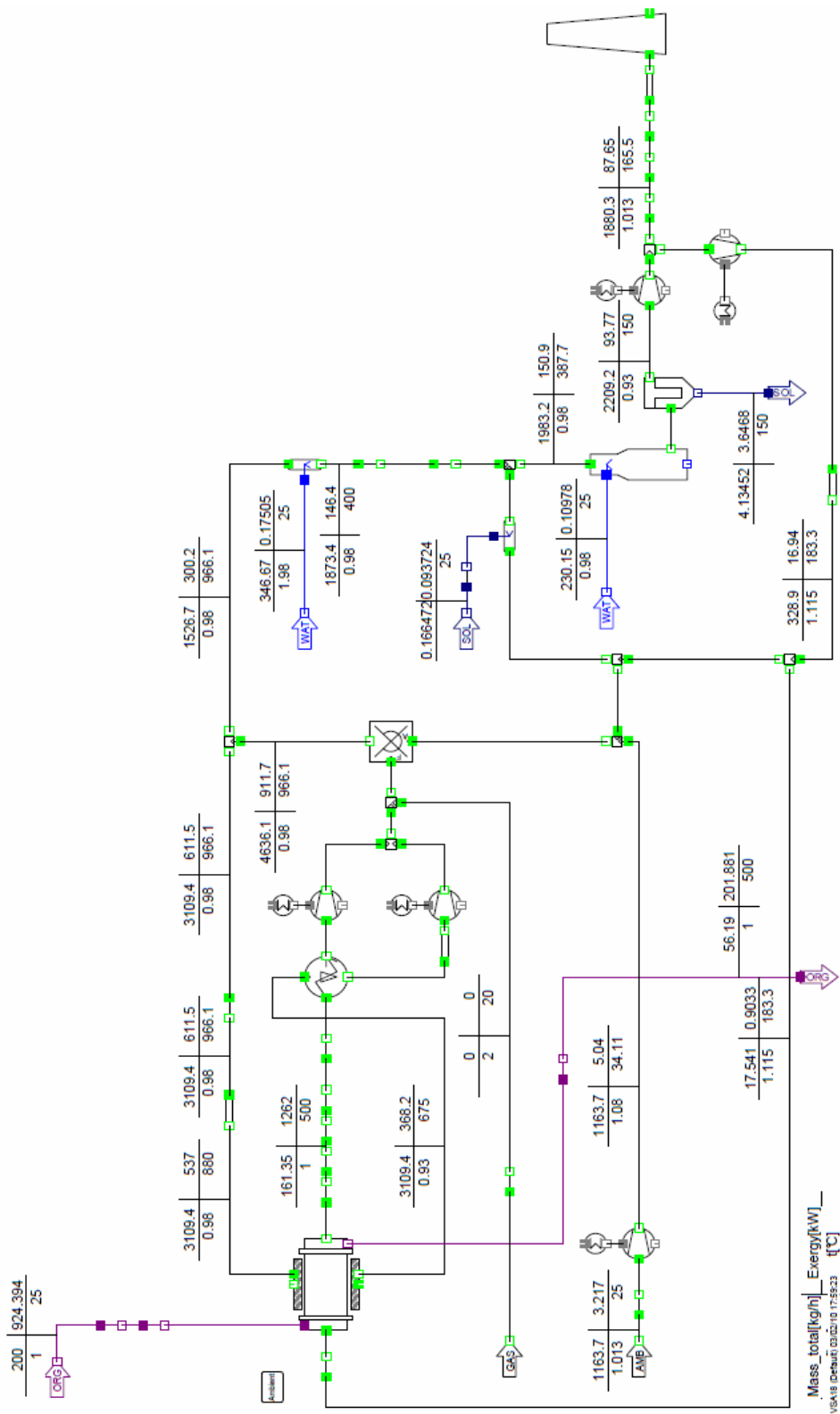


Figure 9-1: Process simulation flow sheet of the pilot plant



**Prozessdaten Versuchsanlage Dürnrohr**

Seite: 1

Ausgeglichene Lösung mit IPSEpro

Messwertbasis: 20.01.2010 12:30 - 12:40 (Stroh aus Lasee, Pyrolysetemperatur 450 °C)

**Prozessbedingungen**

zugeführte Leistung DRO [kW]	112
BWL Brennkammer. [kW]	1812
Pyrolysegastemperatur [°C]	472

**Umgebungsbedingungen**

Seehöhe [m]	182
Temperatur [°C]	5.20
Luftdruck [mbar]	1013.25
Rel. Luftfeuchte [%]	60

**Kaltgaswirkungsgrad Pyrolysegas**

$\eta_{\text{chem}}$	0.55
----------------------	------

**Gasströme**

Luft, Pyrolysegas	Luft vor Gebläse	Luft vor Brennkammer	Pyrolysegas nach DRO	Pyrolysegas nach Pyrol.gasgebläse
Temperatur [°C]	5.2	114.0	472.1	517.6
Absolutdruck [bar]	1.01325	1.03024	1.01302	1.17248
Normvol.strom [Nm <sup>3</sup> /h]	2098	2098	286	286
Betr.vol.strom [m <sup>3</sup> /h]	2138	2925	780	715
Gasmassenstrom [kg/h]	2706	2706	283	283
Staubbelastung [g/Nm <sup>3</sup> ]	---	---	16.6	16.6
Flugkoksbelastung [g/Nm <sup>3</sup> ]	---	---	11.7	11.7
Teerbelastung [g/Nm <sup>3</sup> ]	---	---	229.1	229.1
Gesamtmassenstrom [kg/h]	2706	2706	357	357
Energiestrom [kW]	4.1	86.7	1357.9	1366.5
Zusammensetzung Gas	Umgebungsluft	Umgebungsluft	Pyrolysegas	Pyrolysegas
Zusammensetzung Staub	---	---	Asche Biomasse	Asche Biomasse
Zusammensetzung Flugkoks	---	---	Pyrolysekoks	Pyrolysekoks
Zusammensetzung Teer	---	---	Teer	Teer

Rauchgas, Heißgas, Kaltgas	Luft + Rezigas zu Brennkammer	Heißgas vor DRO	Kaltgas nach DRO	Kaltgas nach Kaltgasgebläse
Temperatur [°C]	141.2	781.6	519.3	423.6
Absolutdruck [bar]	1.03024	1.01248	1.00924	1.07248
Normvol.strom [Nm <sup>3</sup> /h]	3662.0	1381.6	1381.6	1381.6
Betr.vol.strom [m <sup>3</sup> /h]	5463.6	5339.1	4024.0	3329.3
Gasmassenstrom [kg/h]	4346.7	1634.8	1634.8	1634.8
Staubbelastung [g/Nm <sup>3</sup> ]	---	1.19	1.19	1.19
Gesamtmassenstrom [kg/h]	4346.7	1636.5	1636.5	1636.5
Energiestrom [kW]	207.4	466.1	300.8	243.3
Zusammensetzung Gas	Verbr.luftmix	Rauchgas NBK	Rauchgas NBK	Rauchgas NBK
Zusammensetzung Staub	---	Asche Biomasse	Asche Biomasse	Asche Biomasse

Rauchgas, Rauchgas Rezigas mix	Rauchgas nach Brennkammer	Rauchgas vor Sprühkühler	Rauchgas nach Sprühkühler	Rauchgas + Rezigas vor Sprühabsorber
Temperatur [°C]	976.6	976.6	370.4	290.6
Absolutdruck [bar]	1.01248	1.01248	1.01198	1.01198
Normvol.strom [Nm <sup>3</sup> /h]	5384.9	4003.3	5590.1	9498.1
Betr.vol.strom [m <sup>3</sup> /h]	24655.6	18329.8	13185.9	19626.2
Gasmassenstrom [kg/h]	6372.0	4737.1	6012.5	10112.1
Staubbelastung [g/Nm <sup>3</sup> ]	1.19	1.19	0.85	0.50
Gesamtmassenstrom [kg/h]	6378.4	4741.9	6017.3	10116.9
Energiestrom [kW]	2319.8	1724.6	888.6	1190.3
Zusammensetzung Gas	Rauchgas NBK	Rauchgas NBK	Rauchgas Quench	Gasmix vor Desulf
Zusammensetzung Staub	Asche Biomasse	Asche Biomasse	Asche Biomasse	Asche/Kalk mix



<b>Prozessdaten Versuchsanlage Dürnrohr</b>	<i>Seite: 2</i>
---------------------------------------------	-----------------

<i>Rauchgas, Erdgas</i>	Rauchgas nach Sprühabsorber	Abgas nach Gewebefilter	Abgas durch Kamin	Erdgas
Temperatur [°C]	195.7	110.3	138.6	20.0
Absolutdruck [bar]	1.00896	0.99867	1.01325	2.00
Normvol.strom [Nm³/h]	10102.7	10102.7	4625.2	53.5
Betr.vol.strom [m³/h]	17416.1	14390.0	6972.0	29.1
Gasmassenstrom [kg/h]	10598.1	10598.1	4852.1	38.3
Staubbelastung [g/Nm³]	0.47	0.00	0.00	---
Gesamtmassenstrom [kg/h]	10602.8	10598.1	4852.1	38.3
Energiestrom [kW]	871.8	518.7	290.6	532.7
Zusammensetzung Gas	Abgas	Abgas	Abgas	Erdgas
Zusammensetzung Staub	Asche Desulf	---	---	---

<i>Rezigas</i>	Rezigas gesamt	Rezigas zu DRO	Rezigas zu Brennkammer	Rezigas zu Sprühabsorber
Temperatur [°C]	138.6	173.7	173.7	173.7
Absolutdruck [bar]	1.01325	1.03026	1.03026	1.03026
Normvol.strom [Nm³/h]	5477.4	5.6	1563.8	3908.0
Betr.vol.strom [m³/h]	8256.6	9.1	2516.2	6288.0
Gasmassenstrom [kg/h]	5746.0	5.9	1640.5	4099.6
Staub [g/Nm³]	0.00	0.00	0.00	2.30729e-321
Gesamtmassenstrom [kg/h]	5746.0	5.9	1640.5	4099.6
Energiestrom [kW]	344.1	0.4	120.7	301.7
Zusammensetzung Gas	Abgas	Abgas	Abgas	Abgas
Zusammensetzung Staub	---	---	---	Calciumhydroxid

**Biomasse und Pyrolysekoks**

<i>Biomasse, Koks</i>	Biomasse	Pyrolysekoks
Temperatur [°C]	6.3	444.4
Absolutdruck [bar]	1.01302	1.01302
Dichte [kg/m³]	300.0	300.0
Massenstrom [kg/h]	498.5	147.5
Heizwert (wf) [kJ/kg]	18365.2	27005.0
Heizwert [kJ/kg]	16508.0	27005.0
Wassergehalt [Gew. %]	8.93	0.00
Aschegehalt [Gew. % wf]	5.06	12.34
Energiestrom [kW]	2287.0	1129.9
Zusammensetzung org.	Biomasse	Pyrolysekoks
Zusammensetzung anorg.	Asche Biomasse	Asche Biomasse

**Feststoffströme**

	Kalk für Entschwefelung	Gewebefilter Abreinigung
Temperatur [°C]	25.0	110.3
Koksbelastung [kg/kg_anorg.]	0.00	0.00
Massenstrom [kg/h]	0.00	4.74
Energiestrom [kW]	0.00	0.11
Zusammensetzung Organisch	---	---
Zusammensetzung Anorg.	Calciumhydroxid	Asche Desulf

<b>Prozessdaten Versuchsanlage Dürnrohr</b>	Seite: 3
---------------------------------------------	----------

**Wasserströme**

<i>Sprühabsorber und Sprühkühler</i>	Wasser für Sprühkühler	Wasser für Sprühabsorber
Temperatur [°C]	20.0	20.0
Absolutdruck [bar]	2.0	2.0
Enthalpie [kJ/kg]	-15886.8	-15886.8
Betr.vol.strom [m <sup>3</sup> /h]	1.3	0.5
Massenstrom [kg/h]	1275.4	485.9
Energiestrom [kW]	-835.6	-318.4

**Apparate****Nachbrennkammer**

Druckverlust Rauchgas [mbar]	50	Luftzahl $\lambda$ [-]	1.57
Druckverlust Luft [mbar]	18	CO-Schlupf [mol <sub>CO</sub> /mol <sub>CO2</sub> ]	0.0000
		Therm. Leistg. [kW]	1811.6

**Drehrohrreaktor**

Druckverlust Heißgas [mbar]	3.24	zugeführte Leistung über Heißgas [kW]	112
Pyrolysetemperatur [°C]	472	Umgesetzter C in Gas und Teer [%]	50.45
Teer in PG [kg/kg_tr.BSt]	0.15	Exergieverlust [kW]	81.11
Staub in PG [kg/kg_tr.BSt]	0.21		
Flugkoks in PG [kg/kg_tr.BSt]	0.01		

**Sprühkühler**

Druckverlust Gas [mbar]	0.50	Exergieverlust [kW]	543.3
-------------------------	------	---------------------	-------

**Sprühabsorber**

Druckverlust Gas [mbar]	3.02	Exergieverlust [kW]	97.1
Umsatz von CaOH <sub>2</sub> [%]	70.0	Desulfurisation reaction rate [kmol/h]	8.39912e-323

**Gewebefilter**

Druckverlust Gas [mbar]	10.30	rel Wärmeverlust [%]	44.2
Diff.Temp.Austritt [°C]	85.4	Wärmeverlust [kW]	353.0
Abscheidegrad Staub [%]	100.0	Exergieverlust [kW]	108.5

**Exergieflüsse DRO**

Exergie Biomasse [kW]	2475.78
Exergie Heißgas [kW]	269.8
Exergie Rezigas [kW]	0.3
Exergie Pyrolysegas [kW]	1359.7
Exergie Pyrolysekoks [kW]	1147.1
Exergie Kaltgas [kW]	158.0

<b>Prozessdaten Versuchsanlage Dürnrohr</b>	<i>Seite: 4</i>
---------------------------------------------	-----------------

**Zusammensetzungen Gasströme**

<i>Luft und Verbrennungsluftmix</i>	Umgebungsluft	Umgebungsluft wasserfrei	Verbrennungsluftmix	Verbrennungsluftmix wasserfrei
mittlere Molmasse [g/mol]	28.91	28.97	26.60	29.35
Heizwert $H_U$ [MJ/Nm <sup>3</sup> ]	0.00	0.00	0.00	0.00
Ar [vol%]	0.93	0.93	0.71	0.94
C <sub>2</sub> H <sub>4</sub> [vol%]	0.00	0.00	0.00	0.00
C <sub>2</sub> H <sub>6</sub> [vol%]	0.00	0.00	0.00	0.00
C <sub>3</sub> H <sub>8</sub> [vol%]	0.00	0.00	0.00	0.00
CH <sub>4</sub> [vol%]	0.00	0.00	0.00	0.00
CO [vol%]	0.00	0.00	0.00	0.00
CO <sub>2</sub> [vol%]	0.04	0.04	2.58	3.41
H <sub>2</sub> [vol%]	0.00	0.00	0.00	0.00
H <sub>2</sub> O [vol%]	0.52	---	24.23	---
H <sub>2</sub> S [vol%]	0.00	0.00	0.00	0.00
HCl [vol%]	0.00	0.00	0.00	0.00
HCN [vol%]	0.00	0.00	0.00	0.00
N <sub>2</sub> [vol%]	77.67	78.08	59.56	78.60
N <sub>2</sub> O [vol%]	0.00	0.00	0.00	0.00
NH <sub>3</sub> [vol%]	0.00	0.00	0.00	0.00
NO [vol%]	0.00	0.00	0.00	0.00
O <sub>2</sub> [vol%]	20.84	20.95	12.92	17.05
SO <sub>2</sub> [vol%]	0.00	0.00	0.00	0.00

<i>Pyrolysegas, Rauchgas</i>	Pyrolysegas	Pyrolysegas wasserfrei	Rauchgas NBK	Rauchgas NBK wasserfrei
mittlere Molmasse [g/mol]	22.23	26.78	26.52	30.52
Heizwert $H_U$ [MJ/Nm <sup>3</sup> ]	6.94	14.44	0.00	0.00
Ar [vol%]	0.01	0.02	0.65	0.96
C <sub>2</sub> H <sub>4</sub> [vol%]	0.00	0.00	0.00	0.00
C <sub>2</sub> H <sub>6</sub> [vol%]	0.00	0.00	0.00	0.00
C <sub>3</sub> H <sub>8</sub> [vol%]	0.00	0.00	0.00	0.00
CH <sub>4</sub> [vol%]	12.18	25.35	0.00	0.00
CO [vol%]	16.27	33.87	0.00	0.00
CO <sub>2</sub> [vol%]	13.04	27.13	9.29	13.65
H <sub>2</sub> [vol%]	4.82	10.02	0.00	0.00
H <sub>2</sub> O [vol%]	51.95	---	31.96	---
H <sub>2</sub> S [vol%]	0.00	0.01	0.00	0.00
HCl [vol%]	0.00	0.00	0.00	0.00
HCN [vol%]	0.00	0.00	0.00	0.00
N <sub>2</sub> [vol%]	0.90	1.86	54.54	80.17
N <sub>2</sub> O [vol%]	0.00	0.00	0.00	0.00
NH <sub>3</sub> [vol%]	0.02	0.03	0.00	0.00
NO [vol%]	0.00	0.00	0.01	0.01
O <sub>2</sub> [vol%]	0.82	1.70	3.54	5.20
SO <sub>2</sub> [vol%]	0.001	0.00	0.00	0.00

## Prozessdaten Versuchsanlage Dürnrohr

Seite: 5

<i>Rauchgas</i>	Rauchgas Quench	Rauchgas Quench wasserfrei	Gasmix vor Desulf	Gasmix vor Desulf wasserfrei
mittlere Molmasse [g/mol]	24.11	30.52	23.86	30.52
Heizwert $H_U$ [MJ/Nm <sup>3</sup> ]	0.00	0.00	0.00	0.00
Ar [vol%]	0.47	0.96	0.45	0.96
C2H4 [vol%]	0.00	0.00	0.00	0.00
C2H6 [vol%]	0.00	0.00	0.00	0.00
C3H8 [vol%]	0.00	0.00	0.00	0.00
CH4 [vol%]	0.00	0.00	0.00	0.00
CO [vol%]	0.00	0.00	0.00	0.00
CO2 [vol%]	6.65	13.65	6.38	13.65
H2 [vol%]	0.00	0.00	0.00	0.00
H2O [vol%]	51.28	---	53.23	---
H2S [vol%]	0.00	0.00	0.00	0.00
HCl [vol%]	0.00	0.00	0.00	0.00
HCN [vol%]	0.00	0.00	0.00	0.00
N2 [vol%]	39.06	80.17	37.49	80.17
N2O [vol%]	0.00	0.00	0.00	0.00
NH3 [vol%]	0.00	0.00	0.00	0.00
NO [vol%]	0.01	0.01	0.01	0.01
O2 [vol%]	2.54	5.20	2.43	5.20
SO2 [vol%]	0.00	0.00	0.00	0.00

<i>Abgas</i>	Abgas	Abgas wasserfrei
mittlere Molmasse [g/mol]	23.51	30.52
Heizwert $H_U$ [MJ/Nm <sup>3</sup> ]	0.00	0.00
Ar [vol%]	0.42	0.96
C2H4 [vol%]	0.00	0.00
C2H6 [vol%]	0.00	0.00
C3H8 [vol%]	0.00	0.00
CH4 [vol%]	0.00	0.00
CO [vol%]	0.00	0.00
CO2 [vol%]	6.00	13.65
H2 [vol%]	0.00	0.00
H2O [vol%]	56.03	---
H2S [vol%]	0.00	0.00
HCl [vol%]	0.00	0.00
HCN [vol%]	0.00	0.00
N2 [vol%]	35.25	80.17
N2O [vol%]	0.00	0.00
NH3 [vol%]	0.00	0.00
NO [vol%]	0.01	0.01
O2 [vol%]	2.29	5.20
SO2 [vol%]	0.000	0.001

## Organische Zusammensetzungen (wasser- und aschefrei)

	Biomasse	Pyrolysekoks	Teer
C [Gew%]	53.71	86.47	81.65
H [Gew%]	5.29	1.85	7.25
O [Gew%]	40.37	10.29	10.93
N [Gew%]	0.49	0.95	0.17
S [Gew%]	0.01	0.01	0.00
Cl [Gew%]	0.13	0.43	0.00
Heizwert $H_U$ (waf) [kJ/kg]	19343.10	30806.90	38489.50

**Prozessdaten Versuchsanlage Dürnrohr**

Seite: 6

**Zusammensetzungen Feststoffe**

	Asche Biomasse	Asche Desulf	Calciumhydroxid
Asche [Gew%]	100.00	100.00	0.00
K <sub>2</sub> O [Gew%]	0.00	0.00	0.00
MgO [Gew%]	0.00	0.00	0.00
CaO [Gew%]	0.00	0.00	0.00
SiO <sub>2</sub> [Gew%]	0.00	0.00	0.00
Olivin [Gew%]	0.00	0.00	0.00
CaCO <sub>3</sub> [Gew%]	0.00	0.00	0.00
Dolomit [Gew%]	0.00	0.00	0.00
CaSO <sub>4</sub> [Gew%]	0.00	---	0.00
CaOH <sub>2</sub> [Gew%]	0.00	---	100.00

**Prozessdaten Versuchsanlage Dürnrohr**

Seite: 1

Ausgeglichene Lösung mit IPSEpro

Messwertbasis: 19.01.2010 12:35 - 12:45 (Stroh aus Lassee, Pyrolysetemperatur 500 °C)

**Prozessbedingungen**

zugeführte Leistung DRO [kW]	119
BWL Brennkammer. [kW]	1786
Pyrolysegastemperatur [°C]	509

**Umgebungsbedingungen**

Seehöhe [m]	182
Temperatur [°C]	6.80
Luftdruck [mbar]	1013.25
Rel. Luftfeuchte [%]	60

**Kaltgaswirkungsgrad Pyrolysegas**

$\eta_{\text{chem}}$	0.53
----------------------	------

**Gasströme**

Luft, Pyrolysegas	Luft vor Gebläse	Luft vor Brennkammer	Pyrolysegas nach DRO	Pyrolysegas nach Pyrol.gasgebläse
Temperatur [°C]	6.8	122.8	508.7	569.2
Absolutdruck [bar]	1.01325	1.03024	1.01306	1.17249
Normvol.strom [Nm <sup>3</sup> /h]	2016	2016	301	301
Betr.vol.strom [m <sup>3</sup> /h]	2066	2874	860	801
Gasmassenstrom [kg/h]	2599	2599	298	298
Staubbeladung [g/Nm <sup>3</sup> ]	---	---	14.8	14.8
Flugkoksbeladung [g/Nm <sup>3</sup> ]	---	---	11.7	11.7
Teerbeladung [g/Nm <sup>3</sup> ]	---	---	197.1	197.1
Gesamtmassenstrom [kg/h]	2599	2599	365	365
Energiestrom [kW]	5.1	89.8	1335.2	1347.1
Zusammensetzung Gas	Umgebungsluft	Umgebungsluft	Pyrolysegas	Pyrolysegas
Zusammensetzung Staub	---	---	Asche Biomasse	Asche Biomasse
Zusammensetzung Flugkoks	---	---	Pyrolysekoks	Pyrolysekoks
Zusammensetzung Teer	---	---	Teer	Teer

Rauchgas, Heißgas, Kaltgas	Luft + Rezigas zu Brennkammer	Heißgas vor DRO	Kaltgas nach DRO	Kaltgas nach Kaltgasgebläse
Temperatur [°C]	146.7	793.5	603.3	484.4
Absolutdruck [bar]	1.03024	1.01249	1.00877	1.07249
Normvol.strom [Nm <sup>3</sup> /h]	3447.7	1957.7	1957.7	1957.7
Betr.vol.strom [m <sup>3</sup> /h]	5212.4	7650.6	6309.4	5129.4
Gasmassenstrom [kg/h]	4104.7	2320.8	2320.8	2320.8
Staubbeladung [g/Nm <sup>3</sup> ]	---	1.17	1.17	1.17
Gesamtmassenstrom [kg/h]	4104.7	2323.1	2323.1	2323.1
Energiestrom [kW]	202.1	672.3	500.2	396.7
Zusammensetzung Gas	Verbr.luftmix	Rauchgas NBK	Rauchgas NBK	Rauchgas NBK
Zusammensetzung Staub	---	Asche Biomasse	Asche Biomasse	Asche Biomasse

Rauchgas, Rauchgas Rezigas mix	Rauchgas nach Brennkammer	Rauchgas vor Sprühkühler	Rauchgas nach Sprühkühler	Rauchgas + Rezigas vor Sprühabsorber
Temperatur [°C]	967.3	967.3	370.4	285.3
Absolutdruck [bar]	1.01249	1.01249	1.01204	1.01204
Normvol.strom [Nm <sup>3</sup> /h]	5757.2	3799.6	5283.3	9522.4
Betr.vol.strom [m <sup>3</sup> /h]	26165.6	17268.4	12462.6	19491.4
Gasmassenstrom [kg/h]	6825.2	4504.4	5697.0	10153.6
Staubbeladung [g/Nm <sup>3</sup> ]	1.17	1.17	0.84	0.47
Gesamtmassenstrom [kg/h]	6832.0	4508.9	5701.4	10158.0
Energiestrom [kW]	2457.6	1621.9	840.3	1172.8
Zusammensetzung Gas	Rauchgas NBK	Rauchgas NBK	Rauchgas Quench	Gasmix vor Desulf
Zusammensetzung Staub	Asche Biomasse	Asche Biomasse	Asche Biomasse	Asche/Kalk mix

## Prozessdaten Versuchsanlage Dürnrohr

Seite: 2

<i>Rauchgas, Erdgas</i>	Rauchgas nach Sprühabsorber	Abgas nach Gewebefilter	Abgas durch Kamin	Erdgas
Temperatur [°C]	195.3	184.9	143.8	20.0
Absolutdruck [bar]	1.00901	0.99817	1.01325	2.00
Normvol.strom [Nm <sup>3</sup> /h]	10097.7	10097.7	4421.1	54.1
Betr.vol.strom [m <sup>3</sup> /h]	17391.0	17190.3	6748.6	29.4
Gasmassenstrom [kg/h]	10616.1	10616.1	4648.1	38.7
Staubbelastung [g/Nm <sup>3</sup> ]	0.44	0.00	0.00	---
Gesamtmassenstrom [kg/h]	10620.5	10616.1	4648.1	38.7
Energiestrom [kW]	869.7	826.2	287.1	538.6
Zusammensetzung Gas	Abgas	Abgas	Abgas	Erdgas
Zusammensetzung Staub	Asche Desulf	---	---	---

<i>Rezigas</i>	Rezigas gesamt	Rezigas zu DRO	Rezigas zu Brennkammer	Rezigas zu Sprühabsorber
Temperatur [°C]	189.2	176.7	176.7	176.7
Absolutdruck [bar]	1.01325	1.03027	1.03027	1.03027
Normvol.strom [Nm <sup>3</sup> /h]	5676.6	5.7	1431.8	4239.1
Betr.vol.strom [m <sup>3</sup> /h]	9609.2	9.3	2319.3	6866.7
Gasmassenstrom [kg/h]	5968.0	6.0	1505.3	4456.7
Staub [g/Nm <sup>3</sup> ]	0.00	0.00	0.00	0.00
Gesamtmassenstrom [kg/h]	5968.0	6.0	1505.3	4456.7
Energiestrom [kW]	474.5	0.4	112.3	332.5
Zusammensetzung Gas	Abgas	Abgas	Abgas	Abgas
Zusammensetzung Staub	---	---	---	Calciumhydroxid

**Biomasse und Pyrolysekoks**

<i>Biomasse, Koks</i>	Biomasse	Pyrolysekoks
Temperatur [°C]	8.0	470.9
Absolutdruck [bar]	1.01306	1.01306
Dichte [kg/m <sup>3</sup> ]	300.0	300.0
Massenstrom [kg/h]	510.9	151.5
Heizwert (wf) [kJ/kg]	18013.2	27135.2
Heizwert [kJ/kg]	16185.4	27135.2
Wassergehalt [Gew. %]	8.94	0.00
Aschegehalt [Gew. % wf]	5.02	12.48
Energiestrom [kW]	2298.3	1167.6
Zusammensetzung org.	Biomasse	Pyrolysekoks
Zusammensetzung anorg.	Asche Biomasse	Asche Biomasse

**Feststoffströme**

	Kalk für Entschwefelung	Gewebefilter Abreinigung
Temperatur [°C]	25.0	184.9
Koksbelastung [kg/kg_anorg.]	0.00	0.00
Massenstrom [kg/h]	0.00	4.44
Energiestrom [kW]	0.00	0.18
Zusammensetzung Organisch	---	---
Zusammensetzung Anorg.	Calciumhydroxid	Asche Desulf

<b>Prozessdaten Versuchsanlage Dürnrohr</b>	Seite: 3
---------------------------------------------	----------

**Wasserströme**

<i>Sprühabsorber und Sprühkühler</i>	Wasser für Sprühkühler	Wasser für Sprühabsorber
Temperatur [°C]	20.0	20.0
Absolutdruck [bar]	2.0	2.0
Enthalpie [kJ/kg]	-15886.8	-15886.8
Betr.vol.strom [m <sup>3</sup> /h]	1.2	0.5
Massenstrom [kg/h]	1192.6	462.5
Energiestrom [kW]	-781.3	-303.0

**Apparate****Nachbrennkammer**

Druckverlust Rauchgas [mbar]	50	Luftzahl $\lambda$ [-]	1.56
Druckverlust Luft [mbar]	18	CO-Schlupf [mol <sub>CO</sub> /mol <sub>CO2</sub> ]	0.0000
		Therm. Leistg. [kW]	1785.8

**Drehrohrreaktor**

Druckverlust Heißgas [mbar]	3.72	zugeführte Leistung über Heißgas [kW]	119
Pyrolysetemperatur [°C]	509	Umgesetzter C in Gas und Teer [%]	49.40
Teer in PG [kg/kg_tr.BSt]	0.13	Exergieverlust [kW]	96.29
Staub in PG [kg/kg_tr.BSt]	0.19		
Flugkoks in PG [kg/kg_tr.BSt]	0.01		

**Sprühkühler**

Druckverlust Gas [mbar]	0.46	Exergieverlust [kW]	506.8
-------------------------	------	---------------------	-------

**Sprühabsorber**

Druckverlust Gas [mbar]	3.03	Exergieverlust [kW]	91.4
Umsatz von CaOH <sub>2</sub> [%]	70.0	Desulfurisation reaction rate [kmol/h]	1.28595E-32

**Gewebefilter**

Druckverlust Gas [mbar]	10.83	rel Wärmeverlust [%]	5.4
Diff. Temp.Austritt [°C]	10.4	Wärmeverlust [kW]	43.3
Abscheidegrad Staub [%]	100.0	Exergieverlust [kW]	18.8

**Exergieflüsse DRO**

Exergie Biomasse [kW]	2491.25
Exergie Heißgas [kW]	391.6
Exergie Rezigas [kW]	0.3
Exergie Pyrolysegas [kW]	1330.0
Exergie Pyrolysekoks [kW]	1184.6
Exergie Kaltgas [kW]	272.2



## Prozessdaten Versuchsanlage Dürnröhr

Seite: 4

## Zusammensetzungen Gasströme

<i>Luft und Verbrennungsluftmix</i>	Umgebungsluft	Umgebungsluft wasserfrei	Verbrennungsluftmix	Verbrennungsluftmix wasserfrei
mittlere Molmasse [g/mol]	28.90	28.97	26.69	29.35
Heizwert $H_U$ [MJ/Nm <sup>3</sup> ]	0.00	0.00	0.00	0.00
Ar [vol%]	0.93	0.93	0.72	0.94
C <sub>2</sub> H <sub>4</sub> [vol%]	0.00	0.00	0.00	0.00
C <sub>2</sub> H <sub>6</sub> [vol%]	0.00	0.00	0.00	0.00
C <sub>3</sub> H <sub>8</sub> [vol%]	0.00	0.00	0.00	0.00
CH <sub>4</sub> [vol%]	0.00	0.00	0.00	0.00
CO [vol%]	0.00	0.00	0.00	0.00
CO <sub>2</sub> [vol%]	0.04	0.04	2.61	3.42
H <sub>2</sub> [vol%]	0.00	0.00	0.00	0.00
H <sub>2</sub> O [vol%]	0.58	---	23.53	---
H <sub>2</sub> S [vol%]	0.00	0.00	0.00	0.00
HCl [vol%]	0.00	0.00	0.00	0.00
HCN [vol%]	0.00	0.00	0.00	0.00
N <sub>2</sub> [vol%]	77.63	78.08	60.09	78.58
N <sub>2</sub> O [vol%]	0.00	0.00	0.00	0.00
NH <sub>3</sub> [vol%]	0.00	0.00	0.00	0.00
NO [vol%]	0.00	0.00	0.00	0.00
O <sub>2</sub> [vol%]	20.82	20.95	13.05	17.06
SO <sub>2</sub> [vol%]	0.00	0.00	0.00	0.00

<i>Pyrolysegas, Rauchgas</i>	Pyrolysegas	Pyrolysegas wasserfrei	Rauchgas NBK	Rauchgas NBK wasserfrei
mittlere Molmasse [g/mol]	22.24	26.76	26.57	30.58
Heizwert $H_U$ [MJ/Nm <sup>3</sup> ]	6.99	14.47	0.00	0.00
Ar [vol%]	0.01	0.02	0.65	0.96
C <sub>2</sub> H <sub>4</sub> [vol%]	0.00	0.00	0.00	0.00
C <sub>2</sub> H <sub>6</sub> [vol%]	0.00	0.00	0.00	0.00
C <sub>3</sub> H <sub>8</sub> [vol%]	0.00	0.00	0.00	0.00
CH <sub>4</sub> [vol%]	12.29	25.42	0.00	0.00
CO [vol%]	16.38	33.89	0.00	0.00
CO <sub>2</sub> [vol%]	13.09	27.09	9.63	14.13
H <sub>2</sub> [vol%]	4.85	10.04	0.00	0.00
H <sub>2</sub> O [vol%]	51.67	---	31.89	---
H <sub>2</sub> S [vol%]	0.00	0.01	0.00	0.00
HCl [vol%]	0.00	0.00	0.00	0.00
HCN [vol%]	0.00	0.00	0.00	0.00
N <sub>2</sub> [vol%]	0.87	1.80	54.60	80.16
N <sub>2</sub> O [vol%]	0.00	0.00	0.00	0.00
NH <sub>3</sub> [vol%]	0.02	0.03	0.00	0.00
NO [vol%]	0.00	0.00	0.01	0.01
O <sub>2</sub> [vol%]	0.82	1.70	3.23	4.74
SO <sub>2</sub> [vol%]	0.001	0.00	0.00	0.00

## Prozessdaten Versuchsanlage Dürrrohr

Seite: 5

<i>Rauchgas</i>	Rauchgas Quench	Rauchgas Quench wasserfrei	Gasmix vor Desulf	Gasmix vor Desulf wasserfrei
mittlere Molmasse [g/mol]	24.17	30.58	23.90	30.58
Heizwert $H_U$ [MJ/Nm <sup>3</sup> ]	0.00	0.00	0.00	0.00
Ar [vol%]	0.47	0.96	0.45	0.96
C2H4 [vol%]	0.00	0.00	0.00	0.00
C2H6 [vol%]	0.00	0.00	0.00	0.00
C3H8 [vol%]	0.00	0.00	0.00	0.00
CH4 [vol%]	0.00	0.00	0.00	0.00
CO [vol%]	0.00	0.00	0.00	0.00
CO2 [vol%]	6.92	14.13	6.62	14.13
H2 [vol%]	0.00	0.00	0.00	0.00
H2O [vol%]	51.02	---	53.16	---
H2S [vol%]	0.00	0.00	0.00	0.00
HCl [vol%]	0.00	0.00	0.00	0.00
HCN [vol%]	0.00	0.00	0.00	0.00
N2 [vol%]	39.26	80.16	37.55	80.16
N2O [vol%]	0.00	0.00	0.00	0.00
NH3 [vol%]	0.00	0.00	0.00	0.00
NO [vol%]	0.01	0.01	0.01	0.01
O2 [vol%]	2.32	4.74	2.22	4.74
SO2 [vol%]	0.00	0.00	0.00	0.00

<i>Abgas</i>	Abgas	Abgas wasserfrei
mittlere Molmasse [g/mol]	23.56	30.58
Heizwert $H_U$ [MJ/Nm <sup>3</sup> ]	0.00	0.00
Ar [vol%]	0.42	0.96
C2H4 [vol%]	0.00	0.00
C2H6 [vol%]	0.00	0.00
C3H8 [vol%]	0.00	0.00
CH4 [vol%]	0.00	0.00
CO [vol%]	0.00	0.00
CO2 [vol%]	6.24	14.13
H2 [vol%]	0.00	0.00
H2O [vol%]	55.83	---
H2S [vol%]	0.00	0.00
HCl [vol%]	0.00	0.00
HCN [vol%]	0.00	0.00
N2 [vol%]	35.41	80.16
N2O [vol%]	0.00	0.00
NH3 [vol%]	0.00	0.00
NO [vol%]	0.01	0.01
O2 [vol%]	2.09	4.74
SO2 [vol%]	0.000	0.001

**Organische Zusammensetzungen (wasser- und aschefrei)**

	Biomasse	Pyrolysekoks	Teer
C [Gew%]	52.89	86.90	81.70
H [Gew%]	5.28	1.85	7.24
O [Gew%]	41.20	9.85	10.89
N [Gew%]	0.49	0.95	0.17
S [Gew%]	0.01	0.01	0.00
Cl [Gew%]	0.13	0.43	0.00
Heizwert $H_U$ (waf) [kJ/kg]	18965.10	31006.20	38489.50

**Zusammensetzungen Feststoffe**

	Asche Biomasse	Asche Desulf	Calciumhydroxid
Asche [Gew%]	100.00	100.00	0.00
K <sub>2</sub> O [Gew%]	0.00	0.00	0.00
MgO [Gew%]	0.00	0.00	0.00
CaO [Gew%]	0.00	0.00	0.00
SiO <sub>2</sub> [Gew%]	0.00	0.00	0.00
Olivin [Gew%]	0.00	0.00	0.00
CaCO <sub>3</sub> [Gew%]	0.00	0.00	0.00
Dolomit [Gew%]	0.00	0.00	0.00
CaSO <sub>4</sub> [Gew%]	0.00	---	0.00
CaOH <sub>2</sub> [Gew%]	0.00	---	100.00

**Prozessdaten Versuchsanlage Dürnrohr**

Seite: 1

**Ausgeglichene Lösung mit IPSEpro**
**Messwertbasis: 18.01.2010 14:40 - 14:50 (Stroh aus Lassee, Pyrolysetemperatur 550 °C)**
**Prozessbedingungen**

zugeführte Leistung DRO [kW]	120
BWL Brennkammer. [kW]	1688
Pyrolysegastemperatur [°C]	557

**Umgebungsbedingungen**

Seehöhe [m]	182
Temperatur [°C]	5.43
Luftdruck [mbar]	1013.25
Rel. Luftfeuchte [%]	60

**Kaltgaswirkungsgrad Pyrolysegas**

$\eta_{\text{chem}}$	0.46
----------------------	------

**Gasströme**

Luft, Pyrolysegas	Luft vor Gebläse	Luft vor Brennkammer	Pyrolysegas nach DRO	Pyrolysegas nach Pyrol.gasgebläse
Temperatur [°C]	5.4	118.5	557.4	641.4
Absolutdruck [bar]	1.01325	1.03025	1.01306	1.17248
Normvol.strom [Nm <sup>3</sup> /h]	1930	1930	355	355
Betr.vol.strom [m <sup>3</sup> /h]	1969	2722	1081	1028
Gasmassenstrom [kg/h]	2490	2490	354	354
Staubbelastung [g/Nm <sup>3</sup> ]	---	---	13.4	13.4
Flugkoksbelastung [g/Nm <sup>3</sup> ]	---	---	3.4	3.4
Teerbelastung [g/Nm <sup>3</sup> ]	---	---	81.0	81.0
Gesamtmassenstrom [kg/h]	2490	2490	389	389
Energiestrom [kW]	3.9	83.0	1132.6	1150.3
Zusammensetzung Gas	Umgebungsluft	Umgebungsluft	Pyrolysegas	Pyrolysegas
Zusammensetzung Staub	---	---	Asche Biomasse	Asche Biomasse
Zusammensetzung Flugkoks	---	---	Pyrolysekoks	Pyrolysekoks
Zusammensetzung Teer	---	---	Teer	Teer

Rauchgas, Heißgas, Kaltgas	Luft + Rezigas zu Brennkammer	Heißgas vor DRO	Kaltgas nach DRO	Kaltgas nach Kaltgasgebläse
Temperatur [°C]	143.0	812.2	669.7	551.0
Absolutdruck [bar]	1.03025	1.01248	1.00723	1.07248
Normvol.strom [Nm <sup>3</sup> /h]	3266.7	2548.1	2548.1	2548.1
Betr.vol.strom [m <sup>3</sup> /h]	4895.3	10132.8	8847.9	7263.8
Gasmassenstrom [kg/h]	3895.6	3009.4	3009.4	3009.4
Staubbelastung [g/Nm <sup>3</sup> ]	---	1.30	1.30	1.30
Gesamtmassenstrom [kg/h]	3895.6	3012.7	3012.7	3012.7
Energiestrom [kW]	186.5	898.8	729.1	592.1
Zusammensetzung Gas	Verbr.luftmix	Rauchgas NBK	Rauchgas NBK	Rauchgas NBK
Zusammensetzung Staub	---	Asche Biomasse	Asche Biomasse	Asche Biomasse

Rauchgas, Rauchgas Rezigas mix	Rauchgas nach Brennkammer	Rauchgas vor Sprühkühler	Rauchgas nach Sprühkühler	Rauchgas + Rezigas vor Sprühabsorber
Temperatur [°C]	941.6	941.6	370.2	281.8
Absolutdruck [bar]	1.01248	1.01248	1.01200	1.01200
Normvol.strom [Nm <sup>3</sup> /h]	6211.8	3663.7	5031.2	9278.5
Betr.vol.strom [m <sup>3</sup> /h]	27646.0	16305.4	11864.3	18873.0
Gasmassenstrom [kg/h]	7336.3	4326.9	5426.0	9894.8
Staubbelastung [g/Nm <sup>3</sup> ]	1.30	1.30	0.95	0.51
Gesamtmassenstrom [kg/h]	7344.4	4331.7	5430.8	9899.6
Energiestrom [kW]	2577.2	1520.0	799.6	1128.7
Zusammensetzung Gas	Rauchgas NBK	Rauchgas NBK	Rauchgas Quench	Gasmix vor Desulf
Zusammensetzung Staub	Asche Biomasse	Asche Biomasse	Asche Biomasse	Asche/Kalk mix

<b>Prozessdaten Versuchsanlage Dürnrohr</b>	<i>Seite: 2</i>
---------------------------------------------	-----------------

<i>Rauchgas, Erdgas</i>	Rauchgas nach Sprühabsorber	Abgas nach Gewebefilter	Abgas durch Kamin	Erdgas
Temperatur [°C]	196.1	137.0	142.5	20.0
Absolutdruck [bar]	1.00923	0.99879	1.01325	2.00
Normvol.strom [Nm <sup>3</sup> /h]	9811.5	9811.5	4222.2	66.3
Betr.vol.strom [m <sup>3</sup> /h]	16924.0	14946.6	6424.9	36.0
Gasmassenstrom [kg/h]	10323.3	10323.3	4442.5	47.4
Staubbeladung [g/Nm <sup>3</sup> ]	0.49	0.00	0.00	---
Gesamtmassenstrom [kg/h]	10328.0	10323.3	4442.5	47.4
Energiestrom [kW]	847.9	609.5	271.7	659.3
Zusammensetzung Gas	Abgas	Abgas	Abgas	Erdgas
Zusammensetzung Staub	Asche Desulf	---	---	---

<i>Rezigas</i>	Rezigas gesamt	Rezigas zu DRO	Rezigas zu Brennkammer	Rezigas zu Sprühabsorber
Temperatur [°C]	151.9	174.5	174.5	174.5
Absolutdruck [bar]	1.01325	1.03026	1.03026	1.03026
Normvol.strom [Nm <sup>3</sup> /h]	5589.3	5.7	1336.3	4247.3
Betr.vol.strom [m <sup>3</sup> /h]	8698.2	9.2	2154.1	6846.4
Gasmassenstrom [kg/h]	5880.8	6.0	1406.0	4468.8
Staub [g/Nm <sup>3</sup> ]	0.00	0.00	0.00	0.00
Gesamtmassenstrom [kg/h]	5880.8	6.0	1406.0	4468.8
Energiestrom [kW]	381.3	0.4	103.5	329.1
Zusammensetzung Gas	Abgas	Abgas	Abgas	Abgas
Zusammensetzung Staub	---	---	---	Calciumhydroxid

**Biomasse und Pyrolysekoks**

<i>Biomasse, Koks</i>	Biomasse	Pyrolysekoks
Temperatur [°C]	6.9	504.1
Absolutdruck [bar]	1.01306	1.01306
Dichte [kg/m <sup>3</sup> ]	300.0	300.0
Massenstrom [kg/h]	543.7	161.1
Heizwert (wf) [kJ/kg]	16392.9	27846.6
Heizwert [kJ/kg]	14703.0	27846.6
Wassergehalt [Gew. %]	8.97	0.00
Aschegehalt [Gew. % wf]	5.02	12.45
Energiestrom [kW]	2222.0	1276.2
Zusammensetzung org.	Biomasse	Pyrolysekoks
Zusammensetzung anorg.	Asche Biomasse	Asche Biomasse

**Feststoffströme**

	Kalk für Entschwefelung	Gewebefilter Abreinigung
Temperatur [°C]	25.0	137.0
Koksbeladung [kg/kg_anorg.]	0.00	0.00
Massenstrom [kg/h]	0.00	4.78
Energiestrom [kW]	0.00	0.14
Zusammensetzung Organisch	---	---
Zusammensetzung Anorg.	Calciumhydroxid	Asche Desulf

<b>Prozessdaten Versuchsanlage Dürnrohr</b>	<i>Seite: 3</i>
---------------------------------------------	-----------------

**Wasserströme**

<i>Sprühabsorber und Sprühkühler</i>	Wasser für Sprühkühler	Wasser für Sprühabsorber
Temperatur [°C]	20.0	20.0
Absolutdruck [bar]	2.0	2.0
Enthalpie [kJ/kg]	-15886.8	-15886.8
Betr.vol.strom [m <sup>3</sup> /h]	1.1	0.4
Massenstrom [kg/h]	1099.1	428.4
Energiestrom [kW]	-720.1	-280.7

**Apparate****Nachbrennkammer**

Druckverlust Rauchgas [mbar]	50	Luftzahl $\lambda$ [-]	1.62
Druckverlust Luft [mbar]	18	CO-Schlupf [mol <sub>CO</sub> /mol <sub>CO2</sub> ]	0.0000
		Therm. Leistg. [kW]	1688.4

**Drehrohrreaktor**

Druckverlust Heißgas [mbar]	5.25	zugeführte Leistung über Heißgas [kW]	120
Pyrolysetemperatur [°C]	557	Umgesetzter C in Gas und Teer [%]	45.42
Teer in PG [kg/kg_tr.BSt]	0.06	Exergieverlust [kW]	148.13
Staub in PG [kg/kg_tr.BSt]	0.19		
Flugkoks in PG [kg/kg_tr.BSt]	0.00		

**Sprühkühler**

Druckverlust Gas [mbar]	0.48	Exergieverlust [kW]	462.9
-------------------------	------	---------------------	-------

**Sprühabsorber**

Druckverlust Gas [mbar]	2.77	Exergieverlust [kW]	84.2
Umsatz von CaOH <sub>2</sub> [%]	70.0	Desulfurisation reaction rate [kmol/h]	4.70692E-27

**Gewebefilter**

Druckverlust Gas [mbar]	10.44	rel Wärmeverlust [%]	30.6
Diff.Temp.Austritt [°C]	59.1	Wärmeverlust [kW]	238.2
Abscheidegrad Staub [%]	100.0	Exergieverlust [kW]	79.6

**Exergieflüsse DRO**

Exergie Biomasse [kW]	2427.65
Exergie Heißgas [kW]	528.1
Exergie Rezigas [kW]	0.3
<hr/>	
Exergie Pyrolysegas[kW]	1106.8
Exergie Pyrolysekoks [kW]	1293.2
Exergie Kaltgas [kW]	408.0

<b>Prozessdaten Versuchsanlage Dürrohr</b>	<i>Seite: 4</i>
--------------------------------------------	-----------------

**Zusammensetzungen Gasströme**

<i>Luft und Verbrennungsluftmix</i>	Umgebungsluft	Umgebungsluft wasserfrei	Verbrennungsluftmix	Verbrennungsluftmix wasserfrei
mittlere Molmasse [g/mol]	28.91	28.97	26.73	29.35
Heizwert $H_U$ [MJ/Nm <sup>3</sup> ]	0.00	0.00	0.00	0.00
Ar [vol%]	0.93	0.93	0.72	0.94
C2H4 [vol%]	0.00	0.00	0.00	0.00
C2H6 [vol%]	0.00	0.00	0.00	0.00
C3H8 [vol%]	0.00	0.00	0.00	0.00
CH4 [vol%]	0.00	0.00	0.00	0.00
CO [vol%]	0.00	0.00	0.00	0.00
CO2 [vol%]	0.04	0.04	2.59	3.36
H2 [vol%]	0.00	0.00	0.00	0.00
H2O [vol%]	0.53	---	23.09	---
H2S [vol%]	0.00	0.00	0.00	0.00
HCl [vol%]	0.00	0.00	0.00	0.00
HCN [vol%]	0.00	0.00	0.00	0.00
N2 [vol%]	77.67	78.08	60.43	78.57
N2O [vol%]	0.00	0.00	0.00	0.00
NH3 [vol%]	0.00	0.00	0.00	0.00
NO [vol%]	0.00	0.00	0.00	0.00
O2 [vol%]	20.84	20.95	13.17	17.12
SO2 [vol%]	0.00	0.00	0.00	0.00

<i>Pyrolysegas, Rauchgas</i>	Pyrolysegas	Pyrolysegas wasserfrei	Rauchgas NBK	Rauchgas NBK wasserfrei
mittlere Molmasse [g/mol]	22.31	26.71	26.47	30.58
Heizwert $H_U$ [MJ/Nm <sup>3</sup> ]	7.20	14.57	0.00	0.00
Ar [vol%]	0.01	0.01	0.65	0.96
C2H4 [vol%]	0.00	0.00	0.00	0.00
C2H6 [vol%]	0.00	0.00	0.00	0.00
C3H8 [vol%]	0.00	0.00	0.00	0.00
CH4 [vol%]	12.69	25.67	0.00	0.00
CO [vol%]	16.79	33.96	0.00	0.00
CO2 [vol%]	13.35	27.01	9.52	14.15
H2 [vol%]	4.97	10.06	0.00	0.00
H2O [vol%]	50.57	---	32.70	---
H2S [vol%]	0.00	0.01	0.00	0.00
HCl [vol%]	0.00	0.00	0.00	0.00
HCN [vol%]	0.00	0.00	0.00	0.00
N2 [vol%]	0.76	1.54	53.95	80.17
N2O [vol%]	0.00	0.00	0.00	0.00
NH3 [vol%]	0.02	0.03	0.00	0.00
NO [vol%]	0.00	0.00	0.01	0.01
O2 [vol%]	0.84	1.70	3.17	4.71
SO2 [vol%]	0.001	0.00	0.00	0.00

## Prozessdaten Versuchsanlage Dürnrohr

Seite: 5

<i>Rauchgas</i>	Rauchgas Quench	Rauchgas Quench wasserfrei	Gasmix vor Desulf	Gasmix vor Desulf wasserfrei
mittlere Molmasse [g/mol]	24.17	30.58	23.90	30.58
Heizwert $H_U$ [MJ/Nm <sup>3</sup> ]	0.00	0.00	0.00	0.00
Ar [vol%]	0.47	0.96	0.45	0.96
C2H4 [vol%]	0.00	0.00	0.00	0.00
C2H6 [vol%]	0.00	0.00	0.00	0.00
C3H8 [vol%]	0.00	0.00	0.00	0.00
CH4 [vol%]	0.00	0.00	0.00	0.00
CO [vol%]	0.00	0.00	0.00	0.00
CO2 [vol%]	6.94	14.15	6.63	14.15
H2 [vol%]	0.00	0.00	0.00	0.00
H2O [vol%]	50.99	---	53.14	---
H2S [vol%]	0.00	0.00	0.00	0.00
HCl [vol%]	0.00	0.00	0.00	0.00
HCN [vol%]	0.00	0.00	0.00	0.00
N2 [vol%]	39.29	80.17	37.57	80.17
N2O [vol%]	0.00	0.00	0.00	0.00
NH3 [vol%]	0.00	0.00	0.00	0.00
NO [vol%]	0.00	0.01	0.00	0.01
O2 [vol%]	2.31	4.71	2.21	4.71
SO2 [vol%]	0.00	0.00	0.00	0.00

<i>Abgas</i>	Abgas	Abgas wasserfrei
mittlere Molmasse [g/mol]	23.58	30.58
Heizwert $H_U$ [MJ/Nm <sup>3</sup> ]	0.00	0.00
Ar [vol%]	0.42	0.96
C2H4 [vol%]	0.00	0.00
C2H6 [vol%]	0.00	0.00
C3H8 [vol%]	0.00	0.00
CH4 [vol%]	0.00	0.00
CO [vol%]	0.00	0.00
CO2 [vol%]	6.27	14.15
H2 [vol%]	0.00	0.00
H2O [vol%]	55.69	---
H2S [vol%]	0.00	0.00
HCl [vol%]	0.00	0.00
HCN [vol%]	0.00	0.00
N2 [vol%]	35.53	80.17
N2O [vol%]	0.00	0.00
NH3 [vol%]	0.00	0.00
NO [vol%]	0.00	0.01
O2 [vol%]	2.09	4.71
SO2 [vol%]	0.000	0.001

**Organische Zusammensetzungen (wasser- und aschefrei)**

	Biomasse	Pyrolysekoks	Teer
C [Gew%]	49.15	88.66	81.86
H [Gew%]	5.28	1.85	7.20
O [Gew%]	44.94	8.10	10.76
N [Gew%]	0.49	0.95	0.17
S [Gew%]	0.01	0.01	0.00
Cl [Gew%]	0.13	0.43	0.00
Heizwert $H_U$ (waf) [kJ/kg]	17258.90	31806.90	38489.50



**Zusammensetzungen Feststoffe**

	Asche Biomasse	Asche Desulf	Calciumhydroxid
Asche [Gew%]	100.00	100.00	0.00
K <sub>2</sub> O [Gew%]	0.00	0.00	0.00
MgO [Gew%]	0.00	0.00	0.00
CaO [Gew%]	0.00	0.00	0.00
SiO <sub>2</sub> [Gew%]	0.00	0.00	0.00
Olivin [Gew%]	0.00	0.00	0.00
CaCO <sub>3</sub> [Gew%]	0.00	0.00	0.00
Dolomit [Gew%]	0.00	0.00	0.00
CaSO <sub>4</sub> [Gew%]	0.00	---	0.00
CaOH <sub>2</sub> [Gew%]	0.00	---	100.00

**Prozessdaten Versuchsanlage Dürnrohr**

Seite: 1

**Ausgeglichene Lösung mit IPSEpro**
**Messwertbasis: 21.01.2010 10:00 - 10:10 (Stroh aus Lassee, Pyrolysetemperatur 600 °C)**
**Prozessbedingungen**

zugeführte Leistung DRO [kW]	141
BWL Brennkammer. [kW]	1263
Pyrolysegastemperatur [°C]	596

**Umgebungsbedingungen**

Seehöhe [m]	182
Temperatur [°C]	1.07
Luftdruck [mbar]	1013.25
Rel. Luftfeuchte [%]	60

**Kaltgaswirkungsgrad Pyrolysegas**

$\eta_{\text{chem}}$	0.50
----------------------	------

**Gasströme**

Luft, Pyrolysegas	Luft vor Gebläse	Luft vor Brennkammer	Pyrolysegas nach DRO	Pyrolysegas nach Pyrol.gasgebläse
Temperatur [°C]	1.1	140.0	596.4	640.3
Absolutdruck [bar]	1.01325	1.03024	1.01305	1.17297
Normvol.strom [Nm³/h]	1408	1408	337	337
Betr.vol.strom [m³/h]	1413	2094	1073	974
Gasmassenstrom [kg/h]	1816	1816	355	355
Staubbelastung [g/Nm³]	---	---	5.4	5.4
Flugkoksbelastung [g/Nm³]	---	---	15.7	15.7
Teerbelastung [g/Nm³]	---	---	78.4	78.4
Gesamtmassenstrom [kg/h]	1816	1816	389	389
Energiestrom [kW]	0.6	71.4	1367.2	1376.3
Zusammensetzung Gas	Umgebungsluft	Umgebungsluft	Pyrolysegas	Pyrolysegas
Zusammensetzung Staub	---	---	Asche Biomasse	Asche Biomasse
Zusammensetzung Flugkoks	---	---	Pyrolysekoks	Pyrolysekoks
Zusammensetzung Teer	---	---	Teer	Teer

Rauchgas, Heißgas, Kaltgas	Luft + Rezigas zu Brennkammer	Heißgas vor DRO	Kaltgas nach DRO	Kaltgas nach Kaltgasgebläse
Temperatur [°C]	150.5	862.7	732.6	591.1
Absolutdruck [bar]	1.03024	1.01297	1.00783	1.07297
Normvol.strom [Nm³/h]	2095.6	3150.9	3150.9	3150.9
Betr.vol.strom [m³/h]	3196.4	13106.1	11664.2	9414.5
Gasmassenstrom [kg/h]	2563.0	3876.6	3876.6	3876.6
Staubbelastung [g/Nm³]	---	0.77	0.77	0.77
Gesamtmassenstrom [kg/h]	2563.0	3879.0	3879.0	3879.0
Energiestrom [kW]	123.1	1188.9	994.5	789.1
Zusammensetzung Gas	Verbr.luftmix	Rauchgas NBK	Rauchgas NBK	Rauchgas NBK
Zusammensetzung Staub	---	Asche Biomasse	Asche Biomasse	Asche Biomasse

Rauchgas, Rauchgas Rezigas mix	Rauchgas nach Brennkammer	Rauchgas vor Sprühkühler	Rauchgas nach Sprühkühler	Rauchgas + Rezigas vor Sprühabsorber
Temperatur [°C]	932.1	932.1	370.6	263.9
Absolutdruck [bar]	1.01297	1.01297	1.01265	1.01265
Normvol.strom [Nm³/h]	5548.6	2397.7	3279.3	7084.0
Betr.vol.strom [m³/h]	24489.5	10582.4	7732.5	13935.4
Gasmassenstrom [kg/h]	6826.5	2949.9	3658.5	7787.5
Staubbelastung [g/Nm³]	0.77	0.77	0.56	0.26
Gesamtmassenstrom [kg/h]	6830.7	2951.7	3660.3	7789.4
Energiestrom [kW]	2279.8	985.1	520.7	806.1
Zusammensetzung Gas	Rauchgas NBK	Rauchgas NBK	Rauchgas Quench	Gasmix vor Desulf
Zusammensetzung Staub	Asche Biomasse	Asche Biomasse	Asche Biomasse	Asche/Kalk mix

## Prozessdaten Versuchsanlage Dürnrohr

Seite: 2

<i>Rauchgas, Erdgas</i>	Rauchgas nach Sprühabsorber	Abgas nach Gewebefilter	Abgas durch Kamin	Erdgas
Temperatur [°C]	189.7	163.9	135.5	20.0
Absolutdruck [bar]	1.01027	1.00281	1.01325	2.00
Normvol.strom [Nm³/h]	7437.8	7437.8	2939.3	0.2
Betr.vol.strom [m³/h]	12640.3	12025.8	4397.1	0.1
Gasmassenstrom [kg/h]	8071.9	8071.9	3189.9	0.2
Staubbelastung [g/Nm³]	0.25	0.00	0.00	---
Gesamtmassenstrom [kg/h]	8073.8	8071.9	3189.9	0.2
Energiestrom [kW]	619.7	540.6	179.4	2.1
Zusammensetzung Gas	Abgas	Abgas	Abgas	Erdgas
Zusammensetzung Staub	Asche Desulf	---	---	---

<i>Rezigas</i>	Rezigas gesamt	Rezigas zu DRO	Rezigas zu Brennkammer	Rezigas zu Sprühabsorber
Temperatur [°C]	169.6	169.6	169.6	169.6
Absolutdruck [bar]	1.01325	1.03025	1.03025	1.03025
Normvol.strom [Nm³/h]	4498.5	5.7	688.1	3804.7
Betr.vol.strom [m³/h]	7291.9	9.1	1096.9	6065.4
Gasmassenstrom [kg/h]	4882.0	6.2	746.7	4129.1
Staub [g/Nm³]	0.00	0.00	0.00	0.00
Gesamtmassenstrom [kg/h]	4882.0	6.2	746.7	4129.1
Energiestrom [kW]	337.5	0.4	51.6	285.4
Zusammensetzung Gas	Abgas	Abgas	Abgas	Abgas
Zusammensetzung Staub	---	---	---	Calciumhydroxid

**Biomasse und Pyrolysekoks**

<i>Biomasse, Koks</i>	Biomasse	Pyrolysekoks
Temperatur [°C]	3.0	538.6
Absolutdruck [bar]	1.01305	1.01305
Dichte [kg/m³]	300.0	300.0
Massenstrom [kg/h]	546.8	164.5
Heizwert (wf) [kJ/kg]	17705.2	26891.6
Heizwert [kJ/kg]	15929.3	26891.6
Wassergehalt [Gew. %]	8.81	0.00
Aschegehalt [Gew. % wf]	4.79	13.40
Energiestrom [kW]	2420.2	1261.9
Zusammensetzung org.	Biomasse	Pyrolysekoks
Zusammensetzung anorg.	Asche Biomasse	Asche Biomasse

**Feststoffströme**

	Kalk für Entschwefelung	Gewebefilter Abreinigung
Temperatur [°C]	25.0	163.9
Koksbelastung [kg/kg_anorg.]	0.00	0.00
Massenstrom [kg/h]	0.00	1.84
Energiestrom [kW]	0.00	0.07
Zusammensetzung Organisch	---	---
Zusammensetzung Anorg.	Calciumhydroxid	Asche Desulf

<b>Prozessdaten Versuchsanlage Dürrohr</b>	<i>Seite: 3</i>
--------------------------------------------	-----------------

**Wasserströme**

<i>Sprühabsorber und Sprühkühler</i>	Wasser für Sprühkühler	Wasser für Sprühabsorber
Temperatur [°C]	20.0	20.0
Absolutdruck [bar]	2.0	2.0
Enthalpie [kJ/kg]	-15886.8	-15886.8
Betr.vol.strom [m <sup>3</sup> /h]	0.7	0.3
Massenstrom [kg/h]	708.6	284.4
Energiestrom [kW]	-464.2	-186.3

**Apparate****Nachbrennkammer**

Druckverlust Rauchgas [mbar]	50	Luftzahl $\lambda$ [-]	1.87
Druckverlust Luft [mbar]	17	CO-Schlupf [mol <sub>CO</sub> /mol <sub>CO2</sub> ]	0.0000
		Therm. Leistg. [kW]	1262.8

**Drehrohrreaktor**

Druckverlust Heißgas [mbar]	5.14	zugeführte Leistung über Heißgas [kW]	141
Pyrolysetemperatur [°C]	596	Umgesetzter C in Gas und Teer [%]	49.44
Teer in PG [kg/kg_tr.BSt]	0.06	Exergieverlust [kW]	136.55
Staub in PG [kg/kg_tr.BSt]	0.08		
Flugkoks in PG [kg/kg_tr.BSt]	0.01		

**Sprühkühler**

Druckverlust Gas [mbar]	0.33	Exergieverlust [kW]	301.2
-------------------------	------	---------------------	-------

**Sprühabsorber**

Druckverlust Gas [mbar]	2.38	Exergieverlust [kW]	53.6
Umsatz von CaOH <sub>2</sub> [%]	70.0	Desulfurisation reaction rate [kmol/h]	8.79858E-29

**Gewebefilter**

Druckverlust Gas [mbar]	7.45	rel Wärmeverlust [%]	13.9
Diff.Temp.Austritt [°C]	25.7	Wärmeverlust [kW]	79.0
Abscheidegrad Staub [%]	100.0	Exergieverlust [kW]	28.3

**Exergieflüsse DRO**

Exergie Biomasse [kW]	2608.94
Exergie Heißgas [kW]	707.9
Exergie Rezigas [kW]	0.3
Exergie Pyrolysegas[kW]	1333.6
Exergie Pyrolysekoks [kW]	1279.8
Exergie Kaltgas [kW]	567.2

## Prozessdaten Versuchsanlage Dürnrohr

Seite: 4

## Zusammensetzungen Gasströme

<i>Luft und Verbrennungsluftmix</i>	Umgebungsluft	Umgebungsluft wasserfrei	Verbrennungsluftmix	Verbrennungsluftmix wasserfrei
mittlere Molmasse [g/mol]	28.92	28.97	27.41	29.37
Heizwert $H_U$ [MJ/Nm <sup>3</sup> ]	0.00	0.00	0.00	0.00
Ar [vol%]	0.93	0.93	0.77	0.93
C2H4 [vol%]	0.00	0.00	0.00	0.00
C2H6 [vol%]	0.00	0.00	0.00	0.00
C3H8 [vol%]	0.00	0.00	0.00	0.00
CH4 [vol%]	0.00	0.00	0.00	0.00
CO [vol%]	0.00	0.00	0.00	0.00
CO2 [vol%]	0.04	0.04	2.75	3.32
H2 [vol%]	0.00	0.00	0.00	0.00
H2O [vol%]	0.39	---	17.21	---
H2S [vol%]	0.00	0.00	0.00	0.00
HCl [vol%]	0.00	0.00	0.00	0.00
HCN [vol%]	0.00	0.00	0.00	0.00
N2 [vol%]	77.78	78.08	64.48	77.88
N2O [vol%]	0.00	0.00	0.00	0.00
NH3 [vol%]	0.00	0.00	0.00	0.00
NO [vol%]	0.00	0.00	0.00	0.00
O2 [vol%]	20.87	20.95	14.79	17.86
SO2 [vol%]	0.00	0.00	0.00	0.00

<i>Pyrolysegas, Rauchgas</i>	Pyrolysegas	Pyrolysegas wasserfrei	Rauchgas NBK	Rauchgas NBK wasserfrei
mittlere Molmasse [g/mol]	23.60	26.42	27.58	31.06
Heizwert $H_U$ [MJ/Nm <sup>3</sup> ]	9.95	14.97	0.00	0.00
Ar [vol%]	0.01	0.01	0.68	0.92
C2H4 [vol%]	0.00	0.00	0.00	0.00
C2H6 [vol%]	0.00	0.00	0.00	0.00
C3H8 [vol%]	0.00	0.00	0.00	0.00
CH4 [vol%]	17.89	26.91	0.00	0.00
CO [vol%]	22.26	33.48	0.00	0.00
CO2 [vol%]	17.55	26.39	12.56	17.14
H2 [vol%]	6.80	10.23	0.00	0.00
H2O [vol%]	33.52	---	26.71	---
H2S [vol%]	0.01	0.01	0.00	0.00
HCl [vol%]	0.00	0.00	0.00	0.00
HCN [vol%]	0.00	0.00	0.00	0.00
N2 [vol%]	0.82	1.24	56.47	77.05
N2O [vol%]	0.00	0.00	0.00	0.00
NH3 [vol%]	0.02	0.03	0.00	0.00
NO [vol%]	0.00	0.00	0.01	0.02
O2 [vol%]	1.13	1.70	3.57	4.87
SO2 [vol%]	0.001	0.00	0.00	0.00

## Prozessdaten Versuchsanlage Dürnrohr

Seite: 5

<i>Rauchgas</i>	Rauchgas Quench	Rauchgas Quench wasserfrei	Gasmix vor Desulf	Gasmix vor Desulf wasserfrei
mittlere Molmasse [g/mol]	25.01	31.06	24.64	31.06
Heizwert $H_U$ [MJ/Nm <sup>3</sup> ]	0.00	0.00	0.00	0.00
Ar [vol%]	0.49	0.92	0.47	0.92
C2H4 [vol%]	0.00	0.00	0.00	0.00
C2H6 [vol%]	0.00	0.00	0.00	0.00
C3H8 [vol%]	0.00	0.00	0.00	0.00
CH4 [vol%]	0.00	0.00	0.00	0.00
CO [vol%]	0.00	0.00	0.00	0.00
CO2 [vol%]	9.19	17.14	8.70	17.14
H2 [vol%]	0.00	0.00	0.00	0.00
H2O [vol%]	46.41	---	49.21	---
H2S [vol%]	0.00	0.00	0.00	0.00
HCl [vol%]	0.00	0.00	0.00	0.00
HCN [vol%]	0.00	0.00	0.00	0.00
N2 [vol%]	41.29	77.05	39.13	77.05
N2O [vol%]	0.00	0.00	0.00	0.00
NH3 [vol%]	0.00	0.00	0.00	0.00
NO [vol%]	0.01	0.02	0.01	0.02
O2 [vol%]	2.61	4.87	2.47	4.87
SO2 [vol%]	0.00	0.00	0.00	0.00

<i>Abgas</i>	Abgas	Abgas wasserfrei
mittlere Molmasse [g/mol]	24.33	31.06
Heizwert $H_U$ [MJ/Nm <sup>3</sup> ]	0.00	0.00
Ar [vol%]	0.45	0.92
C2H4 [vol%]	0.00	0.00
C2H6 [vol%]	0.00	0.00
C3H8 [vol%]	0.00	0.00
CH4 [vol%]	0.00	0.00
CO [vol%]	0.00	0.00
CO2 [vol%]	8.29	17.14
H2 [vol%]	0.00	0.00
H2O [vol%]	51.63	---
H2S [vol%]	0.00	0.00
HCl [vol%]	0.00	0.00
HCN [vol%]	0.00	0.00
N2 [vol%]	37.27	77.05
N2O [vol%]	0.00	0.00
NH3 [vol%]	0.00	0.00
NO [vol%]	0.01	0.02
O2 [vol%]	2.36	4.87
SO2 [vol%]	0.001	0.002

**Organische Zusammensetzungen (wasser- und aschefrei)**

	Biomasse	Pyrolysekoks	Teer
C [Gew%]	53.51	86.96	81.82
H [Gew%]	4.66	1.87	7.28
O [Gew%]	41.20	9.77	10.73
N [Gew%]	0.49	0.96	0.17
S [Gew%]	0.01	0.01	0.00
Cl [Gew%]	0.13	0.43	0.00
Heizwert $H_U$ (waf) [kJ/kg]	18595.60	31053.00	38489.50

## Prozessdaten Versuchsanlage Dürnrohr

Seite: 6

**Zusammensetzungen Feststoffe**

	Asche Biomasse	Asche Desulf	Calciumhydroxid
Asche [Gew%]	100.00	100.00	0.00
K <sub>2</sub> O [Gew%]	0.00	0.00	0.00
MgO [Gew%]	0.00	0.00	0.00
CaO [Gew%]	0.00	0.00	0.00
SiO <sub>2</sub> [Gew%]	0.00	0.00	0.00
Olivin [Gew%]	0.00	0.00	0.00
CaCO <sub>3</sub> [Gew%]	0.00	0.00	0.00
Dolomit [Gew%]	0.00	0.00	0.00
CaSO <sub>4</sub> [Gew%]	0.00	---	0.00
CaOH <sub>2</sub> [Gew%]	0.00	---	100.00

**Prozessdaten Versuchsanlage Dürnrohr**

Seite: 1

**Ausgeglichene Lösung mit IPSEpro**
**Messwertbasis: 25.08.2009 11:40 - 11:50 (Stroh aus Lassee, Verweilzeitvariation 20%)**
**Prozessbedingungen**

zugeführte Leistung DRO [kW]	143
BWL Brennkammer. [kW]	1365
Pyrolysegastemperatur [°C]	553

**Umgebungsbedingungen**

Seehöhe [m]	182
Temperatur [°C]	27.12
Luftdruck [mbar]	1013.25
Rel. Luftfeuchte [%]	60

**Kaltgaswirkungsgrad Pyrolysegas**

$\eta_{\text{chem}}$	0.54
----------------------	------

**Gasströme**

Luft, Pyrolysegas	Luft vor Gebläse	Luft vor Brennkammer	Pyrolysegas nach DRO	Pyrolysegas nach Pyrol.gasgebläse
Temperatur [°C]	27.1	120.4	552.9	642.7
Absolutdruck [bar]	1.01325	1.03025	1.01306	1.17225
Normvol.strom [Nm <sup>3</sup> /h]	1465	1465	408	408
Betr.vol.strom [m <sup>3</sup> /h]	1611	2076	1234	1182
Gasmassenstrom [kg/h]	1879	1879	406	406
Staubbeladung [g/Nm <sup>3</sup> ]	---	---	7.7	7.7
Flugkoksbeladung [g/Nm <sup>3</sup> ]	---	---	14.6	14.6
Teerbeladung [g/Nm <sup>3</sup> ]	---	---	149.5	149.5
Gesamtmassenstrom [kg/h]	1879	1879	476	476
Energiestrom [kW]	14.8	64.4	1487.4	1510.2
Zusammensetzung Gas	Umgebungsluft	Umgebungsluft	Pyrolysegas	Pyrolysegas
Zusammensetzung Staub	---	---	Asche Biomasse	Asche Biomasse
Zusammensetzung Flugkoks	---	---	Pyrolysekoks	Pyrolysekoks
Zusammensetzung Teer	---	---	Teer	Teer

Rauchgas, Heißgas, Kaltgas	Luft + Rezigas zu Brennkammer	Heißgas vor DRO	Kaltgas nach DRO	Kaltgas nach Kaltgasgebläse
Temperatur [°C]	148.6	816.4	673.2	572.3
Absolutdruck [bar]	1.03025	1.01225	1.00702	1.07225
Normvol.strom [Nm <sup>3</sup> /h]	3011.7	2968.9	2968.9	2968.9
Betr.vol.strom [m <sup>3</sup> /h]	4573.7	11854.4	10349.3	8683.8
Gasmassenstrom [kg/h]	3504.2	3459.1	3459.1	3459.1
Staubbeladung [g/Nm <sup>3</sup> ]	---	0.92	0.92	0.92
Gesamtmassenstrom [kg/h]	3504.2	3461.8	3461.8	3461.8
Energiestrom [kW]	183.7	1068.3	866.4	728.5
Zusammensetzung Gas	Verbr.luftmix	Rauchgas NBK	Rauchgas NBK	Rauchgas NBK
Zusammensetzung Staub	---	Asche Biomasse	Asche Biomasse	Asche Biomasse

Rauchgas, Rauchgas Rezigas mix	Rauchgas nach Brennkammer	Rauchgas vor Sprühkühler	Rauchgas nach Sprühkühler	Rauchgas + Rezigas vor Sprühabsorber
Temperatur [°C]	847.6	847.6	370.4	295.7
Absolutdruck [bar]	1.01225	1.01225	1.01194	1.01194
Normvol.strom [Nm <sup>3</sup> /h]	6382.5	3413.6	4480.9	7265.1
Betr.vol.strom [m <sup>3</sup> /h]	26213.1	14019.7	10571.4	15149.5
Gasmassenstrom [kg/h]	7436.3	3977.2	4835.0	7762.2
Staubbeladung [g/Nm <sup>3</sup> ]	0.92	0.92	0.70	0.43
Gesamtmassenstrom [kg/h]	7442.2	3980.4	4838.2	7765.4
Energiestrom [kW]	2392.9	1279.8	717.5	932.4
Zusammensetzung Gas	Rauchgas NBK	Rauchgas NBK	Rauchgas Quench	Gasmix vor Desulf
Zusammensetzung Staub	Asche Biomasse	Asche Biomasse	Asche Biomasse	Asche/Kalk mix



<b>Prozessdaten Versuchsanlage Dürnrohr</b>	<i>Seite: 2</i>
---------------------------------------------	-----------------

<i>Rauchgas, Erdgas</i>	Rauchgas nach Sprühabsorber	Abgas nach Gewebefilter	Abgas durch Kamin	Erdgas
Temperatur [°C]	193.9	185.8	123.2	20.0
Absolutdruck [bar]	1.01101	1.00510	1.01325	2.00
Normvol.strom [Nm³/h]	7765.9	7765.9	3327.6	0.0
Betr.vol.strom [m³/h]	13307.2	13153.8	4828.7	0.0
Gasmassenstrom [kg/h]	8164.8	8164.8	3498.5	0.0
Staubbelastung [g/Nm³]	0.40	0.00	0.00	---
Gesamtmassenstrom [kg/h]	8167.9	8164.8	3498.5	0.0
Energiestrom [kW]	668.5	642.3	189.6	0.0
Zusammensetzung Gas	Abgas	Abgas	Abgas	Erdgas
Zusammensetzung Staub	Asche Desulf	---	---	---

<i>Rezigas</i>	Rezigas gesamt	Rezigas zu DRO	Rezigas zu Brennkammer	Rezigas zu Sprühabsorber
Temperatur [°C]	187.3	172.4	172.4	172.4
Absolutdruck [bar]	1.01325	1.03026	1.03026	1.03026
Normvol.strom [Nm³/h]	4438.3	107.9	1546.2	2784.2
Betr.vol.strom [m³/h]	7482.1	173.1	2480.4	4466.4
Gasmassenstrom [kg/h]	4666.3	113.5	1625.6	2927.2
Staub [g/Nm³]	0.00	0.00	0.00	0.00
Gesamtmassenstrom [kg/h]	4666.3	113.5	1625.6	2927.2
Energiestrom [kW]	369.9	8.3	119.3	214.8
Zusammensetzung Gas	Abgas	Abgas	Abgas	Abgas
Zusammensetzung Staub	---	---	---	Calciumhydroxid

**Biomasse und Pyrolysekoks**

<i>Biomasse, Koks</i>	Biomasse	Pyrolysekoks
Temperatur [°C]	33.7	493.9
Absolutdruck [bar]	1.01306	1.01306
Dichte [kg/m³]	300.0	300.0
Massenstrom [kg/h]	517.1	154.4
Heizwert (wf) [kJ/kg]	18676.2	26756.9
Heizwert [kJ/kg]	16801.2	26756.9
Wassergehalt [Gew. %]	8.88	0.00
Aschegehalt [Gew. % wf]	4.91	12.95
Energiestrom [kW]	2419.6	1175.5
Zusammensetzung org.	Biomasse	Pyrolysekoks
Zusammensetzung anorg.	Asche Biomasse	Asche Biomasse

**Feststoffströme**

	Kalk für Entschwefelung	Gewebefilter Abreinigung
Temperatur [°C]	25.0	185.8
Koksbelastung [kg/kg_anorg.]	0.00	0.00
Massenstrom [kg/h]	0.00	3.14
Energiestrom [kW]	0.00	0.13
Zusammensetzung Organisch	---	---
Zusammensetzung Anorg.	Calciumhydroxid	Asche Desulf

<b>Prozessdaten Versuchsanlage Dürnrohr</b>	<i>Seite: 3</i>
---------------------------------------------	-----------------

**Wasserströme**

<i>Sprühabsorber und Sprühkühler</i>	Wasser für Sprühkühler	Wasser für Sprühabsorber
Temperatur [°C]	20.0	20.0
Absolutdruck [bar]	2.0	2.0
Enthalpie [kJ/kg]	-15886.8	-15886.8
Betr.vol.strom [m <sup>3</sup> /h]	0.9	0.4
Massenstrom [kg/h]	857.8	402.6
Energiestrom [kW]	-562.0	-263.7

**Apparate****Nachbrennkammer**

Druckverlust Rauchgas [mbar]	50	Luftzahl $\lambda$ [-]	1.68
Druckverlust Luft [mbar]	18	CO-Schlupf [mol <sub>CO</sub> /mol <sub>CO2</sub> ]	0.0000
		Therm. Leistg. [kW]	1364.6

**Drehrohrreaktor**

Druckverlust Heißgas [mbar]	5.24	zugeführte Leistung über Heißgas [kW]	143
Pyrolysetemperatur [°C]	553	Umgesetzter C in Gas und Teer [%]	50.01
Teer in PG [kg/kg_tr.BSt]	0.14	Exergieverlust [kW]	105.03
Staub in PG [kg/kg_tr.BSt]	0.14		
Flugkoks in PG [kg/kg_tr.BSt]	0.01		

**Sprühkühler**

Druckverlust Gas [mbar]	0.32	Exergieverlust [kW]	347.7
-------------------------	------	---------------------	-------

**Sprühabsorber**

Druckverlust Gas [mbar]	0.93	Exergieverlust [kW]	80.1
Umsatz von CaOH <sub>2</sub> [%]	70.0	Desulfurisation reaction rate [kmol/h]	1.91937E-27

**Gewebefilter**

Druckverlust Gas [mbar]	5.91	rel Wärmeverlust [%]	4.3
Diff. Temp.Austritt [°C]	8.1	Wärmeverlust [kW]	26.1
Abscheidegrad Staub [%]	100.0	Exergieverlust [kW]	10.7

**Exergieflüsse DRO**

Exergie Biomasse [kW]	2612.68
Exergie Heißgas [kW]	641.7
Exergie Rezigas [kW]	6.7
Exergie Pyrolysegas[kW]	1464.6
Exergie Pyrolysekoks [kW]	1192.9
Exergie Kaltgas [kW]	498.5

<b>Prozessdaten Versuchsanlage Dürnröhr</b>	<i>Seite: 4</i>
---------------------------------------------	-----------------

**Zusammensetzungen Gasströme**

<i>Luft und Verbrennungsluftmix</i>	Umgebungsluft	Umgebungsluft wasserfrei	Verbrennungsluftmix	Verbrennungsluftmix wasserfrei
mittlere Molmasse [g/mol]	28.73	28.97	26.08	29.59
Heizwert $H_U$ [MJ/Nm <sup>3</sup> ]	0.00	0.00	0.00	0.00
Ar [vol%]	0.91	0.93	0.65	0.93
C2H4 [vol%]	0.00	0.00	0.00	0.00
C2H6 [vol%]	0.00	0.00	0.00	0.00
C3H8 [vol%]	0.00	0.00	0.00	0.00
CH4 [vol%]	0.00	0.00	0.00	0.00
CO [vol%]	0.00	0.00	0.00	0.00
CO2 [vol%]	0.04	0.04	3.66	5.26
H2 [vol%]	0.00	0.00	0.00	0.00
H2O [vol%]	2.13	---	30.32	---
H2S [vol%]	0.00	0.00	0.00	0.00
HCl [vol%]	0.00	0.00	0.00	0.00
HCN [vol%]	0.00	0.00	0.00	0.00
N2 [vol%]	76.42	78.08	54.47	78.18
N2O [vol%]	0.00	0.00	0.00	0.00
NH3 [vol%]	0.00	0.00	0.00	0.00
NO [vol%]	0.00	0.00	0.00	0.01
O2 [vol%]	20.50	20.95	10.89	15.62
SO2 [vol%]	0.00	0.00	0.00	0.00

<i>Pyrolysegas, Rauchgas</i>	Pyrolysegas	Pyrolysegas wasserfrei	Rauchgas NBK	Rauchgas NBK wasserfrei
mittlere Molmasse [g/mol]	22.32	26.79	26.11	30.93
Heizwert $H_U$ [MJ/Nm <sup>3</sup> ]	5.84	11.91	0.00	0.00
Ar [vol%]	0.11	0.22	0.59	0.94
C2H4 [vol%]	0.00	0.00	0.00	0.00
C2H6 [vol%]	0.00	0.00	0.00	0.00
C3H8 [vol%]	0.00	0.00	0.00	0.00
CH4 [vol%]	10.28	20.98	0.00	0.00
CO [vol%]	13.19	26.91	0.00	0.00
CO2 [vol%]	11.03	22.50	10.36	16.53
H2 [vol%]	4.52	9.23	0.00	0.00
H2O [vol%]	50.98	---	37.31	---
H2S [vol%]	0.00	0.01	0.00	0.00
HCl [vol%]	0.00	0.00	0.00	0.00
HCN [vol%]	0.00	0.00	0.00	0.00
N2 [vol%]	9.04	18.45	49.14	78.38
N2O [vol%]	0.00	0.00	0.00	0.00
NH3 [vol%]	0.02	0.03	0.00	0.00
NO [vol%]	0.00	0.00	0.01	0.02
O2 [vol%]	0.82	1.67	2.59	4.13
SO2 [vol%]	0.001	0.00	0.00	0.00

## Prozessdaten Versuchsanlage Dürnrohr

Seite: 5

<i>Rauchgas</i>	Rauchgas Quench	Rauchgas Quench wasserfrei	Gasmix vor Desulf	Gasmix vor Desulf wasserfrei
mittlere Molmasse [g/mol]	24.19	30.93	23.95	30.93
Heizwert $H_U$ [MJ/Nm <sup>3</sup> ]	0.00	0.00	0.00	0.00
Ar [vol%]	0.45	0.94	0.43	0.94
C2H4 [vol%]	0.00	0.00	0.00	0.00
C2H6 [vol%]	0.00	0.00	0.00	0.00
C3H8 [vol%]	0.00	0.00	0.00	0.00
CH4 [vol%]	0.00	0.00	0.00	0.00
CO [vol%]	0.00	0.00	0.00	0.00
CO2 [vol%]	7.89	16.53	7.59	16.53
H2 [vol%]	0.00	0.00	0.00	0.00
H2O [vol%]	52.24	---	54.08	---
H2S [vol%]	0.00	0.00	0.00	0.00
HCl [vol%]	0.00	0.00	0.00	0.00
HCN [vol%]	0.00	0.00	0.00	0.00
N2 [vol%]	37.44	78.38	35.99	78.38
N2O [vol%]	0.00	0.00	0.00	0.00
NH3 [vol%]	0.00	0.00	0.00	0.00
NO [vol%]	0.01	0.02	0.01	0.02
O2 [vol%]	1.97	4.13	1.90	4.13
SO2 [vol%]	0.00	0.00	0.00	0.00

<i>Abgas</i>	Abgas	Abgas wasserfrei
mittlere Molmasse [g/mol]	23.57	30.93
Heizwert $H_U$ [MJ/Nm <sup>3</sup> ]	0.00	0.00
Ar [vol%]	0.40	0.94
C2H4 [vol%]	0.00	0.00
C2H6 [vol%]	0.00	0.00
C3H8 [vol%]	0.00	0.00
CH4 [vol%]	0.00	0.00
CO [vol%]	0.00	0.00
CO2 [vol%]	7.10	16.53
H2 [vol%]	0.00	0.00
H2O [vol%]	57.04	---
H2S [vol%]	0.00	0.00
HCl [vol%]	0.00	0.00
HCN [vol%]	0.00	0.00
N2 [vol%]	33.67	78.38
N2O [vol%]	0.00	0.00
NH3 [vol%]	0.00	0.00
NO [vol%]	0.01	0.02
O2 [vol%]	1.77	4.13
SO2 [vol%]	0.001	0.001

**Organische Zusammensetzungen (wasser- und aschefrei)**

	Biomasse	Pyrolysekoks	Teer
C [Gew%]	54.09	86.31	81.83
H [Gew%]	5.41	1.85	7.19
O [Gew%]	39.88	10.45	10.82
N [Gew%]	0.48	0.96	0.17
S [Gew%]	0.01	0.01	0.00
Cl [Gew%]	0.13	0.43	0.00
Heizwert $H_U$ (waf) [kJ/kg]	19640.50	30736.10	38489.50

**Zusammensetzungen Feststoffe**

	Asche Biomasse	Asche Desulf	Calciumhydroxid
Asche [Gew%]	100.00	100.00	0.00
K <sub>2</sub> O [Gew%]	0.00	0.00	0.00
MgO [Gew%]	0.00	0.00	0.00
CaO [Gew%]	0.00	0.00	0.00
SiO <sub>2</sub> [Gew%]	0.00	0.00	0.00
Olivin [Gew%]	0.00	0.00	0.00
CaCO <sub>3</sub> [Gew%]	0.00	0.00	0.00
Dolomit [Gew%]	0.00	0.00	0.00
CaSO <sub>4</sub> [Gew%]	0.00	---	0.00
CaOH <sub>2</sub> [Gew%]	0.00	---	100.00

**Prozessdaten Versuchsanlage Dürnrohr**

Seite: 1

**Ausgeglichene Lösung mit IPSEpro**

Messwertbasis: 25.08.2009 10:45 - 10:55 (Stroh aus Lassee, Verweilzeitvariation 40%)

**Prozessbedingungen**

zugeführte Leistung DRO [kW]	150
BWL Brennkammer. [kW]	1232
Pyrolysegastemperatur [°C]	569

**Umgebungsbedingungen**

Seehöhe [m]	182
Temperatur [°C]	25.25
Luftdruck [mbar]	1013.25
Rel. Luftfeuchte [%]	60

**Kaltgaswirkungsgrad Pyrolysegas**

$\eta_{\text{chem}}$	0.50
----------------------	------

**Gasströme**

Luft, Pyrolysegas	Luft vor Gebläse	Luft vor Brennkammer	Pyrolysegas nach DRO	Pyrolysegas nach Pyrol.gasgebläse
Temperatur [°C]	25.3	128.6	568.8	642.3
Absolutdruck [bar]	1.01325	1.03025	1.01305	1.17228
Normvol.strom [Nm <sup>3</sup> /h]	1213	1213	493	493
Betr.vol.strom [m <sup>3</sup> /h]	1325	1755	1519	1427
Gasmassenstrom [kg/h]	1556	1556	492	492
Staubbeladung [g/Nm <sup>3</sup> ]	---	---	3.6	3.6
Flugkoksbeladung [g/Nm <sup>3</sup> ]	---	---	2.3	2.3
Teerbeladung [g/Nm <sup>3</sup> ]	---	---	65.4	65.4
Gesamtmassenstrom [kg/h]	1556	1556	527	527
Energiestrom [kW]	11.4	56.9	1373.0	1393.6
Zusammensetzung Gas	Umgebungsluft	Umgebungsluft	Pyrolysegas	Pyrolysegas
Zusammensetzung Staub	---	---	Asche Biomasse	Asche Biomasse
Zusammensetzung Flugkoks	---	---	Pyrolysekoks	Pyrolysekoks
Zusammensetzung Teer	---	---	Teer	Teer

Rauchgas, Heißgas, Kaltgas	Luft + Rezigas zu Brennkammer	Heißgas vor DRO	Kaltgas nach DRO	Kaltgas nach Kaltgasgebläse
Temperatur [°C]	153.6	843.3	665.8	577.5
Absolutdruck [bar]	1.03025	1.01228	1.00655	1.07228
Normvol.strom [Nm <sup>3</sup> /h]	2727.7	2467.1	2467.1	2467.1
Betr.vol.strom [m <sup>3</sup> /h]	4191.0	10093.3	8536.8	7260.6
Gasmassenstrom [kg/h]	3125.5	2824.2	2824.2	2824.2
Staubbeladung [g/Nm <sup>3</sup> ]	---	0.55	0.55	0.55
Gesamtmassenstrom [kg/h]	3125.5	2825.6	2825.6	2825.6
Energiestrom [kW]	174.3	931.5	720.3	618.8
Zusammensetzung Gas	Verbr.luftmix	Rauchgas NBK	Rauchgas NBK	Rauchgas NBK
Zusammensetzung Staub	---	Asche Biomasse	Asche Biomasse	Asche Biomasse

Rauchgas, Rauchgas Rezigas mix	Rauchgas nach Brennkammer	Rauchgas vor Sprühkühler	Rauchgas nach Sprühkühler	Rauchgas + Rezigas vor Sprühabsorber
Temperatur [°C]	856.5	856.5	370.5	293.0
Absolutdruck [bar]	1.01228	1.01228	1.01197	1.01197
Normvol.strom [Nm <sup>3</sup> /h]	5656.4	3189.2	4218.8	6972.4
Betr.vol.strom [m <sup>3</sup> /h]	23416.1	13202.7	9954.2	14470.8
Gasmassenstrom [kg/h]	6475.1	3650.9	4478.4	7331.2
Staubbeladung [g/Nm <sup>3</sup> ]	0.55	0.55	0.42	0.25
Gesamtmassenstrom [kg/h]	6478.3	3652.7	4480.2	7332.9
Energiestrom [kW]	2172.6	1225.0	682.6	896.0
Zusammensetzung Gas	Rauchgas NBK	Rauchgas NBK	Rauchgas Quench	Gasmix vor Desulf
Zusammensetzung Staub	Asche Biomasse	Asche Biomasse	Asche Biomasse	Asche/Kalk mix

<b>Prozessdaten Versuchsanlage Dürnrohr</b>	<i>Seite: 2</i>
---------------------------------------------	-----------------

<i>Rauchgas, Erdgas</i>	Rauchgas nach Sprühabsorber	Abgas nach Gewebefilter	Abgas durch Kamin	Erdgas
Temperatur [°C]	195.5	187.4	121.5	20.0
Absolutdruck [bar]	1.01106	1.00506	1.01325	2.00
Normvol.strom [Nm³/h]	7436.0	7436.0	3039.7	0.0
Betr.vol.strom [m³/h]	12784.7	12638.7	4391.8	0.0
Gasmassenstrom [kg/h]	7703.8	7703.8	3149.2	0.0
Staubbelastung [g/Nm³]	0.24	0.00	0.00	---
Gesamtmassenstrom [kg/h]	7705.5	7703.8	3149.2	0.0
Energiestrom [kW]	651.8	626.5	173.2	0.0
Zusammensetzung Gas	Abgas	Abgas	Abgas	Erdgas
Zusammensetzung Staub	Asche Desulf	---	---	---

<i>Rezigas</i>	Rezigas gesamt	Rezigas zu DRO	Rezigas zu Brennkammer	Rezigas zu Sprühabsorber
Temperatur [°C]	188.9	171.2	171.2	171.2
Absolutdruck [bar]	1.01325	1.03026	1.03026	1.03026
Normvol.strom [Nm³/h]	4396.3	127.7	1514.9	2753.6
Betr.vol.strom [m³/h]	7436.5	204.3	2423.5	4405.1
Gasmassenstrom [kg/h]	4554.6	132.3	1569.5	2852.8
Staub [g/Nm³]	0.00	0.00	0.00	0.00
Gesamtmassenstrom [kg/h]	4554.6	132.3	1569.5	2852.8
Energiestrom [kW]	373.2	9.9	117.4	213.4
Zusammensetzung Gas	Abgas	Abgas	Abgas	Abgas
Zusammensetzung Staub	---	---	---	Calciumhydroxid

**Biomasse und Pyrolysekoks**

<i>Biomasse, Koks</i>	Biomasse	Pyrolysekoks
Temperatur [°C]	34.4	521.0
Absolutdruck [bar]	1.01305	1.01305
Dichte [kg/m³]	300.0	300.0
Massenstrom [kg/h]	564.5	169.7
Heizwert (wf) [kJ/kg]	17392.4	27355.2
Heizwert [kJ/kg]	15617.4	27355.2
Wassergehalt [Gew. %]	8.95	0.00
Aschegehalt [Gew. % wf]	4.79	13.47
Energiestrom [kW]	2456.1	1322.2
Zusammensetzung org.	Biomasse	Pyrolysekoks
Zusammensetzung anorg.	Asche Biomasse	Asche Biomasse

**Feststoffströme**

	Kalk für Entschwefelung	Gewebefilter Abreinigung
Temperatur [°C]	25.0	187.4
Koksbelastung [kg/kg_anorg.]	0.00	0.00
Massenstrom [kg/h]	0.00	1.77
Energiestrom [kW]	0.00	0.07
Zusammensetzung Organisch	---	---
Zusammensetzung Anorg.	Calciumhydroxid	Asche Desulf

<b>Prozessdaten Versuchsanlage Dürrrohr</b>	<i>Seite: 3</i>
---------------------------------------------	-----------------

**Wasserströme**

<i>Sprühabsorber und Sprühkühler</i>	Wasser für Sprühkühler	Wasser für Sprühabsorber
Temperatur [°C]	20.0	20.0
Absolutdruck [bar]	2.0	2.0
Enthalpie [kJ/kg]	-15886.8	-15886.8
Betr.vol.strom [m <sup>3</sup> /h]	0.8	0.4
Massenstrom [kg/h]	827.5	372.6
Energiestrom [kW]	-542.1	-244.1

**Apparate****Nachbrennkammer**

Druckverlust Rauchgas [mbar]	50	Luftzahl $\lambda$ [-]	1.38
Druckverlust Luft [mbar]	18	CO-Schlupf [mol <sub>CO</sub> /mol <sub>CO2</sub> ]	0.0000
		Therm. Leistg. [kW]	1232.2

**Drehrohrreaktor**

Druckverlust Heißgas [mbar]	5.74	zugeführte Leistung über Heißgas [kW]	150
Pyrolysetemperatur [°C]	569	Umgesetzter C in Gas und Teer [%]	47.79
Teer in PG [kg/kg_tr.BSt]	0.07	Exergieverlust [kW]	157.27
Staub in PG [kg/kg_tr.BSt]	0.07		
Flugkoks in PG [kg/kg_tr.BSt]	0.00		

**Sprühkühler**

Druckverlust Gas [mbar]	0.31	Exergieverlust [kW]	333.6
-------------------------	------	---------------------	-------

**Sprühabsorber**

Druckverlust Gas [mbar]	0.90	Exergieverlust [kW]	73.1
Umsatz von CaOH <sub>2</sub> [%]	70.0	Desulfurisation reaction rate [kmol/h]	-3.33539E-28

**Gewebefilter**

Druckverlust Gas [mbar]	6.01	rel Wärmeverlust [%]	4.2
Diff.Temp.Austritt [°C]	8.1	Wärmeverlust [kW]	25.2
Abscheidegrad Staub [%]	100.0	Exergieverlust [kW]	10.4

**Exergieflüsse DRO**

Exergie Biomasse [kW]	2666.49
Exergie Heißgas [kW]	575.5
Exergie Rezigas [kW]	8.6
Exergie Pyrolysegas[kW]	1326.8
Exergie Pyrolysekoks [kW]	1341.2
Exergie Kaltgas [kW]	425.3



## Prozessdaten Versuchsanlage Dürnrohr

Seite: 4

## Zusammensetzungen Gasströme

<i>Luft und Verbrennungsluftmix</i>	Umgebungsluft	Umgebungsluft wasserfrei	Verbrennungsluftmix	Verbrennungsluftmix wasserfrei
mittlere Molmasse [g/mol]	28.76	28.97	25.68	29.72
Heizwert $H_U$ [MJ/Nm <sup>3</sup> ]	0.00	0.00	0.00	0.00
Ar [vol%]	0.92	0.93	0.61	0.93
C2H4 [vol%]	0.00	0.00	0.00	0.00
C2H6 [vol%]	0.00	0.00	0.00	0.00
C3H8 [vol%]	0.00	0.00	0.00	0.00
CH4 [vol%]	0.00	0.00	0.00	0.00
CO [vol%]	0.00	0.00	0.00	0.00
CO2 [vol%]	0.04	0.04	4.13	6.31
H2 [vol%]	0.00	0.00	0.00	0.00
H2O [vol%]	1.91	---	34.52	---
H2S [vol%]	0.00	0.00	0.00	0.00
HCl [vol%]	0.00	0.00	0.00	0.00
HCN [vol%]	0.00	0.00	0.00	0.00
N2 [vol%]	76.59	78.08	51.04	77.95
N2O [vol%]	0.00	0.00	0.00	0.00
NH3 [vol%]	0.00	0.00	0.00	0.00
NO [vol%]	0.00	0.00	0.00	0.01
O2 [vol%]	20.55	20.95	9.70	14.81
SO2 [vol%]	0.00	0.00	0.00	0.00

<i>Pyrolysegas, Rauchgas</i>	Pyrolysegas	Pyrolysegas wasserfrei	Rauchgas NBK	Rauchgas NBK wasserfrei
mittlere Molmasse [g/mol]	22.39	26.59	25.66	31.24
Heizwert $H_U$ [MJ/Nm <sup>3</sup> ]	6.41	12.57	0.00	0.00
Ar [vol%]	0.09	0.19	0.54	0.93
C2H4 [vol%]	0.00	0.00	0.00	0.00
C2H6 [vol%]	0.00	0.00	0.00	0.00
C3H8 [vol%]	0.00	0.00	0.00	0.00
CH4 [vol%]	11.46	22.47	0.00	0.00
CO [vol%]	14.17	27.79	0.00	0.00
CO2 [vol%]	11.54	22.63	10.88	18.82
H2 [vol%]	4.79	9.39	0.00	0.00
H2O [vol%]	49.00	---	42.20	---
H2S [vol%]	0.00	0.01	0.00	0.00
HCl [vol%]	0.00	0.00	0.00	0.00
HCN [vol%]	0.00	0.00	0.00	0.00
N2 [vol%]	8.07	15.81	44.90	77.68
N2O [vol%]	0.00	0.00	0.00	0.00
NH3 [vol%]	0.02	0.03	0.00	0.00
NO [vol%]	0.00	0.00	0.01	0.02
O2 [vol%]	0.85	1.67	1.48	2.56
SO2 [vol%]	0.001	0.00	0.00	0.00

## Prozessdaten Versuchsanlage Dürnrohr

Seite: 5

<i>Rauchgas</i>	Rauchgas Quench	Rauchgas Quench wasserfrei	Gasmix vor Desulf	Gasmix vor Desulf wasserfrei
mittlere Molmasse [g/mol]	23.79	31.24	23.57	31.24
Heizwert $H_U$ [MJ/Nm <sup>3</sup> ]	0.00	0.00	0.00	0.00
Ar [vol%]	0.41	0.93	0.39	0.93
C2H4 [vol%]	0.00	0.00	0.00	0.00
C2H6 [vol%]	0.00	0.00	0.00	0.00
C3H8 [vol%]	0.00	0.00	0.00	0.00
CH4 [vol%]	0.00	0.00	0.00	0.00
CO [vol%]	0.00	0.00	0.00	0.00
CO2 [vol%]	8.22	18.82	7.90	18.82
H2 [vol%]	0.00	0.00	0.00	0.00
H2O [vol%]	56.30	---	58.01	---
H2S [vol%]	0.00	0.00	0.00	0.00
HCl [vol%]	0.00	0.00	0.00	0.00
HCN [vol%]	0.00	0.00	0.00	0.00
N2 [vol%]	33.94	77.68	32.62	77.68
N2O [vol%]	0.00	0.00	0.00	0.00
NH3 [vol%]	0.00	0.00	0.00	0.00
NO [vol%]	0.01	0.02	0.01	0.02
O2 [vol%]	1.12	2.56	1.07	2.56
SO2 [vol%]	0.00	0.00	0.00	0.00

<i>Abgas</i>	Abgas	Abgas wasserfrei
mittlere Molmasse [g/mol]	23.22	31.24
Heizwert $H_U$ [MJ/Nm <sup>3</sup> ]	0.00	0.00
Ar [vol%]	0.37	0.93
C2H4 [vol%]	0.00	0.00
C2H6 [vol%]	0.00	0.00
C3H8 [vol%]	0.00	0.00
CH4 [vol%]	0.00	0.00
CO [vol%]	0.00	0.00
CO2 [vol%]	7.41	18.82
H2 [vol%]	0.00	0.00
H2O [vol%]	60.63	---
H2S [vol%]	0.00	0.00
HCl [vol%]	0.00	0.00
HCN [vol%]	0.00	0.00
N2 [vol%]	30.58	77.68
N2O [vol%]	0.00	0.00
NH3 [vol%]	0.00	0.00
NO [vol%]	0.01	0.02
O2 [vol%]	1.01	2.56
SO2 [vol%]	0.001	0.002

## Organische Zusammensetzungen (wasser- und aschefrei)

	Biomasse	Pyrolysekoks	Teer
C [Gew%]	51.08	88.21	81.92
H [Gew%]	5.41	1.86	7.21
O [Gew%]	42.89	8.53	10.70
N [Gew%]	0.48	0.96	0.17
S [Gew%]	0.01	0.01	0.00
Cl [Gew%]	0.13	0.43	0.00
Heizwert $H_U$ (waf) [kJ/kg]	18267.00	31611.70	38489.50

**Zusammensetzungen Feststoffe**

	Asche Biomasse	Asche Desulf	Calciumhydroxid
Asche [Gew%]	100.00	100.00	0.00
K <sub>2</sub> O [Gew%]	0.00	0.00	0.00
MgO [Gew%]	0.00	0.00	0.00
CaO [Gew%]	0.00	0.00	0.00
SiO <sub>2</sub> [Gew%]	0.00	0.00	0.00
Olivin [Gew%]	0.00	0.00	0.00
CaCO <sub>3</sub> [Gew%]	0.00	0.00	0.00
Dolomit [Gew%]	0.00	0.00	0.00
CaSO <sub>4</sub> [Gew%]	0.00	---	0.00
CaOH <sub>2</sub> [Gew%]	0.00	---	100.00

**Prozessdaten Versuchsanlage Dürnrohr**

Seite: 1

**Ausgeglichene Lösung mit IPSEpro**
**Messwertbasis: 03.12.2009 15:15 - 15:25 (Acti-Prot Pellets, 450 °C)**
**Prozessbedingungen**

zugeführte Leistung DRO [kW]	144
BWL Brennkammer. [kW]	2037
Pyrolysegastemperatur [°C]	456

**Umgebungsbedingungen**

Seehöhe [m]	182
Temperatur [°C]	5.27
Luftdruck [mbar]	1013.25
Rel. Luftfeuchte [%]	60

**Kaltgaswirkungsgrad Pyrolysegas**

$\eta_{\text{chem}}$	0.67
----------------------	------

**Gasströme**

Luft, Pyrolysegas	Luft vor Gebläse	Luft vor Brennkammer	Pyrolysegas nach DRO	Pyrolysegas nach Pyrol.gasgebläse
Temperatur [°C]	5.3	118.2	456.3	520.0
Absolutdruck [bar]	1.01325	1.03025	1.01276	1.17278
Normvol.strom [Nm³/h]	1711	1711	248	248
Betr.vol.strom [m³/h]	1744	2411	662	622
Gasmassenstrom [kg/h]	2207	2207	258	258
Staubbeladung [g/Nm³]	---	---	1.7	1.7
Flugkoksbeladung [g/Nm³]	---	---	3.8	3.8
Teerbeladung [g/Nm³]	---	---	729.9	729.9
Gesamtmassenstrom [kg/h]	2207	2207	440	440
Energiestrom [kW]	3.4	73.3	2125.2	2140.0
Zusammensetzung Gas	Umgebungsluft	Umgebungsluft	Pyrolysegas	Pyrolysegas
Zusammensetzung Staub	---	---	Asche Biomasse	Asche Biomasse
Zusammensetzung Flugkoks	---	---	Pyrolysekoks	Pyrolysekoks
Zusammensetzung Teer	---	---	Teer	Teer

Rauchgas, Heißgas, Kaltgas	Luft + Rezigas zu Brennkammer	Heißgas vor DRO	Kaltgas nach DRO	Kaltgas nach Kaltgasgebläse
Temperatur [°C]	149.8	827.4	550.6	441.8
Absolutdruck [bar]	1.03025	1.01278	1.00826	1.07278
Normvol.strom [Nm³/h]	4051.4	1596.5	1596.5	1596.5
Betr.vol.strom [m³/h]	6169.1	6435.4	4838.5	3946.7
Gasmassenstrom [kg/h]	4602.9	1833.4	1833.4	1833.4
Staubbeladung [g/Nm³]	---	0.09	0.09	0.09
Gesamtmassenstrom [kg/h]	4602.9	1833.6	1833.6	1833.6
Energiestrom [kW]	254.5	588.5	379.7	301.6
Zusammensetzung Gas	Verbr.luftmix	Rauchgas NBK	Rauchgas NBK	Rauchgas NBK
Zusammensetzung Staub	---	Asche Biomasse	Asche Biomasse	Asche Biomasse

Rauchgas, Rauchgas Rezigas mix	Rauchgas nach Brennkammer	Rauchgas vor Sprühkühler	Rauchgas nach Sprühkühler	Rauchgas + Rezigas vor Sprühabsorber
Temperatur [°C]	972.7	972.7	370.1	318.9
Absolutdruck [bar]	1.01278	1.01278	1.01230	1.01230
Normvol.strom [Nm³/h]	5987.5	4391.0	6167.6	8344.2
Betr.vol.strom [m³/h]	27321.2	20036.3	14538.0	18103.3
Gasmassenstrom [kg/h]	6876.0	5042.6	6470.6	8699.1
Staubbeladung [g/Nm³]	0.09	0.09	0.07	0.05
Gesamtmassenstrom [kg/h]	6876.6	5043.0	6471.0	8699.5
Energiestrom [kW]	2638.7	1935.1	999.1	1167.7
Zusammensetzung Gas	Rauchgas NBK	Rauchgas NBK	Rauchgas Quench	Gasmix vor Desulf
Zusammensetzung Staub	Asche Biomasse	Asche Biomasse	Asche Biomasse	Asche/Kalk mix

<b>Prozessdaten Versuchsanlage Dürnrrohr</b>	<i>Seite: 2</i>
----------------------------------------------	-----------------

<i>Rauchgas, Erdgas</i>	Rauchgas nach Sprühabsorber	Abgas nach Gewebefilter	Abgas durch Kamin	Erdgas
Temperatur [°C]	194.9	190.0	136.2	20.0
Absolutdruck [bar]	1.01001	1.00356	1.01325	2.00
Normvol.strom [Nm³/h]	9052.2	9052.2	4455.5	0.0
Betr.vol.strom [m³/h]	15560.0	15495.7	6677.5	0.0
Gasmassenstrom [kg/h]	9268.1	9268.1	4561.7	0.0
Staubbelastung [g/Nm³]	0.05	0.00	0.00	---
Gesamtmassenstrom [kg/h]	9268.6	9268.1	4561.7	0.0
Energiestrom [kW]	794.7	776.0	282.5	0.0
Zusammensetzung Gas	Abgas	Abgas	Abgas	Erdgas
Zusammensetzung Staub	Asche Desulf	---	---	---

<i>Rezigas</i>	Rezigas gesamt	Rezigas zu DRO	Rezigas zu Brennkammer	Rezigas zu Sprühabsorber
Temperatur [°C]	191.8	170.0	170.0	170.0
Absolutdruck [bar]	1.01325	1.03026	1.03026	1.03026
Normvol.strom [Nm³/h]	4596.8	79.7	2340.4	2176.6
Betr.vol.strom [m³/h]	7824.3	127.2	3734.6	3473.3
Gasmassenstrom [kg/h]	4706.4	81.6	2396.2	2228.5
Staub [g/Nm³]	0.00	0.00	0.00	0.00
Gesamtmassenstrom [kg/h]	4706.4	81.6	2396.2	2228.5
Energiestrom [kW]	397.6	6.2	181.2	168.5
Zusammensetzung Gas	Abgas	Abgas	Abgas	Abgas
Zusammensetzung Staub	---	---	---	Calciumhydroxid

**Biomasse und Pyrolysekoks**

<i>Biomasse, Koks</i>	Biomasse	Pyrolysekoks
Temperatur [°C]	6.7	417.6
Absolutdruck [bar]	1.01276	1.01276
Dichte [kg/m³]	500.0	300.0
Massenstrom [kg/h]	531.3	172.9
Heizwert (wf) [kJ/kg]	22083.0	24061.7
Heizwert [kJ/kg]	20516.1	24061.7
Wassergehalt [Gew. %]	6.39	0.00
Aschegehalt [Gew. % wf]	6.91	19.64
Energiestrom [kW]	3029.1	1179.9
Zusammensetzung org.	Biomasse	Pyrolysekoks
Zusammensetzung anorg.	Asche Biomasse	Asche Biomasse

**Feststoffströme**

	Kalk für Entschwefelung	Gewebefilter Abreinigung
Temperatur [°C]	25.0	190.0
Koksbelastung [kg/kg_anorg.]	0.00	0.00
Massenstrom [kg/h]	0.00	0.41
Energiestrom [kW]	0.00	0.02
Zusammensetzung Organisch	---	---
Zusammensetzung Anorg.	Calciumhydroxid	Asche Desulf

## Prozessdaten Versuchsanlage Dürnröhr

Seite: 3

**Wasserströme**

<i>Sprühabsorber und Sprühkühler</i>	Wasser für Sprühkühler	Wasser für Sprühabsorber
Temperatur [°C]	20.0	20.0
Absolutdruck [bar]	2.0	2.0
Enthalpie [kJ/kg]	-15886.8	-15886.8
Betr. vol. strom [m <sup>3</sup> /h]	1.4	0.6
Massenstrom [kg/h]	1427.9	569.0
Energiestrom [kW]	-935.5	-372.8

**Apparate****Nachbrennkammer**

Druckverlust Rauchgas [mbar]	50	Luftzahl $\lambda$ [-]	1.01
Druckverlust Luft [mbar]	17	CO-Schlupf [mol <sub>CO</sub> /mol <sub>CO2</sub> ]	0.0000
		Therm. Leistg. [kW]	2036.5

**Drehrohrreaktor**

Druckverlust Heißgas [mbar]	4.52	zugeführte Leistung über Heißgas [kW]	144
Pyrolysetemperatur [°C]	456	Umgesetzter C in Gas und Teer [%]	59.77
Teer in PG [kg/kg_tr.BSt]	0.39	Exergieverlust [kW]	-10.28
Staub in PG [kg/kg_tr.BSt]	0.01		
Flugkoks in PG [kg/kg_tr.BSt]	0.00		

**Sprühkühler**

Druckverlust Gas [mbar]	0.48	Exergieverlust [kW]	598.4
-------------------------	------	---------------------	-------

**Sprühabsorber**

Druckverlust Gas [mbar]	2.29	Exergieverlust [kW]	117.2
Umsatz von CaOH <sub>2</sub> [%]	70.0	Desulfurisation reaction rate [kmol/h]	-1.2568E-29

**Gewebefilter**

Druckverlust Gas [mbar]	6.45	rel Wärmeverlust [%]	2.6
Diff. Temp. Austritt [°C]	4.9	Wärmeverlust [kW]	18.6
Abscheidegrad Staub [%]	100.0	Exergieverlust [kW]	8.5

**Exergieflüsse DRO**

Exergie Biomasse [kW]	3229.56
Exergie Heißgas [kW]	361.9
Exergie Rezigas [kW]	5.5
<hr/>	
Exergie Pyrolysegas [kW]	2177.2
Exergie Pyrolysekoks [kW]	1212.2
Exergie Kaltgas [kW]	217.9

## Prozessdaten Versuchsanlage Dürnrohr

Seite: 4

## Zusammensetzungen Gasströme

<i>Luft und Verbrennungsluftmix</i>	Umgebungsluft	Umgebungsluft wasserfrei	Verbrennungsluftmix	Verbrennungsluftmix wasserfrei
mittlere Molmasse [g/mol]	28.91	28.97	25.47	29.69
Heizwert $H_U$ [MJ/Nm <sup>3</sup> ]	0.00	0.00	0.00	0.00
Ar [vol%]	0.93	0.93	0.60	0.94
C2H4 [vol%]	0.00	0.00	0.00	0.00
C2H6 [vol%]	0.00	0.00	0.00	0.00
C3H8 [vol%]	0.00	0.00	0.00	0.00
CH4 [vol%]	0.00	0.00	0.00	0.00
CO [vol%]	0.00	0.00	0.00	0.00
CO2 [vol%]	0.04	0.04	4.05	6.35
H2 [vol%]	0.00	0.00	0.00	0.00
H2O [vol%]	0.53	---	36.20	---
H2S [vol%]	0.00	0.00	0.00	0.00
HCl [vol%]	0.00	0.00	0.00	0.00
HCN [vol%]	0.00	0.00	0.00	0.00
N2 [vol%]	77.67	78.08	50.32	78.87
N2O [vol%]	0.00	0.00	0.00	0.00
NH3 [vol%]	0.00	0.00	0.00	0.00
NO [vol%]	0.00	0.00	0.01	0.01
O2 [vol%]	20.84	20.95	8.82	13.83
SO2 [vol%]	0.00	0.00	0.00	0.00

<i>Pyrolysegas, Rauchgas</i>	Pyrolysegas	Pyrolysegas wasserfrei	Rauchgas NBK	Rauchgas NBK wasserfrei
mittlere Molmasse [g/mol]	23.33	32.19	25.74	31.09
Heizwert $H_U$ [MJ/Nm <sup>3</sup> ]	1.37	3.66	0.00	0.00
Ar [vol%]	0.11	0.31	0.56	0.95
C2H4 [vol%]	0.00	0.00	0.00	0.00
C2H6 [vol%]	0.00	0.00	0.00	0.00
C3H8 [vol%]	0.00	0.00	0.00	0.00
CH4 [vol%]	2.76	7.35	0.00	0.00
CO [vol%]	3.02	8.04	0.00	0.00
CO2 [vol%]	11.43	30.46	10.94	18.52
H2 [vol%]	0.02	0.05	0.00	0.00
H2O [vol%]	62.47	---	40.93	---
H2S [vol%]	0.00	0.01	0.00	0.00
HCl [vol%]	0.00	0.00	0.00	0.00
HCN [vol%]	0.00	0.00	0.00	0.00
N2 [vol%]	18.68	49.77	47.48	80.39
N2O [vol%]	0.00	0.00	0.00	0.00
NH3 [vol%]	0.01	0.03	0.00	0.00
NO [vol%]	0.00	0.00	0.02	0.04
O2 [vol%]	1.50	3.99	0.06	0.11
SO2 [vol%]	0.001	0.00	0.00	0.00

## Prozessdaten Versuchsanlage Dürnrohr

Seite: 5

<i>Rauchgas</i>	Rauchgas Quench	Rauchgas Quench wasserfrei	Gasmix vor Desulf	Gasmix vor Desulf wasserfrei
mittlere Molmasse [g/mol]	23.52	31.09	23.37	31.09
Heizwert $H_U$ [MJ/Nm <sup>3</sup> ]	0.00	0.00	0.00	0.00
Ar [vol%]	0.40	0.95	0.39	0.95
C2H4 [vol%]	0.00	0.00	0.00	0.00
C2H6 [vol%]	0.00	0.00	0.00	0.00
C3H8 [vol%]	0.00	0.00	0.00	0.00
CH4 [vol%]	0.00	0.00	0.00	0.00
CO [vol%]	0.00	0.00	0.00	0.00
CO2 [vol%]	7.79	18.52	7.58	18.52
H2 [vol%]	0.00	0.00	0.00	0.00
H2O [vol%]	57.95	---	59.08	---
H2S [vol%]	0.00	0.00	0.00	0.00
HCl [vol%]	0.00	0.00	0.00	0.00
HCN [vol%]	0.00	0.00	0.00	0.00
N2 [vol%]	33.80	80.39	32.90	80.39
N2O [vol%]	0.00	0.00	0.00	0.00
NH3 [vol%]	0.00	0.00	0.00	0.00
NO [vol%]	0.02	0.04	0.02	0.04
O2 [vol%]	0.04	0.11	0.04	0.11
SO2 [vol%]	0.00	0.00	0.00	0.00

<i>Abgas</i>	Abgas	Abgas wasserfrei
mittlere Molmasse [g/mol]	22.95	31.09
Heizwert $H_U$ [MJ/Nm <sup>3</sup> ]	0.00	0.00
Ar [vol%]	0.36	0.95
C2H4 [vol%]	0.00	0.00
C2H6 [vol%]	0.00	0.00
C3H8 [vol%]	0.00	0.00
CH4 [vol%]	0.00	0.00
CO [vol%]	0.00	0.00
CO2 [vol%]	6.99	18.52
H2 [vol%]	0.00	0.00
H2O [vol%]	62.28	---
H2S [vol%]	0.00	0.00
HCl [vol%]	0.00	0.00
HCN [vol%]	0.00	0.00
N2 [vol%]	30.32	80.39
N2O [vol%]	0.00	0.00
NH3 [vol%]	0.00	0.00
NO [vol%]	0.02	0.04
O2 [vol%]	0.04	0.11
SO2 [vol%]	0.000	0.001

**Organische Zusammensetzungen (wasser- und aschefrei)**

	Biomasse	Pyrolysekoks	Teer
C [Gew%]	59.87	79.74	80.65
H [Gew%]	5.22	1.92	8.06
O [Gew%]	24.68	4.44	11.12
N [Gew%]	9.95	12.96	0.17
S [Gew%]	0.10	0.33	0.00
Cl [Gew%]	0.19	0.61	0.00
Heizwert $H_U$ (waf) [kJ/kg]	23722.00	29942.80	38489.50



## Prozessdaten Versuchsanlage Dürnrohr

Seite: 6

**Zusammensetzungen Feststoffe**

	Asche Biomasse	Asche Desulf	Calciumhydroxid
Asche [Gew%]	100.00	100.00	0.00
K <sub>2</sub> O [Gew%]	0.00	0.00	0.00
MgO [Gew%]	0.00	0.00	0.00
CaO [Gew%]	0.00	0.00	0.00
SiO <sub>2</sub> [Gew%]	0.00	0.00	0.00
Olivin [Gew%]	0.00	0.00	0.00
CaCO <sub>3</sub> [Gew%]	0.00	0.00	0.00
Dolomit [Gew%]	0.00	0.00	0.00
CaSO <sub>4</sub> [Gew%]	0.00	---	0.00
CaOH <sub>2</sub> [Gew%]	0.00	---	100.00

**Prozessdaten Versuchsanlage Dürnrohr**

Seite: 1

Ausgeglichene Lösung mit IPSEpro

Messwertbasis: 02.12.2009 15:05 - 15:15 (Acti-Prot Pellets, 500 °C)

**Prozessbedingungen**

zugeführte Leistung DRO [kW]	139
BWL Brennkammer. [kW]	1875
Pyrolysegastemperatur [°C]	503

**Umgebungsbedingungen**

Seehöhe [m]	182
Temperatur [°C]	10.54
Luftdruck [mbar]	1013.25
Rel. Luftfeuchte [%]	60

**Kaltgaswirkungsgrad Pyrolysegas**

$\eta_{chem}$	0.64
---------------	------

**Gasströme**

Luft, Pyrolysegas	Luft vor Gebläse	Luft vor Brennkammer	Pyrolysegas nach DRO	Pyrolysegas nach Pyrol.gasgebläse
Temperatur [°C]	10.5	114.2	503.1	572.1
Absolutdruck [bar]	1.01325	1.03025	1.01270	1.17272
Normvol.strom [Nm³/h]	1582	1582	247	247
Betr.vol.strom [m³/h]	1643	2206	702	660
Gasmassenstrom [kg/h]	2038	2038	250	250
Staubbeladung [g/Nm³]	---	---	28.3	28.3
Flugkoksbeladung [g/Nm³]	---	---	20.5	20.5
Teerbeladung [g/Nm³]	---	---	662.0	662.0
Gesamtmassenstrom [kg/h]	2038	2038	426	426
Energiestrom [kW]	6.2	65.6	1970.6	1986.4
Zusammensetzung Gas	Umgebungsluft	Umgebungsluft	Pyrolysegas	Pyrolysegas
Zusammensetzung Staub	---	---	Asche Biomasse	Asche Biomasse
Zusammensetzung Flugkoks	---	---	Pyrolysekoks	Pyrolysekoks
Zusammensetzung Teer	---	---	Teer	Teer

Rauchgas, Heißgas, Kaltgas	Luft + Rezigas zu Brennkammer	Heißgas vor DRO	Kaltgas nach DRO	Kaltgas nach Kaltgasgebläse
Temperatur [°C]	149.2	821.8	584.0	491.2
Absolutdruck [bar]	1.03025	1.01272	1.00721	1.07272
Normvol.strom [Nm³/h]	3826.4	1775.3	1775.3	1775.3
Betr.vol.strom [m³/h]	5818.9	7120.2	5604.6	4692.8
Gasmassenstrom [kg/h]	4335.7	2031.0	2031.0	2031.0
Staubbeladung [g/Nm³]	---	1.68	1.68	1.68
Gesamtmassenstrom [kg/h]	4335.7	2033.9	2033.9	2033.9
Energiestrom [kW]	240.7	651.5	450.9	375.9
Zusammensetzung Gas	Verbr.luftmix	Rauchgas NBK	Rauchgas NBK	Rauchgas NBK
Zusammensetzung Staub	---	Asche Biomasse	Asche Biomasse	Asche Biomasse

Rauchgas, Rauchgas Rezigas mix	Rauchgas nach Brennkammer	Rauchgas vor Sprühkühler	Rauchgas nach Sprühkühler	Rauchgas + Rezigas vor Sprühabsorber
Temperatur [°C]	947.3	947.3	369.6	320.1
Absolutdruck [bar]	1.01272	1.01272	1.01234	1.01234
Normvol.strom [Nm³/h]	5931.5	4156.1	5766.9	7732.4
Betr.vol.strom [m³/h]	26516.3	18579.7	13582.4	16808.3
Gasmassenstrom [kg/h]	6785.5	4754.5	6049.2	8060.9
Staubbeladung [g/Nm³]	1.68	1.68	1.21	0.90
Gesamtmassenstrom [kg/h]	6795.4	4761.5	6056.2	8067.9
Energiestrom [kW]	2545.7	1783.7	935.1	1088.4
Zusammensetzung Gas	Rauchgas NBK	Rauchgas NBK	Rauchgas Quench	Gasmix vor Desulf
Zusammensetzung Staub	Asche Biomasse	Asche Biomasse	Asche Biomasse	Asche/Kalk mix

<b>Prozessdaten Versuchsanlage Dürnrohr</b>	<i>Seite: 2</i>
---------------------------------------------	-----------------

<i>Rauchgas, Erdgas</i>	Rauchgas nach Sprühabsorber	Abgas nach Gewebefilter	Abgas durch Kamin	Erdgas
Temperatur [°C]	194.1	190.1	138.3	20.0
Absolutdruck [bar]	1.01037	1.00463	1.01325	2.00
Normvol.strom [Nm³/h]	8399.6	8399.6	4122.4	0.0
Betr.vol.strom [m³/h]	14408.5	14367.9	6209.1	0.0
Gasmassenstrom [kg/h]	8597.2	8597.2	4219.3	0.0
Staubbelastung [g/Nm³]	0.83	0.00	0.00	---
Gesamtmassenstrom [kg/h]	8604.2	8597.2	4219.3	0.0
Energiestrom [kW]	736.9	722.6	265.9	0.0
Zusammensetzung Gas	Abgas	Abgas	Abgas	Erdgas
Zusammensetzung Staub	Asche Desulf	---	---	---

<i>Rezigas</i>	Rezigas gesamt	Rezigas zu DRO	Rezigas zu Brennkammer	Rezigas zu Sprühabsorber
Temperatur [°C]	191.7	170.9	170.9	170.9
Absolutdruck [bar]	1.01325	1.03024	1.03024	1.03024
Normvol.strom [Nm³/h]	4277.2	67.0	2244.7	1965.5
Betr.vol.strom [m³/h]	7279.6	107.2	3588.8	3142.3
Gasmassenstrom [kg/h]	4377.8	68.6	2297.5	2011.7
Staub [g/Nm³]	0.00	0.00	0.00	0.00
Gesamtmassenstrom [kg/h]	4377.8	68.6	2297.5	2011.7
Energiestrom [kW]	370.9	5.2	175.1	153.3
Zusammensetzung Gas	Abgas	Abgas	Abgas	Abgas
Zusammensetzung Staub	---	---	---	Calciumhydroxid

**Biomasse und Pyrolysekoks**

<i>Biomasse, Koks</i>	Biomasse	Pyrolysekoks
Temperatur [°C]	11.7	441.9
Absolutdruck [bar]	1.01270	1.01270
Dichte [kg/m³]	500.0	300.0
Massenstrom [kg/h]	522.1	164.9
Heizwert (wf) [kJ/kg]	21153.9	24490.8
Heizwert [kJ/kg]	19645.2	24490.8
Wassergehalt [Gew. %]	6.39	0.00
Aschegehalt [Gew. % wf]	7.39	17.66
Energiestrom [kW]	2851.0	1147.1
Zusammensetzung org.	Biomasse	Pyrolysekoks
Zusammensetzung anorg.	Asche Biomasse	Asche Biomasse

**Feststoffströme**

	Kalk für Entschwefelung	Gewebefilter Abreinigung
Temperatur [°C]	25.0	190.1
Koksbelastung [kg/kg_anorg.]	0.00	0.00
Massenstrom [kg/h]	0.00	6.99
Energiestrom [kW]	0.00	0.30
Zusammensetzung Organisch	---	---
Zusammensetzung Anorg.	Calciumhydroxid	Asche Desulf

<b>Prozessdaten Versuchsanlage Dürnrohr</b>	<i>Seite: 3</i>
---------------------------------------------	-----------------

**Wasserströme**

<i>Sprühabsorber und Sprühkühler</i>	Wasser für Sprühkühler	Wasser für Sprühabsorber
Temperatur [°C]	20.0	20.0
Absolutdruck [bar]	2.0	2.0
Enthalpie [kJ/kg]	-15886.8	-15886.8
Betr.vol.strom [m³/h]	1.3	0.5
Massenstrom [kg/h]	1294.7	536.3
Energiestrom [kW]	-848.2	-351.3

**Apparate****Nachbrennkammer**

Druckverlust Rauchgas [mbar]	50	Luftzahl $\lambda$ [-]	1.02
Druckverlust Luft [mbar]	18	CO-Schlupf [mol <sub>CO</sub> /mol <sub>CO2</sub> ]	0.0000
		Therm. Leistg. [kW]	1874.8

**Drehrohrreaktor**

Druckverlust Heißgas [mbar]	5.51	zugeführte Leistung über Heißgas [kW]	139
Pyrolysetemperatur [°C]	503	Umgesetzter C in Gas und Teer [%]	57.24
Teer in PG [kg/kg_tr.BSt]	0.36	Exergieverlust [kW]	2.59
Staub in PG [kg/kg_tr.BSt]	0.19		
Flugkoks in PG [kg/kg_tr.BSt]	0.01		

**Sprühkühler**

Druckverlust Gas [mbar]	0.38	Exergieverlust [kW]	537.6
-------------------------	------	---------------------	-------

**Sprühabsorber**

Druckverlust Gas [mbar]	1.97	Exergieverlust [kW]	110.4
Umsatz von CaOH <sub>2</sub> [%]	70.0	Desulfurisation reaction rate [kmol/h]	-4.47823E-27

**Gewebefilter**

Druckverlust Gas [mbar]	5.74	rel Wärmeverlust [%]	2.1
Diff.Temp.Austritt [°C]	4.0	Wärmeverlust [kW]	14.0
Abscheidegrad Staub [%]	100.0	Exergieverlust [kW]	6.5

**Exergieströme DRO**

Exergie Biomasse [kW]	3050.95
Exergie Heißgas [kW]	403.4
Exergie Rezigas [kW]	4.7
<hr/>	
Exergie Pyrolysegas [kW]	2018.2
Exergie Pyrolysekoks [kW]	1174.2
Exergie Kaltgas [kW]	264.0

## Prozessdaten Versuchsanlage Dürnrohr

Seite: 4

## Zusammensetzungen Gasströme

<i>Luft und Verbrennungsluftmix</i>	Umgebungsluft	Umgebungsluft wasserfrei	Verbrennungsluftmix	Verbrennungsluftmix wasserfrei
mittlere Molmasse [g/mol]	28.88	28.97	25.40	29.71
Heizwert $H_U$ [MJ/Nm <sup>3</sup> ]	0.00	0.00	0.00	0.00
Ar [vol%]	0.93	0.93	0.59	0.94
C <sub>2</sub> H <sub>4</sub> [vol%]	0.00	0.00	0.00	0.00
C <sub>2</sub> H <sub>6</sub> [vol%]	0.00	0.00	0.00	0.00
C <sub>3</sub> H <sub>8</sub> [vol%]	0.00	0.00	0.00	0.00
CH <sub>4</sub> [vol%]	0.00	0.00	0.00	0.00
CO [vol%]	0.00	0.00	0.00	0.00
CO <sub>2</sub> [vol%]	0.04	0.04	4.11	6.50
H <sub>2</sub> [vol%]	0.00	0.00	0.00	0.00
H <sub>2</sub> O [vol%]	0.75	---	36.88	---
H <sub>2</sub> S [vol%]	0.00	0.00	0.00	0.00
HCl [vol%]	0.00	0.00	0.00	0.00
HCN [vol%]	0.00	0.00	0.00	0.00
N <sub>2</sub> [vol%]	77.49	78.08	49.77	78.86
N <sub>2</sub> O [vol%]	0.00	0.00	0.00	0.00
NH <sub>3</sub> [vol%]	0.00	0.00	0.00	0.00
NO [vol%]	0.00	0.00	0.02	0.03
O <sub>2</sub> [vol%]	20.79	20.95	8.63	13.67
SO <sub>2</sub> [vol%]	0.00	0.00	0.00	0.00

<i>Pyrolysegas, Rauchgas</i>	Pyrolysegas	Pyrolysegas wasserfrei	Rauchgas NBK	Rauchgas NBK wasserfrei
mittlere Molmasse [g/mol]	22.72	32.16	25.64	31.10
Heizwert $H_U$ [MJ/Nm <sup>3</sup> ]	1.21	3.65	0.00	0.00
Ar [vol%]	0.10	0.29	0.55	0.94
C <sub>2</sub> H <sub>4</sub> [vol%]	0.00	0.00	0.00	0.00
C <sub>2</sub> H <sub>6</sub> [vol%]	0.00	0.00	0.00	0.00
C <sub>3</sub> H <sub>8</sub> [vol%]	0.00	0.00	0.00	0.00
CH <sub>4</sub> [vol%]	2.43	7.32	0.00	0.00
CO [vol%]	2.67	8.03	0.00	0.00
CO <sub>2</sub> [vol%]	10.08	30.32	10.80	18.52
H <sub>2</sub> [vol%]	0.02	0.05	0.00	0.00
H <sub>2</sub> O [vol%]	66.77	---	41.70	---
H <sub>2</sub> S [vol%]	0.00	0.01	0.00	0.00
HCl [vol%]	0.00	0.00	0.00	0.00
HCN [vol%]	0.00	0.00	0.00	0.00
N <sub>2</sub> [vol%]	16.60	49.96	46.81	80.29
N <sub>2</sub> O [vol%]	0.00	0.00	0.00	0.00
NH <sub>3</sub> [vol%]	0.01	0.03	0.00	0.00
NO [vol%]	0.00	0.00	0.06	0.10
O <sub>2</sub> [vol%]	1.32	3.98	0.08	0.14
SO <sub>2</sub> [vol%]	0.000	0.00	0.00	0.00

## Prozessdaten Versuchsanlage Dürrrohr

Seite: 5

<i>Rauchgas</i>	Rauchgas Quench	Rauchgas Quench wasserfrei	Gasmix vor Desulf	Gasmix vor Desulf wasserfrei
mittlere Molmasse [g/mol]	23.51	31.10	23.37	31.10
Heizwert $H_U$ [MJ/Nm <sup>3</sup> ]	0.00	0.00	0.00	0.00
Ar [vol%]	0.40	0.94	0.39	0.94
C2H4 [vol%]	0.00	0.00	0.00	0.00
C2H6 [vol%]	0.00	0.00	0.00	0.00
C3H8 [vol%]	0.00	0.00	0.00	0.00
CH4 [vol%]	0.00	0.00	0.00	0.00
CO [vol%]	0.00	0.00	0.00	0.00
CO2 [vol%]	7.78	18.52	7.58	18.52
H2 [vol%]	0.00	0.00	0.00	0.00
H2O [vol%]	57.99	---	59.09	---
H2S [vol%]	0.00	0.00	0.00	0.00
HCl [vol%]	0.00	0.00	0.00	0.00
HCN [vol%]	0.00	0.00	0.00	0.00
N2 [vol%]	33.73	80.29	32.85	80.29
N2O [vol%]	0.00	0.00	0.00	0.00
NH3 [vol%]	0.00	0.00	0.00	0.00
NO [vol%]	0.04	0.10	0.04	0.10
O2 [vol%]	0.06	0.14	0.06	0.14
SO2 [vol%]	0.00	0.00	0.00	0.00

<i>Abgas</i>	Abgas	Abgas wasserfrei
mittlere Molmasse [g/mol]	22.94	31.10
Heizwert $H_U$ [MJ/Nm <sup>3</sup> ]	0.00	0.00
Ar [vol%]	0.36	0.94
C2H4 [vol%]	0.00	0.00
C2H6 [vol%]	0.00	0.00
C3H8 [vol%]	0.00	0.00
CH4 [vol%]	0.00	0.00
CO [vol%]	0.00	0.00
CO2 [vol%]	6.97	18.52
H2 [vol%]	0.00	0.00
H2O [vol%]	62.34	---
H2S [vol%]	0.00	0.00
HCl [vol%]	0.00	0.00
HCN [vol%]	0.00	0.00
N2 [vol%]	30.24	80.29
N2O [vol%]	0.00	0.00
NH3 [vol%]	0.00	0.00
NO [vol%]	0.04	0.10
O2 [vol%]	0.05	0.14
SO2 [vol%]	0.000	0.001

**Organische Zusammensetzungen (wasser- und aschefrei)**

	Biomasse	Pyrolysekoks	Teer
C [Gew%]	57.79	79.41	80.83
H [Gew%]	5.31	1.89	7.91
O [Gew%]	26.83	4.94	11.08
N [Gew%]	9.78	12.83	0.17
S [Gew%]	0.10	0.33	0.00
Cl [Gew%]	0.19	0.60	0.00
Heizwert $H_U$ (waf) [kJ/kg]	22841.10	29742.10	38489.50

## Prozessdaten Versuchsanlage Dürnröhr

Seite: 6

**Zusammensetzungen Feststoffe**

	Asche Biomasse	Asche Desulf	Calciumhydroxid
Asche [Gew%]	100.00	100.00	0.00
K <sub>2</sub> O [Gew%]	0.00	0.00	0.00
MgO [Gew%]	0.00	0.00	0.00
CaO [Gew%]	0.00	0.00	0.00
SiO <sub>2</sub> [Gew%]	0.00	0.00	0.00
Olivin [Gew%]	0.00	0.00	0.00
CaCO <sub>3</sub> [Gew%]	0.00	0.00	0.00
Dolomit [Gew%]	0.00	0.00	0.00
CaSO <sub>4</sub> [Gew%]	0.00	---	0.00
CaOH <sub>2</sub> [Gew%]	0.00	---	100.00

**Prozessdaten Versuchsanlage Dürrohr**

Seite: 1

**Ausgeglichene Lösung mit IPSEpro**

Messwertbasis: 01.12.2009 10:15 - 10:25 (Acti-Prot Pellets, 550 °C)

**Prozessbedingungen**

zugeführte Leistung DRO [kW]	110
BWL Brennkammer. [kW]	1279
Pyrolysegastemperatur [°C]	554

**Umgebungsbedingungen**

Seehöhe [m]	182
Temperatur [°C]	10.64
Luftdruck [mbar]	1013.25
Rel. Luftfeuchte [%]	60

**Kaltgaswirkungsgrad Pyrolysegas**

$\eta_{\text{chem}}$	0.48
----------------------	------

**Gasströme**

Luft, Pyrolysegas	Luft vor Gebläse	Luft vor Brennkammer	Pyrolysegas nach DRO	Pyrolysegas nach Pyrol.gasgebläse
Temperatur [°C]	10.6	113.2	553.8	644.1
Absolutdruck [bar]	1.01325	1.03026	1.01299	1.17261
Normvol.strom [Nm³/h]	1070	1070	414	414
Betr.vol.strom [m³/h]	1111	1488	1254	1202
Gasmassenstrom [kg/h]	1378	1378	438	438
Staubbelastung [g/Nm³]	---	---	11.3	11.3
Flugkoksbelastung [g/Nm³]	---	---	11.6	11.6
Teerbelastung [g/Nm³]	---	---	240.1	240.1
Gesamtmassenstrom [kg/h]	1378	1378	547	547
Energiestrom [kW]	4.2	43.9	1411.2	1436.2
Zusammensetzung Gas	Umgebungsluft	Umgebungsluft	Pyrolysegas	Pyrolysegas
Zusammensetzung Staub	---	---	Asche Biomasse	Asche Biomasse
Zusammensetzung Flugkoks	---	---	Pyrolysekoks	Pyrolysekoks
Zusammensetzung Teer	---	---	Teer	Teer

Rauchgas, Heißgas, Kaltgas	Luft + Rezigas zu Brennkammer	Heißgas vor DRO	Kaltgas nach DRO	Kaltgas nach Kaltgasgebläse
Temperatur [°C]	149.7	827.3	670.1	554.0
Absolutdruck [bar]	1.03026	1.01261	1.00651	1.07261
Normvol.strom [Nm³/h]	2816.9	2023.0	2023.0	2023.0
Betr.vol.strom [m³/h]	4288.3	8155.4	7032.4	5786.9
Gasmassenstrom [kg/h]	3172.2	2293.9	2293.9	2293.9
Staubbelastung [g/Nm³]	---	1.42	1.42	1.42
Gesamtmassenstrom [kg/h]	3172.2	2296.7	2296.7	2296.7
Energiestrom [kW]	179.6	755.5	601.0	490.8
Zusammensetzung Gas	Verbr.luftmix	Rauchgas NBK	Rauchgas NBK	Rauchgas NBK
Zusammensetzung Staub	---	Asche Biomasse	Asche Biomasse	Asche Biomasse

Rauchgas, Rauchgas Rezigas mix	Rauchgas nach Brennkammer	Rauchgas vor Sprühkühler	Rauchgas nach Sprühkühler	Rauchgas + Rezigas vor Sprühabsorber
Temperatur [°C]	863.0	863.0	368.1	297.4
Absolutdruck [bar]	1.01261	1.01261	1.01221	1.01221
Normvol.strom [Nm³/h]	5299.0	3276.0	4364.2	6836.5
Betr.vol.strom [m³/h]	22054.1	13634.4	10256.0	14295.6
Gasmassenstrom [kg/h]	6008.4	3714.5	4589.2	7127.6
Staubbelastung [g/Nm³]	1.42	1.42	1.07	0.68
Gesamtmassenstrom [kg/h]	6015.9	3719.2	4593.8	7132.3
Energiestrom [kW]	2072.9	1281.5	708.2	900.2
Zusammensetzung Gas	Rauchgas NBK	Rauchgas NBK	Rauchgas Quench	Gasmix vor Desulf
Zusammensetzung Staub	Asche Biomasse	Asche Biomasse	Asche Biomasse	Asche/Kalk mix



<b>Prozessdaten Versuchsanlage Dürnrohr</b>	<i>Seite: 2</i>
---------------------------------------------	-----------------

<i>Rauchgas, Erdgas</i>	Rauchgas nach Sprühabsorber	Abgas nach Gewebefilter	Abgas durch Kamin	Erdgas
Temperatur [°C]	193.8	187.8	135.0	20.0
Absolutdruck [bar]	1.01027	1.00454	1.01325	2.00
Normvol.strom [Nm³/h]	7322.4	7322.4	2955.3	0.0
Betr.vol.strom [m³/h]	12555.0	12463.0	4416.2	0.0
Gasmassenstrom [kg/h]	7518.2	7518.2	3034.3	0.0
Staubbelastung [g/Nm³]	0.64	0.00	0.00	---
Gesamtmassenstrom [kg/h]	7522.8	7518.2	3034.3	0.0
Energiestrom [kW]	644.2	625.4	187.5	0.0
Zusammensetzung Gas	Abgas	Abgas	Abgas	Erdgas
Zusammensetzung Staub	Asche Desulf	---	---	---

<i>Rezigas</i>	Rezigas gesamt	Rezigas zu DRO	Rezigas zu Brennkammer	Rezigas zu Sprühabsorber
Temperatur [°C]	189.4	169.2	169.2	169.2
Absolutdruck [bar]	1.01325	1.03031	1.03031	1.03031
Normvol.strom [Nm³/h]	4367.1	147.5	1747.2	2472.4
Betr.vol.strom [m³/h]	7395.1	235.0	2782.8	3937.8
Gasmassenstrom [kg/h]	4483.9	151.5	1793.9	2538.5
Staub [g/Nm³]	0.00	0.00	0.00	0.00
Gesamtmassenstrom [kg/h]	4483.9	151.5	1793.9	2538.5
Energiestrom [kW]	376.0	11.5	135.7	192.0
Zusammensetzung Gas	Abgas	Abgas	Abgas	Abgas
Zusammensetzung Staub	---	---	---	Calciumhydroxid

**Biomasse und Pyrolysekoks**

<i>Biomasse, Koks</i>	Biomasse	Pyrolysekoks
Temperatur [°C]	9.6	452.2
Absolutdruck [bar]	1.01299	1.01299
Dichte [kg/m³]	500.0	300.0
Massenstrom [kg/h]	581.4	185.9
Heizwert (wf) [kJ/kg]	17091.8	25636.0
Heizwert [kJ/kg]	15849.0	25636.0
Wassergehalt [Gew. %]	6.36	0.00
Aschegehalt [Gew. % wf]	7.15	18.44
Energiestrom [kW]	2561.5	1353.5
Zusammensetzung org.	Biomasse	Pyrolysekoks
Zusammensetzung anorg.	Asche Biomasse	Asche Biomasse

**Feststoffströme**

	Kalk für Entschwefelung	Gewebefilter Abreinigung
Temperatur [°C]	25.0	187.8
Koksbelastung [kg/kg_anorg.]	0.00	0.00
Massenstrom [kg/h]	0.00	4.66
Energiestrom [kW]	0.00	0.20
Zusammensetzung Organisch	---	---
Zusammensetzung Anorg.	Calciumhydroxid	Asche Desulf

<b>Prozessdaten Versuchsanlage Dürnrohr</b>	<i>Seite: 3</i>
---------------------------------------------	-----------------

**Wasserströme**

<i>Sprühabsorber und Sprühkühler</i>	Wasser für Sprühkühler	Wasser für Sprühabsorber
Temperatur [°C]	20.0	20.0
Absolutdruck [bar]	2.0	2.0
Enthalpie [kJ/kg]	-15886.8	-15886.8
Betr.vol.strom [m <sup>3</sup> /h]	0.9	0.4
Massenstrom [kg/h]	874.6	390.5
Energiestrom [kW]	-573.0	-255.9

**Apparate****Nachbrennkammer**

Druckverlust Rauchgas [mbar]	50	Luftzahl $\lambda$ [-]	1.02
Druckverlust Luft [mbar]	18	CO-Schlupf [mol <sub>CO</sub> /mol <sub>CO2</sub> ]	0.0000
		Therm. Leistg. [kW]	1278.5

**Drehrohrreaktor**

Druckverlust Heißgas [mbar]	6.10	zugeführte Leistung über Heißgas [kW]	110
Pyrolysetemperatur [°C]	554	Umgesetzter C in Gas und Teer [%]	47.53
Teer in PG [kg/kg_tr.BSt]	0.20	Exergieverlust [kW]	84.25
Staub in PG [kg/kg_tr.BSt]	0.12		
Flugkoks in PG [kg/kg_tr.BSt]	0.01		

**Sprühkühler**

Druckverlust Gas [mbar]	0.41	Exergieverlust [kW]	351.2
-------------------------	------	---------------------	-------

**Sprühabsorber**

Druckverlust Gas [mbar]	1.93	Exergieverlust [kW]	76.7
Umsatz von CaOH <sub>2</sub> [%]	70.0	Desulfurisation reaction rate [kmol/h]	1.42268E-28

**Gewebefilter**

Druckverlust Gas [mbar]	5.74	rel Wärmeverlust [%]	3.2
Diff. Temp. Austritt [°C]	6.1	Wärmeverlust [kW]	18.6
Abscheidegrad Staub [%]	100.0	Exergieverlust [kW]	7.9

**Exergieflüsse DRO**

Exergie Biomasse [kW]	2762.58
Exergie Heißgas [kW]	475.1
Exergie Rezigas [kW]	10.5
Exergie Pyrolysegas [kW]	1413.6
Exergie Pyrolysekoks [kW]	1385.0
Exergie Kaltgas [kW]	365.3

## Prozessdaten Versuchsanlage Dürnrohr

Seite: 4

## Zusammensetzungen Gasströme

<i>Luft und Verbrennungsluftmix</i>	Umgebungsluft	Umgebungsluft wasserfrei	Verbrennungsluftmix	Verbrennungsluftmix wasserfrei
mittlere Molmasse [g/mol]	28.88	28.97	25.24	29.91
Heizwert $H_U$ [MJ/Nm <sup>3</sup> ]	0.00	0.00	0.00	0.00
Ar [vol%]	0.93	0.93	0.56	0.92
C <sub>2</sub> H <sub>4</sub> [vol%]	0.00	0.00	0.00	0.00
C <sub>2</sub> H <sub>6</sub> [vol%]	0.00	0.00	0.00	0.00
C <sub>3</sub> H <sub>8</sub> [vol%]	0.00	0.00	0.00	0.00
CH <sub>4</sub> [vol%]	0.00	0.00	0.00	0.00
CO [vol%]	0.00	0.00	0.00	0.00
CO <sub>2</sub> [vol%]	0.04	0.04	4.80	7.89
H <sub>2</sub> [vol%]	0.00	0.00	0.00	0.00
H <sub>2</sub> O [vol%]	0.76	---	39.23	---
H <sub>2</sub> S [vol%]	0.00	0.00	0.00	0.00
HCl [vol%]	0.00	0.00	0.00	0.00
HCN [vol%]	0.00	0.00	0.00	0.00
N <sub>2</sub> [vol%]	77.49	78.08	47.45	78.09
N <sub>2</sub> O [vol%]	0.00	0.00	0.00	0.00
NH <sub>3</sub> [vol%]	0.00	0.00	0.00	0.00
NO [vol%]	0.00	0.00	0.03	0.04
O <sub>2</sub> [vol%]	20.79	20.95	7.93	13.05
SO <sub>2</sub> [vol%]	0.00	0.00	0.00	0.00

<i>Pyrolysegas, Rauchgas</i>	Pyrolysegas	Pyrolysegas wasserfrei	Rauchgas NBK	Rauchgas NBK wasserfrei
mittlere Molmasse [g/mol]	23.70	32.70	25.41	31.45
Heizwert $H_U$ [MJ/Nm <sup>3</sup> ]	1.49	3.84	0.00	0.00
Ar [vol%]	0.12	0.31	0.50	0.90
C <sub>2</sub> H <sub>4</sub> [vol%]	0.00	0.00	0.00	0.00
C <sub>2</sub> H <sub>6</sub> [vol%]	0.00	0.00	0.00	0.00
C <sub>3</sub> H <sub>8</sub> [vol%]	0.00	0.00	0.00	0.00
CH <sub>4</sub> [vol%]	3.00	7.75	0.00	0.00
CO [vol%]	3.22	8.32	0.00	0.00
CO <sub>2</sub> [vol%]	13.15	33.98	11.42	20.72
H <sub>2</sub> [vol%]	0.02	0.05	0.00	0.00
H <sub>2</sub> O [vol%]	61.29	---	44.90	---
H <sub>2</sub> S [vol%]	0.00	0.01	0.00	0.00
HCl [vol%]	0.00	0.00	0.00	0.00
HCN [vol%]	0.00	0.00	0.00	0.00
N <sub>2</sub> [vol%]	17.62	45.52	43.03	78.10
N <sub>2</sub> O [vol%]	0.00	0.00	0.00	0.00
NH <sub>3</sub> [vol%]	0.01	0.03	0.00	0.00
NO [vol%]	0.00	0.00	0.06	0.11
O <sub>2</sub> [vol%]	1.56	4.02	0.09	0.16
SO <sub>2</sub> [vol%]	0.001	0.00	0.00	0.00

## Prozessdaten Versuchsanlage Dürnrohr

Seite: 5

<i>Rauchgas</i>	Rauchgas Quench	Rauchgas Quench wasserfrei	Gasmix vor Desulf	Gasmix vor Desulf wasserfrei
mittlere Molmasse [g/mol]	23.57	31.45	23.37	31.45
Heizwert $H_U$ [MJ/Nm <sup>3</sup> ]	0.00	0.00	0.00	0.00
Ar [vol%]	0.37	0.90	0.36	0.90
C2H4 [vol%]	0.00	0.00	0.00	0.00
C2H6 [vol%]	0.00	0.00	0.00	0.00
C3H8 [vol%]	0.00	0.00	0.00	0.00
CH4 [vol%]	0.00	0.00	0.00	0.00
CO [vol%]	0.00	0.00	0.00	0.00
CO2 [vol%]	8.57	20.72	8.26	20.72
H2 [vol%]	0.00	0.00	0.00	0.00
H2O [vol%]	58.64	---	60.14	---
H2S [vol%]	0.00	0.00	0.00	0.00
HCl [vol%]	0.00	0.00	0.00	0.00
HCN [vol%]	0.00	0.00	0.00	0.00
N2 [vol%]	32.30	78.10	31.13	78.10
N2O [vol%]	0.00	0.00	0.00	0.00
NH3 [vol%]	0.00	0.00	0.00	0.00
NO [vol%]	0.05	0.11	0.04	0.11
O2 [vol%]	0.07	0.16	0.06	0.16
SO2 [vol%]	0.00	0.00	0.00	0.00

<i>Abgas</i>	Abgas	Abgas wasserfrei
mittlere Molmasse [g/mol]	23.01	31.45
Heizwert $H_U$ [MJ/Nm <sup>3</sup> ]	0.00	0.00
Ar [vol%]	0.34	0.90
C2H4 [vol%]	0.00	0.00
C2H6 [vol%]	0.00	0.00
C3H8 [vol%]	0.00	0.00
CH4 [vol%]	0.00	0.00
CO [vol%]	0.00	0.00
CO2 [vol%]	7.71	20.72
H2 [vol%]	0.00	0.00
H2O [vol%]	62.78	---
H2S [vol%]	0.00	0.00
HCl [vol%]	0.00	0.00
HCN [vol%]	0.00	0.00
N2 [vol%]	29.07	78.10
N2O [vol%]	0.00	0.00
NH3 [vol%]	0.00	0.00
NO [vol%]	0.04	0.11
O2 [vol%]	0.06	0.16
SO2 [vol%]	0.001	0.002

## Organische Zusammensetzungen (wasser- und aschefrei)

	Biomasse	Pyrolysekoks	Teer
C [Gew%]	49.07	83.17	81.44
H [Gew%]	4.62	1.91	7.78
O [Gew%]	34.65	1.42	10.62
N [Gew%]	11.37	12.57	0.17
S [Gew%]	0.10	0.33	0.00
Cl [Gew%]	0.19	0.61	0.00
Heizwert $H_U$ (waf) [kJ/kg]	18408.50	31431.10	38489.50

**Zusammensetzungen Feststoffe**

	Asche Biomasse	Asche Desulf	Calciumhydroxid
Asche [Gew%]	100.00	100.00	0.00
K <sub>2</sub> O [Gew%]	0.00	0.00	0.00
MgO [Gew%]	0.00	0.00	0.00
CaO [Gew%]	0.00	0.00	0.00
SiO <sub>2</sub> [Gew%]	0.00	0.00	0.00
Olivin [Gew%]	0.00	0.00	0.00
CaCO <sub>3</sub> [Gew%]	0.00	0.00	0.00
Dolomit [Gew%]	0.00	0.00	0.00
CaSO <sub>4</sub> [Gew%]	0.00	---	0.00
CaOH <sub>2</sub> [Gew%]	0.00	---	100.00

## 9.7 Chromatograms from the GC-MS/FID detection

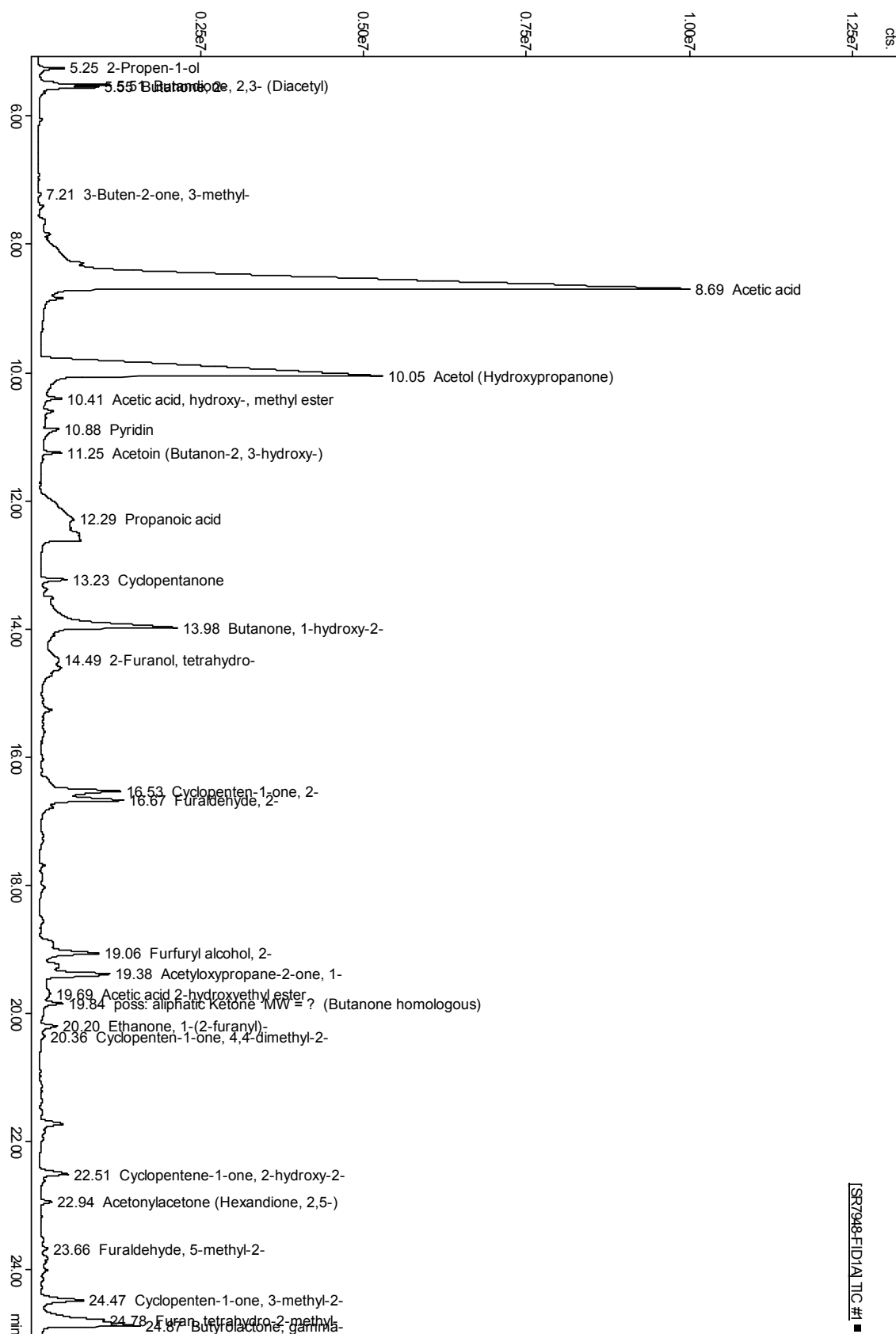


Figure 9-3: Sample 7948 – liquid phase

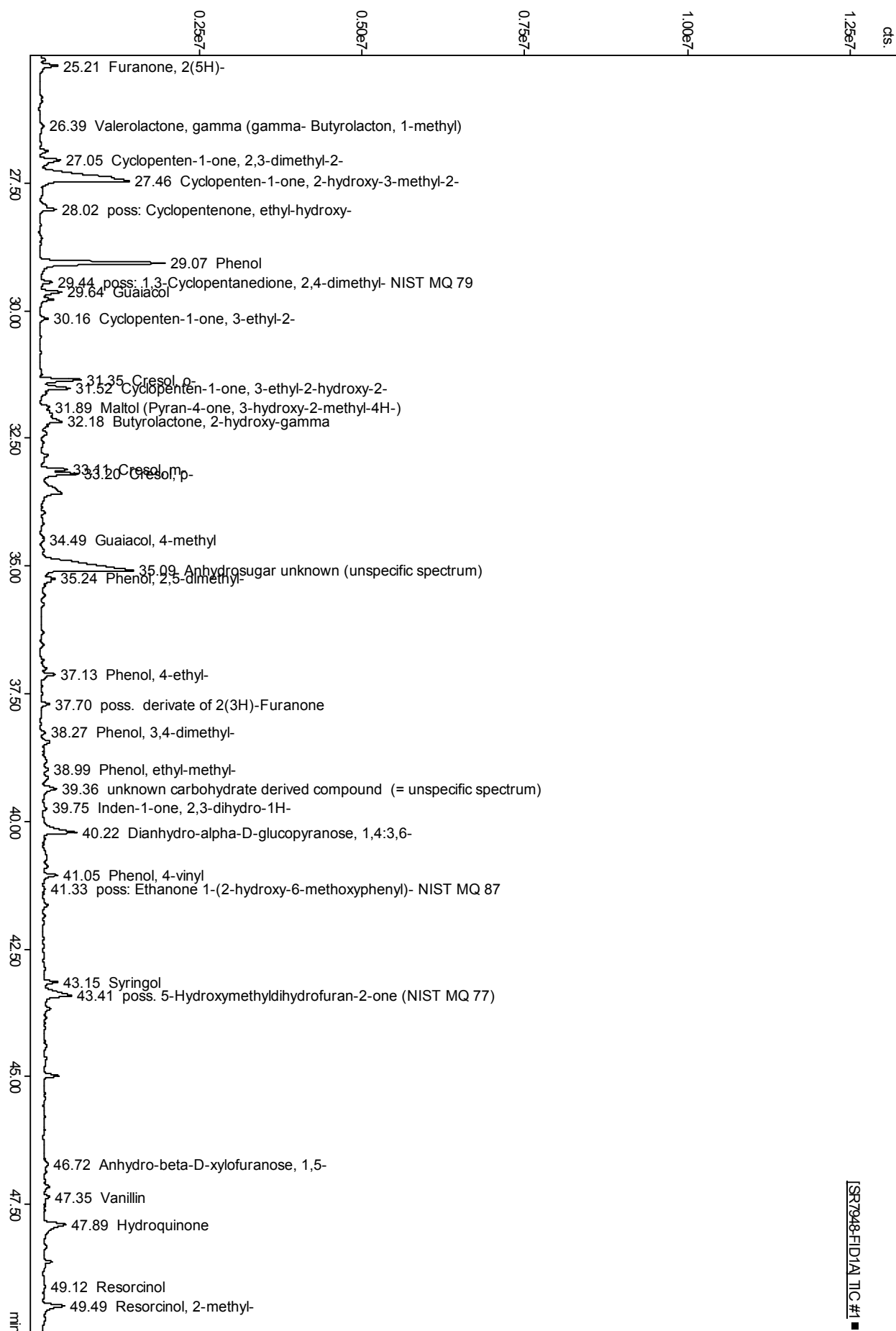


Figure 9-4: Sample 7948 – liquid phase

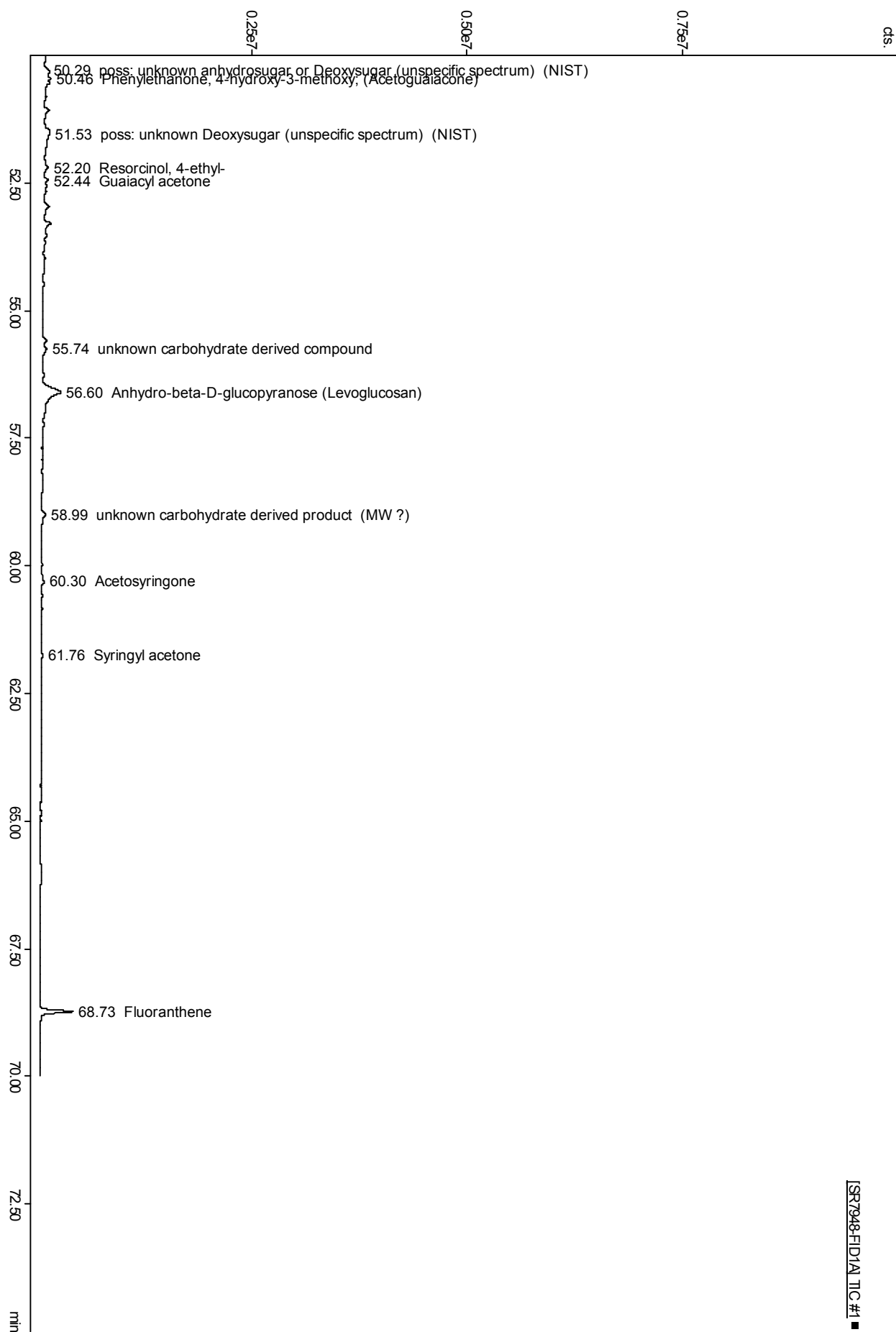


Figure 9-5: Sample 7948 – liquid phase



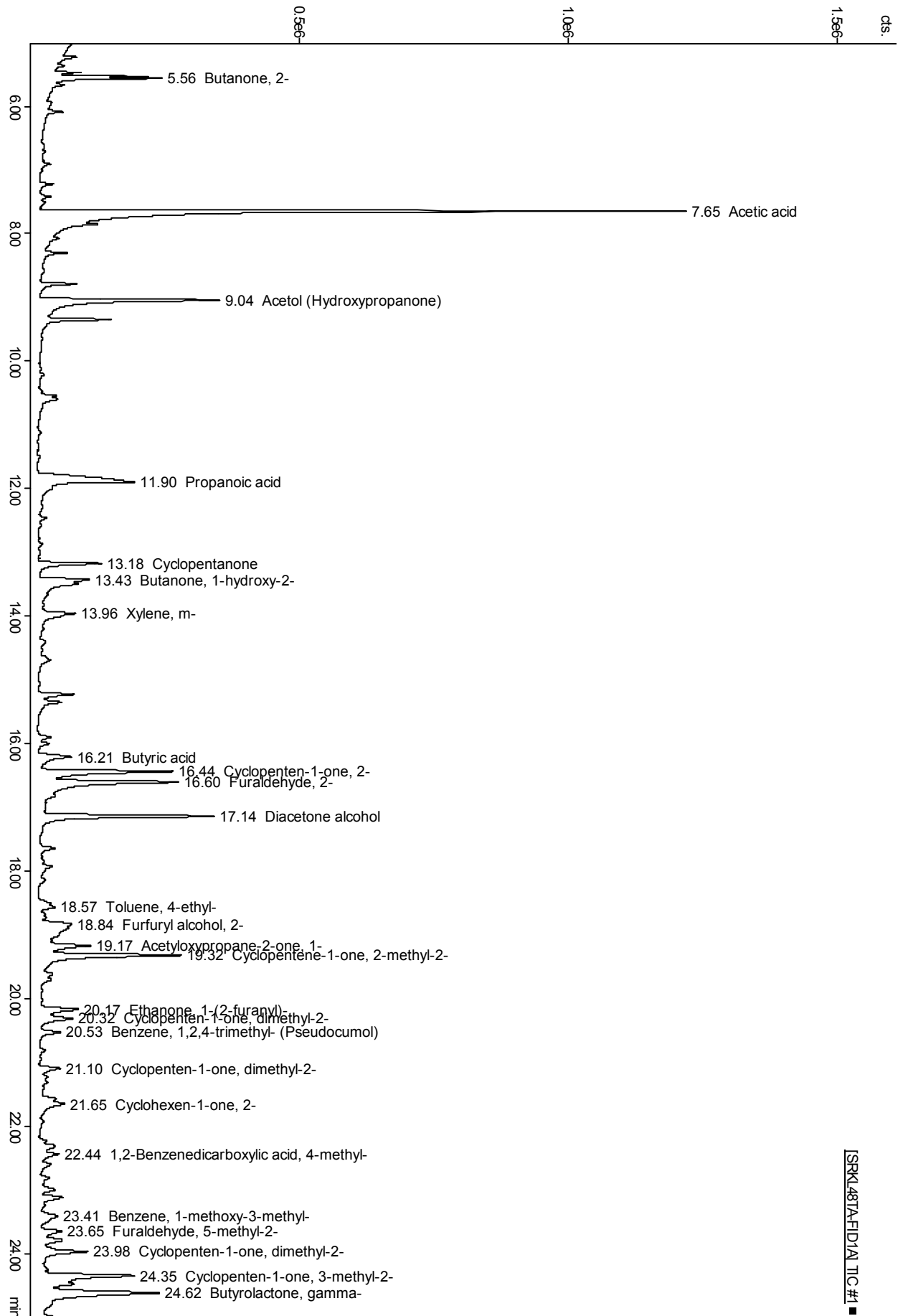


Figure 9-6: Sample 7948 - tarry phase

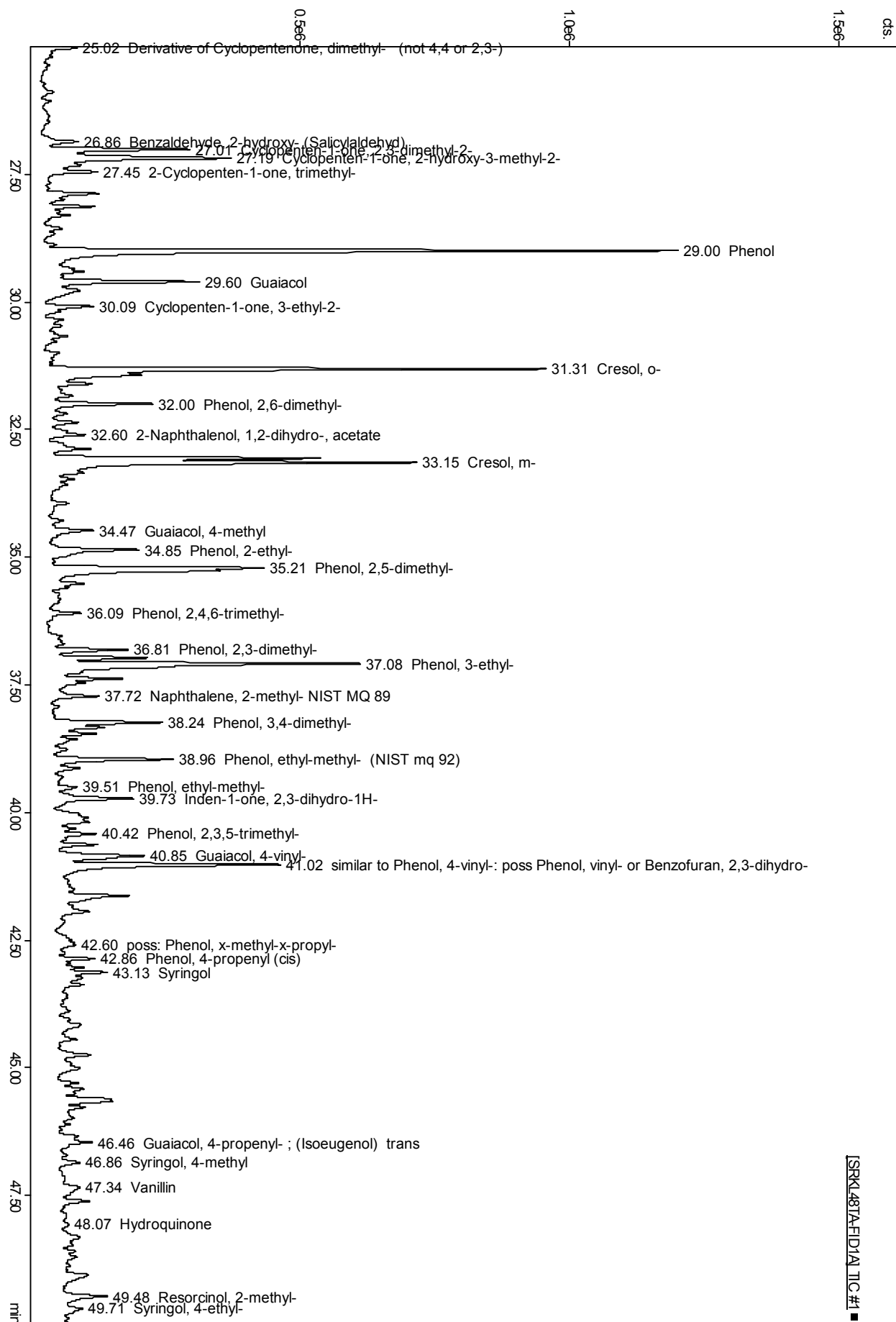


Figure 9-7: Sample 7948 - tarry phase

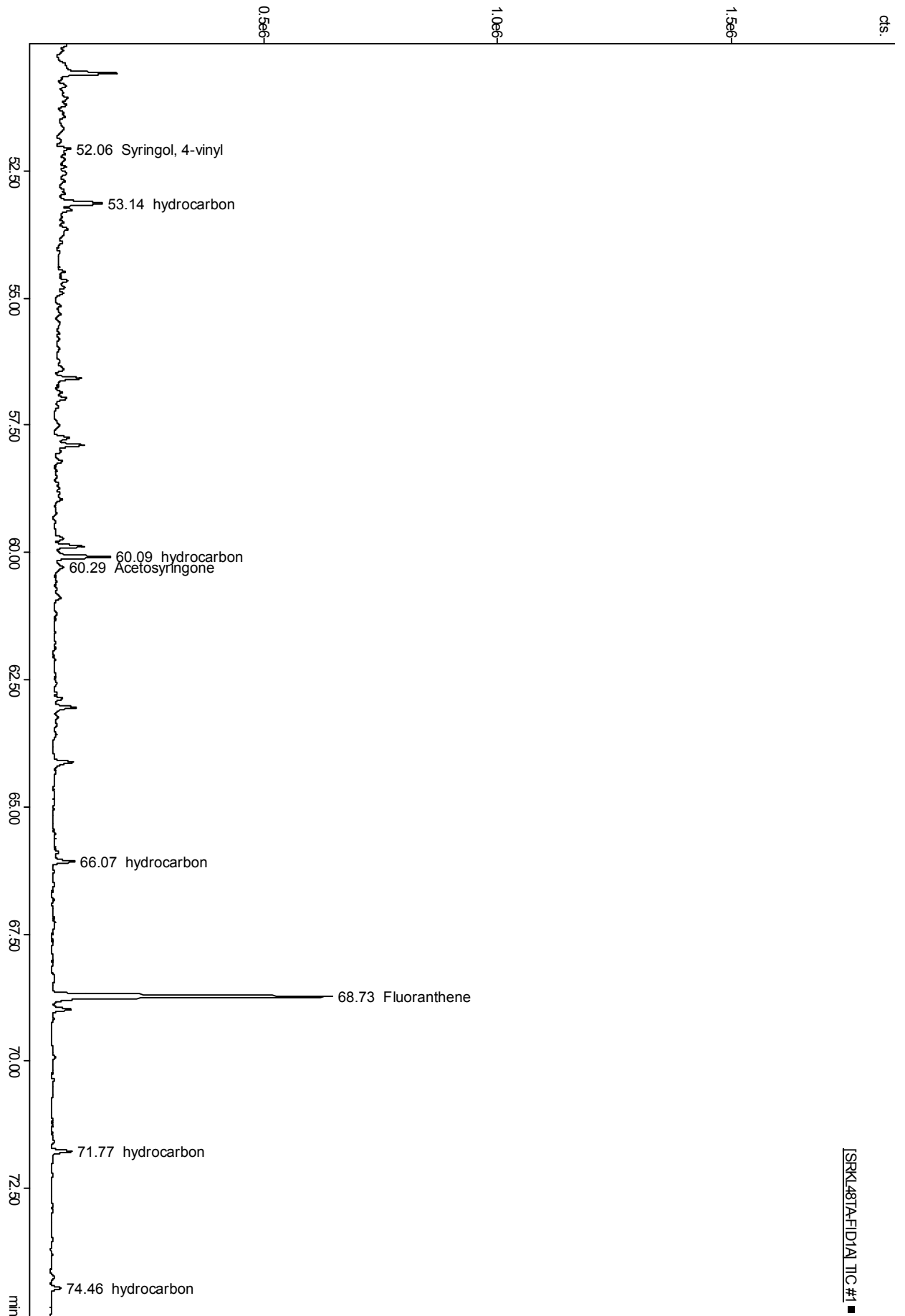


Figure 9-8: Sample 7948 – tarry phase

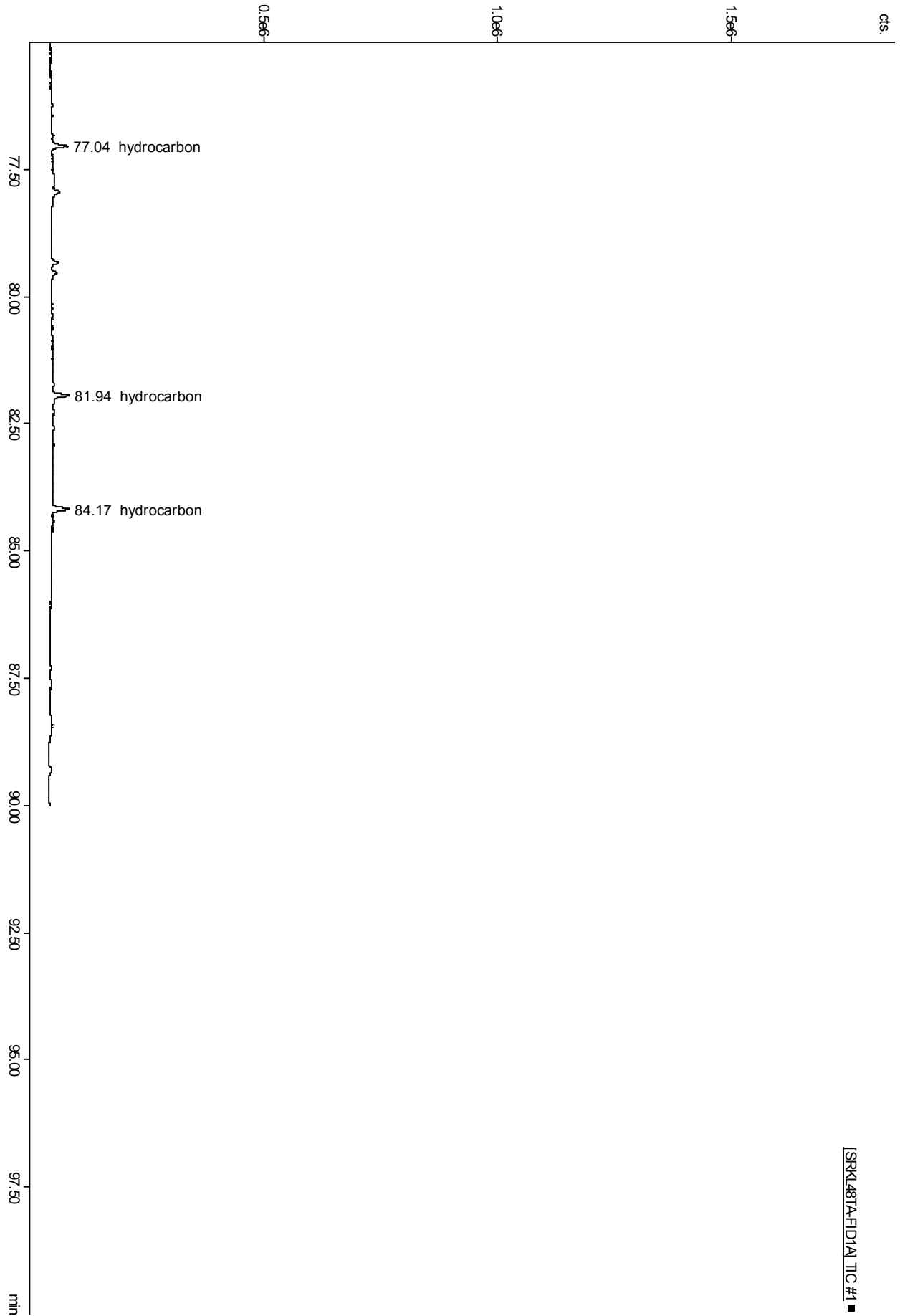


Figure 9-9: Sample 7948 – tarry phase

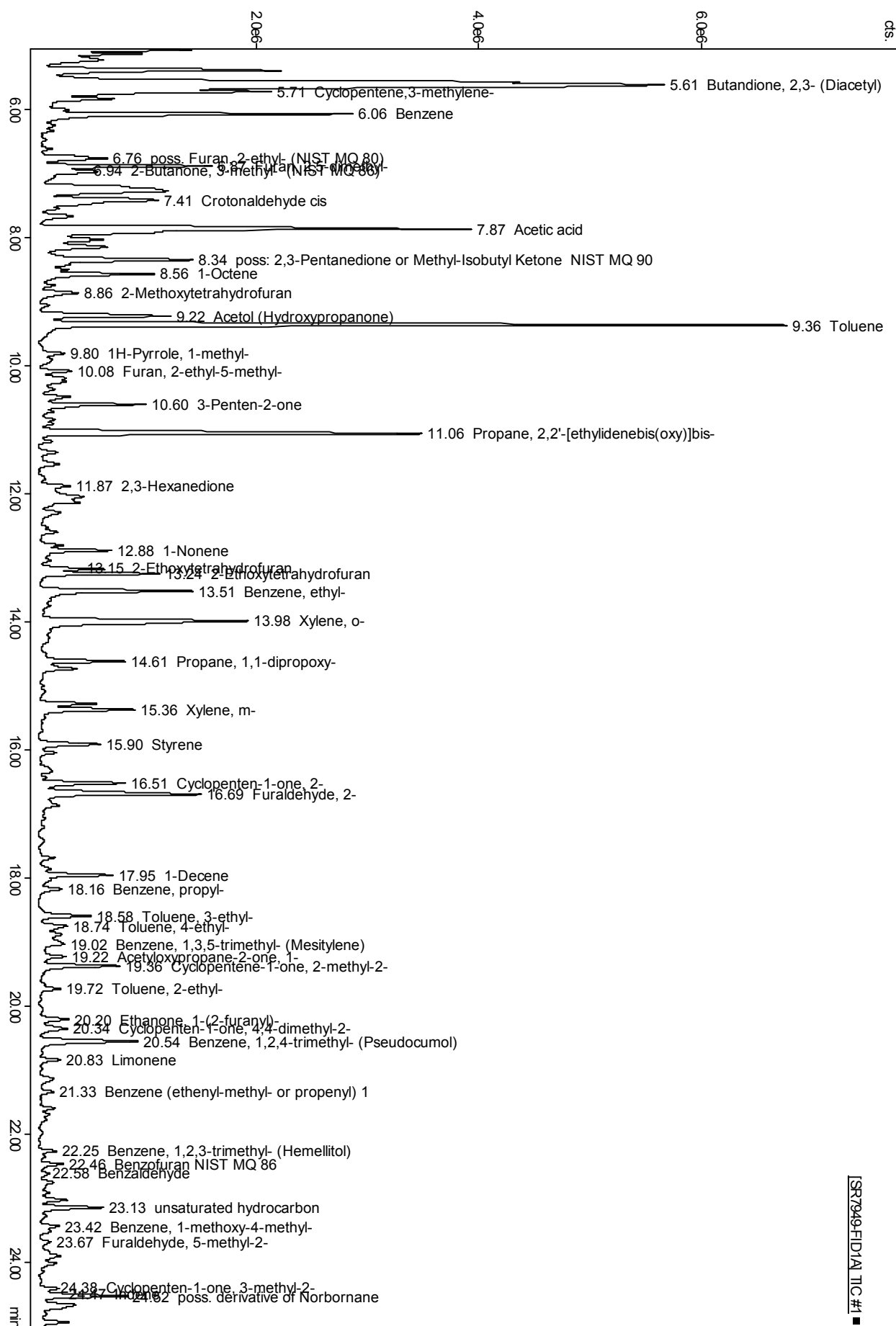


Figure 9-10: Sample 7949



Figure 9-11: Sample 7949

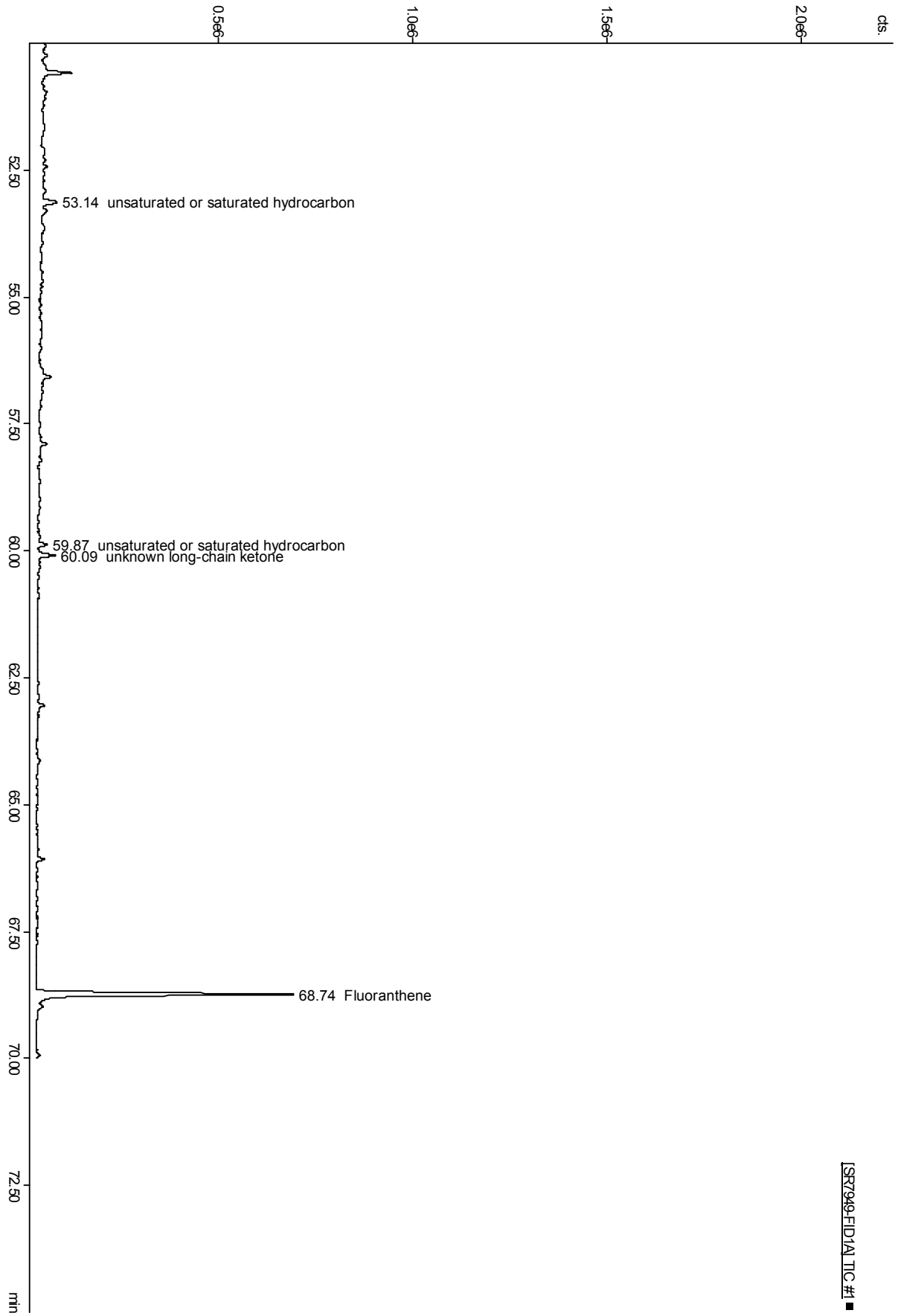


Figure 9-12: Sample 7949

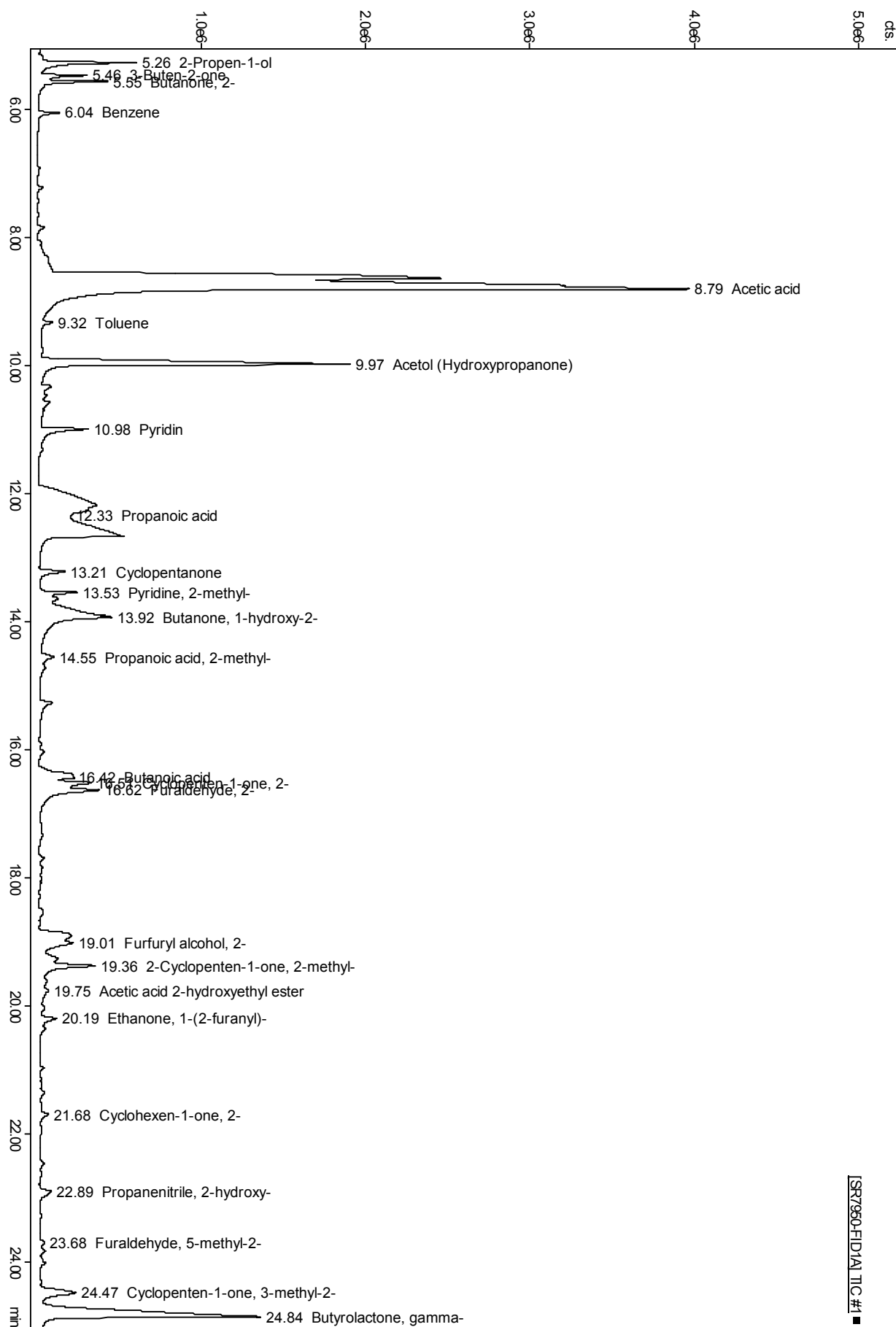


Figure 9-13: Sample 7950



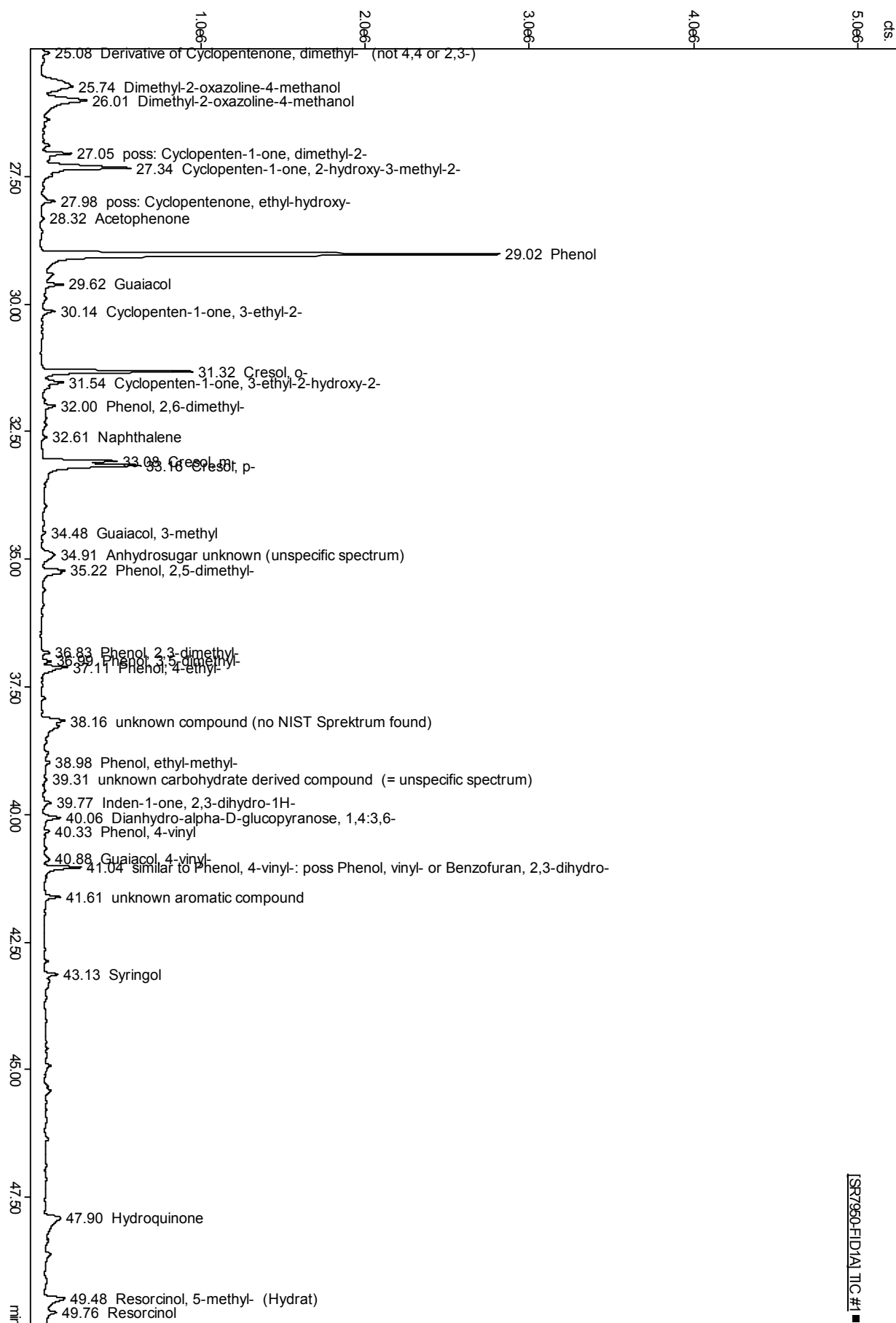


Figure 9-14: Sample 7950

Table 9-10: Detected single components in the pyrolysis oil samples by using GC-MS/FID

<b>Acids</b>	<b>Furans</b>
Acetic acid	Furfuryl alcohol, 2-
Propionic acid	Furanone, 2(5H)-
Butanoic acid	Furaldehyde, 2-
<b>Nonaromatic Aldehydes</b>	Furaldehyde, 5-methyl-2-
Crotonaldehyde, cis	Ethanone, 1-(2-furanyl)-
<b>Nonaromatic Ketones</b>	Valerolactone, $\gamma$ - (gamma-Butyrolactone, 1-methyl-)
Acetol (Hydroxypropanone)	Butyrolactone, $\gamma$ -
Acetylacetone (Hexandion, 2,5-)	Butyrolactone, 2-hydroxy-, $\gamma$ -
Butanone, 2-	2-Furanol, tetrahydro-
Butanone, 1-hydroxy-2-	Furan, 2,5-dimethyl-
Butandione, 2,3- (Diacetyl)	2-Methoxytetrahydrofuran
Acetoin (Hydroxy-2-butanone, 3-)	Furan, 2-ethyl-5-methyl-
Propanone, acetyloxy-2-	2-Ethoxytetrahydrofuran
Cyclopentanone	Benzofuran
Cyclopenten-1-one, 2-	Benzofuran, 7-methyl-, overlapping with unsaturated hydrocarbon
Cyclopenten-1-one, 4,4-dimethyl-2-	poss. 5-Hydroxymethylidihydrofuran-2-one
Cyclopenten-1-one, 2,3-dimethyl-2-	poss. Furan, 2-ethyl-
Cyclopenten-1-one, 3-methyl-2-	poss. Benzofuran, dimethyl-
Cyclopenten-1-one, 3-ethyl-2-	poss. derivate of 2(3H)-Furanone
Cyclopenten-1-one, 2-hydroxy-2-	<b>Sugars</b>
Cyclopenten-3-one, 2-hydroxy-1-methyl-1-	Anhydro- $\beta$ -D-xylofuranose, 1,5-
Cyclopenten-1-one, 3-ethyl-2-hydroxy-2-	Anhydro- $\beta$ -D-glucopyranose, 1,6- (Levoglucozan)
3-Buten-2-one, 3-methyl-	Dianhydro- $\alpha$ -D-glucopyranose, 1,4:3,6- poss: unknown anhydrosugar or Deoxysugar (unspecific spectrum)
Furan, tetrahydro-2-methyl-	poss: unknown Deoxysugar (unspecific spectrum)
Diacetone alcohol	derivative of glucofuranurono-lactone overlapping with hydrocarbon un- or saturated
Cyclopenten-1-one, 2-methyl-2-	<b>Catechols</b>
3-Buten-2-one	Hydroquinone (Benzene, 1,4-dihydroxy-)
2-Cyclopenten-1-one, 2-methyl-	Resorcinol (Benzene, 1,3-dihydroxy)
Derivative of Cyclopentenone, dimethyl- (not 4,4 or 2,3-)	Resorcinol, 2-methyl-
Cyclohexen-1-one, 2-	Resorcinol, 4-ethyl-
Cyclopenten-1-one, dimethyl-2-	Resorcinol (Benzene, 1,3-dihydroxy)
Derivative of Cyclopentenone, dimethyl- (not 4,4 or 2,3-)	Resorcinol, 5-methyl-, Hydrat (Orcinol)
2-Cyclopenten-1-one, trimethyl-	<b>Aromatic Aldehydes</b>
2-Butanone, 3-methyl-	Benzaldehyde, 2-hydroxy (Salicylaldehyd)
poss: 2,3-Pentanedione or Methyl-Isobutyl Ketone NIST MQ 90	Benzaldehyde
3-Penten-2-one	<b>Aromatic Ketones</b>
2,3-Hexanedione	Acetophenone
poss: aliphatic Ketone (Butanone homologous)	<b>Syringols (Dimethoxy phenols)</b>
poss: Cyclopentenone, ethyl-hydroxy-	Syringol
poss: 1,3-Cyclopentanedione, 2,4-dimethyl-	Acetosyringone
<b>Pyrans</b>	Syringylacetone
Maltol (Pyran-4-on, 3-hydroxy-2-methyl-4H-)	Syringol, 4-methyl-
<b>Benzenes</b>	

Inden-1-one, 2,3-dihydro-1H-	Syringol, 4-ethyl-
Toluene	Syringol, 4-vinyl-
Toluene, 2-ethyl-	<b>Lignin derived Phenols</b>
Toluene, 3-ethyl-	Phenol
Toluene, 4-ethyl-	Phenol, 2,6-dimethyl-
Xylene, m- (Benzene, 1,3-dimethyl-)	Phenol, 2,3-dimethyl-
Benzene, 1,2,4-trimethyl-	Phenol, 2,3,5-trimethyl-
Benzene, 1-methoxy-3-methyl-	Phenol, 2,4,6-trimethyl-
Benzene	Phenol, 2-ethyl-
Benzene, ethyl-	Phenol, 3-ethyl-
Benzene, 1,3,5-trimethyl-	Phenol, 4-propenyl-, cis
Benzene, 1,2,3-trimethyl-	Phenol, 3,5-dimethyl-
Benzene, propyl-	Phenol, 2,5-dimethyl-
2-Naphthalenol, 1,2-dihydro-, acetate	Phenol, 3,4-dimethyl-
Naphthalene, 2-methyl-	Phenol, 4-ethyl-
Styrene	Phenol, 4-vinyl-
Benzene, 1-methoxy-4-methyl-	Phenol, ethyl-methyl-
Naphthalene	Derivative of Phenol, (2,3,4- or 2,4,5-)trimethyl-
Indene	Cresol, o-
Benzofuran, 2-methyl-	Cresol, p-
Xylene, o-	Cresol, m-
Benzene (ethenyl-methyl- or propenyl) 1	similar to Phenol, 4-vinyl-: poss Phenol, vinyl- or Benzofuran, 2,3-dihydro-
Benzene, 1-butenyl	poss: Phenol, allyl-
1H-Indene, 2-methyl-	poss: Phenol, x-methyl-x-propyl-
poss. 2-Cyclopenten-1-ol, 1-phenyl-	<b>Miscellaneous</b>
<b>Guaiacols (Methoxy phenols)</b>	Pyridine
Guaiacol	Acetic acid 2-hydroxyethyl ester
Guaiacol, 4-methyl-	2-Propen-1-ol
Vanillin	Acetic acid, hydroxy-, methyl ester
Phenylethanone, 4-hydroxy-3-methoxy- (Acetoguaiacone)	Cyclopentene,3-methylene-
Guaiacyl acetone	1-Octene
Guaiacol, 4-propenyl-(trans) (Isoeugenol)	1H-Pyrrole, 1-methyl-
Guaiacol, 4-vinyl-	Propane, 2,2'-[ethylidenebis(oxy)]bis-
Guaiacol overlapping with 1H-Indene, 3-methyl-	1-Nonene
Guaiacol, 4-ethyl overlapping with 3,4-Dimethylphenol	Propane, 1,1-dipropoxy-
Guaiacol, 3-methyl-	1-Decene
poss: Ethanone 1-(2-hydroxy-6-methoxyphenyl)-	Limonene
poss. x-(x-Hydroxyphenyl)buta-x,x-diene	Pyridine, 2-methyl-
	Propanoic acid, 2-methyl-
	Propanenitrile, 2-hydroxy-
	Dimethyl-2-oxazoline-4-methanol
	Dimethyl-2-oxazoline-4-methanol
	1,2-Benzenedicarboxylic acid, 4-methyl-
	Bicyclo[3.3.0]oct-2-en-8-one, 3-methyl-
	poss. derivative of Norbornane
	similar to Bicyclo[3.3.0]oct-2-en-8-one, 3-methyl-
	poss. 2-Acetyl-5-norbornene
	similar to Phenol, 4-vinyl-: poss Phenol, vinyl- or Benzofuran, 2,3-dihydro-

# Lebenslauf

## Michael Halwachs

geboren am: 29. März 1981  
 wohnhaft in: 7400 Oberwart, Burgenland  
 Familienstand: Ledig  
 Staatsbürgerschaft: Österreich



## Schulische Laufbahn

1987 - 1991 Volksschule in A-7423 Pinkafeld  
 1991 - 2000 Bundesrealgymnasium mit Schwerpunkt Darstellende Geometrie in A-7432 Oberschützen  
 10 / 2001 - 10 / 2006 Fachhochschule für Energie- und Umweltmanagement in A-7423 Pinkafeld  
 10 / 2005 - 10 / 2006 Diplomstudium Verfahrenstechnik an der Technischen Universität Wien  
 Seit 10 / 2006 Doktoratsstudium Verfahrenstechnik : TU Wien - Institut für Verfahrenstechnik, Umwelttechnik und technische Biowissenschaften

## Berufserfahrung

10 / 2003 - 10 / 2005 Messung, Auswertung und Interpretation von Produktgasproben im Biomasseblockheizkraftwerk Güssing für das Institut für Verfahrenstechnik, Umwelttechnik und Technische Biowissenschaften der TU Wien (Projekt Renewable Energynetwork), A-1040 Wien  
 04 / 2007 - 12 / 2008 Projektassistent an der TU Wien - Institut für Verfahrenstechnik, Umwelttechnik und technische Biowissenschaften, Forschungsbereich Chemische Verfahrenstechnik und Wirbelschichttechnik, Arbeitsgruppe Zero Emission Energy Technology, A-1060 Wien Getreidemarkt 9/166  
 01 / 2009 - 12 / 2010 Junior Researcher: Kompetenzzentrum Bioenergy 2020+ GmbH  
 02 / 2010 bis dato Lektor an der FH Pinkafeld – Studiengang Energie- und Umweltmanagement, Umweltlabor für Wasseraufbereitung und Wasseranalyse sowie Staubmessung, Studiengang Nachhaltige Energiesysteme, ILV Energetische Nutzung von Biomasse